

**Potential for Contaminant Release from Fracturing UK  
Gas Prospective Black Shale Formations**

by

**Adeolu Oluwatosin Adegbulugbe**

Submitted in accordance with the requirements for the degree of  
Doctor of Philosophy

The University of Leeds  
School of Civil Engineering

November, 2015

The candidate confirms that the work submitted is his own and that appropriate credit has been given where reference has been made to the work of others.

The copy has been supplied on the understanding that it is a copyright material and that no quotation from the thesis may be published without proper acknowledgement

© 2015 The University of Leeds and Adeolu Adegbulugbe

## **Dedication**

This thesis is dedicated to all those aspiring to make a meaning in life and to my next employer for giving me the chance to build a career.

## **Acknowledgements**

I would like to express my gratitude to Prof. Nigel Wright, who believed I could successfully complete the research and was willing to give me a chance. I would like to thank Dr. Andy Sleigh for his invaluable contribution. I am indebted to Dr. Miller Alonso Camargo-Valero for his remarkable assistance and much needed motivation when I was overwhelmed with challenges. Your guidance and encouragements made this possible.

I am particularly grateful for the assistance given by Dr. Adriana Matamoros-Veloza who pushed me in the right direction. Her huge contribution remains priceless, Mr. Simon Lloyd for his patient and immense help when I was in dire need of one, Dave and Sheena at the public health laboratory for their assistance.

I acknowledge the colossal contributions of my wife, Adebukola, for her patience, care and love while research took a greater part of my sanity, my son Oluwatimilehin who gave me a reason to push and fight harder. Adebukola without you, none of this would have been possible. I am also indebted to my loving parents and siblings. Your immeasurable contributions have always surpassed all others. To my friends Dr. Frederick Pessu, Dr. Oladipo Adewale and Dr. Seun Akinrinola, I will never forget your colossal contributions. You guys are dear to my heart.

I would like to express my gratitude to my colleagues at the School of Civil Engineering, Mechanical Engineering and the School of Chemical and Process Engineering. You all have made the journey bearable.

Above all, I am grateful to God almighty, the maker of heaven and earth, the alpha and Omega, the rose of Sharon, the author and finisher of my faith.

## Abstract

This thesis investigates the potential for contaminant releases from three prospective shale gas formations following operational and environmental conditions common to the industrial extraction of shale gas. The overall aim was to assess the likelihood for these potentially toxic contaminants posing a substantial risk to existing water resource and infrastructure. This knowledge is geared towards providing the UK oil and gas industry with a quantitative risk assessment of flowback and produced water quality in the likelihood of the UK involvement in shale gas development.

Physical and geochemical characterisations of sampled black shales from three UK prospective Lancashire (LAN), Derbyshire (DRB) and Whitby (CLV) formations are presented to supplement the proposed contaminant release investigation with a record of empirical baseline data of the mineralogical and elemental compositions of the sampled shales. Black shale from Lancashire showed notably larger mean compositions of Cr (131ppm  $\pm$ 16), Rb (308ppm  $\pm$ 20), Ni (291ppm  $\pm$ 21), Zn (378ppm  $\pm$ 41) and Cu (285ppm  $\pm$ 43) and Pb (160  $\pm$ 17) in comparison with data from two documented world shale averages and the currently producing Marcellus formation in the US. Likewise, quantitative mineralogical data suggest a predominantly phyllosilicate (clay) and silicate (quartz) enriched shale matrix with the exception of the Carboniferous Edale shale with a sizable brittle carbonate content (22.27%). A risk weighing evaluation based on quantified trace elements, bioavailability and severity of toxicity highlighted Cr, Cu, Ni and Zn having the largest risk impacts investigated in the sampled shales. An assessment of the potential for acid rock drainage is assessed by static acid base accounting method and all three shales appear to be potentially acid producing with mean NPR at LAN( 0.66  $\pm$ 0.24), DRB ( 0.76  $\pm$ 0.19) and CLV( 0.71  $\pm$ 0.23). Heavy metal fractionation by sequential chemical extraction show a richly mobile carbonate phase Cr and a thermodynamically unstable Ni and Zn, possibly mobile via microbial mediation in all three sampled shales.

Based on these findings, laboratory scale kinetic leaching experiments were developed to simulate the release of the selected high risk heavy metals following weathering in their natural environment and subsequently following anthropogenic disturbances from operational fracture treatments. Natural weathering simulated releases were to

serve as baseline data on heavy metal mobility trends for comparison with hydraulic fracture influenced releases. We reported the characteristics of the leachate obtained and a quantification of the potential toxic Elements (PTEs) indicator in both leaching kinetic experiments and these trends allowed a prediction of future releases. Both simulated releases revealed an accelerated release activated in the later stages of leaching (between week 3 and 6) indicating a non-solely diffusion controlled release and an approximate exponential release rate was observed. Results showed a rise from one to three orders of a magnitude increase in PTE release rates from all three black shale types. In the natural weathering simulated releases, Cr recorded the highest release rates of  $9.31\text{E-}09$ ,  $8.7\text{E-}09$  and  $2.86\text{E-}08\text{mol/m}^2/\text{day}$  in the Lancashire, Derbyshire and Whitby black shales respectively. Acid base predictions showed higher percentage pyrite dissolution rate in comparison with carbonate rates in the LAN and DRB shales signifying the possible generation of acid mine drainage (AMD) in the Lancashire and Derbyshire black shales while carbonate dissolution rates sulphur rates exceeding sulphur rates in the CLV shale. Speciation analysis by geochemical modelling in both simulated releases revealed the presence of  $\text{CrO}_4^{2-}$ ,  $\text{Cr}^{3+}$ ,  $\text{Cu}^{2+}$ ,  $\text{Ni}^{2+}$  and  $\text{Zn}^{2+}$ , as toxic species but suggested the predominant reduction of Cr(VI) to Cr(III) following the acidic characteristics of the resulting leachates. In both simulated studies, predictions of the 5 to 10 year released concentrations all exceed the Environment Agency (EA) environmental quality standard (EQS) for inland surface water and transitional/coastal waters permissible concentration. Our findings suggests that significantly higher released concentrations of investigated PTEs were observed in the fractured simulated leaching kinetic experiment to suggest the increased risks from hydraulic fracturing. However, non-anthropogenic influences alone are capable of releasing toxic concentrations of the investigated trace metals.

The influence of additional environmental and operational factors prevalent during the development of shale gas wells were further investigated in a microcosm experiments. In particular, the mobility and release of the investigated PTEs influenced by prevailing anaerobic conditions in the presence of proliferating sulphur reducing bacteria. Our result showed that chemolithrophic bacterium like *Thiobacillus denitrificans*, is capable of anaerobic nitrate dependent pyrite oxidation and if present during fracture conditions can play a role in heavy metal mobility during fluid rock interaction. Mobilization and release of potentially toxic trace metals such as

investigated in the study, is accelerated by operational fracturing conditions such as chemical use and environmental factors such as the anaerobic conditions and bacteria proliferation in fracture wells. Data collected has shown that a significant immobilization of heavy metals can be achieved by the eradication of bacteria in fracture wells and during drilling operations.

## Table of Content

<b>Dedication .....</b>	<b>ii</b>
<b>Acknowledgements.....</b>	<b>iii</b>
<b>Abstract.....</b>	<b>iv</b>
<b>Table of Content.....</b>	<b>vii</b>
<b>List of Figures and Plates .....</b>	<b>xiii</b>
<b>List of Tables .....</b>	<b>xvii</b>
<b>List of Acronyms/Abbreviations.....</b>	<b>xxii</b>
<b>Chapter 1. Introduction.....</b>	<b>1</b>
1.1 Focus and Rationale .....	1
1.2 The UK Drivers for Unconventional Gas Development .....	4
1.3 Hydraulic Fracturing and Associated Risks .....	5
1.4 Contaminants and Contaminant Pathway.....	6
1.5 Assessing UK indigenous Water Contamination Risks .....	8
1.6 Scope, Aim and Objectives .....	9
<b>Chapter 2. Literature Review .....</b>	<b>12</b>
2.1 Overview of UK Prospective Shale Gas Formations .....	13
2.1.1 Black (Carboniferous) Shale .....	16
2.1.2 Thermal Maturity .....	17
2.1.3 Total Organic Carbon.....	17
2.1.4 Edale Basin Shale.....	18
2.1.5 Lancashire Carboniferous Shale .....	19
2.1.6 Cleveland Basin Jurassic Shale .....	20
2.2 Risk Evaluation on UK Water Resources .....	20
2.2.1 Hydraulic Fracturing Water Life Cycle .....	21
2.2.2 Water Sourcing Impact .....	22
2.2.3 Chemical Additives .....	26
2.2.4 Flowback and Produced Water Impact .....	29
2.3 Review of Fracturing Additive Use in the UK.....	30
2.3.1 Applications and Regulations .....	31
2.3.2 Disclosed Fracturing Additives.....	35
2.3.3 Examining Safety Records for Disclosed Additives.....	35
2.3.4 Friction Reducers FR-40 .....	36
2.3.4.1 De-polymerization and degradation of Polyacrylamide .....	37

2.3.4.2	Stability and Reactivity of Polyacrylamides.....	38
2.3.4.3	Health and Environmental Risk.....	39
2.3.4.4	Human Epidemiological Studies .....	39
2.3.4.5	Routes of Exposure.....	40
2.3.5	Acids and Tracers.....	41
2.4	Black shale contamination.....	43
2.5	Heavy metals as Indicators for Contaminant Mobility.....	45
2.6	Flowback and AMD/ARD Analogy.....	46
2.7	Microbial Influence on Contaminant Release .....	46
2.8	Knowledge Gap.....	47
<b>Chapter 3.</b>	<b>Research Methodology and Analytical Methods .....</b>	<b>49</b>
3.1	Investigated Formations .....	49
3.1.1	Lancashire Carboniferous Shale (LAN).....	49
3.1.2	Edale Basin Shale (DRB).....	50
3.1.3	Cleveland Basin Jurassic Shale (CLV) .....	50
3.2	Rock Sampling .....	50
3.3	Rock Preparation and Storage .....	51
3.4	General Methods .....	52
3.4.1	Spectrometry Instrumentations .....	52
3.4.2	Chromatograph Instrumentation .....	53
3.4.3	Laboratory Analysis of Metal Release.....	54
<b>Chapter 4.</b>	<b>Shale Characterisation Study .....</b>	<b>56</b>
4.1	Introduction .....	56
4.2	Chapter Objectives .....	56
4.3	Methodology .....	57
4.3.1	Physical Characterisation of Shales .....	58
4.3.1.1	Particle Size Reconstruction .....	58
4.3.1.2	Surface Area Determination (BET Analysis).....	59
4.3.2	Chemical Characterisation of Shales .....	60
4.3.2.1	Mineralogical Determination by XRD .....	60
4.3.2.2	XRF Whole Rock Elemental Determination .....	60
4.3.2.3	Total Carbon and Total Sulphur Determination .....	61
4.3.2.4	Bulk Compositional Assay by Total Acid Extraction .....	61
4.3.2.5	Acid Base Accounting (ABA) – Static Method.....	62
4.3.2.6	Mobility Assessment by Sequential Extraction .....	65

4.4	Results and Discussion: Physical Characterisation .....	67
4.4.1	Lithological Characteristics .....	67
4.4.2	Standardized Particle Size Distribution .....	68
4.4.3	Surface Area Determination.....	69
4.5	Results and Discussion: Geochemical Characterisation .....	72
4.5.1	Mineralogical Composition.....	72
4.5.2	XRF Whole Rock Composition .....	74
4.5.2.1	Justification for Selected PTE Indicators.....	78
4.5.2.2	Trace Element Correlation.....	80
4.5.3	Acid Base Analysis .....	83
4.5.4	Sequential Batch Extraction.....	86
4.6	General Discussion/Result Significance.....	91
4.7	Limitations of Experimental Study .....	95
4.8	Summary and Conclusion .....	96
<b>Chapter 5.</b>	<b>Column Kinetics: Natural Weathering Simulation .....</b>	<b>97</b>
5.1	Introduction .....	97
5.2	Chapter Objectives .....	99
5.3	Methodology .....	100
5.3.1	Laboratory Simulation of Natural (Weathering) Releases.....	100
5.3.2	Justification of the Chosen Leaching Method.....	101
5.3.3	Sample Preparation .....	103
5.3.4	Experimental Design and Setup.....	103
5.3.5	Analysis and Spectrometric Determinations.....	107
5.3.6	Quality Control .....	108
5.4	Results .....	111
5.4.1	Presentation of Data .....	111
5.4.2	Leachate Analysis .....	112
5.4.2.1	Alkalinity, Conductivity and pH Effect on Metal Release .....	112
5.4.2.2	Dissolution and Contaminant Release Kinetics.....	114
5.4.2.3	Predicting Long Term Leachate Composition.....	119
5.4.2.4	Pyrite and Carbonate Weathering Rates .....	122
5.5	Geochemical Modelling for Metal Speciation .....	126
5.6	General Discussion.....	130
5.6.1	Chromium .....	132
5.6.2	Copper.....	133

5.6.3	Nickel .....	134
5.6.4	Zinc .....	134
5.7	Limitations of Experimental Study .....	135
5.8	Summary & Conclusion .....	135
<b>Chapter 6.</b>	<b>Column Kinetics: Fracture Simulated Releases .....</b>	<b>137</b>
6.1	Introduction .....	137
6.2	Chapter Objectives .....	138
6.3	Methodology .....	138
6.3.1	Composition and Preparation of Simulated Fracture Fluid .....	138
6.3.2	Sample Preparation .....	139
6.3.3	Experimental Design and Setup .....	140
6.4	Results .....	142
6.4.1	Presentation of Data .....	142
6.4.2	Leachate Analysis .....	143
6.4.2.1	Leachate Characteristics .....	143
6.4.2.2	Weathering Pattern .....	145
6.4.2.3	Trace Metal Release Kinetics (Dissolution Rate).....	148
6.4.2.4	Predicting Long term Leachate Composition .....	150
6.4.2.5	Pyrite and Carbonate Weathering Rates .....	153
6.5	Geochemical Modelling for Metal Speciation .....	157
6.6	General Discussion .....	161
6.6.1	Column Leachate Chemistry .....	161
6.6.2	Release Quantification .....	162
6.6.3	Release Predictions .....	163
6.6.4	Predicting Flowback Quality (Acidity/Alkalinity Characteristics)....	165
6.6.5	SFF Effects of Metal Mobility .....	166
6.6.5.1	Chromium .....	166
6.6.5.2	Copper.....	167
6.6.5.3	Nickel.....	168
6.6.5.4	Zinc .....	168
6.7	Limitations of Experimental Study .....	169
6.8	Summary & Conclusion .....	169
<b>Chapter 7.</b>	<b>Comparative Analysis: Natural and Fracture Enhanced .....</b>	<b>172</b>
7.1	Introduction .....	172
7.2	Variations in pH, Conductivity and Alkalinity.....	173

7.3	PTEs Releases and Reaction Rate .....	178
7.4	Flowback Quality .....	182
7.5	Heavy Metal Speciation .....	185
7.6	Chapter Summary .....	189
7.7	Conclusion.....	192
<b>Chapter 8. Microcosm Investigation of Biochemical Release Potential.. 193</b>		
8.1	Introduction .....	193
8.2	Chapter Objectives .....	195
8.3	Design of Experiment.....	197
8.3.1	Microcosm Design .....	197
8.3.2	The Choice of Inoculum.....	198
8.3.3	Design of Oxidation Experiment .....	199
8.3.3.1	Statistical Design of Experiment Iteration.....	199
8.3.3.2	Test of Quantifiable Concentrations .....	200
8.3.3.3	Analytical Determinations .....	201
8.4	Methodology .....	202
8.4.1	Sample Preparation .....	202
8.4.2	Cultivation and Adaptation of Thiobacillus Denitrificans.....	202
8.4.2.1	Monitoring Bacterial Growth.....	205
8.4.2.2	Maintaining Anoxic Conditions.....	206
8.4.2.3	Harvesting Growing Cells .....	207
8.4.3	Microbial Mediated Oxidation Experiment .....	207
8.4.3.1	Volumetric Composition of Oxidation Medium.....	207
8.4.3.2	Oxidation Experiment.....	209
8.4.4	Analytical Determinations .....	210
8.4.4.1	Fe (II) and Total Fe Determination.....	210
8.4.4.2	Trace Metal Determination.....	211
8.4.4.3	Elemental Transformation Rate .....	212
8.5	Results and Discussion.....	212
8.5.1	Cultivation and Adaptation Results .....	212
8.5.2	Shale Oxidation Experiment: Proof of Nitrate Dependent Pyrite Oxidation.....	217
8.5.2.1	pH and Bacterial Count.....	217
8.5.2.2	Oxidation of Fe <sup>2+</sup> and Formation of Fe <sup>3+</sup> .....	219
8.5.2.3	Nitrate Reduction.....	221

8.5.3	Anaerobic Bio-mediated PTE Releases .....	223
8.5.3.1	No SFF Amended Leachant.....	223
8.5.3.2	With SFF Amended Leachant.....	224
8.5.4	Anaerobic Non Bio-Mediated PTE Releases.....	226
8.5.5	Comparative Analysis of PTE Releases.....	226
8.6	Limitations of Experimental Study .....	231
8.7	Summary and Conclusion .....	231
<b>Chapter 9.</b>	<b>Conclusion and Recommendations .....</b>	<b>233</b>
<b>Reference.....</b>	<b>.....</b>	<b>237</b>
<b>APPENDIX A: Shale Characterisation Data .....</b>	<b>.....</b>	<b>253</b>
<b>APPENDIX B: Quality Control Results .....</b>	<b>.....</b>	<b>257</b>
9.1	GFAAS Quality Control Results .....	257
9.2	FAAS Quality Control Results.....	259
9.3	IC Quality Control Results .....	260
<b>APPENDIX C: Leachate Characteristics .....</b>	<b>.....</b>	<b>261</b>

## List of Figures and Plates

<b>Figure 2.1:</b> UK Northern Petroleum Province, Basins, and Shale Gas Prospective Areas(EIA 2011) .....	13
<b>Figure 2.2:</b> Summary of prospective areas for gas in the upper and lower parts Bowland-Hodder unit in relation to urban areas of central Britain (Andrews 2013). 15	
<b>Figure 2.3:</b> Modern Analog for Organic Rich Shale (Alexander et al. 2011).....	16
<b>Figure 2.4:</b> Illustration of fracturing water life cycle (EPA 2011).....	21
<b>Figure 2.5:</b> Underground, Under Threat: The State of Ground Water in England and Wales" retrieved from (Environment Agency 2006) .....	23
<b>Figure 2.6:</b> Abstractions from non-tidal surface water and groundwater by use, England and Wales, 2000-2011 (Moore <i>et al.</i> 2014).....	23
<b>Figure 2.7:</b> Wastewater Constituents from Shale Gas Exploration (The Royal Society 2012) .....	29
<b>Plate 3.1:</b> (A) The Varian spectrometer setup for FAAS (B) The Varian spectrometer setup for GFAAS .....	52
<b>Plate 3.2:</b> (A) The Metrohm 850 Professional Ion Chromatograph (B) Cations, Anion and Regenerant Solutions.....	53
<b>Figure 4.1:</b> Sequential extraction scheme (modification of the Tessier 4 stage chemical extraction scheme) .....	66
<b>Plate 4.2:</b> (A) Weathered mass of Edale black shale (DRB) showing brownish colouration, an indication of iron enrichment (B) Unweather Edale shale.....	67
<b>Plate 4.3:</b> (C) Jurassic black shale from the Cleveland basin (CLV) (D) Numarian grey to black shale from Bowland basin, Lancashire (LAN).....	68
<b>Figure 4.4:</b> Comparison of Trace metal distribution in sampled shales and World shale averages compiled by (1) Vinogradov (1967) and (2) Li and Schoonmaker (2005b).....	77
<b>Figure 4.5:</b> (a) Cross plot of Fe/Al ration versus Ni from the LAN black shale (b) Cross plot of SiO <sub>2</sub> versus Cu from the LAN sample set.....	81
<b>Figure 4.6:</b> (a) Cross plot of Fe/Al ration versus Zn (b) Cross plot of Ni versus V from the Edale shale formation at the Peak National District park in Derbyshire (DRB)..	82
<b>Figure 4.7:</b> (a) Cross plot of Fe/Al ration versus Zn (b) Cross plot of Ni versus V from the Edale shale formation at the Whitby Formation, Cleveland Basin (CLV). .....	82

<b>Figure 4.8:</b> Plots of NPR test methods for mean Static ratios computed in all three investigated formations using three methodologies i.e. Standard Sobek method, modified Sobek method and the modified Lawrence ABA method .....	84
<b>Figure 4.9:</b> Plots of the Static ABA analysis for sampled shales (a) Modified Acid Base Method by (Lawrence and Wang 1997) (b) Standard Sobek Method by (Sobek et al. 1978) (c) Studies Modification to the Sobek Method. ....	85
<b>Figure 4.10 [A-H]:</b> Distribution of indicator PTEs in the Sequential Extraction protocols applied, [A-D] in percentages, [E-H] in concentration ( $\mu\text{g/g}$ ). ....	89
<b>Figure 4.11:</b> Mineralogical distribution of quartz, carbonate, and clay in all three investigated formations. ....	92
<b>Figure 4.12:</b> Comparison of Average NP values determined by the standard Sobek and the Modified Sobek Method.....	93
<b>Figure 5.1:</b> Schematic diagram of fabricated single leaching column.....	104
<b>Plate 5.2:</b> Fabricated Leaching Rig .....	105
<b>Figure 5.3:</b> Weekly pH trend in Leachate .....	113
<b>Figure 5.4:</b> Alkalinity Concentrations for all Three Investigated Black Shales .....	113
<b>Figure 5.5:</b> Conductivity Trends overtime for all Three Sampled Shales .....	114
<b>Figure 5.6:</b> Cumulative Plots of Weighted Released Heavy Metal Concentrations Leached in tap water .....	116
<b>Figure 5.7:</b> Comparison of Normalized Heavy metal Release from Sampled Shales .....	118
<b>Figure 5.8:</b> Curve fitting to flux computation .....	120
<b>Figure 5.9:</b> Curve fitting to flux computation (contd.) .....	121
<b>Figure 5.10:</b> Ten year prediction of released heavy metal concentrations.....	121
<b>Figure 5.11:</b> Curve fitting on cumulative percentage sulphur and carbonated data	124
<b>Figure 5.12:</b> A 10 year Prediction of pyrite dissolution in comparison with carbonate dissolution rate .....	125
<b>Figure 5.13:</b> Heavy metal speciation in leachate from the Lancashire (LAN), Derbyshire (DRB) and Whitby (CLV) black shale formations. ....	129
<b>Figure 6.1:</b> Weekly pH trend in Leachate .....	143
<b>Figure 6.2:</b> Alkalinity Concentrations for all Three Investigated Black Shales .....	144
<b>Figure 6.3:</b> Weekly Conductivity Trends for all Three Sampled Shales .....	145

<b>Figure 6.4:</b> Leaching Data showing weighted Concentrations and Cumulative Weighted concentrations .....	146
<b>Figure 6.5:</b> Comparison of Normalized Heavy metal Release from Sampled Shales .....	149
<b>Figure 6.6:</b> Curve fitting to flux computation .....	152
<b>Figure 6.7:</b> Ten year prediction of release concentrations .....	153
<b>Figure 6.8:</b> Curve fitting on cumulative percentage sulphur and carbonate data ...	155
<b>Figure 6.9:</b> A 10 year Prediction of pyrite dissolution in comparison with carbonate dissolution rate .....	157
<b>Figure 7.1:</b> pH data for both simulated leaching scenarios in (a) Lancashire Bowland Shale (b) Derbyshire Edale shale (c) Whitby Bituminous Shale .....	174
<b>Figure 7.2:</b> Conductivity data for both simulated leaching scenarios in (a) Lancashire Bowland Shale (b) Derbyshire Edale shale (c) Whitby Bituminous Shale.....	176
<b>Figure 7-3:</b> Alkalinity data for both simulated leaching scenarios in (a) Lancashire Bowland Shale (b) Derbyshire Edale shale (c) Whitby Bituminous Shale.....	177
<b>Figure 7.4:</b> Leach curves for Cr, Cu, Ni and Zn in (A) Natural weathering simulated leaching experiment (B) Fracture Enhanced all other concentrations ate in $\mu\text{g/L}$ ...	179
<b>Figure 7.5:</b> A comparison of mean computed elemental mass loss ( $NL_i$ ) in the natural weathering simulate leaching and the Fracture enhanced simulated leaching experiment.....	180
<b>Figure 7-6:</b> A comparison of chemical flux from the simulated natural weathering and fracture enhanced simulated leaching experiment .....	181
<b>Figure 7.7:</b> Combined plots of cumulative sulphur and $\text{CaCO}_3$ leaching rates in (a) Natural weathering leaching simulation (b) Fracture enhanced leaching simulation .....	183
<b>Figure 7.8:</b> Results of aqueous PTE speciation for: (a) average natural weathering simulated leaching (b) average fractured enhanced weathering simulated leaching	186
<b>Figure 7.9:</b> Speciation of (a) $\text{Cr(VI)}$ ( $10^{-6}\text{M}$ ) (b) $\text{Cr(III)}$ ( $10^{-6}\text{M}$ ) (c) $\text{Cu(2)}$ ( $10^{-7}\text{M}$ ) (d) $\text{Ni}$ ( $10^{-7}\text{M}$ ) and (e) $\text{Zn}$ ( $10^{-6}\text{M}$ ) from the Bowland black shale leached with SFF. .	188
<b>Figure 7.10:</b> 5 year predicted release concentrations of investigated traces in the fractured simulated and natural weathering simulated leaching scenarios .....	191
<b>Plate 8.1:</b> Laboratory Items and accessories use in designing the microcosm.....	198
<b>Plate 8.2:</b> (a) Freeze dried ampoules vials of <i>Thiobacillus denitrificans</i> ATCC©25259TM .....	203

<b>Plate 8.3:</b> (a) 150ml borosilicate glass serum bottle used as growth cells (b) Incubation of growth cells in a systematic rotary incubator at 37 <sup>0</sup> C .....	205
<b>Plate 8.4:</b> 3.5L AnaeroPack Rectangular jar containing streaked plates.....	207
<b>Plate 8.5:</b> Microcosm vessels filled with shale and reaction media.....	209
<b>Plate 8.6:</b> (A) The non-Zeeman Work-head (B) Capillary Tip Positioning.....	211
<b>Figure 8.7:</b> Mean concentrations of SO <sub>4</sub> <sup>2-</sup> , NO <sub>3</sub> <sup>-</sup> and NO <sub>2</sub> <sup>-</sup> over sampling duration in both (A) Ordinary growth media and (B) SFF Modified growth media and evidence of nitrate dependent oxidation. ....	213
<b>Figure 8.8:</b> Count of cells in the cultivating growth cells.....	215
<b>Figure 8.9:</b> Plots of pH trends and counts of colony forming units (CFU) .....	218
<b>Figure 8.10:</b> Proof of anaerobic, nitrate dependent oxidation of pyritic molecules from black shales by <i>T.denitrificans</i> . Plots shows the production of Fe <sup>3+</sup> and oxidation of Fe <sup>2+</sup> and Fe <sup>2+</sup> in sterile controls (MRC 3, 6 and 9) .....	219
<b>Figure 8.11:</b> Sulphate (SO <sub>4</sub> <sup>2-</sup> ), Nitrate (NO <sub>3</sub> <sup>-</sup> ) and Nitrite (NO <sub>2</sub> <sup>-</sup> ) trends in reactors (A) MRC 1 (Bioleaching of LAN shale without SFF amendment) (B) MRC 5 (Bioleaching of LAN shale with SFF amendment) oxidation experiment. ....	221
<b>Figure 8.12:</b> Release trends of investigated trace metals in the bio-mediated oxidation experiments with no introduction of SFF.....	224
<b>Figure 8.13:</b> Release trends of investigated trace metals in the bio-mediated oxidation experiments with amended with SFF. Plots (a-d) represent bio-mediated oxidation results (e-h) represents non- bio-mediated oxidation results .....	225
<b>Figure 8.14:</b> A comparison between results from varying simulated leaching configuration for releases of Cr from studies investigated shales.....	227
<b>Figure 8.15:</b> Semi Log plot comparing bulk matrix composition with average daily released concentrations from both leaching column and oxidation experiments ....	228
<b>Figure C-1:</b> Plots of Raw Release Concentration (non-cumulative) for both Majors and trace Heavy Metals .....	265

## List of Tables

<b>Table 1.1:</b> Structure of the Thesis .....	2
<b>Table 2.1:</b> IOD’s Estimate of Water Use and Flowback water (IOD 2013) .....	24
<b>Table 2.2:</b> Identified Risk Impacts from Water Sourcing and the Probability of Occurrence .....	25
<b>Table 2.3:</b> Disclosed Chemicals Used at Preese Hall Site. ....	27
<b>Table 2.4:</b> Identified Risk Impacts from Chemical Additives and the Probability of Occurrence .....	28
<b>Table 2.5:</b> Compiled Fracturing Additives and their Applications .....	32
<b>Table 3.1:</b> Definition of Utilised Quality Control Parameters .....	54
<b>Table 4.1:</b> Particle size distribution of reconstructed samples .....	58
<b>Table 4.2:</b> Carbonate rating based on percent insoluble residue with corresponding acid volumes and acid strengths.....	63
<b>Table 4.3:</b> Particle size distribution of reconstructed samples .....	69
<b>Table 4.4:</b> Surface Area Measurement for all Sampled Shale Pre-leaching .....	70
<b>Table 4.5:</b> Surface Area Measurement Post-leaching (Simulated Natural Weathering) .....	71
<b>Table 4.6:</b> Surface Area Measurement Post-leaching (Fracture Enhanced Weathering) .....	71
<b>Table 4.7:</b> Summary of the before and after changes in the observed BET.....	72
<b>Table 4.8:</b> Normalised Mineralogical composition of sampled Black shale from all three investigated UK formations .....	73
<b>Table 4.9:</b> Chemical Composition of Sampled Shale, Numerian Lancashire Shale (LAN), Derbyshire Edale Shale (DRB) and Whitby Toarcian Bituminous Shale (CLV) .....	76
<b>Table 4.10:</b> Toxicity ranking and a risk index for selection of high risk trace element .....	79
<b>Table 4.11:</b> Sulphur and Acid Potential (AP) Determination .....	83
<b>Table 4.12:</b> Distribution of PTE Indicators Extracted from the 6 Stage Sequential Extraction Protocols .....	87

<b>Table 4.13:</b> Summary of Characterisation Results for all Three Investigated Black Shale Formations.....	90
<b>Table 5.1:</b> Summary Experimental Column Design .....	106
<b>Table 5.2:</b> Analysis and Appropriate Method Utilised .....	107
<b>Table 5.3:</b> Definition of Utilised Quality Control Parameters for GFAAS .....	109
<b>Table 5.4:</b> Definition of Utilised Quality Control Parameters for the FAAS .....	109
<b>Table 5.5:</b> Quality Control Parameters for IC Determinations .....	110
<b>Table 5.6:</b> Computation Result for Dissolution Rate and Goodness of Fit.....	117
<b>Table 5.7:</b> Normalised Release Rates [ $\text{mol}/\text{m}^2/\text{day}$ ] .....	119
<b>Table 5.8:</b> Estimated Decay (rate of change) Constants for Cr, Cu, Ni and Zn.....	120
<b>Table 5.9:</b> Summary computation for Cumulative percentage of sulphur and carbonate weathered in all three investigated shales .....	123
<b>Table 5.10:</b> Fitting Parameters of Sulphur and Carbonate Extraction for curves in Figure 5.10 .....	124
<b>Table 5.11:</b> Computation of predicted percentage pyrite and carbonate rates .....	125
<b>Table 5.12:</b> Dominant Chemical Species of Metals in Soils and Natural Waters...	126
<b>Table 5.13:</b> Summary of Physiochemical Parameters from Selected Weekly Leachate .....	127
<b>Table 5.14:</b> Result of PHREEQC output, containing predicted concentrations of selected ionic species .....	128
<b>Table 5.15:</b> Summarised concentration of a 10 years release prediction .....	131
<b>Table 5.16:</b> Summarised mean percentages for identified toxic species from speciation results in Table 5.14 .....	132
<b>Table 6.1:</b> Summary Properties of Loaded Experimental Column .....	141
<b>Table 6.2:</b> Computation for Dissolution Rates and Goodness of fit for the Cumulative Leaching Data .....	147
<b>Table 6.3:</b> Normalised Release Rates [ $\text{mol}/\text{m}^2/\text{day}$ ] .....	150
<b>Table 6.4:</b> Estimated rate of change (decay) constants for Cr, Cu, Ni and Zn.....	151
<b>Table 6.5:</b> Summary computation for Cumulative percentage sulphur and carbonate weathered in all three investigated shales .....	154

<b>Table 6.6:</b> Curve Fitting Parameters for Sulphur and Carbonate plots in Figure 6.8 .....	155
<b>Table 6.7:</b> Computation of predicted percentage pyrite and carbonate rates .....	156
<b>Table 6.8:</b> Summary of Physiochemical Parameters from Selected Weekly Leachate .....	158
<b>Table 6.9:</b> Result of PHREEQC output file containing activities and concentrations of some ionic species.....	159
<b>Table 6.10:</b> Comparison of emperical rates with normalised dissolution rate constant for investigated traces heavy metals .....	163
<b>Table 6.11:</b> Summarised mean percentages for identified toxic species from speciation results in Table 5.19 .....	164
<b>Table 6.12:</b> Summarised total concentration of a 10 years release prediction.....	165
<b>Table 7.1:</b> Comparing modelled 10 year predictions of Fracture and natural weathering simulated leaching of sampled shales .....	182
<b>Table 7.2:</b> Summary of Sulphur and Carbonate content in experimental Column .	184
<b>Table 7.3:</b> Computed percentages for toxic species from geochemical modelling of dissolved species .....	185
<b>Table 8.1:</b> Matrix of proposed microcosm experiment to study the effect of environmental and operational condition on PTE releases .....	196
<b>Table 8.2:</b> Description of Experiment Runs.....	199
<b>Table 8.3:</b> Computation of Reactor Configuration for Rock Fluid volume in Reactor .....	200
<b>Table 8.4:</b> Analysis and Appropriate Method .....	201
<b>Table 8.5:</b> ATCC medium: 450 T2 medium for Thiobacillus .....	204
<b>Table 8.6:</b> Computation of growth rate and generation time for both cultures.....	214
<b>Table 8.7:</b> Cultivation data showing count of CFU/mL and absorbance at OD600 for growth cells in recommended ATCC media.....	216
<b>Table 8.8:</b> Cultivation data showing count of CFU/mL and absorbance at OD600 for growth cells in SFF amended media .....	216
<b>Table 8.9:</b> Computation of Elemental transformation rate for Fe <sup>2+</sup> .....	220
<b>Table 8.10:</b> Computation of Elemental transformation rate for Fe <sup>3+</sup> .....	220

<b>Table 8.11:</b> Computation of Elemental transformation rate Sulphate (SO <sub>4</sub> <sup>2-</sup> ) from raw concentration (ppm) .....	222
<b>Table 8.12:</b> Computation of Elemental transformation rate Nitrate (NO <sub>3</sub> <sup>-</sup> ) from raw concentration (ppm) .....	222
<b>Table 8.13:</b> Computation of Elemental transformation rate Nitrite (NO <sub>2</sub> <sup>-</sup> ) from raw concentration (ppm) .....	222
<b>Table 8.14:</b> Trace metal oxidation rates in (mol m <sup>-2</sup> hr <sup>-1</sup> ) computed from linear regression .....	228
<b>Table 8.15:</b> Comparative summary of bulk metal composition in sampled shales with cumulative releases from leaching column and microcosm oxidation experiments	230
<b>Table A-1:</b> Correlation Matrix for Black Shale Sampled from the Bowland Lancashire Formation (Coefficient of R <sup>2</sup> values for Majors, Minors and Traces).....	253
<b>Table A-2:</b> Correlation Matrix for Black Shale Sampled from the Edale formation (Coefficient of R <sup>2</sup> values for Majors, Minors and Traces).....	254
<b>Table A-3:</b> Correlation Matrix for Black Shale Sampled from the Toarcian Whitby formation (R <sup>2</sup> values for Majors, Minors and Traces) .....	255
<b>Table A-4</b> Computed Neutralization Potential for All Three Investigated Formations .....	256
<b>Table B-1:</b> Computation of MDL for GFAAS from spiked LRB.....	258
<b>Table B-2:</b> Results for adopted 5 point statistical Check test for GFAAS Determinations .....	259
<b>Table B-3:</b> Summary results for MDL determinations .....	259
<b>Table B-4:</b> Sample and LFB recoveries and percentage differences of triplicate spikes adopted for FAAS determinations .....	260
<b>Table B-5:</b> Quality Control Test with a Certified Multi Anion Standard for IC....	260
<b>Table C-1:</b> Reactor 1 (LAN) Weekly Monitoring Report for Natural Weathering Simulation .....	261
<b>Table C-2:</b> Reactor 2 (DRB) Weekly Monitoring Report for Natural Weathering Simulation .....	261
<b>Table C-3:</b> Reactor 3 (CLV) Weekly Monitoring Report for Natural Weathering Simulation .....	262
<b>TableC-4:</b> Summary Computation of Weathered Mass .....	263
<b>Table C-5:</b> Raw Concentration of Major Elements .....	264

<b>Table C-6:</b> Raw Concentration of Minor (Trace) Elements .....	264
<b>Table C-7:</b> Computed Cumulative weighted Concentrations for Major Elements..	266
<b>Table C-8:</b> Computed Cumulative weighted Concentrations for Trace Elements..	266
<b>Table C-9:</b> Computation of percentage weekly weathered CaCO <sub>3</sub> in the Lancashire Bowland Shale .....	267
<b>Table C-10:</b> Computation of percentage weekly weathered CaCO <sub>3</sub> in the Derbyshire Edale shale .....	268
<b>Table C-11:</b> Computation of percentage weekly weathered CaCO <sub>3</sub> in the Whitby Bituminous shale.....	269
<b>Table C-12:</b> Computation of cumulative sulphur weathered from analytical sulphur determination.....	270

## **List of Acronyms/Abbreviations**

AAS	Atomic Absorption Spectrometer
ABA	Acid Base Accounting
AP	Acid Production Potential
ATCC	American Type Culture Collection
BET	Brunauer, Emmett and Teller Surface Area Determination
BGS	British Geological Survey
BP	British Petroleum
CLV	Whitbian Bituminous Shale from the Cleveland Basin
DBP	Disinfection By-Products
DECC	Department of Energy and Climate Change
DEFRA	Department for Environment, Food and Rural Affairs
DRB	Edale Shale from Derbyshire
EA	Environmental Agency
EPA	US Environmental Protection Agency
EU	European Union
FAAS	Flame Atomic Absorption Spectrometer
GTA	Graphite Tube Atomizer
HAA	Halo-acetic Acids
HDPE	High Density Polyethylene
HDF	Hydraulic Fracture
IC	Ion Chromatography
ICI	International Chemical Industry
IDL	Instrument Detection Limit
IOD	Institute of Directors
LAN	Black Shale from Bowland Formation Lancashire

LFB	Laboratory Fortified Blank
LOI	Loss of Ignition
LRB	Laboratory Reagent Blank
MDL	Method Detection Limit
MSDS	Material safety data sheet
NORM	Naturally Occurring Radionuclides
NP	Neutralisation Potential
NRC	US Nuclear Regulatory Commission
OD	Optical Density
OFGEM	Office of Gas and Electricity Markets
OGP	Oil and Gas Producers
PTE	Potentially Toxic Trace Elements
QCS	Quality Control Sample
QCS	Quality Control Sample
REACH	Registration, Evaluation, Authorization and Restriction of Chemicals Regulation
SDS	Safety Data Sheets
SFF	Simulated Fracture Fluid
TCF	Trillion Cubic Feet
THM	Tri-halomethane
TOC	Total Organic Carbon
UK	United Kingdom
US	United States
W.H.O	World Health Organization
XRD	X-Ray Diffraction Analysis
XRF	X-Ray Fluorescence

# Chapter 1. Introduction

## 1.1 Focus and Rationale

In the UK, surface and ground water are abstracted by water utilities and serve as potable water resources. Major UK aquifers such as the Chalk and Permo-Triassic sandstones supply more than 85% of total abstracted groundwater in the UK while the Rivers Itchen, Medway and Teise are licenced rivers for water abstraction (Hlavay *et al.* 2004). Hence, hydrological cycles and anthropogenic interferences within supply catchments are strategically monitored to avoid widespread resource contamination. Over the years, water resources in the UK suffer from so much anthropogenic pressures, negatively impacting their ability to provide sustainably for both abstraction and effluent demands of a growing population. It is clear however, that with the current discovery of shale gas in the UK and the application of the extraction technique known as “Hydraulic Fracturing”, a further strain is expected on this dwindling resource.

The Royal Society has called for proper risk evaluations and implications on the UK’s current water resource status and together with the Royal Academy of Engineering, have reported that limited understanding of UK shales and the composition of returning wastewater have hindered a true assessment of potential risks (The Royal Society 2012). The identification of potential risks, though a responsibility of the EA in England and Wales, is jointly shared from a policy perspective by the Department for Environment, Food and Rural Affairs (Defra), one of the principal organisations with the statutory undertaking powers for setting national level policies and strategies for the management of water. A proper evaluation of the risks from this new industry is therefore vital to the adoption of appropriate regulatory policies required to guide shale exploration and the protection of human health and the environment.

This thesis presents an investigative study undertaken to assess the likelihood for potential water resource contamination from the industrial extraction of shale gas from UK prospective shale gas formations. This project was initiated following debates on the planned moratorium on shale gas exploration and search for scientific understanding of the potential risk impact on water resource in the UK. The research objectives are designed to provide scientific knowledge of the likelihood of contaminant release and mobility from these prehistoric shale formations. The

investigation has been confined to three (3) UK shale formations with identified shale gas prospectivity. The study adopts the synthesis of fracture formation returning wastewater (Flowback) from all three sampled formations for the experimental determination of contaminant release. The investigation compares the impact of both environmental and operational factors to the release and mobility of contaminants from the sampled formations. A structure of the thesis has been provided (Table 1.1) as a summary of work presented here.

**Table 1.1:** Structure of the Thesis

<b>Chapter Title</b>	<b>Chapter Content</b>
Chapter 1: Introduction: Overview of UK exploration drivers, the extraction techniques, potential contaminants and scope of investigative study	A summary of thesis structure. A general introduction to shale gas exploration in the UK, the research aim, objectives and scope of the study. An overview of UK drivers for unconventional gas exploration, the environmental and health impact of gas exploration in the US and avoiding risk assessments: a US case study.
Chapter 2: A critical review of extraction techniques, potential for risk and the implications for water resource in the UK.	A critical look at shale extraction in the UK, prospective UK shale gas formations, the fundamentals regarding metal mobility from fluid rock interactions, the feasible pathways involved in heavy metal mobility and the possible risk to water resource, the environment and human health.
Chapter 3: Materials and Methods:	This Chapter describes the general methodology adopted for the study, the choice of analytical techniques and sample preparation methods generally adopted during the study.

<b>Chapter Title</b>	<b>Chapter Content</b>
Chapter 4: Sampled black shale characterisation study	In Chapters 4, the results and discussion from both the physical and chemical characterisation studies are reported and analysed for comparison with established knowledge. Chapter 4 presents the results for characterisation study on samples from all three investigated shale formations.
Chapter 5: Leaching column kinetic test simulating natural weathering releases	Results for experiments investigating the release of PTEs under natural environmental degradation of the sampled shales are presented and discussed.
Chapter 6: Leaching column kinetic test simulating fracture enhanced releases	This Chapter discusses results from experiments investigating the release of PTEs following anthropogenic interferences from Hydraulic fracturing operational conditions.
Chapter 7: Microcosm study of release potential	This Chapter compares and discusses results obtained from both simulated leaching kinetic studies in Chapters 5 and 6.
Chapter 8: General Discussion	This study presents and discusses results obtained from the experimental study of both environmental and operational condition on heavy metal releases.
Chapter 9: Conclusions and recommendations	General conclusions from the research and avenues for further research are discussed.

## 1.2 The UK Drivers for Unconventional Gas Development

Global uncertainties affecting the energy sector have driven the world to seek alternative sources of energy that are sustainable and allow the attainment of statutory commitments on CO<sub>2</sub> reduction. The task of achieving this dual objective within an economic climate, plagued with rising costs, increasing demands and an economic recession is taking its toll on most economies, the United Kingdom included. Towards the end of the last century, there has been a global push to exploit other forms of fossil and non-fossil fuel. Over the past few decades unconventional gas has moved from a minority interest to centre stage focus in natural gas circles. This is driven largely, by unforeseen growth in North American shale gas production, which in 2006 effected a reversal of the decline in total US natural gas production. Estimates of global unconventional gas resources have, since the late 1990s, exceeded those of conventional gas. However, doubts as to their viability at prevailing natural gas market prices, served to limit the expectation of future production from these sources.

More than any other fuel in the UK energy mix, gas is widely used in the UK. In 2011, gas accounted for just 30% of final energy consumption and since 2004, the majority of this being imports primarily due to the decline in UK North Sea production. It became obvious that the UK gas prices were vulnerable to fluctuations in the international price and these fears were worsened by the US's declaration of a shale gas boom following successful applications of the technology. The resulting effect was a rise in UK gas import prices, driving off investment and further worsening the energy crisis. There were several debates suggesting that to compete in the global gas market, the UK's shale gas resource had to be exploited. Extracting commercially viable quantities of the unconventional gas could equally change the energy landscape for the UK. The news of viable quantities of UK shale gas in place could not have come at a better time, as the energy regulator OFGEM, reported the UK having a 2 day gas storage capacity in March 2013. Drawing analogies with the US, when shale gas replaced other fossil-fuels, lower emissions of greenhouse gases and local pollutants were reported (DTI 2003, Arthur *et al.* 2008, Consulting Regeneris 2011, OGP 2012). This further helped to diversify energy supply, and so improve energy security (Scheetz *et al.* 1981). This could provide the flexibility and back-up capacity needed

as more variable capacity comes online in power generation, a much needed flexibility for the UK (Pederson *et al.* 1983).

### **1.3 Hydraulic Fracturing and Associated Risks**

Like with every other fossil fuel, shale gas exploration has its share of environmental and human health hazards and up until recently, this was largely embedded in the technique for extraction “Hydraulic Fracturing”. Hydraulic fracturing is a well stimulation technique that has been employed in the oil and gas industry since the late 1940s. The process involves the injection of fracture fluids, a carefully formulated product containing water, proppant and chemical additives, into a subsurface geologic formation containing oil and/or gas at a force sufficient to induce fractures through which oil or natural gas can flow to a producing wellbore. Following fracturing activities, formation water returns to the surface as ‘flowback’ usually within the first 30 days after drilling and as “produced water” subsequently, throughout the gas production life of the well. It is with these returning wastewaters, this research study is mainly concerned. Of course, other risks arise such as air pollution, faulty casings during drilling, gas migration, earthquakes and light tremors but all are a consequence of the extraction technique and can be controlled through engineering schemes. However, risks arising from the nature of the formation are inevitable, and would occur irrespective of the formation fractured by manifesting in the return wastewater from the fractured formation.

This returning wastewater stream contains a huge deposit of suspended and dissolved salts, usually from geological formations characteristic to the site, hydrocarbons, heavy metals, and traces of chemicals used to enhance fracturing and a range of other contaminants. The treatment and disposal of this waste stream has been challenging and environmental experts have raised concerns over a lack of best practices to minimize the impact on the environment. Most treatment plants are equipped to remove organic waste however, with inorganic wastes embedded in returning flowback, tertiary treatment techniques have to be designed. The problem is, most tertiary treatments are case specific. Therefore, wastewater treatment plants have to be specifically designed to remove these inorganic non-biodegradable contaminants from influent waste and this is the major challenge with flowback and produced water.

## 1.4 Contaminants and Contaminant Pathway

Shale gas extraction is yet to commence commercially in the UK and with the exception of the Environment Agency's analysis of returning flow from the Preese Hall site at Weeton, the typical contaminants in UK returning waste fluid is largely unknown. However, there is a wealth of data on the nature of returning waste fluid from the United States from over 30 years of shale gas exploration. Returning waste fluids from fractured formations are known to contain high levels of salinity, toxic metals, radioactivity, high concentrations of some inorganic solutes and have the potential to return some organic additives (Langmuir 1997, Hornberger *et al.* 2004b, Peng *et al.* 2004, Hornberger *et al.* 2005, Mor *et al.* 2006). The Environment Agency report on the Preese Hall, UK return waste fluid showed concentrations of Lead (Pb) having 1438 times tap water values, Cadmium (Cd) having 150 times tap water values, Bromide (Br) having 2297 times tap water values, Chromium (Cr) having 636 times tap water values, Aluminium (Al) having 197 times tap water values, Arsenic (As) having 20 times tap water values and levels of Radioactivity at up to 90 Bq/l (EA 2012).

Mor *et al.* (2006) reported salinity levels for typical waste fluid from the Pennsylvania shale plays in the US to vary from 5000 mg/L to >200000 mg/L. These concentrations include sodium ion (50–40000 mg/L), chloride ion (5000–80000 mg/L) and may contain high concentrations of brines mostly due to fluid interactions with the formation. In addition, other components such as barium (50–9000mg/L), strontium (50–6000mg/L), magnesium (50–2000mg/L), calcium (500–12000mg/L), iron (50–160mg/L), manganese (5–7mg/L), sulphate (10–400mg/L) and silica (50–300mg/L) have been reported in the Marcellus shale plays of Pennsylvania. Total dissolved solids range reported 1000–150,000 ppm, toxic inorganic constituents such as arsenic and selenium, radionuclides, organics and other noxious inorganic constituents are found in flowback water (Chen *et al.* 2008). These concentrations may vary in flowback water from different areas and shales, and this illustrates the need for similar data gathering for the UK. In addition to this, the productions of surrogate contaminants have also been reported. In the US state of Pennsylvania, returning waste fluid was prevented from being treated at wastewater treatment plants due to high levels of bromide, which when disinfected, creates a compound called brominated

trihalomethanes linked to several types of cancer and birth defects (Bhattacharya and Parkin 1988). These and many more contaminants and surrogate contaminants raises the concern over treatment technologies, disposal route or reuse.

The most obvious pathway for contamination is leakage of fracturing fluid into underground aquifers. In the UK, data released by the British Geological Survey (BGS) and the Environment Agency (EA) have shown that almost half the area of England and Wales where major drinking water aquifers are located have shale gas deposits below them (Environment Agency 2009a). Although the maps suggest that the vertical distance between the water and the gas are sometimes several kilometres, making water pollution by fracture propagation very unlikely, data from the US state of Ohio where aquifer contaminations have been reported suggest the likelihood of occurrence of possible contamination. Well casing integrity represents another pathway for contaminant introduction and is simply the leakage of fracking fluid and returning waste fluid into adjacent aquifers due to structural failures in the wells protective casing. Around 27% of the UK population, including London and much of south-east England gets drinking water from underground supplies hence imagine the scale of the risk to human health here in the UK. The leakage from just one exploratory well has the potential to cause widespread damage to the environment and poses a risk to public health, therefore the scale of the potential health risk is increased with several wells needed to recreate a US shale gas boom here in the UK.

In the north and west of England however, water supplies come predominantly from surface water and the possible contamination pathway can be explained by a review of the waste handling processes following return of wastewater to the surface. Returning waste fluid is classified as trade effluent as the Water Industry Act 1991 states that any liquid produced wholly or in part from any trade or business activity carried out on any trade premises qualifies as trade effluent and therefore requires consent from the water utility provider. In the UK, discharge of trade effluent can only be made to the foul sewer and cannot be discharged to surface waters. Provisions exist where certain trade effluent deemed unsuitable for discharge are transported by tankers to waste management centres. Effluent discharges from these waste centres are eventually discharged to surface waters following treatment completion and this constitutes a

threat to the environment and human health if treatment is inadequate. Potential risks to water resource and human health could therefore occur via a number of pathways;

- Shallow aquifers contaminated by fugitive natural gas (i.e., stray gas contamination) from leaking shale gas and conventional oil and gas wells, potentially followed by water contamination from hydraulic fracturing fluids and/or formation waters from the deep formations.
- Surface water contamination from spills, leaks, and the disposal of inadequately treated wastewater or hydraulic fracturing fluids.

## **1.5 Assessing UK indigenous Water Contamination Risks**

A critical requirement for the UK just at the verge of developing her shale gas resource is an inclusive risk assessment of potential water resource contamination. For the appropriate engineering and policy decision to be made, it is essential that potential UK risks arising from this new industry be understood. For example, important engineering decisions on treatment type, effluent quality, disposal methods and reuse options based on a UK scenario are vital. Policy decisions on the environmental permitting systems required to protect water resource, the environment and human health is equally vital. It is already agreed that wastewater management is one of the biggest challenges for the UK at the verge of shale gas exploration but what constitutes the challenge is virtually unknown as stated by the Royal Society report *“Produced water will continue to return to the surface over the well’s lifetime. Very little is currently known about the properties of UK shales to explain what fraction of fracture fluid will return as flow back water, as well as the composition of formation waters and produced water”* (The Royal Society 2012). Even in the US, current treatment efforts to render this complex waste stream safe for disposal fall short mainly because of the variable nature of the waste and its deteriorating quality with respect to time (Blauch *et al.* 2009, Hayes and Severin 2012). Engineering a suitable treatment solution is estimated to cost the US. shale gas industry a yearly investment of \$10 million (£6.70 million) (Acharya *et al.* 2011).

However for the UK, the challenge is critically unique. The Preese Hall well site at Weeton remains to date the only fractured shale gas well in the UK. Although abandoned due to technical problems, plans are currently underway to fracture

additional wells at Anna's Road, Banks and Singleton with the prospect of more wells as recent surveys have also identified prospective UK shale gas formations in Derbyshire and Scarborough (Andrews 2013). Therefore, a risk assessment of possible water resource and contamination risk would require a predictive approach due to a lack of an active UK fractured wells.

To resolve this challenge, this study will assess the quantitative mineralogical and geochemical properties of the source rock. Other research have shown that flowback is a function of the characteristics of the source formation and chemical use during fracturing (Halliburton 2008, Basu 2011, EPA 2011, Hayes 2011, Considine *et al.* 2012). Since industry chemical use can be predetermined, the unknown variables are the mineralogy and geochemical characteristics of the source rock, shale. Hence, unknowns like the variability in flowback composition over time are largely a function of the unknowns in the fluid-rock interactions within the formation. This all too important risk assessment must provide information on the likely contaminant release from fracturing these prospective formations and this is the basis for the research in this thesis.

## **1.6 Scope, Aim and Objectives**

With the UK's efforts to develop her potential shale gas resource, there are several concerns that the water contamination risks from shale development activities have been overlooked and not adequately researched (Green *et al.* 2011, Wood *et al.* 2011, CIEH 2012, The Royal Society 2012). Key aspects with pressing information gaps such as flowback treatment, water resource management and the possibility of ground water contamination have prevented the assessment of direct risk implications for this unconventional resource development. This research provides an investigative look at the source rock with the aim to understand the release of potentially toxic elements (PTEs) and the kinetics that control contaminant release from the source formation, black shale, resulting in the generation of returning waste fluid. This thesis intends to utilise the kinetics of fluid-rock interactions in the study of the release and mobility of PTEs from black shale. A simulation of both environmental and operational conditions during fracture is planned to enable the study of the controlling factors responsible for the flowback and produced water characteristics and as such provide a quantitative prediction of the quality of returning waste fluid. The main objectives related to this

research work are enumerated below with sub-objectives (itemised in Roman numeral) listed under each main objective:

1. Identify UK prospective black shale and provide a characterisation study of the sampled prospective formations (Chapter 4 objective).
  - i. Sample three prospective UK shale gas formations and provide a physical and geochemical characterisation of the sampled formations
  - ii. Select identifier PTEs of notable toxicity for proposed mobility and release assessment.
  - iii. Provide bulk quantification and fractionation data on selected PTEs via total acid extraction and Sequential batch extraction (SBE).
2. Assess the release patterns of the selected trace element under prevailing natural environmental conditions (Chapter 5 objective).
  - i. Using the studied shale lithologies, run a laboratory scale simulation of fluid rock interactions typically occurring during natural degradation and weathering, noting any observable weathering patterns and its influence on long term releases of trace heavy metal compositions.
  - ii. Using the leaching data, observe the potential for the investigated shales to produce acidic, circumneutral or alkaline drainages. This being a function of the relative weathering rates of the carbonates and pyrite compositions
3. Assess the time dependent release of PTEs using industrial chemical additives as leaching solvent (Chapter 6 objective).
  - i. Using the studied shale lithologies, run a laboratory scale simulation of fluid rock interactions resulting from fracture induced weathering, noting observable weathering patterns and its influence on long term releases of indicator trace heavy metal compositions.
  - ii. Observe the influence on the leachate quality and potential for the investigated shales to produce acidic, circumneutral or alkaline drainages.

- iii. Compare data with results obtained in the simulated natural weathering kinetic study in the previous Chapter.
4. Provide a comparative analysis on simulation results obtained from both natural and fracture enhanced PTE release experiments aimed at determining the risk contribution of shale gas development to contaminant mobility (Chapter 7 objective).
  5. Investigate the release of heavy metals under the prevailing anoxic conditions (environmental conditions) and chemical use, (operational conditions) typifying conditions during hydraulic fracturing (Chapter 8 objective).
    - i. Evaluating the extent to which a solely chemically controlled oxidation process can influence PTE release
    - ii. Evaluating the extent to which a solely biological controlled oxidation process can influence PTE release
    - iii. Evaluating the extent to which a combination of chemical and biological oxidation process can influence PTE release

## Chapter 2. Literature Review

A UK holistic view of potential risks to water resource requires a critical look at five vital areas. Firstly, a general look at shale gas prospectivity in the UK, examining the prospective formations with reported gas-in-place and a critical evaluation of characteristics of these formations in light of their geochemical properties. A study of how the locations of these formations, their proximity to established water resource both surface and underground impacts the potential for risk. The water resource status in these areas, wastewater treatment facilities within these localities and a review of the geochemical study of these rock formations, gives a broad overview of the likelihood for water resource contamination.

Secondly, this review will assess the water usage in fracturing operations to identify the potential impact on UK water resources. Thirdly, the identification of potential contaminants as identified from the review of mineralogical and geochemical characterisation of UK formations previously reviewed. This will help to establish the contaminant indicators to be monitored during the assessment of UK risk arising. This section will also include a review of contaminant identification from the source rock “Black Shale” and other associated toxic elements. A review of the pathways to contamination exposures while drawing analogies with the US scenarios will further help to review implications of UK wastewater and water treatments. Fourthly, this review will evaluate the use of several indicators for the intended risk assessment, the suitability of radionuclides, heavy metals, total dissolved solids or other suitable indicators.

Lastly, the review will not be complete without critical analysis of the state of the art in the field of fluid rock interactions resulting in accelerated degradation, shale compositional and heavy metal release from shale rock. It is postulated that these factors are responsible for the release of contaminants to generation of returning waste fluid, however the impact of both environmental conditions during fracturing and microbial mediated degradation will be reviewed. This review will outline the problem with the use of literature, identifying the knowledge gap and defining the importance of the research to current knowledge.

## 2.1 Overview of UK Prospective Shale Gas Formations

A review of the UK's potential shale formations is necessary to identify potential sampling locations for the proposed experimental work. In the UK, shale was until recently (1980) not considered a hydrocarbon reservoir rock, organic rich shale however, has been studied as a source rock in which oil and gas matured before migrating into conventional fields (DECC 2011). The earliest reports of onshore hydrocarbons date back to a well drilled at Heathfield in Sussex in 1895 which produced sufficient gas to fuel a gas light for the railway station. Although shale gas potential was highlighted in the 1980s (Selley 2005a) it was only in the 13th Onshore Licensing Round in 2008 that companies specifically sought to explore for shale gas. Up until 2013, the UK could boast of 8 onshore gas fields, 3 coalbed methane and 18 vent gas where methane was extracted from abandoned coal mines, all producing gas, signifying a shift to coal bed methane, vent gas and shale gas exploration (Andrews 2013).

One of the earliest reports from EIA (2011) on UK shale gas prospectivity reported its findings as under the two UK petroleum systems made up of several formations and basins (Figure 2.1).

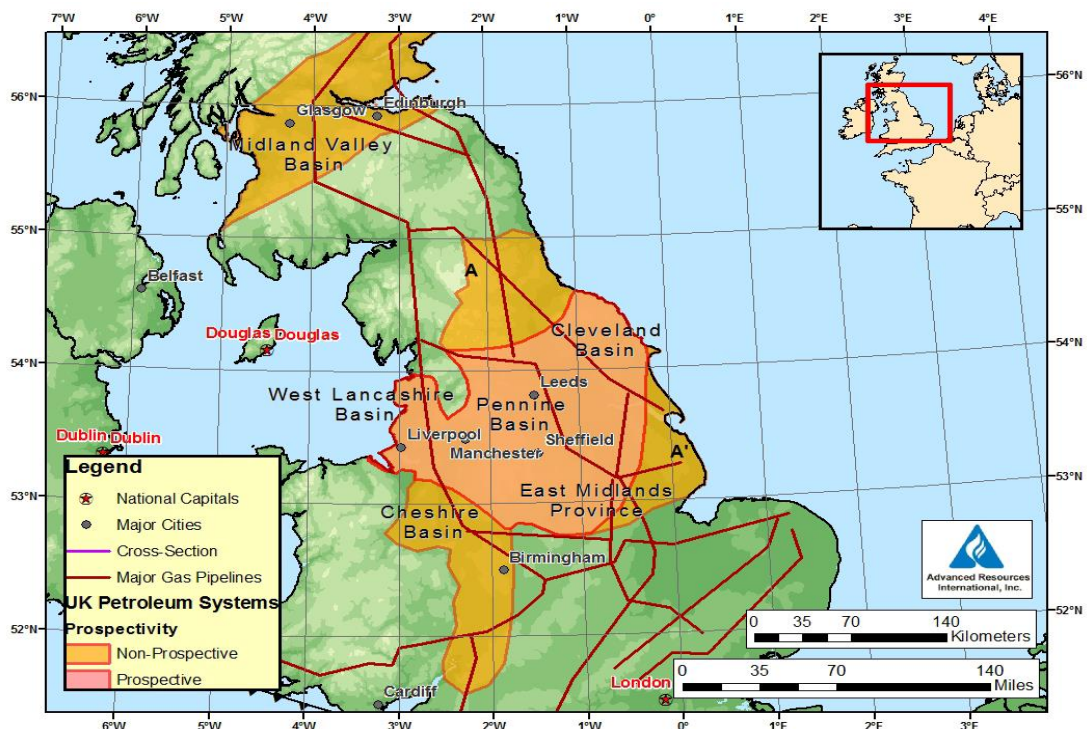


**Figure 2.1:** UK Northern Petroleum Province, Basins, and Shale Gas Prospective Areas(EIA 2011)

These include the Northern Petroleum System with a mainly Carboniferous basin and the Southern Petroleum System, mainly of Jurassic geological age. The EIA report was mainly speculative as conclusions were based on data from UK onshore oil basins which had similarly depositional and tectonic history with reviewed shale gas formations rather than a true measure of prospectivity from data on the type of organic matter held in the shale, its thermal maturity, burial history, micro-porosity and fracture spacing and orientation. However, this report did identify the Namurian Bowland Shale, Liassic shale from the Cleveland basin, shale from the Carboniferous Pennine Basin, as well as the Cheshire, West Lancashire and Scottish Midland Valley basins as part of the potential prospective shale formation in the Northern petroleum system. Based on the expanse of shale cover for the Bowland shale, the report estimated a risk shale gas in-place of 95 Trillion cubic feet (Tcf) of which it estimated 19 Tcf was technically recoverable.

In contrast, Smith *et al.* (2010) provided a geological information system combining information on hydrocarbon shows, thermal maturity, fracture orientation, gas composition, and isotope data to identify potential UK prospective areas for shale gas. The Lower Palaeozoic shale basins on the Midland Microcraton, the Mississippian shales in the Pennine Basin, the Pennsylvanian shales in the Stainmore and Jurassic shales in Wessex and Weald basins. Perhaps the only criticism of this study would be the use of analogies with the prospective formations in the US. One could argue that reporting UK prospectivity based on formation analogues with the US do not provide reliable data to suggest the prospectivity of UK formations. However, Smith *et al.* (2010) based their study on three main factors that controlled prospectivity in the Barnett shale, thermal maturity, thickness and total organic carbon (TOC) content of the shale as also supported by Zhao *et al.* (2007). Hence, by assessing these controls in a regional UK context, the authors were able to identify prospective UK shale gas target formations. Again this study identified the Carboniferous black shale of the Mississippian shale units has having the highest potential for gas. This conclusion was based on the high Total Organic Carbon (TOC) values reported by Armstrong *et al.* (1997)

Following increased interest in UK shale gas prospects, the British Geological Survey (BGS) embarked on a gas in place survey and produced the most convincing UK shale

gas prospectivity survey to date. Relying on a 3D geological model generated using seismic mapping, the BGS study provided a preliminary gas in-place estimate for the Bowland-Hodder (Carboniferous) shale gas play (Figure 2.2) across a large area of central Britain. The BGS convincingly reported a combined average total in-place gas resource estimate for the upper and lower Bowland-Hodder unit shales across central Britain of 1329Tcf (37.6Ttcm) at a 50<sup>th</sup> percentile (P50) (Andrews 2013). The study significantly identified the Bowland, Blacon, Gainsborough, Widmerpool, Edale and Cleveland basins as having the right formation thicknesses and TOC content (Organic matter) to generate considerable amounts of hydrocarbon.

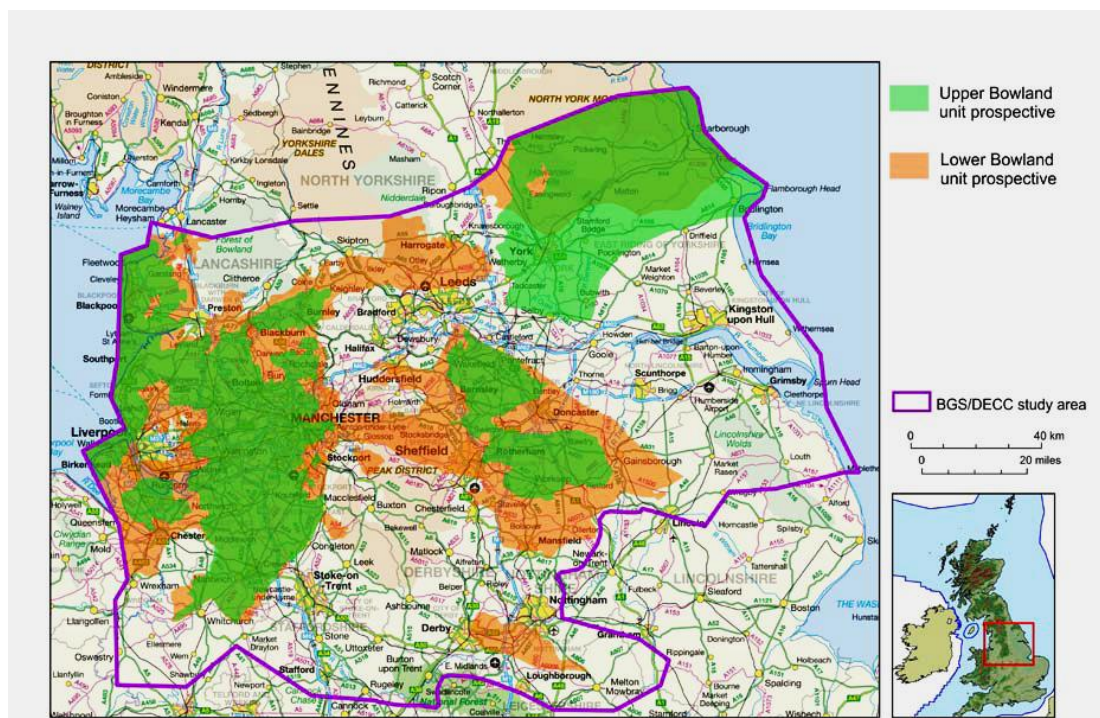


**Figure 2.2:** Summary of prospective areas for gas in the upper and lower parts Bowland-Hodder unit in relation to urban areas of central Britain (Andrews 2013)

To determine UK prospectivity for the purpose of obtaining environmental samples, a critical scrutiny of UK reported prospective formations is examined. To identify potentially prospective shales, geologists look for specific geochemical properties, which are typically derived from core data. Some of the properties can be measured with downhole sensors; however, petrophysicists refine and characterise downhole measurements by calibrating log data to core data. Geochemical properties needed to adequately characterise shale resources include TOC, gas volume and capacity, thermal maturity, permeability and mineralogy. Hence the desired shales will show

some evidence of original TOC, with evidence that significant amounts of gas have formed from that TOC during thermal maturation. These and other useful indicators of prospectivity are adopted, in comparison to US active gas formations, to provide a review of likely UK prospective shale formations.

### 2.1.1 Black (Carboniferous) Shale

Active US shale gas rich formations like the Marcellus, Barnett and Atrim shales have the lithological characteristics of being mostly black shales, similar to identified UK formations like the Bowland shale, Edale shale and the Laissic shales of Jurassic geological age. The colour ‘black’ is of course associated with the abundance of organic matter and pyrite content, which petro-physicists identify as having the potential to hold gas. Interestingly, Jones and Plant (1989) reported that UK Lower Palaeozoic black shales often show preferential enrichment of various heavy elements including As, Co, Cr, Cu, Mo, Ni, Pb, S, U and V, a discovery also reported by Leggett (1980) and in most cases referred to as Carboniferous. The modern analog for organic rich shales suggests decay of organic material is a bacterial process that occurs under aerobic conditions, limited anaerobic bacterial activity can also occur under anoxic conditions (Figure 2.3). Black, organic-rich sediments accumulate on the bottom. Anaerobic bacteria strip oxygen from the sulphates and give off hydrogen sulphides ( $H_2S$ ) as a waste product. The  $H_2S$  may react with iron in the sediments to form pyrite ( $FeS_2$ ), which is frequently observed in organic –rich shale deposits (Alexander *et al.* 2011).

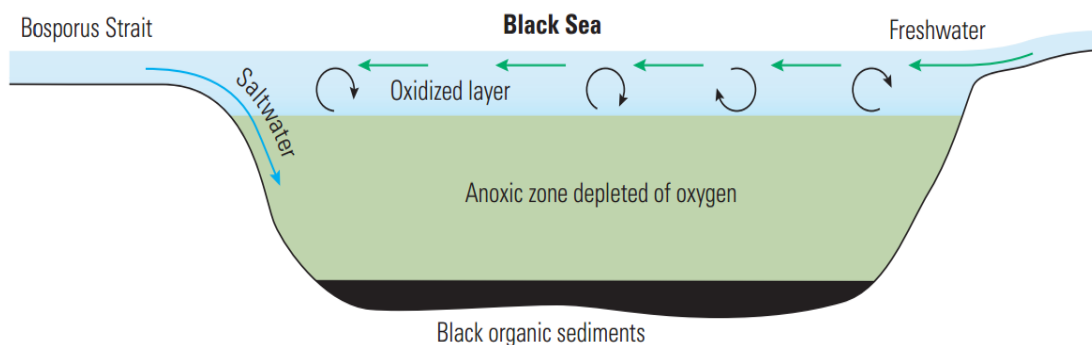


**Figure 2.3:** Modern Analog for Organic Rich Shale (Alexander *et al.* 2011)

### **2.1.2 Thermal Maturity**

Thermal maturity is a function of depositional history and gives a measure of how much pressure and temperature the rock has undergone over time and also whether oil or gas has been generated during the process. As kerogen is exposed to progressively higher temperatures over time, vitrinite cell wall materials and woody plant tissue preserved in the rock undergo irreversible alteration and develop increased reflectance. This vitrinite reflectance ( $R_o$ ) is measured microscopically and typically ranges from 0% to 3% for a prospective shale formation. Measurements in excess of 1.5% are a sign of dry gas generating source rock, a positive indicator for gas shale.  $R_o$  ranges of 0.6% to 0.8 % indicate oil and ranges of 0.8% to 1.1% indicate wet gas. A reflectance value below 0.6% is indicative of kerogen that is immature, not having been exposed to sufficient thermal conditions over adequate time for conversion of the organic matter to hydrocarbons. Hence, prospective formations usually show a high vitrinite reflectance ( $>1.1\%R_o$ ). Data from the active Marcellus shale report values ranging from 0.6% to 2.47% with the highest recorded from the Allegheny County in Pennsylvania. In the UK, the BGS and Department of Energy & Climate Change (DECC) report (Andrews 2013) provided data on part of the Bowland-Hodder unit (includes Carboniferous Numarian grey shale from Lancashire and Black shale the Edale shale basin in Derbyshire) of central England, and reported a  $R_o$  of 1.1% for present day depth of anything between outcrop and 2900m. Although, the report suggested data obtained for vitrinite reflectance showed large variability, this has been generally accepted as valuable data suggesting shale gas prospectivity.

### **2.1.3 Total Organic Carbon**

Organic shale, by definition, must have organic carbon and the TOC governs the resource potential of shale, therefore petro-physicists target formations having TOC values in the general range of 2% to 10%. Surprisingly, rocks with TOC above 10% are usually too immature for development and ideally should be over 2%, with 5% around the maximum encountered in typical prospective shale gas formations. The presence of TOC often dictates the porosity of the shale, as most of the shale's porosity is contained within the microscopic pore space of the organic matter itself. The total carbon in a shale sample includes both inorganic and organic carbon. To quantify organic carbon, engineers use a combustion technique after pre-treating the sample

with phosphoric acid to remove inorganic carbon. The combustion allows the conversion of organic carbon to CO<sub>2</sub>, which is then measured as a weight percent of the rock. However, for more accurate measurements, Petro-physicists commonly use downhole data from geochemical and conventional logging suites to quantify the volume of kerogen in the rock and then compute TOC values from these data. Active US shale formations like the Utica Shales are known to have a TOC values ranging from 0.5% to 3% (Nyahay *et al.* 2014), the Barnett shale have reported values in the range of 3.3% to 5.2% (Nyahay *et al.* 2014) and the Marcellus shales have reported up to 12% (Bruner and Smosna 2011). In the UK, there are a few published data on organic carbon contents in the Bowland-Hodder unit (Smith *et al.* 2010, DECC 2011) and these published data suggest that Namurian marine shales have generally higher TOC values (average 4.5%) compared to non-marine shales, which have an average value of 2.7% (Spears and Amin 1981a). Maynard *et al.* (1991) found that two thin Namurian black shale marine bands have a TOC of between 10 and 13%, whereas values within interbedded strata ranged between 2 and 3%. The Numarian Holywell Shale of North Wales has TOC values in the range 0.7-5%, with an average of 2.1% (Armstrong *et al.* 1997). More recently, the Ince Marshes 1 well encountered shales with TOC values of 1.18 – 6.93% (average 2.73%) in the ‘Bowland Shale’ (iGas 2012). These three prospectivity controlling factors were subsequently used to select potential UK shale gas formations for the proposed experimental work as part of this research study. These include the Carboniferous Numarian grey shale from the trough of Bowland Lancashire UK, Black shale from the Mam Tor landslide at the Peak District National Park, North Derbyshire UK and Grey to black Jurassic aged shale specimen from coast of Scarborough UK.

#### **2.1.4 Edale Basin Shale**

Some of the oldest and blackest shale outcrops in the UK can be found at the Mam Tor landslide at the Peak District National Park. This shale has a sequence of interbedded sandstone, siltstone and shale of Dinantian age. Shale stratigraphy consists of laminated, sub fissile, very dark grey to black shale. The Edale Basin is a fault-bounded structure (Gutteridge 1991) that has a preserved cover of Millstone Grit and a relatively thin overlying unit of late Carboniferous Coal Measures. This shale unit forms part of the BGS and DECC report shales forming the Bowland-Hodder unit.

Ewbank *et al.* (1993) noted that Alportian-Pendleian mudstones exposed at an outcrop in the Edale Gulf area predominantly contained gas-prone Type III kerogen. Younger shale gas targets include the Bowland (Edale) Shales and the Sabden Shales (Namurian). The shortened black Edale Shale sequence outcropping in the Derbyshire Peak District was until recently regarded as thin and immature for hydrocarbon generation. Towards the East however, these units thicken and represent the main source rocks that charged the East Midlands hydrocarbon system suggesting the likelihood for gas prospectivity. Borehole cores from these units have a TOC content average of 4.48% in marine bands and 2.66% in non-marine shale sequences suggesting the higher prospects of gas finds. Already, several DECC exploration licences have been issued for shale gas exploration in this unit with iGas being the most likely investor to commence operations sometime in 2015 (Andrews 2013). Black shale from the Mam Tor landslide at the Peak District National Park, North Derbyshire UK (Grid Reference SK 1270083600) has been sampled for the study.

### **2.1.5 Lancashire Carboniferous Shale**

The oldest rocks present in Lancashire comprise limestones and mudstones that were deposited in the sea and are now collectively known as the Carboniferous Limestone. These units also form part of the Bowland shale formation and the Hodder Mudstone Formation of Lancashire. These are dark grey shale mudstones, with occasional thin calcareous mudstones and siltstones with well exposed sections at the Pendle Grit formation in the trough of the section. This distinctive unit of rock outcrops in two separate parts of the County. In the south it underlies the tract of land from north of Preston, through the Ribble Valley via Clitheroe to Barnoldswick and around the southern and eastern flanks of the Forest of Bowland. In the north the Carboniferous Limestone outcrops between Kirby Lonsdale and Silverdale on the coast, where the outcrop gives rise to some of the best examples of limestone pavement in the country. This unit to date contains the only hydraulically fractured shale unit in the UK, fractured by a Spanish based exploration firm, Cuadrilla Resources. Surprisingly, not far from this well location, in the West Lancashire basin is the Formby oil seeps, used since the 17th century, and responsible for the discovery of the very shallow Formby Oilfield in 1939 which has produced 71,560 barrels of oil. The region is also home to the Daw Hill Colliery, the largest UK coal producer. In 2008 alone, Daw Hill

excavated a record 3.25 million tons of coal. The south coast is also bounded by the Wytch Farm giant field which has produced over 450mmbbls of oil. Carboniferous Numarian grey shale from the trough of Bowland Lancashire UK (Grid Reference SD 6265252722) has been sampled for the study.

### **2.1.6 Cleveland Basin Jurassic Shale**

The Cleveland Basin, includes the North York Moors, Cleveland Hills, Hambleton Hills, Howardian Hills and the North Yorkshire coast. It is an onshore extension of the Southern Permian Basin petroleum system and is known to hold minor (gas) petroleum systems (DECC 2011). Most of the Cleveland Basin is within the gas window, with the southern line of gas fields (e.g. Kirby Misperton) at a lower level of maturity on the crests of structures. Already this part of North East England has contributed to onshore gas supplies. In 1937, British Petroleum (BP) and International Chemical Industry (ICI) drilled at Eskdale and tested gas from the Permian Magnesian Limestone. These gas supplies were used in nearby Whitby until 1967. Coal has also been mined in this unit as the now closed Eskdale and Lockton gasfields and other still producing gas fields like the Kirby Misperton, Malton and the Pickering gasfields. Lithologically, these are mudstone, intercalated with relatively thin units of calcareous sandstone, calcareous mudstone and calcareous siltstone. Although, their stratigraphy may vary generally across the basin, the shale consists of a generally grey to black of Jurassic age. This grey to black Jurassic shale specimen from the coast of Scarborough UK (Grid Reference TA 0351091180) that form part of the Cleveland basin. All three sampling location were selected due to their characteristic greyish to black natured shale, mostly reported has holding mature natural gas, documented gas prospects and close stratigraphic similarities to the currently explored Carboniferous formations in Lancashire.

## **2.2 Risk Evaluation on UK Water Resources**

It is generally agreed that a thorough life cycle assessment of an impact is required to fully conduct a proper risk evaluation. Therefore, this section provides a critical review of the life cycle of water use during fracturing operations here in the UK, with the aim of identifying risks to water resources and its potential impact. This lifecycle assessment will evaluate water use in fracturing shale gas, from sourcing to reuse or

disposal, will eventually identify the driving factors that may affect the severity and frequency of such impacts.

### 2.2.1 Hydraulic Fracturing Water Life Cycle

Water use is essential to hydraulic fracturing and according to Cuadrilla Resources Ltd, constitutes 99.8% of the resource used to fracture the sole fractured shale gas well in Preese Hall here in the UK. Water is essential for the success of each well, and is in fact used in the initial drilling process for each well. During Cuadrilla's operations at Preese Hall, 8,400m<sup>3</sup> of water were used for the fracture treatments and an additional 900m<sup>3</sup> of water was used during the drilling phase. It is estimated that in the US, a single horizontal shale gas well will use between 9,000m<sup>3</sup> and 29,000m<sup>3</sup> of water during a multi-stage fracturing operation (Wood et al. 2011), with an average of around 18,000m<sup>3</sup> and an additional 2,000m<sup>3</sup> per well typically required for drilling vertical and horizontal components, maintaining hydrostatic pressure in the wellbore and cooling the drill head and removing drill cuttings. A typical illustration of fracturing water life cycle is shown in Figure 2.4.

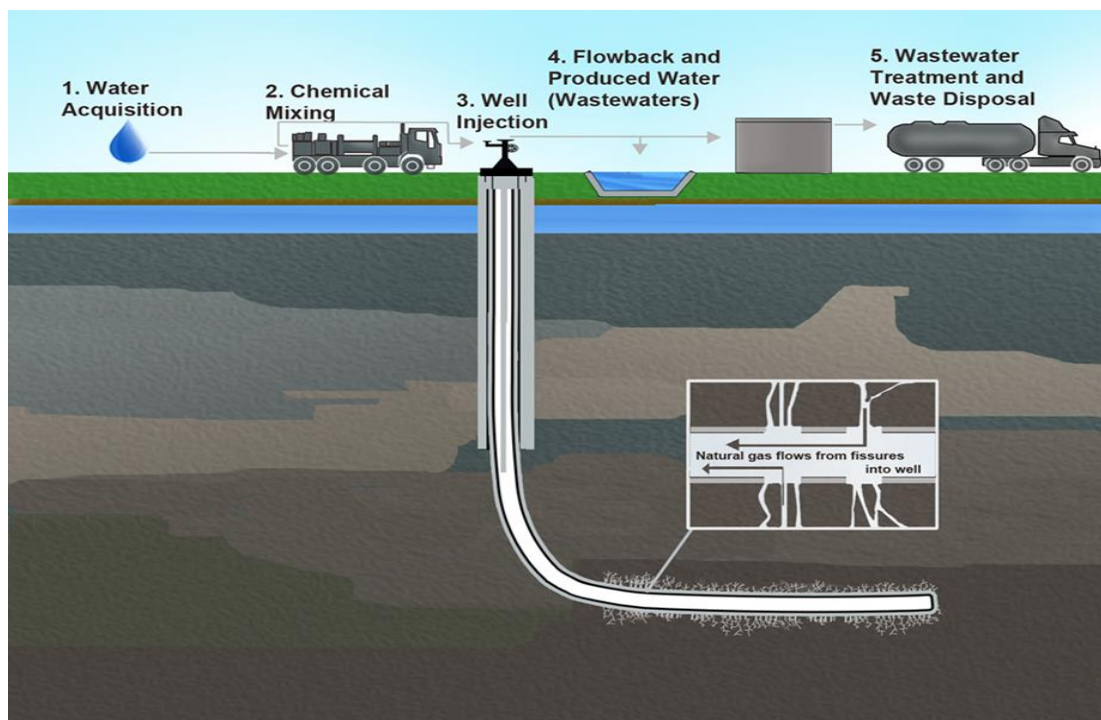


**Figure 2.4:** Illustration of fracturing water life cycle (EPA 2011)

Therefore it is generally known that the scale of water used during the development of a single well exceeds the scale of water use during the drilling of conventional gas

wells. A critical look at the potential for interaction between hydraulic fracturing and water resources reveals five stages that form the hydraulic fracturing water cycle.

- Water Sourcing
- Chemical Addition
- Flowback and Produced Water
- Treatment and Disposal

At each individual stage of the hydraulic fracturing water cycle, there are potential risks to water resource that have to be identified in a UK context. Water sourcing refers to the acquisition of water for fracturing purposes and the review will aim to find within a UK context the possible scenario leading to risk implication on UK water resources. Chemical addition describes the preparation of fracturing fluid a term used for stimulating the wells. The likelihood of risk to water resources at the well injection stage will be considered as well as the risk from flowback and produced water, the wastewater fractions that return during the life time of a well. Finally, risk at treatment and disposal will help provide conclusions to the risk evaluation.

### **2.2.2 Water Sourcing Impact**

The Environment Agency (EA) is charged with the responsibility of managing water resources, and in March 2009, published a water resources strategy for England and Wales. It reported that water demand is likely to increase in the future, as more homes are built, and drier weather, brought about by climate change, could lead to more water being used for irrigation consequently lowering water availability (Environment Agency 2009b). The severe drought of 2011 and early 2012 reminded us that the UK's water resources were vulnerable particularly for ground water in the UK in much of the Midlands and South of England (Figure 2.5). Water sourcing refers to the acquisition of water for fracturing and drilling and other site related purposes. To aid the risk assessment, it is necessary to start with the generic manufacturing/industry question, "Exactly how much is needed".

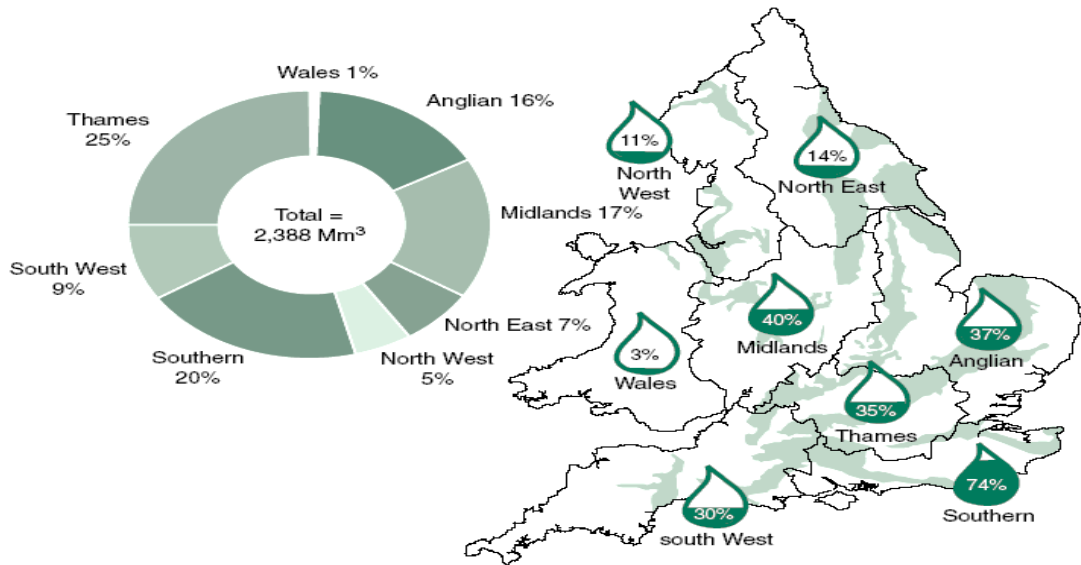


**Figure 2.5:** Underground, Under Threat: The State of Ground Water in England and Wales" retrieved from (Environment Agency 2006)

Due to the infancy of shale gas exploration in the UK, not much data or peer reviewed publications exist that characterize the amounts and sources of water currently in use for hydraulic fracturing operations, including recycled water. The Tyndall centre (Wood et al. 2011) reported that for shale gas to make a meaningful contribution, an estimated 9 billion cubic meter/year is require for 20 years, it further estimated that a total water consumption of 0.027-0.113 megalitres would be required to sustain this figure. Averaged over the 20 year period, this is equivalent to an annual water demand of 1,300-5,600megalitres. Annual abstraction by industry (excluding electricity generation) in England and Wales is some 905,000megalitres/year as can be deduced from Figure 2.6.

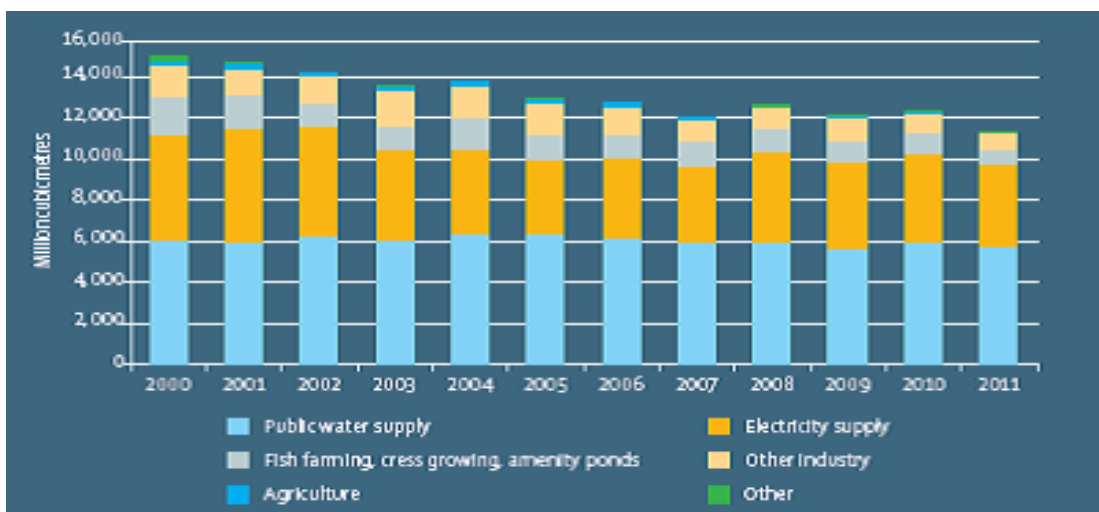


**Figure 2.6:** Abstractions from non-tidal surface water and groundwater by use, England and Wales, 2000-2011 (Moore *et al.* 2014)

As such, development of shale reserves at levels sufficient to deliver gas at a level equivalent to only 10% of UK gas consumption would increase industrial water abstraction across England and Wales by up to 0.6%. Perhaps the best estimate of exactly how much water is required comes from the Institute of Directors (IOD) report of May 2013 and summarised in Table 2.1 below. The report suggests that to meet less than half of the UK’s gas demand, we would need about 5.4 million m<sup>3</sup> of water per annum and generate 1.6 million m<sup>3</sup> of waste fluids, suggesting a yearly 10.8 million m<sup>3</sup> of water and 3.2 million m<sup>3</sup> of wastewater to achieve full demand. Putting this in prospective, to extract just 10% of the available UK shale gas in-place resource estimates, would require water equal to the annual water consumption of 12.4 million UK household.

**Table 2.1:** IOD’s Estimate of Water Use and Flowback water (IOD 2013)

	Water Use	Amount	Comments
Estimates for 10 pad with 40 wells (Larger gas production development)	Water Use for Fracturing	544,000 m <sup>3</sup>	Will be heavily concentrated in early years
	Flowback Water	163,200 m <sup>3</sup>	Will be heavily concentrated in early years
Estimates for 10 pad with 10 wells (smaller gas production development)	Water Use for Fracturing	136,000 m <sup>3</sup>	Will be heavily concentrated in early years
	Flowback Water	40,800 m <sup>3</sup>	Will be heavily concentrated in early years

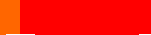
Then the question arises “Where do we source this water from?” Cuadrilla published reports suggesting that for the fractured gas wells at the Preese Hall Cuadrilla site; all waters were sourced from mains serviced by United Utility. The Utility firm have stated a majority of their water supplied is sourced from rivers and reservoirs with a minimal supply sourced from groundwater (figure 2.5). Hence, with regards to water sourcing, the impacts are clear;

1. Possible strain on surface water and ground water resource resulting in the lowering of available water resource. Although, data from the Environment

Agency report (Environment Agency 2006) have shown a minimal reliance on ground water resource around prospective formations within the north central areas of the UK, surface water abstraction data (Figure 2.6) from the Institute of Directors report (IOD 2013) reveal that over 40% of abstracted water resources are used as public water supply. Hence, although the risk is arguably reduced the impact is substantially high as depicted in Table 2.2.

2. Lowering of the water table and the adverse effects on water quality. One of the consequences of excessive abstraction of large volumes of ground water is the exposure of naturally occurring minerals in the aquifer to the oxic environment resulting in chemical changes that affect mineral solubility, causing chemical contamination of the water by encouraging bacterial growth, which causes taste and odour problems. This would suggest a significantly high likelihood of risk arising as depicted in Table 2.2.

**Table 2.2:** Identified Risk Impacts from Water Sourcing and the Probability of Occurrence

Identified Risk	Risk Probability				
Strain on ground and surface water Abstraction					
	<b>Very Unlikely</b>	<b>Unlikely</b>	<b>Probable</b>	<b>Likely</b>	<b>Very Likely</b>
					
Lowering of the water Table and the adverse effects on water quality					
	<b>Very Unlikely</b>	<b>Unlikely</b>	<b>Probable</b>	<b>Likely</b>	<b>Very Likely</b>
					

### 2.2.3 Chemical Additives

Water supplied to site is mixed with chemicals that serve a number of functions down the fractured well. This mixture of water and chemicals serve two main purposes, the creation of fractures and lastly as a carrier of proppants and chemicals use to achieve several functions during well simulation. Chemicals are added to the fluid to optimize the performance of the fluid. Very little chemical is required, usually between 1 and 1.5% of the fluid volume however, considering the annual 5million m<sup>3</sup> of water used, an equivalent annual chemical use of 75000m<sup>3</sup> is expected. One major concern is that fracturing fluids contain numerous chemicals that could harm human health and the environment, especially when the likelihood of migration to drinking water supplies is considered. A US. Congressional hearing reported that between 2005 and 2009, oil and gas service companies used hydraulic fracturing products containing 29 chemicals that were;

1. Known or possible human carcinogens
2. Regulated under the Safe Drinking Water Act for their risks to human health
3. Listed as hazardous air pollutants under the Clean Air Act.

These 29 chemicals were components of more than 650 different products used during hydraulic fracturing. Concerns have also been raised on the ultimate outcome of chemicals that are recovered and disposed of as wastewater. A 2011 report in the New York Times raised questions about the safety of surface water discharge and the ability of wastewater treatment facilities to process wastewater from natural gas drilling operations (Urbina 2011). Perhaps the most glaring example of the impact of chemical use on water resources was reported in April 2011, when bad weather and mechanical faults during a routine fracturing operation caused a leak at the Atgas 2H well in rural Leroy Township, about 175 miles northwest of Philadelphia. This incident released thousands of gallons of chemical laced and highly saline water from the drill site toward a tributary of a popular trout-fishing stream and forced seven families nearby to temporarily evacuate their homes (McGraw 2011). In the UK, the drill operator at the Bowland formation, released an itemized list (Table 2.3) of additives used in its 6 stage fracturing exercise at the Preese Hall site in Lancashire (Cuadrilla Resources 2012). This investigative review will be limited to these listed additives, their compounds and the likely by-products formed during use. By-product formation is not

uncommon in water and wastewater works. The formation of carcinogenic disinfection by-products (DBPs) such as trihalomethanes (THMs) and haloacetic acids (HAAs) is well known in the water and wastewater treatment industry when disinfection with CL2 is performed.

Despite the numerous chemical combinations available to a drill operator in the UK, the uses of these chemicals are guided by regulatory laws. The Chemicals Hazard Information and Packaging for Supply Regulations 2002 (CHIP3) is the regulatory legislation covering Great Britain which implements several EU Directives, such as the Dangerous Substances Directive, the Dangerous Preparations Directive and the Safety Data Sheets Directive (SDS). Safety Data Sheets also called material safety data sheets (MSDS) are one of the key tools in hazard communication. Perhaps the most applicable regulation to chemical disclosure for shale gas development is the Registration, Evaluation, Authorization and restriction of Chemicals regulation (REACH), passed into UK law on 1st June 2007.

**Table 2.3:** Disclosed Chemicals Used at Preese Hall Site.

<b>Common Name</b>	<b>Supplier Chemical name</b>	<b>Purpose</b>	<b>Ingredients listed on MSDS</b>	<b>Total Volume Injected</b>
Fresh Water	United Utilities	Carry sand, Open Fracture	Nil	100%
Congleton Sand	Sibelco UK	Prop open Fracture	Nil	100%
Chelford Sand	Sibelco UK	Prop open Fracture	Nil	100%
Friction Reducer	CESI Chemical	Reduce pressure required to pump down pipe	Polyacrylamide emulsion in hydrocarbon oil	90%
Chem Tracer	Spectrachem	Identify Frac water in Flowback	Water and Sodium Salt	10%
Hydrochloric Acid (HCl)	Undisclosed	Drilling and simulation	Undisclosed	Undisclosed

Compiled from (Cuadrilla Resources 2012)

The aim of REACH is to ensure that the risks of substances are properly understood and managed appropriately. REACH requires manufacturers or importers of

substances in the EU to register their substances. In addition, this provision requires the preparation of safety data sheets for both substances and mixtures, and it specifically spells out what information needs to be provided on the SDS. This section explores the use of additives in fracturing formations by investigating the list of fracturing additives used at the Preese Hall shale gas site, examining the chemical ingredients of all listed additives and investigates the toxicity of those ingredients. Nevertheless, the identified risk and impact from chemical additives on water resources are highlighted in Table 2.4. However, there is growing recognition that REACH is not the mechanism to address public disclosure concerns regarding the chemical constituents of hydraulic fracturing fluid. The inadequacy of the REACH regulatory policy in the protection of human health and the prevention of environmental hazards has been repeatedly stated since the start of prospecting for shale gas in Europe.

**Table 2.4:** Identified Risk Impacts from Chemical Additives and the Probability of Occurrence

Identified Risk	Risk Probability				
Release to surface and ground water through on-site spills or leaks					
	Very Unlikely	Unlikely	Probable	Likely	Very Likely
Disposal of untreated or improper treatment of returning wastewater.					
	Very Unlikely	Unlikely	Probable	Likely	Very Likely

Brussels law firm Philippe & Partners, concluded that the existing regulatory framework in Europe is adequate for shale gas activities as they currently stand (Philippe & Partners 2011), although there are still limitations with these policies in protecting our fragile ecosystem. It is clear that for the UK, a clearer assessment of the potential risk and impacts would require a thorough review of the current industrial practice and UK regulatory controls. Hence, Section 2.3 of this review documents a thorough investigative review of fracturing additives and UK applications.

## 2.2.4 Flowback and Produced Water Impact

Like every industrial process waste is produced which requires either treatment, recycling or disposal and shale exploration is no different. Wastewater returns throughout the life span of a well, representing 40% to 70% of the initial fluid injected into the well. The distinction between flowback and produced water borders around the time of return. Negative pressure following a lowering of initial injection pressure results in the return of fracturing fluid to the surface. This return flow is mostly designated flowback. Produced water on the other hand, refers to fluid returned to the surface after the well has been placed into production. Flowback from the wells are usually black briny fluids with high suspended materials and in some cases in the United States, have recorded residual hydrocarbon, bacterial contents and colloidal materials. These characteristics may vary from site to site and therefore it is essential to conduct onsite specific investigations on the characteristics of effluent flowback quality. This is so far the biggest challenge for a shale gas ready UK and could not have been better stated by the Royal Society and the Royal Academy of Engineers *“Produced water will continue to return to the surface over the well’s lifetime... VERY LITTLE is currently known about the properties of UK shales to explain what fraction of fracture fluid will return as flow back water, as well as the composition of formation waters and produced water”* (The Royal Society 2012). However, based on an analogy with the US, the constituents of flowback and produced water can be seen as illustrated in Figure 2.7 below.

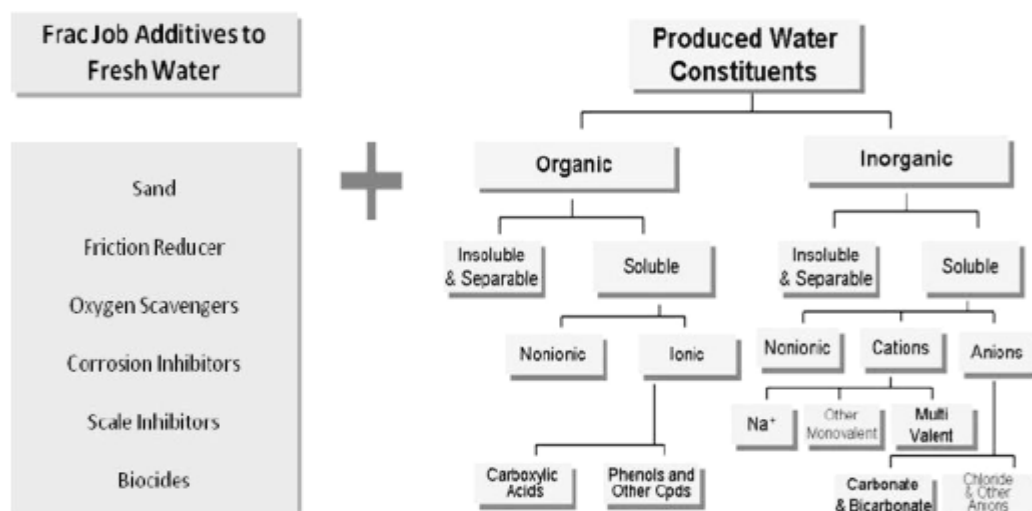


**Figure 2.7:** Wastewater Constituents from Shale Gas Exploration (The Royal Society 2012)

Flowback from fractured wells in the US show compositions of fractured fluid chemicals, shale mineralogical compositions and dissolved solids from the reservoir. Returning wastewater from shale gas developments are known to show footprints of shale mineralogical compositions leached during the actions of hydraulic fracturing. There is an extensive body of research in support of this dispersion and migration of elements from weathering shale into the environment. One feature that enhances the potential for dispersion or migration of shale minerals is its ability to undergo chemical weathering when exposed to air or moisture. Jeng (1991), researched extensively on this phenomena while studying the acidity of Norwegian alum shale. The study reported on the vulnerability of black shale to chemical weathering due to its sulphide and organic material content. The study also reported that one dominant mechanism of dispersion is surface streams or underground water. Research by Puura *et al.* (1999) further pointed out that mining activities also contributed to the dispersion of elements from geological materials.

### **2.3 Review of Fracturing Additive Use in the UK**

The objective of identifying compositions making up the fracturing fluid is an essential part of the much larger objectives of determining contamination in flowback that limit its reuse options. The intended objectives of reviewing UK fracturing additive use however is to provide information on the following:

- Distinguishing UK industry practice in Chemical use from US practises by identifying contributions from chemical use to indigenous contamination risk
- Providing data necessary for the simulation of fracture fluid for intended laboratory investigation

Contamination, is referred to in this research as “Constituents of concern”. Ideally, these possibly harmful compounds would have been easily investigated if samples of the fracturing fluid are readily attainable from the UK site operators. Unfortunately, access to this fracturing fluid is highly restricted and is considered as trade secrets and as such a desk study approach has been adopted to investigate these chemicals. Although it is expected that some or all of these additives may return in the Flowback, no literature has yet reported or confirmed the presence and concentrations of these recovered additives. A possible hypothesis considered in this research is that these

compounds become decomposed or altered, under conditions expected during gas exploration or during hydraulic fracturing. Acharya et al. (2011) stated *“It is likely that these compounds may get chemically, physically or microbiologically altered or destroyed during the hydro-fracturing process or become lost in the shale formation”* (Acharya et al. 2011). While the experimental analysis designed in this research should prove this hypothesis, this study seeks to understand the risks associated if in fact the hypothesis is confirmed.

Therefore, the study begins by assuming the hypothesis is proven. If in fact fracturing additives contribute to contaminants found in Flowback, it is necessary to investigate the consequences of human and environmental exposure to these chemicals.

The study has adopted the following methodology.

1. Investigate the use of additives in fracturing formations by obtaining and compiling the list of fracturing additives used at the Bowland shale gas drill site.
2. Examine the chemical ingredients of the listed additives compiled above.
  - Obtain the material safety data sheets (MSDS) or safety data sheets (SDS) for the listed chemicals for a full description of chemical ingredients
  - Investigate the toxicity of identified ingredients and evaluate the impact of these identified contaminants and by-product compounds to human health and the environment.

### **2.3.1 Applications and Regulations**

There have been several advancements in fracturing simulation in the last decade, resulting in the development of fracturing additives that ultimately improve permeability and allows the extraction of substantial gas quantities from shale formations. However, there are several roles additives play during a completion process that define every successful well completion. The fracturing fluids employed consist largely of water and sand but in addition, a selection of chemical additives are introduced specifically to achieve predetermined objectives. Table 2.5 shows a list of common additives and their general fracturing engineering purposes. The number of

chemical additives used in a typical fracture treatment varies depending on the conditions of the specific well fractured. The drill operator then determines the specific conditions required before deciding on the appropriate additive to achieve the engineering purpose. It is therefore not unusual for some fracturing exercises to omit some compound categories if their properties are not required for the specific application.

**Table 2.5:** Compiled Fracturing Additives and their Applications

<b>Additive Type</b>	<b>Common Chemical Additives Used</b>	<b>Engineering Purpose in Fracturing</b>
<b>Diluted Acid (15%)</b>	1). Hydrochloric Acid	Help dissolve minerals and initiate cracks in the rock
<b>Biocide</b>	1). Glutaraldehyde 2). Quaternary Ammonium-Chloride	Eliminates bacteria in the water that produce corrosive by-products
<b>Breaker</b>	1). Ammonium Persulfate 2). Sodium Chloride 3). Magnesium Peroxide 4). Calcium Chloride	Allows a delayed break down of the gel polymer chains
<b>Corrosion Inhibitor</b>	1). Isopropanol 2). Methanol 3). Formic Acid 4). Acetaldehyde	Prevents the corrosion of the pipe
<b>Cross linker</b>	1). Ethylene Glycol 2). Borate Salts 3). Methanol 4). Petroleum Distillate	Maintains fluid viscosity as temperature increases
<b>Friction Reducer</b>	1). Polyacrylamide 2). Petroleum Distillate 3). Ethylene Glycol 4). Hydro treated Light-Petroleum Distillate	Minimizes friction between the fluid and the pipe
<b>Gel</b>	1). Polysaccharide Blend 2). Guar Gum 3). Methanol	Thickens the water in order to suspend the sand
<b>Iron Control</b>	1). Citric Acid 2). Acetic Acid 3). Thioglycolic Acid 4). Sodium Erythorbate	Prevents precipitation of metal oxides
<b>KCl</b>	1). Potassium chloride	Creates a brine carrier fluid

<b>Additive Type</b>	<b>Common Chemical Additives Used</b>	<b>Engineering Purpose in Fracturing</b>
<b>Oxygen Scavenger</b>	1). Ammonium Bisulphate	Removes oxygen from the water to protect the pipe from corrosion
<b>pH Adjusting Agent</b>	1). Isopropanol 2). Ethylene Glycol 3). Sodium Hydroxide 4). Acetic Acid	Maintains the effectiveness of other components, such as cross linkers
<b>Scale Inhibitor</b>	1). Copolymer of Acrylamide and Sodium Acrylate 2). Sodium Polycarboxylate 3). Phosphoric Acid Salt	Prevents scale deposits in the pipe
<b>Surfactant</b>	1). Lauryl Sulfate 2). Ethanol 3). Naphthalene 4). Methanol 5). Isopropyl Alcohol	Used to increase the viscosity of the fracture fluid
<b>Non-Emulsifier</b>	1). Lauryl Sulfate 2). Isopropanol 3). Ethylene Glycol	Used to prevent the formation of emulsions in the fracture fluid also acts as a product stabilizer and a winterizing agent.
<b>Tracers</b>	1). Deuterium oxide	To identify and trace the Frac water in flowback

There is growing recognition that REACH is not the mechanism to address public disclosure concerns regarding the chemical constituents of hydraulic fracturing fluid. In the US, a means for public disclosure of chemicals used by drilling operators is made possible via the FracFocus website. Subsequently, representatives of the EU institutions are receptive to a similar style public disclosure avenue and the consensus is building around a FracFocus-like reporting. This was eloquently stated by the International organization of oil and gas producers (OGP) in their April 2012 report *“Chemical substances are already registered and approved under the REACH Regulation. However, OGP supports disclosure of the contents of fracturing fluids to the public, for example, an initiative such as “Frac Focus” specifically for EU citizens”* (OGP 2012).

The inadequacy of the REACH regulatory policy in the protection of human health and the prevention of environmental hazards has been repeatedly pointed out since the

start of prospecting for shale gas in Europe. The most supportive proof of this argument is the confidentiality provision within the REACH regulation. Some industrial players have raised the concern that inclusion of the full registration number in the SDS will reveal information about their supply chains and could even allow their customers to bypass them in the supply chain. Hence the confidentiality provision clause, allows a distributor or downstream user to omit the part of the registration number referring to the individual registrant of a joint submission.

Another aspect of the confidentiality clause excuses the provision of the full chemical identity of dangerous substances within a preparation. The regulations require the disclosure of toxicology information and ecological information in the SDS or MSDS. This should reveal the full composition of the commercial formulations and aid in risk assessment and prevention. However, this clause allows the use of confidential names for certain substances in dangerous preparations. Therefore, since prospecting for shale gas became a reality in European nations, there have been rising public concerns that chemicals used in hydraulic fracturing are not properly registered for use in REACH, under the guise of the confidentiality provisional clause. This is not peculiar to the EU. Chemical disclosure, though enforced in the US has come under huge criticism lately. (2012) reported disclosure laws in 17 states of the United States and uncovered flaws in the adherence to and interpretations of these regulations (Moulton and Plagakis 2012). The most prominent being an exemption that allows companies to withhold disclosure of chemical used on the grounds of “confidential business information”, a similar trend already discussed above in the UK scenario. In the United State, this loophole allows companies to conceal specific information on ingredients in their products by claiming that disclosure would undermine their business model or give competitors an advantage. If water infrastructures are to be effectively protected, full disclosure is necessary. The water and wastewater industries as a matter of necessity need to know full details of chemical compositions used during production or exploration activities. It is only then that water fit for municipal and industrial consumption can be supplied.

### **2.3.2 Disclosed Fracturing Additives**

Here in the UK, the drill operator at the Bowland formation, released an itemized list of additives used in its 6 stage fracturing exercise at the Preese Hall site in Lancashire (Cuadrilla Resources 2012). Table 2.5 contains a detailed summary of the additives used during exploratory drilling works. The scope of this research will be limited to these listed additives, their compounds and likely by-products formed during use. To effectively investigate the possibility of harm to humans and the ecosystem, it is important to consider the possible formation of by-products.

### **2.3.3 Examining Safety Records for Disclosed Additives**

A full disclosure of chemicals and mixtures should be documented in the SDS according to the REACH regulation. This regulatory provision allows the ease in assessing the toxicity of disclosed additives listed in Table 2.5. An evaluation of the Material safety data sheets or safety data sheets for the listed additives is examined for hazards to human health and the environment. Amongst the additives disclosed, is a blend of chemicals used as a friction reducer and produced by CESI Chemicals under the chemical name 'FR-40'. Figures from the drilling operator at the Bowland gas wells shows 3,700 liters (813 gallons) of FR-40, a friction reducer was used at the Preese Hall site in Lancashire. FR-40 is classed under US Environment Agency regulations as an "immediate (acute) health hazard" and a "delayed (chronic) health hazard" (Lieber 1991). It is an irritant and can cause defatting or dermatitis of the skin. In September, the European Chemicals Agency, reported that the use of this friction reducer for fracking could technically be illegal, as it has not been registered, authorized or passed safety assessments (R. Gallagher, 2011). Another additive reported by the exploratory drill operator is a chemical tracer supplied by Spectra-chem with the chemical name "Chem Tracer". Further examination on the manufacturers catalog reveal that tracer combinations utilized could range from a minimum of 2 different compounds and any selection from a maximum of 22 possible compounds. The site operator used a total of 4,252 grams of this additive in its six stage fracturing exercise. Although concentrations appear minute, chemical additions of any magnitude could result in considerable changes in the quality and reuse option. Hence, a study of these additives was conducted.

### **2.3.4 Friction Reducers FR-40**

FR-40 is the supplier's chemical name given to a specially prepared blend of fracturing additive used at the Bowland shale gas site. The MSDS for this listed additive reveal very little detail on the ingredients (probably taking advantage of the confidentiality provision) when thoroughly investigated. A summary of the finding from the MSDS is outlined as follows;

- Mild irritation, defatting and dermatitis of the skin were the only human health hazards recorded.
- No information on environmental hazard.
- No values were reported for the Lethal dose indicators, LD<sub>50</sub> (which measures the short term poisoning potential of a material) representing the amount of a material, given all at once, which causes the death of 50% of a group of test animals.
- Stated no possibility of hazardous polymerization but affirmed hazardous decomposition producing oxides of Carbon and oxides of Nitrogen.
- Toxicological information reported acute effects to both eyes and skin, with no toxicity concerns if inhaled and no ingestion hazards.
- None of the compositional ingredients was considered carcinogenic.

However, following a consultative hearing by the DECC, the firm revealed its main composition as "polyacrylamide emulsion in hydrocarbon oil". This blend of chemical is used to reduce friction between the water and the pipe when pumping into the well. Polyacrylamides are not toxic and in fact are environmentally friendly compounds when in their polymerized form. However, the de-polymerizations of polyacrylamide have been known to occur under certain environmental condition. Hence, conditions resulting into the de-polymerization or degradation of polyacrylamide were investigated.

### ***2.3.4.1 De-polymerization and degradation of Polyacrylamide***

Polymerization is a process of reacting monomer molecules together in a chemical reaction to form polymer chains or three dimensional networks. Polymerization that is not sufficiently moderated and proceeds at a fast rate can be very hazardous. This phenomenon is known as hazardous polymerization and can cause fires and explosions. Therefore, the MSDS or SDS should provide information on hazardous polymerization or decomposition of a chemical or mixture if the likely hood of occurrence is high. There are concerns that polyacrylamide may depolymerize to form acrylamide, a lethal neurotoxin found to be carcinogenic, easily penetrating the skin and inhalable, and other research findings that suggest the environmental degradation of Polyacrylamides to form acrylamide. Woodrow *et al.* (2008) provided data that suggest that commercially available polyacrylamide contains minute residual amounts of acrylamide remaining from its production, usually less than 0.05% w/w (Woodrow et al. 2008). Woodrow and his team were concerned that the use of Polyacrylamide has a potential of contributing acrylamide monomer to aquifers, and considering that some seepage was inevitable, these monomers could migrate to receiving surface waters. Hence, a laboratory investigation was conducted to study the efficacy and stability of commercial Polyacrylamide as a flocculating agent when applied to earthen irrigation canals and ditches. Their studies were to find and characterize the environmental conditions that might lead to acrylamide release. Results showed residual monomer in polyacrylamide can contribute acrylamide to irrigation water, but concentrations would remain below detectable limits of 0.5 ppb.

Smith *et al.* (1996) also investigated the effect of environmental conditions on polyacrylamide, and their results showed that degradation of polyacrylamide under certain conditions does in fact cause the release of acrylamide (Smith et al. 1996). They investigated under agricultural settings, the effects of various environmental conditions such as pH, light exposure and temperature on a polyacrylamide thickening agent formulated with and without an herbicide. Their finds suggested that under artificial environmental conditions, polyacrylamides may degrade to acrylamide and thus creates a potential environmental/health hazard (i.e., contamination of surface water and/or ground water systems) (Smith et al. 1996).

### ***2.3.4.2 Stability and Reactivity of Polyacrylamides***

In dilute aqueous solution, such as is commonly used for enhanced oil recovery applications, polyacrylamide polymers are susceptible to chemical, thermal, and mechanical degradation. Chemical degradation occurs when the labile amine moiety hydrolyzes at elevated temperature or pH, resulting in the evolution of ammonia and a remaining carboxyl group as reported by (Leung *et al.* 1987) Thermal degradation of the vinyl backbone can occur through several possible radical mechanisms, including the auto-oxidation of small amounts of iron and reactions between oxygen and residual impurities from polymerization at elevated temperature as reported by (Audibert *et al.* 1992). This is also reiterated in the MSDS, thermal decomposition stated as may result in the production of carbon oxides and nitrogen oxides (NO<sub>x</sub>). Mechanical degradation can also be an issue at the high shear rates experienced in the near-wellbore region. Therefore drawbacks of this product are a high temperature sensitivity, low salinity tolerance, poor shear stability and poor dissolution properties, all suggesting the possible de-polymerization of polyacrylamide. Unfortunately, the MSDS for the listed FR-40 fails to provide this information and generally fails to mention the presence of this compound entirely.

Another detrimental effect of the use of friction reducers is the need to increase the quantity of this additive during fracturing. As mentioned earlier, adding of friction reducers allows fracturing fluids and proppant to be pumped to the target zone at a higher rate and reduced pressure than if water alone were used. However, friction reducers' interactions with the base fluid vary depending on factors like the TDS concentrations and hardness. Reusing flowbacks with high levels of total dissolved solids (TDS) can lead to adverse interactions between the friction reducer and the base fluid. The adverse interactions result in elevated treating pressures, and this is often overcome by introducing more of the friction reducer into the mixture, consequently leading to higher chemical costs for the treatment (Bull *et al.* 1984, Ferguson and Johnson 2009). Because synthetic polymers are known to not readily breakdown in the environment, most polyacrylamides used in fracture simulation are pumped with liquid emulsion, making them easy to pump and disperse and able to hydrate in water (Kaaufman *et al.* 2008).

### ***2.3.4.3 Health and Environmental Risk***

Several studies have been reported on the hazardous potential of polyacrylamide and its monomers, with the main concern centered on its depolymerized monomer, acrylamide. Many reported the lethal neurotoxicity of depolymerized polyacrylamide with several epidemiological studies documenting the effect of acrylamide in human, particularly reproductive toxicity, genotoxicity/clastogenicity, and carcinogenicity. The earliest carcinogenicity studies relied on animal testing. Toxicological studies reported acrylamide inducing an increased incidence of cancers of the brain and central nervous system, the thyroid and other endocrine glands, and reproductive organs of mice (Bull et al. 1984). M. Friedman reviewed current data on the toxicological study of acrylamide covering exposure from the environment and diet and reported the carcinogenic nature of acrylamide (Friedman 2003). The toxicological effect of acrylamide on the reproductive health was also investigated using male Sprague–Dawley rats, by studying the Leydig cells in their testes. The research results concluded that acrylamide toxicity appears to increase Leydig cell death and perturb gene expression level in the rat testis, contributing to sperm defects and various abnormalities (Yanga *et al.* 2005). Although, these were recorded potential human health risks on the basis of only animal studies, there are strong validated results to suggest a similar fate in humans.

### ***2.3.4.4 Human Epidemiological Studies***

A workplace survey at a polyacrylamide manufacturing plant identified 5 out of 71 workers with clinical signs of peripheral neuropathy, with one worker also suffering cerebellar and ocular impairment. Recovery was reported to be incomplete even after 5 years without exposure to acrylamide. Sixty-three of the remaining workers were evaluated for neuro-pathological effects. At the factory there were no unexposed individuals, no engineering measures to reduce exposure and no respiratory protection. Some protective clothing was available but its efficacy was unclear. Twenty two workers were exposed to airborne levels of  $<0.3 \text{ mg/m}^3$ , and 41 exposed to levels above this with four workers apparently subjected to levels of about  $0.75 \text{ mg/m}^3$ . A higher prevalence of effects was reported in those exposed to  $>0.3 \text{ mg/m}^3$ . Symptoms include weakness, effects on sensation, skin peeling, sweating and changes in skin pigmentation (Myers and Macun 1991).

### ***2.3.4.5 Routes of Exposure***

Studies on the route of exposure revealed sources such as acrylamide entrapped in polyacrylamide, depolymerized polyacrylamide in the soil and in food packaging, microbial enzyme catalyzed transformation of acrylonitrile to acrylamide, and tobacco smoke. Chronic environmental studies carried out in polyacrylamide production plants over a period of 5 years indicated that workers were being exposed to polymer dust through inhalation. Average airborne concentrations of the polymer were reported to be 1 mg/m<sup>3</sup>. Approximately 5 mg/day of the dust, with a diameter greater than 50 pm per particle, had the potential to be trapped in the upper respiratory passages and swallowed (Lieber 1991). There are also incidences of indirect exposure via the environment. A potential source of public exposure is through drinking water. A World Health Organization (WHO) report stated that the most important source of drinking water contamination by acrylamide is the use of polyacrylamide flocculants containing residual levels of acrylamide monomer (WHO 2011). For drinking water treatment by flocculation, a monomer level of <0.05% in polyacrylamide dosed at 1 ppm (1 mg/L) is required. It results in a maximal possible concentration of acrylamide at 0.5 µg/L in drinking water. Assuming 2L consumption per day for a male or female of 70kg, it is estimated that maximum exposure would be  $1.42 \times 10^{-5}$  mg/kg bw/day.

Based on its toxicity and human health consideration, the Australian Drinking Water Guideline (NHMRC 1996) stipulated that the concentration of acrylamide in drinking water should not exceed 0.2 µg/L. In the UK, the current limit for acrylamide concentrations in drinking water is based on the product specification for polyacrylamide used in the treatment process, and is 0.1 µg/l (EA 2004). Acrylamide was detected at levels of <5 µg/L in both river water and tap water in an area where polyacrylamides were used in the treatment of potable water. Samples from public drinking water supply wells in West Virginia, USA, contained 0.024–0.041 µg of acrylamide per liter. In one study in the United Kingdom, tap water levels in the low µg/liter range were reported (Brown and Rhead 1979).

In summary, the investigation of this fracturing additive suggests a high possibility of contamination from the use of polyacrylamide concentration in the additive. Polyacrylamides are not toxic, but un-polymerized acrylamide can be present in the polymerized acrylamide and based on well conditions during hydraulic fracturing, the

decomposition of polyacrylamide is a possibility that cannot be ruled out. The agency's December Northwest monitoring report included the analysis of acrylamide as a possible breakdown product from polyacrylamide use as fracking fluid. In the reported result, representative sampling done on 17th August 2011 representing 110 days from well fracturing, recorded acrylamide concentration of 0.05µg/L. No results of analysis were reported for all prior sampling dates representing day 7, 14, 20, 47, and 95. Hence, concentrations of acrylamide in early flowback from shale gas fractured wells in the UK are not known till date.

### **2.3.5 Acids and Tracers**

The use of hydrochloric acid shale gas exploration has been downplayed by several drilling firms until disclosure laws required that firms ensure chemical disclosure. The acid was listed as used under 2 stages, drilling and well development. It was noted primarily to help dissolve minerals and initiate cracks in the rock however, it has also been used to clear the channels from the borehole into the shale. Surprisingly, its use was never disclosed by Cuadrilla at the Preese Hall UK site, until two occasions in 2011, during a consultation meeting at Balcombe in West Sussex and in a written defence produced by the firm in response to a parliamentary inquest requiring the firm to provide written evidence into their operations in the UK (Cuadrilla Resources 2011). In the written response, the firm reported between 11,000L and 20,000L of HCl acid were injected into the Lancashire formation (Bowens 2014). Cuadrilla claims the acid use is naturally found in the human stomachs, however experts suggest that gastric acid or acid found in the stomach is a dilute concentration of the acid, usually 0.1M and 0.01M concentration in comparison to 12.08M Concentrated HCl used at the Lancashire site. A critical look at the facts suggest that since the acid is added as an additive (smaller volume in comparison to the entire fracturing fluid), the resulting concentration of HCl acid is much lower than a 12.08M concentration suggested by opponents. It was vital for this study however to arrive at an estimated concentration of HCl acid used in the stage fracture operation at the Preese Hall site and therefore the following data was used.

- Data reported by Cuadrilla suggests 99.75% of fracturing fluid make-up contained water and sand, 0.125% Hydrochloric acid (HCl) and 0.075% represents Polyacrylamide oil based Friction Reducer (Cuadrilla Resources

2011, North Meols News 2011).

- A total 8399.2m<sup>3</sup> (8,399,200Ltrs) of fresh water was reported to have been used for all six stages (Cuadrilla Resources 2012).
- Fracture fluid make-up contained a percentage volume of 99.75% of water and sand. From the total water volume used at the Preese Hall site, this represents 8378.2m<sup>3</sup> (8378200 litres) of fresh water.
- Fracture fluid make-up contained a percentage volume of 0.125% Hydrochloric acid (E507 food grade). From the total water volume used at the Preese Hall site, represents 10.499m<sup>3</sup> (10499 litres) of HCl acid.
- Acid specification for E507 (37%) concentrated HCl acid has a stated concentration of 12.08M (FSA 2012).

Assuming other fluids contribute negligible effect in diluting concentrated acid, a 10,499 litre 12.08M concentration of HCl acid, diluted in 8,378,200 litres will result in an empirical concentration of 0.02M of HCl acid and quite rightly affirms Cuadrilla's claim of dilute concentration similar to stomach acids. This computation gives an approximate acid concentration in the fractured fluid used at the Lancashire site. Acid use in oil and water wells is not uncommon and has been in use for several years. A clearer picture emerges of certain reactions within the formation, acid interactions with clay minerals in shale will result in the acid base neutralisation reaction promoted by carbonate minerals in the shale. The resultant effect on PTE release is however unknown at this stage, as this would depend on a number of factors including;

- Specific PTE concerned
- Mobility of PTE concerned (easy of degradation of the host mineral phase and release of the PTE)
- Other compositions within the formation inhibiting or catalysing the release of the PTE concerned
- Other factors affecting the rates of the reactions within the formation.

Tracers are employed by drilling operators to initially monitor the movement of frac

water in flowback but of recent are used during hydraulic fracturing of a producing formation to monitor changes in activity that might suggest movement of fracturing fluid into groundwater and the environment. Successful fracture stimulation requires maximum controlled placement of fracture proppant in the reservoir zone, while avoiding fracture development into water producing strata and adjacent non-productive zones of a formation. The injection of radioactive tracers, along with the other substances in hydraulic fracturing fluid, is often used to determine the injection profile and location of fractures created by hydraulic fracturing. The US. Nuclear Regulatory Commission (NRC), lists some of the most commonly used tracers and these include; Antimony-124, Bromine-82, Iodine-125, Iodine-131, Iridium-192, and Scandium-46 (U.S. Nuclear Regulatory Commission 2000). These tracers are also used extensively because they are easily identified and measured. The engineering functionality required of an ideal tracer is its ease in detection, ability to flow within the water flow, chemically immiscibility, unreactiveness with passing substrates, and should not alter the properties of the water. It is therefore assumed in this study that tracers have negligible chemical influence on the fracture fluid. Nevertheless, because of its potential risk impact at larger concentrations to water resource, this review has investigated the spectrachem's Chem tracer listed by Cuadrilla.

## **2.4 Black shale contamination**

This section is aimed at illustrating the possible occurrence of contamination associated with black shale. One of the earliest studies providing evidence of the potential widespread contamination from black shale was by Lee *et al.* (1998). This study showed that black shale could have a viable influence on the geochemistry in an area. Lee *et al.* (1998), showed how the shale rich bedrock of the Okchon Zone in Korea, influenced the geochemistry of the overlying soil. The study showed the mobility of potentially toxic elements such as Cd was significantly absorbed by plants. Aside enrichments in soil, the study showed elements such as As, Cd, Cu, Mo, U and Zn to be readily mobile thus increasing their bioavailability. Loukola-Ruskeeniemi *et al.* (1998), also studied the influence of the bedrock geochemistry on sediment, lakes and stream in Eastern Finland. The study showed that Ni, Zn and Cd were significantly enriched where the underlying bedrock was predominantly black shale. The study concluded that glacial melting and wave actions had resulted in the weathering of

substantial black shale bedrock over thousands of years and this had impacted sediments and sub-lake sediments in the area. The resulting effect was the occurrence of acidic sediments (pH 3.8) and the abundance of trace metals. In a popular study by Peng *et al.* (2004), the release of 25 different elements from weathering black shales in western China was investigated. Sediments and water samples analyzed showed elevated concentrations of Cr, Co, Cu, Pb and Cd, indicating severe incidences of contamination by heavy metals. Although the study had provided no indication of background data, other possible explanations to the occurrence of contamination were considered unlikely. The study further suggested the releases observed were possible factors behind the high incidence of endemic diseases prevalent in the Western Hunan region of China. In a similar study by Yu *et al.* (2010), weathering intensity studies was used to show that sediments in the Dongping and the Yanxi areas of the South China Hunan province inherited a heterogeneous geochemical character from their parent materials, the lower Cambrian black shales. The study show that the resulting acid sulfate soils, was mostly responsible for the associated environmental and health issues reported in the area. In particular the abundance, distribution, and exposure of Cd and Cu was widely reported. Black shale influences on ground water have also been widely documented. Woo *et al.* (2002), studied groundwater quality in black shale areas in Korea, in attempt to identify if heavy metal enrichments in soil and stream reported in a previous study in the area had any effects on associated groundwater. Although concentrations of investigated heavy metals observed from the study were well within the Korean and US EPA drinking water guideline, it was concluded that the major factor controlling the behaviour of the elements were adsorption to Fe<sup>-</sup> and Mn<sup>-</sup> hydroxides in the ground. Therefore, the depletion of the ground's buffer capacity due to acid drainage, and changes in hydrological and chemical conditions could remobilise adsorbed elements. Several other studies have also shown a link between black shale formations and contaminations observed in surface waters, surface water sediments, soils and crops (Horan *et al.* 1994, Kelley and Taylor 1997, Peng *et al.* 2005, Lavergren *et al.* 2009b, Peng *et al.* 2009b, Yu *et al.* 2014). Most studies have shown the high incidence of heavy metals that occur in trace compositions in the shale matrix and this have been used in all previous studies to assess the mobility of contaminants.

## 2.5 Heavy metals as Indicators for Contaminant Mobility

By nature of compositional matrix, heavy metals are naturally the first observable potential toxicants in black shale. Most studies associated with contamination mobility in shale have studied the mobility of heavy metals because their ability to provide information on the matrix properties of the formation. Most high risk contaminants reported in flowbacks are associated with reported heavy metals or trace element concentrations, for example, the detection of naturally occurring radionuclides materials (NORMs), are discovered in association with trace element compositions like Uranium (U), Strontium (Sr), Radium (Ra) and Vanadium (V) (Lavergren et al. 2009b, Bank *et al.* 2010). On the other hand, high TDS concentrations which are a major concern with flowbacks and produced water are also associated with metal ions like Na, Ca, Mg, K, Fe and Ba (Blauch et al. 2009, Hayes and Severin 2012). Black shale, the source rock for shale gas is known to be enriched in metals, heavy metals, rare earth metals and other trace elements. The release of these potentially toxic trace elements (PTEs) are a function (amongst other factors) of the metal enrichments in the shale matrix (El Kammar and El Kammar 1996, Loukola-Ruskeeniemi et al. 1998, Lavergren et al. 2009b, Bank 2011) but this vary widely by location (Smith and Young 1967, Fisher *et al.* 1998) and therefore serve as a good indicator for contamination mobility. Hence, the quantification of trace element concentration in flowback fluid and their release rates from unweathered shale would provide a useful way of assessing contamination build-up in flowback and consequently the risk contributions of shale gas exploration and development. Monitoring changes in trace element released can therefore indicate or help predict flowback quality over time. Trace element speciation and factors controlling their mobility such as pH, Eh, temperature, surface properties of the solids, abundance and speciation of ligands, ionic composition, presence or absence of dissolved and/or particulate organic matter and biological activity as reported by Jeng (1991) and Plant *et al.* (1996) all play a part in the formation of this relatively new waste. But first, geochemical studies on the parent material can reveal substantial information on the heavy metals risk of shale gas mining operations. Interestingly, a bulk of the processes resulting in flowback generation can be derived from our understanding of acid mine drainage.

## **2.6 Flowback and AMD/ARD Analogy**

Acid production in acid mine drainage may provide a theoretical explanation to the geo-biological processes responsible for flowback formation. First, a few similarities that suggest comparable processes result in both waste formations. Primarily, both processes are influenced by the same rate limiting factors. These primary factors include the presence of water, oxygen, sulphide minerals, ferric iron, bacteria to catalyse oxidation reactions, and heat. All these primary factors are present in the reservoir or induced by the actions of hydraulic fracturing. Therefore, there is no doubt that fluid-rock interaction enhanced by hydraulic fracturing result in the processes that generate flowback from shale gas wells. Secondly, both are influenced by secondary factors that act to either neutralize the acid produced or change the effluent character by adding metals ions mobilized by residual acid. However, while acid mine drainage is known to result from a slow and chemically induced weathering processes, flowback is generated from a rather forcefully induced chemical weathering and in addition, the use of chemical additives. The resulting effect on the drilled reservoir, the organics and inorganics released and consequently the quality of the return flowback is largely unknown.

## **2.7 Microbial Influence on Contaminant Release**

Microbial processes that impact oil production from conventionally developed reservoirs are well documented (Van Hamme *et al.* 2003, Orem *et al.* 2014). In these reservoirs, the stimulation of bacteria may result in detrimental issues such as reservoir fouling, bio-corrosion and product souring (sulphurization). They are understood to contribute to degradation of polymers in HDF fluids, souring, well plugging, corrosion in well conduits and therefore limits gas flow within the well (Murali Mohan *et al.* 2013, Vidic *et al.* 2013, Elliott *et al.* 2014). Microbes however, are intimately involved in metal biogeochemistry with a variety of other processes determining mobility. Microorganisms can mobilize metals through chelation by microbial metabolites such as autotrophic and heterotrophic leaching which can result in volatilization (Gadd 2004). These processes can lead to dissolution of insoluble metal compounds and minerals and even more complex mineral ores and therefore render them bioavailable. Alternatively, immobilization can result from sorption to biomass or exo-polymers (Macaskie and Dean 1989), transport and intracellular sequestration or precipitation as

organic and inorganic compounds (Beveridge and Doyle 1989, Southam 2000). For example, the reduction of higher valency species may effect mobilization like the typical case of Mn(IV) to Mn(II), or immobilization caused by the reduction of Cr(VI) to Cr(III) (Lovley and Coates 1997, McLean *et al.* 2002). Both mobilization and immobilization may even occur simultaneously and the balance between both processes would determine the prevailing effect within the system.

Therefore, there is a substantial knowledge gaps regarding the effect of microbial population in unconventional wells, particularly regarding the mobilization or immobilization of PTEs. It is widely known that dissimilatory sulphate-reducing bacteria (SRB) play an important role in the sulphur cycle and the mineralization of organic matter even in anoxic marine and freshwater environments (Rabus *et al.* 2006). It hypothesized that microbial presence play a greater influence in contamination mobility in fractured wells and a key objective of the research study was to assess the potential for PTE release following microbial proliferation in the characteristic prevailing anoxic ecosystem. A test of releases impacted by the prevailing environmental and operational conditions most common during fracturing operations is proposed as a research objective. A review of prevailing downhole conditions at most US well sites suggest that anoxic conditions are quite predominant with temperatures in the range of 66°C -125°C (Salbu *et al.* 1998), little or no oxygen (Jorgensen *et al.* 2009), elevated CO<sub>2</sub> typical with most hydrocarbon wells and abundance of acidophilic bacteria (Struchtemeyer and Elshahed 2011, Murali Mohan *et al.* 2013, Elliott *et al.* 2014). By assessing the combined effect of these environmental conditions on the mobility or immobility of our investigated PTEs, a better understanding of the gravity of impending treatment needs can be achieved.

## **2.8 Knowledge Gap**

One of the most pressing needs in the UK at the verge of developing its shale gas resource is an assessment of the risk contributions of hydraulic fracturing and shale gas development. Besides the general environmental concerns, the water and wastewater industry in particular are already faced with the challenge of what to expect from released quantities of returning waste. The knowledge of the risk contributions will ensure the right mitigating measures are proposed. In addition, a pre-requirement for developing shale gas formations in the UK is the development of treatment plans

to manage return flowback (EA, 2012). Operating companies are aware that inadequate water management solutions associated with fracturing operations may become a limiting factor in the development of unconventional gas reserves. The EA has mandated that no permits will be approved for flowback storage in double skinned tanks on site while methods for disposal or treatment are considered. Flowback management will henceforth be determined pre-drilling and before fracturing treatment (EA 2012). Consequently, there are concerted efforts to understand the chemistry of returning wastewater from this new industry. Knowledge of factors that influence the variation in flowback quality, the parameters responsible and the process chemistry involved in the formation of flowback (Hayes 2009, Bank 2011). Fluid-rock interactions suggest flowback is more of a geochemical consequence with environmental implication than existing saline deposits unearthed during drilling. The chief culprits are possible soluble trace elements in black shale that exist in more ways than one and of several chemical species. Kinetic tests afford the study of trace element mobility as well as the rate of acid production and subsequently, the flowback quality potentially produced. Hence, since every formation is unique in terms of its acid generation potential. Engineers can predict the nature and size of the associated risk and feasibility of a mitigation options that vary by location. Having illustrated the similarities with returning fracturing wastewater and AMD, similar assessment techniques employed in AMD become useful assessment tools for investigating flowback characteristics and potential risk contributions from shale gas development.

With the UK's efforts to develop her potential shale gas resource, there are several concerns that the risks contributions from shale development activities have been overlooked and are not adequately researched (Green et al. 2011, Wood et al. 2011, CIEH 2012, The Royal Society 2012). This research provides a quantitative risk analysis of the potential release of toxic contaminants as a result of fracturing prospective shale gas formations in the UK. This research will endeavour to provide answers to key questions with regards to contamination risk to water resource in the UK from shale gas development techniques. Important contribution to knowledge will include a quantitative determination of the extent of specific PTEs mobility following hydraulic fracturing and therefore provide essential knowledge of expected returning wastewater treatment challenges.

## **Chapter 3. Research Methodology and Analytical Methods**

This Chapter describes the samples, materials and methodologies adopted in the investigation of potentially toxic trace element release from three prospective UK black shale formations. The choice of sampling location and analytical technique adopted are also discussed. Details are provided on the concepts, design and fabrication of experimental rigs and microcosm reactor vessels used in simulating release reactions. The Chapter provides details of the constituent characterisation study on sampled shales from all three selected formations. A detailed description of experiments conducted to investigate the natural release rates under varying environmental conditions via the sequential batch extraction technique is reported herein. Details are also provided on the experiments to investigate the effect of both operational and environmental conditions on the release of PTEs during fracturing operation on the investigated formations. Finally, methodologies adopted on the microbial simulated weathering of all three sampled prospective black shale are detailed.

### **3.1 Investigated Formations**

The targeted formations have been selected due to their prospectivity for gas contents as reported by the British Geological Survey (BGS) and a number of peer reviewed papers (Ebukanson and Kinghorn 1986, Selley 1987, Maynard et al. 1991, Selley 2005b, Smith et al. 2010, Andrews 2013).

#### **3.1.1 Lancashire Carboniferous Shale (LAN)**

Grey to Black shale found in much of central England is most likely part of the extensive high calcareous shale of Numarian age jointly called the Bowland shale. Probably holding the largest composition of mature gas content (Smith et al. 2010), this carboniferous shale holds the first modern shale gas exploratory sites in the UK. Carboniferous Numarian grey shale from the trough of Bowland Lancashire (Grid Reference SD 6265252722) was chosen to be sampled for the study. These form part of the Bowland shale formation and the Hodder Mudstone Formations of Lancashire studied by the BGS gas-in-place investigation. Structurally, shale comprises dark grey shaly mudstones, with occasional thin calcareous mudstones and siltstones with well

exposed sections at the Pendle Grit formation in the trough of the section. These shale samples are herein designated as Lancashire shale (LAN).

### **3.1.2 Edale Basin Shale (DRB)**

The black rocks of Derbyshire found at the Derbyshire Peak District represent one of the visible outcrops of black shale in the UK. Known as the Edale shale formation, these shales of Dinantian age is thought to be the source formation responsible for residual oil shows in the Castleton area of Derbyshire (Ziegler *et al.* 1997). Black shale from the Mam Tor landslide at the Peak District National Park, North Derbyshire (Grid Reference SK 1270083600) is sampled for the study. Some of the oldest and blackest shale outcrop can be found here with a sequence of inter-bedded sandstone, siltstone and shale of Dinantian age. This shale is structurally laminated, sub-fissile, very black shale with weathered portions showing brownish colourations possibly from oxidation of iron enrichments. Sampled shale is herein designated as Derbyshire shale (DRB).

### **3.1.3 Cleveland Basin Jurassic Shale (CLV)**

The Toarcian Whitby Mudstone Formation contains bands of grey to black shale with visible outcrops at the Whitby East Cliff and was sampled as part of this study. This forms part of the Cleveland basin and is estimated to contain approximately 1,300 trillion cubic feet of shale that stretches from Whitby right through the coast of Robin Hoods bay to the coast of Scarborough (Andrews 2013). Morris (1979) categorised this as part of the bituminous shale facies based on its sedimentary structures and contained faunas. Powell (1984) in his redefinition of the formations, categorised it as part of the jet rock member, or more commonly the jet rock series. All sampling locations were selected due to their characteristic greyish to black natured shale, mostly reported has holding mature natural gas, documented gas prospects and close stratigraphic similarities to the currently explored Carboniferous formations in Lancashire.

## **3.2 Rock Sampling**

The objective of the sampling exercise was to collect non-core (destructive) representative fractions from each investigated formation, removed by approved methods, guarded against accidental or fraudulent adulteration, and tested or analysed in order to determine the nature, composition, percentage of specified constituents, etc.

and possibly their reactivity. Drilling methods are used to obtain bulk samples of black shale from each prospective formation. Extreme precaution was taken during sampling to ensure bulk samples were a true representation of the nature and condition of the rock represented. Because of the need to obtain unweathered rock samples several sampling methods were adopted depending on the structure and hardness of the rock. In all sampled formations, sections with visible outcrops of shale showing minimal or no evidence of weathering were selected. At the Peak District National Park for example, vertical slanting plains measuring 7 to 8fts, allowed the collection of samples at random depths, by the use of a simple rock hammer chiselling technique. It was necessary to remove (by chiselling off) the outer top surface of the rock. This exposed unweathered surface of the rock mass, allowed the collection of undisturbed samples from the formation. Sampling at each site was in no particular order (random) to account for the typically spatial distributed nature of geochemical data, However, care was taken to ensure each sample correspond to a layer of nearly uniform composition. A set of 15 (n=15) representative samples were collected from each outcropping black shale formation. During sampling, all rocks were subsequently logged, weighed, dated and wrapped in protective bubble wraps before transportation to the laboratory. High priority was given to the collection of only unweathered samples in clean and pristine conditions because samples exposed to the environment may be physically and/or chemically altered and therefore not representative of the underlying material.

### **3.3 Rock Preparation and Storage**

At the laboratory, samples were stored to, minimise, the oxidation of certain compositions such as pyrite  $\text{FeS}_2$  resulting in the formation soluble acid sulphate salts. Prior to analysis, samples were stored in sealed, high density polyethylene (HDPE) containers to maintain airtightness. These were then keep under dark dry and cool conditions within the laboratory. Depending on the specific method implementation, samples were retrieved from storage and prepared (dried, pulverised and sieved) for analysis when due. Hence no treated samples were stored kept in storage longer than six weeks. All rocks sampled from the same formations were pooled together before pulverising in the gyro mill. In preparation for analytical determinations, samples were then pulverised and homogenized in a ring type gyro mill to achieve particle sizes  $<75\mu\text{m}$ .

### 3.4 General Methods

A number of spectrometric analytical instrumentations were adopted during the study. The flame atomic absorption spectrometer (FAAS) and the graphite furnace atomic absorption spectrometer (GFAAS) were both used for the determination of trace metal concentrations in aqueous leachate samples. The Ion Chromatography (IC) was mainly used for the determination of anions and major cations while the Spectrophotometer was used for the determination of  $\text{Fe}^{2+}$  and  $\text{Fe}^{3+}$

#### 3.4.1 Spectrometry Instrumentations

Trace metals in the leaching column experiments were analysed using the Varian AA240FS Atomic Absorption Spectrometer in the School of Chemical and Process Engineering. Fuelled by acetylene, the spectrometer adopts fuel support by a nitrous oxide or air supply. The device is equipped with 4 fixed lamp positions with automatic lamp selection to enable fast sequential multi-element determinations. For background correction the AA240FS adopts a high speed deuterium background corrector for accurate correction of background signals. The study adopts varying configurations to the fuel and fuel support flames to combat interferences. All standard solutions were prepared with HCl before dilution to the required concentrations.

The Varian Graphite Tube Atomizer (GTA) (Plate 3.1) 120 furnace atomic absorption spectrometer is a robust analytical spectrometer with varied applications. The inert gas, Argon is used at the 'Normal' gas inlet to the GTA to shroud the hot graphite components and prevent oxidation.

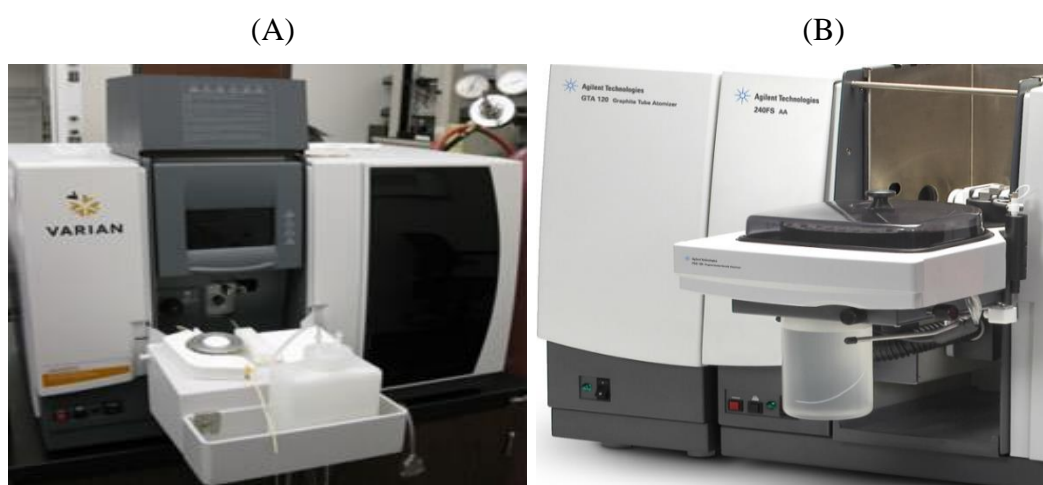


**Plate 3.1:** (A) The Varian spectrometer setup for FAAS (B) The Varian spectrometer setup for GFAAS

Gas pressure is maintained at 25psi with a normal flow rate of 2.5 L/min. Water supply is maintained at 20<sup>0</sup>C with a minimum flow rate maintained at 1.5 L/min at 27 psi. The Plateau, pyrolytically coated graphite tube is the choice of graphite tube for the analysis. No matrix modifiers were adopted for the various metal determinations during this study as very good recoveries were observed during instrument and laboratory performance assessments.

### 3.4.2 Chromatograph Instrumentation

The Metrohm 850 Professional Ion Chromatography system (Plate 3.2) equipped with the 896 professional Amperometric detectors and an 858 Professional Sample Processor was use for the determination of anion concentrations. A Metrosep A Supp 5 - 150/4.0 anion exchange column was used for the separation of the analytes and the column temperature is maintained at 45°C. An isocratic elution was adopted with 3.2mM aqueous Na<sub>2</sub>CO<sub>3</sub> and 1.0mM aqueous NaHCO<sub>3</sub> as mobile phase. A regenerant solution comprising of 100mmol H<sub>2</sub>SO<sub>4</sub> and 100mmol Oxalic acid, supplies the regenerant ions required for suppression or regeneration of the ion exchange surface and removes the eluent and analyte counter ions.

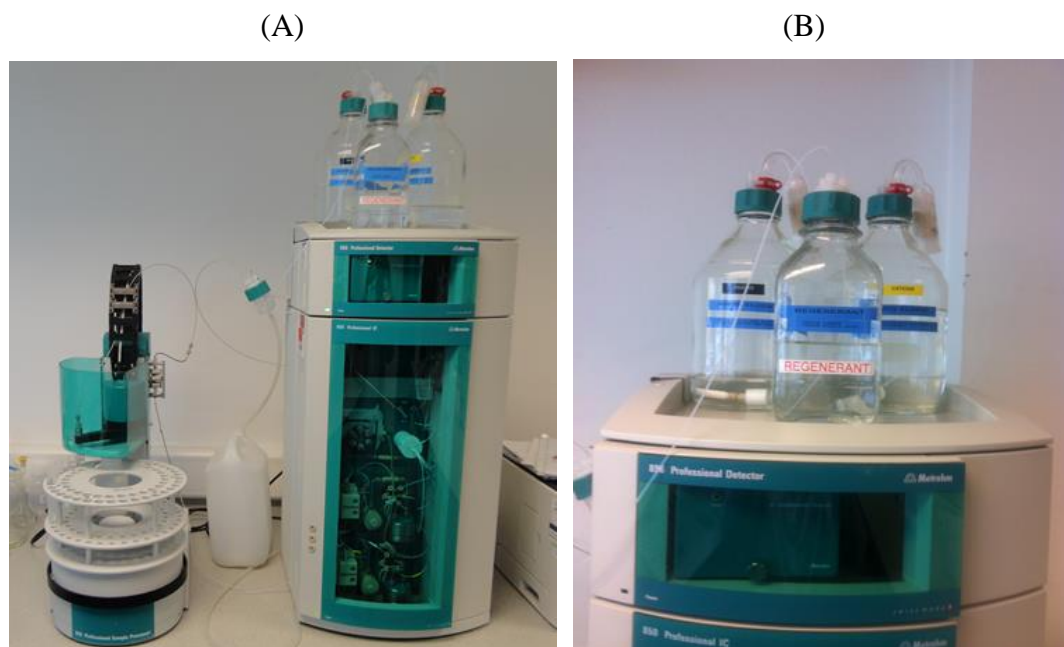


**Plate 3.2:** (A) The Metrohm 850 Professional Ion Chromatograph (B) Cations, Anion and Regenerant Solutions

### 3.4.3 Laboratory Analysis of Metal Release

Leachates were analysed for major metals Al, Fe, Ca and Mg and trace elements Cr, Cu, Ni and Zn via the flame atomic absorption spectrometer (FAAS). A quality control standard US EPA Method 7000B for metal determination by FAAS was also adopted. All measurement of metal releases in part per billion (ppb) is done via the Varian GTA 120 furnace atomic absorption spectrometer. The EPA standard method 200.9<sup>1</sup> (Determination of Trace Elements by Stabilized Temperature Graphite Furnace Atomic Absorption) in adherence to a formal quality control scheme is adopted. The standard requires that a characterisation of both instrument and laboratory performance be assessed prior to samples being analysed by the chosen analytical method. This involves the determination of the instrument detection limit (IDL) and method detection limit (MDL) judged over a 5 point statistical check test. The quality control standard also requires the intermittent analysis of Laboratory Reagent Blank (LRB), Quality Control Sample (QCS) and Laboratory Fortified Blank (LFB) alongside samples from the experimental study. The NIST-1643e reference material from the National Institute of Standard and Technology is adopted as the QCS. Concentrations adopted for the all other quality control parameters are listed in Table 3.1 below.

**Table 3.1:** Definition of Utilised Quality Control Parameters

Quality Control Parameter	Definition
Laboratory Reagent Blank (LRB)	Milli-Q Water (18Ωm)
Method Detection Limit (MDL) (µg/L)	Cr(0.06), Cu(0.10), Ni(0.08) & Zn(0.13)
Quality Control Sample (QCS)	NIST-1643e
Instrument Detection Limit (IDL)	Cr(0.069), Cu(0.071), Ni(0.114), Zn(.091)
Laboratory Fortified Blank (LFB) (µg/L)	Cr(7.5), Cu(30), Ni(24) & Zn(75)

**Procedure:** Using the SpectrAA program development application, each single element hollow cathode lamp is aligned and optimized before the Plateau, pyrolytically coated graphite tube is inserted into the centre cooling block. Once aligned, the capillary tip can be positioned in relation to the cuvette floor. Lamp probe positioning is optimized to ensure smooth sample collection, injection and rinse.

Calibration standards as described above are made freshly for each batch of sample analysis. The LFB and LRB are analysed at the start and intermittently during each batch of samples analysed to investigate matrix interferences. Recovery range is checked with values specified by the EPA standard method 200.9<sup>1</sup> (70-130%) and are computed as described in Equation 3.1 and 3.2.

$$LFB, R\% = \frac{(LFB)}{\text{Spike Level}} \times 100 \text{ -----Eq. 3.1}$$

Where R% is the LFB Percentage recovery, LFB is the LFB results (µg/L) and the Spike Level is the LFB true value (µg/L).

$$Sample, R\% = \frac{(\text{Avg.Spiked sample})}{(\text{Spike Level} + \text{Sample Test Result})} \times 100 \text{ -----Eq. 3.2}$$

Where Sample, R% is Sample Percentage recovery, Avg. Spiked Sample is Average of spiked sample triplicate result (µg/L). Spike Level is LFB true value (µg/L) and Sample Test Result is the sample results when analysed. For quality control adherence, 10 replicates of a laboratory blank (Deionized water) are analysed to determine the instrument detection limit (IDL) from Equation 3.3 and the method detection limit (MDL) was subsequently computed from Equation 3.4.

$$IDL = 3 \times ST.DEV \text{ -----Eq. 3.3}$$

Where *ST.DEV*, is the Standard deviation of the 10 replicate analyses

$$MDL = t \times S \text{ -----Eq. 3.4}$$

Where *t* is the student's t value for a 99% confidence level and a standard deviation estimate with n-1 degrees of freedom [*t* = 2.821 for 10 replicates]. *S* is the standard deviation of the replicate analyses Analysis of the quality control sample is done following IDL and MDL determinations.

## **Chapter 4. Shale Characterisation Study**

### **4.1 Introduction**

Black shale is a dark coloured mud-rock containing organic matter that may have produced hydrocarbons in the subsurface or that may yield hydrocarbons by pyrolysis (Tourtelot 1979). Usually, shale having more than 2% organic carbon would have a greyish to black appearance. Perhaps the most relevant characteristics of black shale to this study are its enrichment in metals usually found in concentrations exceeding expected amounts in ordinary shale. Krauskopf and Bateman (1955), reported that black shale beds enriched in metals by factors greater than 50 for Silver (Ag) and 10 for Molybdenum (Mo). In addition black shales are a known sink for radionuclides and other potentially toxic elements mainly because of their potential as a reservoir for hydrocarbon. The release of these potentially toxic trace elements (PTEs) are a function (amongst other factors) of the trace metal enrichments in the shale matrix (El Kammar and El Kammar 1996, Loukola-Ruskeeniemi et al. 1998, Lavergren et al. 2009b, Bank 2011) but this varies widely by location (Smith and Young 1967, Fisher et al. 1998). Hence, the quantification of trace elements and their release from unweathered shale provide useful data for assessing the bulk composition of liable contamination. The characterisation study presented here has looked at both the physical and chemical characteristics of the sampled shales to identify the potential for contamination.

### **4.2 Chapter Objectives**

The study's hypothesis was based on the premise that potentially toxic trace elements are enriched in UK black shale and may be found distributed in larger concentrations than averagely expected. In line with achieving the research objective of providing a characterisation study of the sampled prospective formations (objective 1), this Chapter is designed to assess the properties of the sampled shales that suggested the ease of toxicant release and the likelihood of contamination exposure. Additionally, the study presented in this chapter will provide baseline empirical data for comparison with results to be obtained from proposed kinetic leaching investigation. Therefore, the following tasks were designed to achieve the chapter objectives as stated in objective 1;

- i. Provide a physical and geochemical characterisation of the sampled formations
- ii. Select identifier PTEs of notable toxicity for subsequently mobility and release assessment in objective 2 of the research study.
- iii. Provide bulk quantification and fractionation data on selected PTEs via total acid extraction and Sequential batch extraction (SBE).

### **4.3 Methodology**

Firstly, the lithological and stratigraphy properties of the samples collected were studied and compiled to provide useful information on any properties that might affect contamination release from the studied shale. X-ray spectrometric methods such as X-ray Diffractive (XRD) analysis and X-ray Fluorescence (XRF) analysis were adopted to quantitatively assess the mineralogical and elemental composition of the sampled shales. By adopting a risk weight scheme based on abundance, bioaccumulation, bioavailability and toxicity limits in drinking water, identified trace metals from the geochemical assessments were reduced to a select few assessed throughout the study. These trace metals serve as the PTE indicators adopted to assess, mobility and release kinetics for the research study. Since the fate of PTEs depends on their potential for release, the study investigates their potential for release by first investigating the sampled shales tendency to produce acid waste.

The widely used static acid base analysis method that assesses the balance between the acid generating potential and the rock neutralization potential is adopted for each ( $n=15$ ) sample sets collected for the study. Acid potential was obtained following microanalysis to determine sulphur weighted percentages for all three shales and the analysis adopts flash combustion in a Thermo Flash EA 1112 series performed in the school of Chemistry, University of Leeds. Three widely used methods are adopted to determine the shales neutralization potential. These methods include the standard Sobek NP determination method by, a modification to the standard Sobek method and the modified acid base analysis method developed by Skousen *et al.* (1997). Modifications to the standard Sobek method which formed the modified Sobek method adopted included the use of a carbonate rating test as a replacement for the subjective Fizz test, the application 5ml peroxide ( $H_2O_2$ ) for siderite correction, the use of ambient HCl during digestion and the adoption of a pH titration end point of 8.3.

Subsequently, a modification of Tessier *et al.* (1979) sequential batch extraction scheme was developed to study trace element fractionation and mobility for the three sampled shale formations. Ten sample sets (n=10) were prepared for each sampled formation and a six stage extraction sequence was designed for extraction of the partitioning particulate heavy metals into chemical forms likely to be released in solution under various environmental conditions.

### 4.3.1 Physical Characterisation of Shales

The main purpose of the physical characterisation study is to provide details of the lithology and other physical properties of the sampled shales, which might contribute or affect toxicant release subsequently causing contamination exposure. Most black shale formations lay in adjacent beds with sandstone, mudstone and other clay mineral formations, identifying the target formation by its physical characteristics is pertinent to the sampling exercise.

#### 4.3.1.1 Particle Size Reconstruction

Collected sample were reconstructed to particle sizes shown in Table 4.1 to standardize conditions of exposure for all sampled shale types and facilitate uniform expose of sample to weathering conditions and collection of leachate. Following sample crushing, all shales were passed through a 3/8 inch mesh to ensure that no particle size greater than 3/8 inch is added to the column.

**Table 4.1:** Particle size distribution of reconstructed samples

S/No	Sieve Size	Size	Weight (g)	Percent of Total Weight
1	+3/8	9.52mm	-	-
2	+3/8 - #4	4.76mm	800	40
3	#4 - #10	2.00mm	500	25
4	#10 - #16	1.18mm	300	15
5	#16 - #35	0.60µm	200	10
6	#35 - #60	0.250µm	100	5
7	#60	Less than 0.250µm	100	5

A number of methods were adopted in this study to ensure better control over the weathering rate and consistency of the test procedure to all three sampled shales. Firstly, the adoption of the same particle size distribution amongst all sampled shales and secondly the determination of the surface area from the BET analysis as described in the next section.

#### ***4.3.1.2 Surface Area Determination (BET Analysis)***

The Brunauer, Emmett and Teller (BET) surface area of each fraction of sieved and reconstructed shale was determined using a Micrometrics Tristar Surface Area and porosity Analyser using N<sub>2</sub> gas bulk adsorption. The analysis was carried out in the School of Chemical and Process Engineering. Samples were first degassed in a Micrometric Flowprep 060 degas system for 20mins and subsequently heated below boiling point for 1.5 hours to remove residual gas on the surface of particles. Shale samples were heated to 300°C in the temperature jacket for 1.5 hours and condensation on the sample tubes were removed by air drying during heating. The sample tubes are reweighed following heating before surface areas are analysed in the Tristar analyser. Surface areas were measured for all particle sizes used in the column experiments before introduction columns are loaded and following completion of the leaching test. The bulk surface areas for each column were determined for the post-leaching rock by taking the individual masses of the sieve fractions listed in Table 4.1 above, multiplying each mass by the surface area (SA), and combining their fractional percent of the total as a weighted linear average as shown in equation 4.1.

$$A \times SA_{\text{Sieve1}} + B \times SA_{\text{Sieve2}} + C \times SA_{\text{Sieve3}} + D \times SA_{\text{Sieve4}} + E \times SA_{\text{Sieve5}} = \mathbf{SA_{\text{bulk}}}$$
 -----Eq. 4.1

Where:  $A + B + C + D + E = 1$

A is fraction of total sieve 1 size, B is fraction of total sieve 2 size and C is fraction of total sieve 3 size, D is fraction of total sieve 4 size, E is fraction of total sieve 5 size. The determination of the surface area aids the computation of the surface area to volume ratio. Surface area to volume ratio is used in the determination of the normalised mass loss which quantifies the release of ions into a leaching solvent.

### **4.3.2 Chemical Characterisation of Shales**

Chemical characterization plays a critical role in risk assessment by allowing at first glance the identification of potential hazards in the compositional structure of the material investigated. Knowledge of the chemical composition such as the abundance of metals, heavy metals and trace elements in the sampled shales provides the ground work for determining the hazard components of the investigated shales. In this study, a mineralogical and elemental quantification of the each investigated composite shale matrix was examined to identify potential hazardous or toxic compositions that contribute to the risks from exposures to these pre-historic formations. All sampled shales were examined mineralogical by X-ray diffraction analysis (XRD) and elementally by X-ray fluorescence analysis (XRF).

#### ***4.3.2.1 Mineralogical Determination by XRD***

Mineralogical data for the sampled formation is required for two main reasons; firstly to determine the range and quantity of minerals present which may host potentially toxic elements and secondly, to aid with phase identification. Mineralogical compositions were determined by XRD in the X-ray Laboratory in the School of Earth and Environment, University of Leeds. Bulk mineralogical analysis was performed on samples passing through 75 $\mu$ m sieves, oven dried at 105°C and analysed on a Bruker B8 diffractometer, fitted with a lynx eye detector using a Cu K-alpha 1 radiation wavelength. The interpretation was carried out using Bruker EVA software and International Centre for Diffraction Data Powder Diffraction File (ICDD-PDF) database.

#### ***4.3.2.2 XRF Whole Rock Elemental Determination***

Bulk whole rock chemical analysis was done by pressed pellet analysis on samples dried at 105°C, ground and passed through 75 $\mu$ m sieves. The sample was then pressed with 280kN pressure for 20 seconds into an Aluminium cup. For the determination of loss on ignition (LOI), samples were ashed at 900°C for 2hrs and allowed to cool in a desiccator. The LOI values obtained represent the loss of volatiles from the samples due to reactions such as carbonate and organic matter decomposition, sulphide oxidation and the loss of moisture and structural water. Weights are recorded to 4d.p on an analytical balance. Chemical analysis of all samples obtained at random depths

was performed by XRF analysis on an ARL Advantx XRF wavelength spectrometer. Fused glassed beads were prepared using 0.5g of the oven dried samples mixed with 5g of dilithiumtetraborate ( $\text{Li}_2\text{B}_4\text{O}_7$ ) (ratio 10:1) in a gold-platinum vessel at c. 1250°C. Lithium tetraborate (Fluxana, Germany) was used to dissolve the samples prior to element determinations and as a wetting agent, 0.05g of Lithium bromide was added and controlled fusion was achieved after 30mins. The concentrations of elements in the unknown samples were measured by comparing the X-ray intensity for each element with the intensity for beads prepared from standard samples (i.e. ARSTM 010-2 coal ash, EURO-CRM 776-1, CCRMP blast furnace slag SL1 and BCS No. 309 Sillimanite).

#### ***4.3.2.3 Total Carbon and Total Sulphur Determination***

Total carbon and sulphur were determined through microanalysis using microgram/milligram quantities of the sample. Adopting a Sartorius SE2 Ultra-micro balance, with a readability of 0.1µg and verified for use in legal metrology. Dried, powdered and homogenised samples completely free from contamination were prepared for the analysis. The analysis adopts flash combustion in a Thermo Flash EA 1112 series. 2 to 3 mg of the prepared homogenised sample was weighed into a tin capsule and approximately 5mg of Vanadium Pentoxide ( $\text{V}_2\text{O}_5$ ) was added to aid combustion. After sealing the capsule, the sample was placed in the auto-sampler. The tin capsule enclosing the sample falls into the reactor chamber at 900°C where excess oxygen is introduced. Tin, coming in contact with the extremely oxidizing environment, triggers a strong exothermic reaction. The temperature rises to approximately 1800°C instantly causing the combustion of the sample. High purity helium is used as the carrier gas. The resulting reaction produces  $\text{SO}_2$  which passes through and separate in a chromatography column. The quantities are detected using a Thermal Conductivity detector and then compared with 4 standards (BBOT, dl-Methionine, L-Cystine & Sulphanilamide) to give a linear calibration plot for determination of the percentages of Sulphur.

#### ***4.3.2.4 Bulk Compositional Assay by Total Acid Extraction***

In assessing the bulk releasable compositions of the sampled shale, whole compositional analysis is adopted via total acid extraction. These release quantities

serve as baseline data for further comparison with mobility data. Total decomposition of rock specimens is known to be achieved by hydrofluoric acid however, issues with its corrosive nature and harm to equipment was a deterrent to its use. Alternatively, total digestion by Aqua regia was considered as a safe alternative to obtaining acid extractible trace element composition. Ure (1990), Berrow and Stein (1983) all reported reasonable and achievable decomposition of shale in Aqua regia except for the detection of matrice containing As, Se, and Cd. Niskavaara *et al.* (1997) suggested that residual elements that are not released by Aqua regia digestion are mostly bound to silicate minerals and are considered unimportant for estimating the mobility and behaviour of the elements. Hence digestion by hotplate aquaregia was adopted.

Digestion was completed in a 50mL conical flask equipped with a sealing funnel. To provide a steady supply of heat, the hot plate was equipped with a sand bath. 0.5g of the sample was accurately weighed to 4 decimal places into a sealed 50mL conical flask and allowed to heat up for 1 hour at 200°C. After digestion, the samples were transferred quantitatively to the digested solution and diluted to achieve a 10% acid solution in the final volume. The extracted solutions were analysed in a high resolution continuum source Atomic Absorption Spectrometer (AAS, ContrAA 700, Analytik Jena) using the HydrEA technique.

#### ***4.3.2.5 Acid Base Accounting (ABA) – Static Method***

The widely used static acid base analysis method that assesses the balance between the acid generating potential and the rock neutralization potential was adopted for each ( $n=15$ ) sample sets collected for the study. Firstly the carbonate rating method was adopted as a more objective analytical process to determine the acid to be added for NP determination. The procedure was performed for ( $n=5$ ) sample sets for each sampled shale. Pulverised sampled shales were sieved (<60 mesh) and oven dried at 105°C overnight. A 0.45µm filter was dried and weighed in preparation for filtration. 2 g of the dried sample was placed in a 250 mL Erlenmeyer flask and 20.0 mL of 10% (0.1 M) HCl was added and agitated until all CO<sub>2</sub> evolution ceased. The suspension was then filtered in a pump controlled vacuum filter, the residue was washed onto the filter with distilled water. The filter was oven dried at 105°C overnight before final measurements of dried filter and residue weights are recorded. The percentage insoluble residue was computed by dividing the weight (g) of residue by the weight of

the sample (g) (equation 4.2). Based on results obtained, samples are rated according to Table 4.2 and this was adopted in the computation of NP values for each sample set.

$$\% \text{ Insoluble Residue} = \frac{\text{Residue Weight (g)}}{\text{Weight of Sample (g)}} \text{-----Eq. 4.2}$$

**Table 4.2:** Carbonate rating based on percent insoluble residue with corresponding acid volumes and acid strengths

<b>Carbonate Rating</b>	<b>Percent Insoluble Residue (%)</b>	<b>Amount of Acid (mL)</b>	<b>Strength of Acid (M)</b>
0	95 - 100	20	0.1
1	90 - 94	40	0.1
2	75 - 89	40	0.5
3	< 75	80	0.5

Sample digestion for acid base accounting analysis (ABA) was carried out with 15 replicates of all three sampled shales 2g each were placed in 15 beakers with a 16<sup>th</sup> beaker serving as a blank and containing no shale. The beakers were covered with watch glasses, and the content were boiled gently for 5 min to a maximum of 90 to 95°C. Reaction was assumed to be complete when no bubbles were seen rising through the suspension and the sediment settled evenly over the bottom of the beakers when the temperature was reduced to 80°C. Distilled water was then added to bring the volume in the beakers to 100 mL and the solution boiled gently for 5mins. After cooling, the contents of the beakers were gravity filtered using 0.45micron filters and the filtered solution was then treated with 5 mL of 30% H<sub>2</sub>O<sub>2</sub> (to exclude neutralization by siderite) and boiled for an additional 5 min.

The study adopted the standard Sobek method as described in Sobek *et al.* (1978) with a slight modification on the Sobek procedure for NP determination. A back titration end point of 8.3, siderite correction with 5ml peroxide (H<sub>2</sub>O<sub>2</sub>) (Skousen et al. 1997), use of ambient HCl during digestion and the use of the carbonate rating for the selection of acid addition rather than the subjective fizz test were modifications adopted for the modified Sobek method. The digested solution was back titrated to pH

7 using the same concentration of acid adopted from the carbonate rating in Table 4.2. Total NaOH added is recorded and used in the computation of the acid remaining. Hence the volume of base used in obtaining pH values 2.0, 2.5, 3.0, 3.5, 4.0, 4.5, 5.0, 6.0 and the end point at 7.0 was recorded and used in obtaining the back titration curve. The computation of NP requires the determination of the constant (C), the volume of acid consumed from Equations 4.3, 4.4 and 4.5 as shown below.

$$\text{Constant (C)} = \frac{(\text{Volume (ml) acid in blank})}{(\text{Volume (ml) base in blank})} \text{-----Eq. 4.3}$$

$$\text{Vol. acid consumed} = (\text{Vol. acid added}) - (\text{Vol. base added} \times C) \text{----Eq. 4.4}$$

$$\text{NP (kg CaCO}_3\text{/t)} = (\text{Vol. of acid consumed}) \times (25.0) \times (N \text{ of add}) \text{----Eq. 4.5}$$

However, because of known limitations with the Sobek method for NP determination, such as the tendency to over-estimates NP values, the Lawrence modified acid base accounting method was used to provide NP computations for the same sample sets. Also adopted is the modified ABA NP determination method. Originally developed by Lawrence (1990), this method prevents the overestimation of the NP value by performing the HCl acid digestion for 24 hours at lower temperature of 20 to 35°C. Two other modifications include the control of pH by limiting the addition of acid to a pH range of 1.5 to 2.0 and the use of an 8.3 pH value as end point during back titration. This study also adopts the carbonate rating instead of the subjective fizz test. NP values are obtained from Equation 4.6, where Acid Normality = 0.5M or 0.1M HCl and Base Normality= 0.1 N NaOH.

NP (kg CaCO<sub>3</sub>/t) is computed as follows;

$$\frac{(\frac{\text{Acid Normality} \times \text{Acid}}{\text{Volume}}) - ((\frac{\text{Base Normality} \times \text{Base}}{\text{Volume}}) \times 50)}{\text{Weight of Sample}} \text{----- Eq. 4.6}$$

#### ***4.3.2.6 Mobility Assessment by Sequential Extraction***

A modification of Tessier's sequential extraction scheme (Tessier et al. 1979) was developed to study trace element fractionation and mobility for the three sampled shale formations. Ten sample sets ( $n=10$ ) were prepared for each sampled formation and a six stage extraction sequence was designed for extraction of the partitioning particulate heavy metals into chemical forms likely to be released in solution under various environmental conditions. The schemes (Figure 4.1) show similarities with the Tessier's four stage extraction scheme, except for the inclusion of a water soluble fraction and the use of Aquaregia for digestion of the residual fraction. One gram of shale sample was weighed and placed in a 100 ml polycarbonate centrifuge tube and the following extractions were made sequentially. 1 gram of sample was extracted with 5ml of deionized water for 2hrs at room temperature with a continuous agitation at 180rpm. Mean room temperatures were recorded at 23-25°C. Solid phase after extraction was washed in 5mL of tap water before the next extraction step. Exchangeables were extracted with 8mL 1M  $MgCl_2$  to pH 7 at room temperature with continuous agitation. The washed residual from the exchangeable fraction was extracted with 8mL 1M sodium acetate (NaOAc) maintained at pH 5 with Acetic Acid (HOAc) for 5hrs at continuous agitation at room temperature. Residuals were washed as before (10mL deionized water) and extracted with 20mL 0.04M  $NH_2OH \cdot HCl$  in 25% (v/v) HOAc. Agitation is occasionally in a water bath to maintain temperature at  $96 \pm 30C$  for 6hrs. Trace metals abound to organic matter was extracted with 3mL 0.02M  $HNO_3$  with 5mL 30%  $H_2O_2$ . The solution was cooled to within room temperature before another addition of 3mL of 30%  $H_2O_2$ . Final cooled solution was reacted with 5mL of 3.2M  $NH_4OAc$  in 20% v/v  $HNO_3$  with pH 2 using  $HNO_3$  at  $85 \pm 2^0C$  in a water bath for 2hrs with occasional agitation. The finale solid phase at this stage holds residual trace metal fractions and was extracted by hotplate digestion in Aquaregia. Supernatants are extracted at each sequence and was analysed by the FAAS.

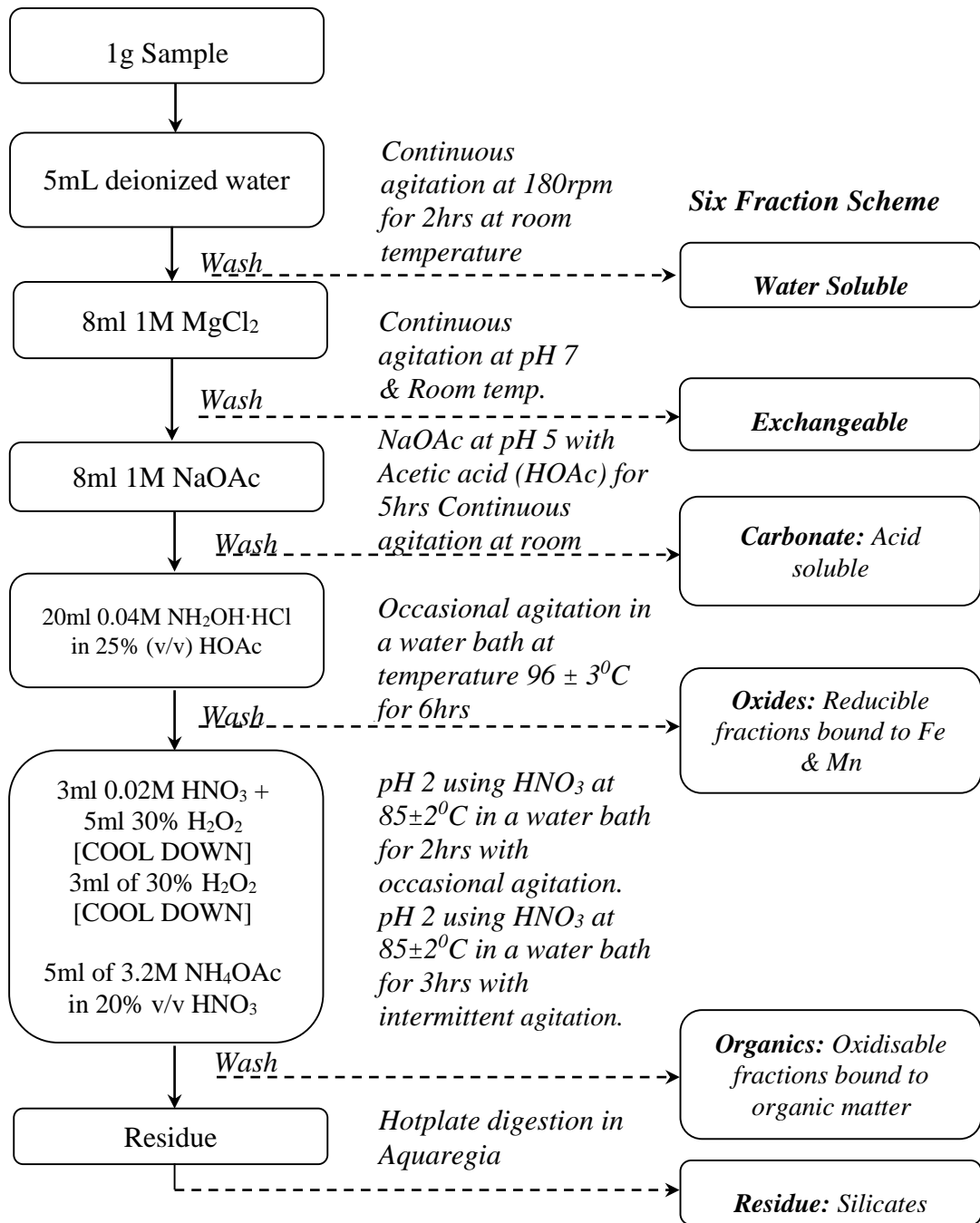


**Figure 4.1:** Sequential extraction scheme (modification of the Tessier 4 stage chemical extraction scheme)

## 4.4 Results and Discussion: Physical Characterisation

Results for the physical characterisation study on the sampled black shales are discussed here. This include lithological observations, sample particle size preparation exercises and results obtained from the surface area determination experimental study.

### 4.4.1 Lithological Characteristics

The blackest of all three sampled shales is the Edale basin shale at the peak district National park. Also known as the shivering mountain, the eastern face of the peak show physical evidence of frequent landslides preventing the sampling of unweathered rocks at this face. Various strata of sandstone and limestone that form the peak are visible at this section but at the base of the Mam-Tor, a band of black shale overlaid by another band of tubiditic sandstone is evident. Shale stratigraphy consists of laminated, sub fissile, very dark grey to black shale.



**Plate 4.2:** (A) Weathered mass of Edale black shale (DRB) showing brownish colouration, an indication of iron enrichment (B) Unweather Edale shale

Texturally fine grained and structurally laminated splitting into thin plates (Plate 4.1B). A visible brownish decolouration (Plate 4.1A) showing evidence of iron oxides can be seen on the overly weathered samples. Unweathered rock mass however, displays a shiny lustre (Plate 4.1B) where laminated faces are split. The Toarcian Whitby Mudstone Formation contains bands of grey to black shale with visible outcrops at the Whitby East Cliff. These rocks are of Jurassic age with a brassy colour and metallic lustre, almost jet black in appearance (Plate 4.2C). Major parts of the cliff show signs of sea erosion but between the cliff ends on the east of the river Esk provides ample outcrops for sampling of unweathered samples. Shale stratigraphy consists of mudstone, intercalated with relatively thin units of calcareous sandstone, calcareous mudstone and calcareous siltstone. Texturally, fine grained with visible

shiny lustre and not structurally laminated in appearance (Figure 4.2C). This shale is considerably hard with an estimated Mohs hardness ranging between 2.5 to 4.

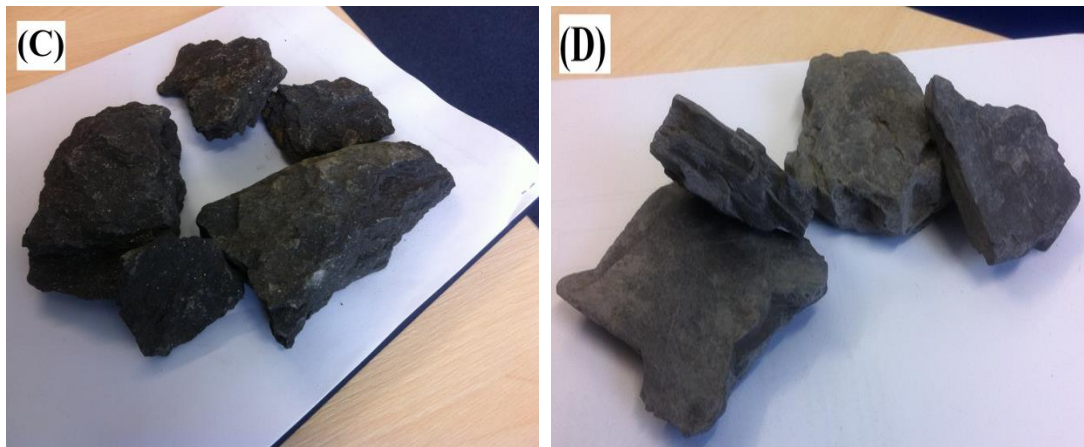


**Plate 4.3:** (C) Jurassic black shale from the Cleveland basin (CLV) (D) Numarian grey to black shale from Bowland basin, Lancashire (LAN)

Dark to very dark grey shale lines the head of the valley pass, a high pass in the Forest of Bowland reaching up to 960ft at the highest point. The hill is formed by Upper Carboniferous shales and sandstones with the Pendle Grit Formation and occasional thin calcareous mudstones and siltstones with well exposed sections at the Pendle Grit formation in the trough of the section. Appreciable dig reveals very dark grey unweather shale on the sides of the valley pass. Texturally, it appears mainly as a thinly fissile mudstone (Plate 4.2D). Structure is also laminated and its hardness can be described as soft and can be loosened by scratching.

#### **4.4.2 Standardized Particle Size Distribution**

As with most mobility and release investigations on rocks, preparation required grinding into varying particle sizes to obtain a more holistic nature of the consolidated overburden strata. Sampling rocks however, introduces a new challenge with obtaining site representative samples. The mass of rock will quite often be pulverised to obtain varying particle samples that enhances reactivity. Leaching experiments on rock samples follow similar trends. Generally, the finer the particle size, the more reactive the samples because the more bonds within the shale matrix that need to be broken, the slower the dissolution. Also, the more bonds exposed to the interaction with water, the more ions will be taken into solution and equally the more the dissolution. Hence, the particle size of crushed samples can affect weatherability and composition

dissolution. This concept was widely documented by Ethridge *et al.* (1979); and Hornberger *et al.* (2004a) who demonstrated the effect of particle size distribution on results from leaching kinetics. Therefore, as part of the physical characterisation study, it is important to assess the operational properties of the rock particularly following sample crushing. Extreme caution is needed when selecting appropriate particle sizes for any leaching exercise as a greater percentage of fine particles increase the surface area available for reaction (Hornberger and Brady 2009). In line with this study's aim however, it is more appropriate to adopt a standardized particle size distribution to enable a comparative analysis of leaching rates and facilitate better control in determining the reaction kinetics for all three sampled shale types and Table 4.3 shows the particle size adopted with equivalent weights.

**Table 4.3:** Particle size distribution of reconstructed samples

S/No.	Sieve Size	Size	Weight (g)	% Total Weight
1	+3/8	9.52mm	-	-
2	+3/8 - #4	4.76mm	800	40
3	#4 - #10	2.00mm	500	25
4	#10 - #16	1.18mm	300	15
5	#16 - #35	0.60µm	200	10
6	#35 - #60	0.250µm	100	5
7	#60	Less than 0.250µm	100	5

#### 4.4.3 Surface Area Determination

The surface area for the various particle sizes in Table 4.3 was determined using the Brunauer, Emmet and Teller (BET) method. Results for the three sampled formations are displayed in Table 4.4. With these data, an effective area of materials that were leached could be calculated for each column. The table contains the weight fractions retained on individual sieves, the BET surface area for each fraction and the modelled effective surface area (normalised S.A) for all sampled shale before the leaching test. Using the percentage retained on the sieves, the normalised BET surface area can be computed from Equation 4.7 below.

$$\text{Normalised S.A (m}^2\text{/g)} = \% \text{ retained} \times \text{BET Surface Area (m}^2\text{/g)} \text{---Eq. 4.7}$$

Determination of the surface area aids the computation of the surface area to volume ratio. Surface area to volume ratio is used in the determination of the normalised mass loss which quantifies the release of ions into a leaching solvent.

**Table 4.4:** Surface Area Measurement for all Sampled Shale Pre-leaching

Sieve Size	Aperture Size	BET SA (m <sup>2</sup> /g)			% Retd. on Sieve	Normalised SA (m <sup>2</sup> /g)		
		LAN	DRB	CLV		LAN	DRB	CLV
+3/8	9.52mm	24.03	25.32	11.24	-	0.00	0.00	0.00
+3/8 - #4	4.75mm	21.73	21.15	10.99	40	8.69	8.46	4.39
#4 - #10	2.00mm	20.62	21.25	10.65	25	5.15	5.31	2.66
#10 - #16	1.18mm	21.60	22.21	6.50	15	3.24	3.33	0.98
#16 - #35	600µm	24.29	21.53	7.32	10	2.43	2.15	0.73
#35 - #60	250µm	22.36	23.36	6.32	5	1.12	1.17	0.32
#60 (Pan)	< 250µm	22.31	23.12	8.56	5	1.12	1.16	0.43
						<b>21.75</b>	<b>21.58</b>	<b>9.51</b>

Following the completion of the leaching test, the analysis is repeated and the observed surface area measurements are shown in Table 4.5 for the leaching protocol simulating natural weathering and Table 4.6 for the leaching protocol simulating fractured enhanced weathering. All shales exhibited increases in surface area following leaching in contrast to the expected reduction in surface area as a result of preferential dissolution of small high surface energy particles. This however, is common with shale due to their variability in mineralogical composition. Shales that have more soluble, fine-grained components will in general present a larger measured surface area after leaching primarily because of the layered structure of the phyllosilicate such as micas, chlorite and clay minerals. Therefore, these results indicate that the mineralogical composition of black shales sampled are enriched in phyllosilicate, mostly clay minerals and these contribute to increased surface area observed.

**Table 4.5:**Surface Area Measurement Post-leaching (Simulated Natural Weathering)

Aperture Size	BET SA (m <sup>2</sup> /g)			% Retd. on Sieve			Normalised SA (m <sup>2</sup> /g)		
	LAN	DRB	CLV	LAN	DRB	CLV	LAN	DRB	CLV
9.52mm	-	-	-	-	-	-	-	-	-
4.75mm	26.74	23.15	11.33	34.40	31.06	38.03	9.20	7.19	4.31
2.00mm	23.02	24.31	12.04	33.91	35.19	25.66	7.80	8.55	3.09
1.18mm	23.22	23.47	7.49	14.92	15.99	15.66	3.47	3.75	1.17
600µm	27.01	22.64	9.01	8.05	8.47	8.89	2.17	1.92	0.80
250µm	22.97	24.16	8.20	3.58	3.84	4.61	0.82	0.93	0.38
< 250µm	24.54	25.66	11.66	5.14	5.45	7.15	1.26	1.40	0.83
<b>Total</b>							<b>24.72</b>	<b>23.74</b>	<b>10.58</b>

**Table 4.6:**Surface Area Measurement Post-leaching (Fracture Enhanced Weathering)

Aperture Size	BET SA (m <sup>2</sup> /g)			% Retd. on Sieve			Normalised SA (m <sup>2</sup> /g)		
	LAN	DRB	CLV	LAN	DRB	CLV	LAN	DRB	CLV
9.52mm	-	-	-	-	-	-	-	-	-
4.75mm	22.00	24.20	9.23	31.20	30.5	32.00	6.86	7.38	2.95
2.00mm	21.11	22.22	9.57	33.60	29.6	23.80	7.09	6.58	2.28
1.18mm	20.59	20.52	8.96	12.10	15.2	14.80	2.49	3.12	1.33
600µm	23.66	20.95	8.70	8.91	11.0	12.90	2.11	2.30	1.12
250µm	19.97	23.63	10.22	6.84	6.3	6.80	1.37	1.49	0.70
< 250µm	20.35	21.57	11.70	7.35	7.4	9.70	1.50	1.60	1.13
<b>Total</b>							<b>21.42</b>	<b>22.47</b>	<b>9.51</b>

A summary of the surface area data is shown in Table 4.7, apart from the black shale sampled from Whitby (Cleveland Basin) leached in SFF, an increase in surface area after leaching accounts for the negative percentage change in surface area measurement. The usefulness of these surface area measurements will become evident during the computation of leaching rates, where the surface area/volume parameter allows leaching rates varying over several orders of magnitude to be scaled onto the same plot.

**Table 4.7:** Summary of the before and after changes in the observed BET

Sample I.D	Natural Weathering			Fractured Simulated		
	*SA before (m <sup>2</sup> g)	*SA after (m <sup>2</sup> g)	% Change	SA before (m <sup>2</sup> g)	SA after (m <sup>2</sup> g)	% Change
LAN	21.75	24.72	-13.68	20.99	21.42	-2.04
DRB	21.58	23.74	-10.02	22.31	22.47	-0.73
CLV	9.51	10.58	-11.30	10.81	9.51	12.00

\*SA (Surface area)

## 4.5 Results and Discussion: Geochemical Characterisation

The chapter objectives were to provide a chemical trail of chemical constituents of all sampled shales, largest at its mineralogical level and smallest at the elemental level. For this study, the range and quantity of minerals present in all sampled shales as well as their elemental composition have been used to shortlist potentially toxic elements and provide a means to aid trace element phase identification.

### 4.5.1 Mineralogical Composition

Mineralogical compositions were determined by X-Ray Diffraction Spectrometer (XRD) analysis on pulverised samples of collected shales. Details of the methodology and analytical procedures adopted are provided in Section 3.2.2.1. Quantitative whole rock mineralogical compositions are displayed in Tables 4.8. Identification and classification of abundance are based on relative peak heights and mineral crystalline structure. Adopting the Yitagesu *et al.* (2009) classification, mica is a major rock mineral (31.96%) detected in Lancashire black shale (Table 4.8) and mineral distributions show it is enriched in phyllosilicates as previously anticipated from the surface area BET results obtained. A pyrite composition of 5.62% (Table 4.8), the largest observed in all sampled shales is indicative of a relatively larger acid potential in comparison to all other investigated shale types. Also observed is that the Lancashire black shale is the only sampled shale not largely composed of quartz. Calcite, dolomite and siderite are the carbonate minerals present in the Lancashire black shale, all together forming a combined percentage of 7.23% of the entire mineral composition in the matrix indicative of a poor neutralisation potential. One of the earliest mineralogical data provided on the Numarian bowland formation was reported

by Spears and Amin (1981b) and document the mean quartz content of the shale at 19% slightly short of reported 14.23% in this study. It is important to note however that Spears and Amin (1981b) study was on the Mam Tor Beds which they considered an extension of the Namurian shale in the central Pennines. Observed mineralogical data for the studied Lancashire black shale showed good agreements with Hillier (2006) results on similar shale sampled from littledale, Lancashire.

**Table 4.8:** Normalised Mineralogical composition of sampled Black shale from all three investigated UK formations

Mineral	Mineral Formula	LAN (%)	DRB (%)	CLV (%)
Quartz	SiO <sub>2</sub>	14.23	30.47	41.46
Albite	NaAlSi <sub>3</sub> O <sub>8</sub>	2.92	4.02	4.27
Microcline	KAlSi <sub>3</sub> O <sub>8</sub>	0	1.07	0.93
Calcite	CaCO <sub>3</sub>	5.05	22.27	0.84
Dolomite	(CaMg)(CO <sub>3</sub> ) <sub>2</sub>	1.02	0.92	1.91
Mica	X <sub>2</sub> Y <sub>4-6</sub> Z <sub>8</sub> O <sub>20</sub> (OH,F) <sub>4</sub>	31.96	22.39	22.61
Illite-smectite	(Mixed Layered)	16.59	3.23	6.40
Kaolinite	Al <sub>2</sub> Si <sub>2</sub> O <sub>5</sub> (OH) <sub>4</sub>	16.22	5.69	9.84
Chlorite	(Mg <sub>5</sub> Al)(AlSi <sub>3</sub> )O <sub>10</sub> (OH) <sub>8</sub>	5.23	7.52	8.76
Pyrite	FeS <sub>2</sub>	5.62	1.50	2.99
Siderite	Fe <sub>2</sub> CO <sub>3</sub>	1.16	0.93	0.00

Mineral distribution in the sampled Edale shale show a rich quartz (30.47%), Mica (22.39%) and Calcite (22.27%) (Table 4.8). Having a rich composition of carbonate mineral, Calcite suggest the probability of a low acid generating potential particularly with a pyrite composition as low as 1.50%. Depending on heavy metal association, the edale black shale may eventually release mobile heavy metals if found to be associated with the weak and easily soluble calcite mineral phase. Other carbonate minerals like Dolomite (0.92%) and siderite (0.93%) only appear at negligible concentrations.

The Whitby black shale show an average quartz composition of 41.46% with mica recording the next largest at 22.61% (Table 4.8). Pyrite composition is averaged at 2.99% and carbonate minerals record the lowest of all three investigated formations, with a calcite averaged at 0.84% and dolomite at 1.91%. No Siderite was detected in the whitby black shale. Pye and Krinsley (1986) in their study of the microfabric, mineralogy and early diagenetic history of the Whitby Mudstone Formation reported that bituminous facies shales similar to those sampled for the study composed mainly

of quartz, kaolinite, fine-grained micas, dolomite, illite-smectite, chlorite, pyrite and calcite. Dolomite, a carbonate mineral composed of calcium and magnesium carbonate commonly found in shale, particularly of Jurassic as reported by Scotney *et al.* (2012) and Hillier (2006) was not observed in any of the shales analysed. However, all peak plots did show possible unidentified peaks at spacings of 2.89 and 2.79 which show similar patterns suggesting dolomite. Hillier reported similar observation of the appearance of a peak at about  $17\text{\AA}$  in diffraction patterns of glycolated clay samples of Jurassic origin. According to Hillier (2006), this peak is due to the presence of random mixed layer of illite-smectite.

When compared with the results compiled in Hillier's appendix (Hillier 2006), the composition of silicate mineral, aggregated as trilayer silicates and dilayer silicates minerals are in good agreement. Because of its unreactive nature, silicate minerals can incorporate trace amounts of otherwise incompatible elements into its atomic lattice during crystallisation and it is not uncommon for this to hold most trace elements in the matrix (White 2013). The degree of dissolution of the mineral and release of PTEs will depend on the capability of forming acids to attack the various phases within the crystalline structure. The presence of pyrite here is indicative of the acid forming composition in shale while calcite show the presence of a buffering potential. It would be interesting to note by static test the maximum acid production potential (AP) with its maximum neutralization potential (NP) and how this affects PTE release potentials during the kinetic release experiments.

#### **4.5.2 XRF Whole Rock Composition**

Major and trace element compositions were determined by X-ray fluorescence (XRF) analysis using an ARL Advantx XRF wavelength spectrometer. Samples ( $n=15$ ) were prepared for analysis by pressing to pellet after passing samples through  $75\mu\text{m}$  aperture sieves are dried at  $105^\circ\text{C}$ . Details of the methodology and analytical procedures adopted are provided in Section 3.2.2.1. Subsequently, precise compositional analysis was done by XRF fused bead analysis after samples were ashed at  $900^\circ\text{C}$  to obtain the loss of ignition (LOI). Results are displayed in Table 4.9. An analytical mass balance was carried out by summing the mean total LOI at  $900^\circ\text{C}$  with the sum of XRF determined elemental composition, assuming all elements were present as oxides. Mean mass recoveries are also shown in Table 4.9. Consequently,

using major and trace element data established for all three shales in the study, interelement correlation matrices have been computed to show major/trace correlations and corroborate some of the observations and conclusions made. For the purpose of this study, results are discussed under two aspects, majors and trace element compositions.

Distribution of major elements in all three sampled formations as shown in Table 4.9 are relatively similar. Si and Al weighted percentages depicting the abundance of silicate fractions in all three formations. A comparison of trace element compositions in all three sampled formation together with similarly assessed trace element compositions in the US. Marcellus formation, as reported by (Bank et al. 2010, Bank 2011) is shown in Figure 4.3. Loss on ignition values are generally much higher in the Lancashire black shale and is not uncommon for high carboniferous shales to have high LOI due to their rich organic matter content. Identified major compositions are largely as expected, showing larger compositions of Si, Ca and Al in all three investigated formations. The predominantly clay associated elements, namely silicate,  $Al_2O_3$ ,  $K_2O$ ,  $Fe_2O_3$  and  $MgO$ , show higher abundance than expected in typical shale and the abundance of calcium in the CLV and DRB black shales suggest the likelihood of an inhibition to acid formation because of its affinity to carbonates or the abundance of calcite.

**Table 4.9:** Chemical Composition of Sampled Shale, Numerian Lancashire Shale (LAN), Derbyshire Edale Shale (DRB) and Whitby Toarcian Bituminous Shale (CLV)

Whole Rock Chemical Composition: Major Elements (%wt)											1	2	Whole Rock Traces Elements Composition (ppm)											
	SiO <sub>2</sub>	CaO	Al <sub>2</sub> O <sub>3</sub>	Fe <sub>2</sub> O <sub>3</sub>	K <sub>2</sub> O	MgO	Na <sub>2</sub> O	TiO <sub>2</sub>	SO <sub>3</sub>	MnO	LOI	Net Total	P <sub>2</sub> O <sub>5</sub>	Sr	Cr	V	Zr	Rb	Ni	Zn	Cu	Ba	Pb	
<i>n. Avg.</i>	15	15	15	15	15	15	15	15	15	15	15	15	15	15	15	15	15	15	15	15	15	15	15	15
<i>Unit</i>	%	%	%	%	%	%	%	%	%	%	%	%	(ppm)	(ppm)	(ppm)	(ppm)	(ppm)	(ppm)	(ppm)	(ppm)	(ppm)	(ppm)	(ppm)	(ppm)
<b>LAN</b>	41.49	4.16	23.30	12.00	3.70	1.53	2.14	1.04	7.11	0.65	<b>10.13</b>	<b>99.76</b>	0.238	883	131	108	174	308	291	378	285	287	160	
<i>S.D</i>	±1.03	±0.12	±0.51	±0.69	±0.17	±0.27	±0.30	±0.08	±0.40	±35.08			±0.08	±37.64	±16.62	±30.93	±9.61	±20.72	±21.11	±41.04	±43.06	±64.25	±17.83	
<b>DRB</b>	34.02	18.92	15.73	11.76	3.96	1.30	2.32	0.92	6.19	0.25	<b>7.04</b>	<b>99.53</b>	450.60	983	83	155	665	234	96	174	244	1107	163	
<i>S.D</i>	±1.59	±0.82	±0.47	±0.59	±0.16	±0.22	±0.35	±0.04	±0.27	±0.05			±7.09	±4.72	±2.11	±6.80	±0.52	±2.98	±2.10	±2.75	±3.11	±4.46	±2.59	
<b>CLV</b>	34.46	23.98	14.92	13.42	13.61	1.45	2.34	1.09	3.78	0.30	<b>7.31</b>	<b>99.48</b>	911	716	79	78	823	287	115	138	140	679	152	
<i>S.D</i>	±1.55	±3.61	±1.10	±1.62	±19.28	±0.25	±0.37	±0.11	±0.74	±0.04			±17.57	±25.03	±7.77	±8.27	±36.74	±31.48	±9.88	±25.76	±23.09	±36.38	±24.14	

*n. Avg.*: Number of Samples Averaged

% wt.: Percentage Weighted Concentration

S.D: Standard Deviation

Columns 1 show the % Loss of Ignition (LOI) and column 2 shows % summation (which is sum of aggregate % wt. and LOI).

Standard Reference Materials: ARSTM 010-2 coal ash, EURO-CRM 776-1, CCRMP blast furnace slag SL1, BCS No. 309 Sillimanite.

Trends in Al and Fe for all sampled formations are important to the study because of their affinity for hosting trace metals. Trace metals distributions offer the most important indication for contaminant identification, not only because of their toxicity but also because they constitute the inorganic compositions that contribute the largest risk to water resource when mobilised from their parent rock. Results show similarities to reported min-eralogical data by Hillier (2006) except for the absence of Arsenic (As). Strontium (Sr) is found in large concentration in all three formations and is indicative of the presence of naturally occurring radionuclides (NORMs), as 12 out of the 16 known naturally occurring Sr are NORMs (Skoryna *et al.* 1964, USEPA 2012). With the exception of Zr and Rb not assessed in Hillier’s compilation and clear differences in reported quantities, all other results show similar trends. Pressed pellet analysis adopted to determine quantitatively the compositions in sampled shale revealed Sr, Cl, Ba, Mn, V, Rb, Ni, Zr, Cr, Zn, Pb, Cu, Mo, Nb, Sb and Ce compositions with Sr and Cl recording the most abundant at (867ppm – 981ppm) and (960ppm – 10,100ppm). Pye and Krinsley (1986) reported similar finds with Jet rock shale from the Whitby Mudstone Formation assessed from pressed powder pellets. Fused bead analysis detailed in Table 4.9 represents the mean of abundance for majors and traces. Cu records 3 to 5 times average compositions in sampled formation in comparison to Vinogradov’s world shale average (Figure 4.4) while Zn and Ni are enriched upto 1.5 times and in some cases 4 times in comparison to Li and Schoonmaker’s reported world shale averages respectively (Li and Schoonmaker 2005a).

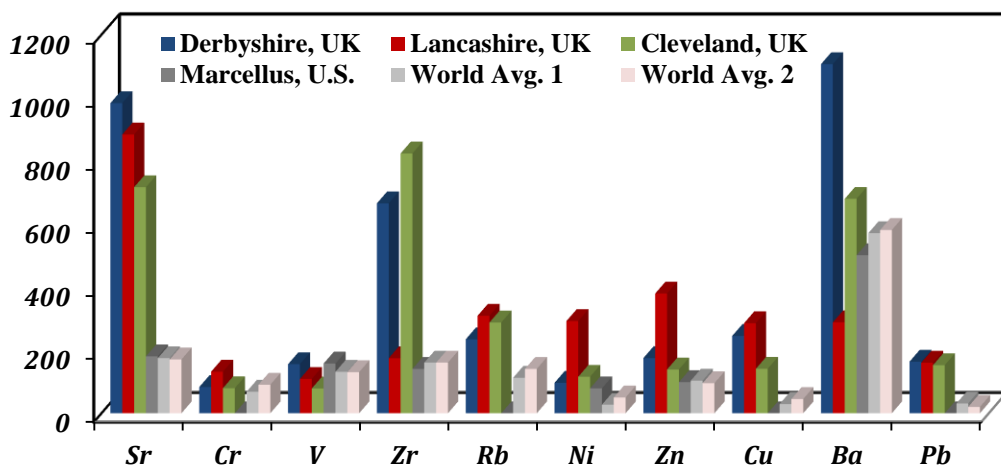


**Figure 4.4:** Comparison of Trace metal distribution in sampled shales and World shale averages compiled by (1) Vinogradov (1967) and (2) Li and Schoonmaker (2005b)

Fused bead trace element composition showed enrichment in V, Cr, Ni, Mn, Rb, Ba, Sr, Zn and Cu. Sr however, remains the most abundant in all three formations. There are however clear disparity in trace element concentrations observed here in comparison with those reported by Hillier (2006) in similar Jurassic shale in the Cleveland basin. Differences in analytical methods could account for this, as well as large variations in stratigraphy for Jurassic aged black shale formations in the Yorkshire area (Scotney et al. 2012). Trace element compositional results showed large signature consistencies with shale values compiled by (Hillier 2006) in clay materials from the British Isles. In all, these data suggest the abundance of trace element in the Numerian Carboniferous black shales from the Forrest of Bowland in Lancashire, the Carboniferous Edale formations of Derbyshire and butiminous black shales from the Whitby formations.

The study has placed particular interest on trace/heavy metal formations in these formation because they constitute the bulk of the inorganic contaminants problematic to treat. In addition, a good number of these heavy metals are known carcinogens and toxic to both the ecosystem and human health. Take for example, Nickle, a known high risk heavy metal that contributes to severe environmental and human health disorders. Nickel's adult inhalation mean daily intake (MDI inhalation) estimated at 0.06 $\mu$ g per day and oral mean daily intake (MDI oral) from food and water combined at approximately 130 $\mu$ g per day is sufficient data that suggest potentially serious health hazards could result from exposure from weathered concentrations alone. Therefore, it is important to draw a clear distinction between bulk concentrations observed and releasable quantities that have the potential to cause contamination. The challenge therefore to determine is what concentrations of observed bulk concentrations would become labile.

#### ***4.5.2.1 Justification for Selected PTE Indicators***

Several trace elements can be detected in any single shale mineralogical study, making it extremely time consuming and cumbersome to accurately monitor in the vast majority of any laboratory investigations. In addition, certain elements detected in trace concentrations are insignificant with regards to mobility studies as they remain largely evasive or unreactive in nature. In a bid to narrow down all identified trace elements to potentially toxic species with greater health or hazardous environmental

implications, a number of selection criteria were employed. The magnitude of detected concentrations, toxicity ranking (maximum concentration limits in drinking water) and the data on the degree of bioaccumulation in humans were used to select indicator trace elements for the rest of the research study (Table 4.10). The drinking water standard is used because risk associated with HDF could have profound effects on drinking water, groundwater or surface waters used as abstraction sources, constituting a risk to human health. Computations for this are presented in Table 4.10 below. The order of magnitude of the ratio between the detected concentration and the toxicity limit in drinking water is recorded as the risk index. The higher the order of magnitude the more severe the risk impact. Results from the risk index identified Pb and the biophile element Ni and V as having the most potential to create significant contamination risk. In terms of detected concentrations, together with the rankings, Cr, Ni, Zn and Cu were selected as indicator PTEs for release monitoring in the ensuing study's objectives. The data on bioaccumulation provides a secondary weight criterion to assess the magnitude of the risk impact. It is additionally important where the values of the risk index are identical (in the case of Ni and V).

**Table 4.10:** Toxicity ranking and a risk index for selection of high risk trace element

Trace	mean Concentration (ppm)			Max Conc. In DW (mg/L)	Ranked by Detected Concentration			Ranked by Toxicity in humans	Risk Index <sup>2</sup>	Biological Half Life in Humans
	LAN	DRB	CLV		LAN	DRB	CLV			
<b>Cr</b>	131	83	79	0.05	8	9	8	4	3	15days for 50%
<b>Cu</b>	285	244	140	2.0	5	3	5	5	2	4 weeks
<b>Ni</b>	291	96	115	0.02	4	8	7	3	4	20-34 hrs.
<b>Pb</b>	160	163	152	0.015	7	6	4	1	4+	28 days
<b>Rb</b>	308	234	287	-	3	4	3	8	-	31-46 days
<b>Sr</b>	883	983	716	4.0	1	1	2	7	2+	18 years
<b>V</b>	108	155	78	0.015	9	7	9	1	4	20 to 40 hours
<b>Zn</b>	378	174	138	3.0	2	5	6	6	2-	154 days
<b>Zr</b>	174	665	823	-	6	2	1	8	-	67 and 65 days

\*Very low toxicity recorded for Rb, no EU or W.H.O limits in drinking water

<sup>1</sup> Mol. weight of the element is computed from the mol. weight of compounds

<sup>2</sup> Index derived from order of magnitude (ratio of mean concentration and maximum concentration in drinking water)

#### ***4.5.2.2 Trace Element Correlation***

The principles governing the distribution of elements in rocks and minerals are well known. Goldschmidt (1958), explained the chemical affinity of an element determines the rock type in which an element will be concentrated, while its ionic radius governs the position it can occupy in a mineral structure. This is important to this study, as trace metal mobility is greatly influenced by the host (associated fraction or phase) in which the trace elements are bound. Any change in the environmental conditions affecting redox environments can have an impact on the major dissolve minerals containing Fe, Al or organic matter and consequently, affect heavy metals associated with such minerals. Correlation is an effective tool that can be used to determine element association with major elements, trace elements and their ratios. In its application, statistical evaluation of the geochemical data was done to reveal trends in distribution of the trace elements using Al and Fe. The relative compositional constancy of natural crustal material such as Al is frequently used as the basis of data interpretation because of its high natural abundance and the relatively small inputs from anthropogenic sources. Lopez *et al.* (2006), stated that proxies employed in the study of sedimentary material should be based on a known relationship between geochemical processes for example, the known similarity in reactivity between Al and Fe. This is because element concentration data suffer from the ‘constant sum effect’ that may lead to spurious correlations. Therefore, the use of elemental ratios between Al and Fe was adopted in investigating correlation (Turekian and Wedepohl 1961, Calvert and Pedersen 1993). However, there are some established associations common in trace element geochemistry. One of such is that Cu, V, Ni, Mo, Co and U are mainly present in organic matter and Sulphur bearing minerals and this correlations have been investigated from the data obtained (Fu *et al.* 2011, Mohialdeen and Raza 2013). Results obtained from the Bowland black shale formations in Lancashire (LAN) show strong positive correlation between V ( $r = 0.90$ ) and Cu ( $r = 0.97$ ) and the silicate fraction. However, trace metals associated with silicates are known to be less readily mobile due to their strong tetrahedral structure which are ionic and partially covalent (Adriano 2001, Bank 2011) and could suggest poor mobility in the Lancashire formations. Regression plots (Figure 4.5 a and b) show the relationships for Ni and Cu.

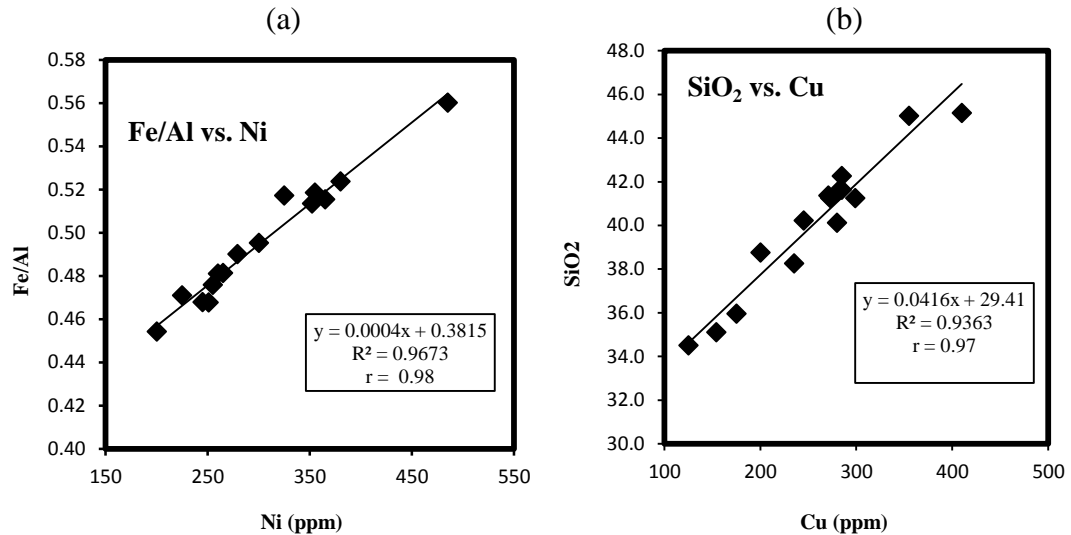


**Figure 4.5:** (a) Cross plot of Fe/Al ratio versus Ni from the LAN black shale (b) Cross plot of SiO<sub>2</sub> versus Cu from the LAN sample set.

There are strong correlations between Fe/Al and Zn (Figure 4.6a) in the Edale formation suggesting Zn association with either the Fe-Mn oxides or the sulphide fractions of the shale matrix. Barwise (1990), suggested that source rock type and depositional environment have a significant effect on the concentrations of V and Ni in source rocks. Barwise (1990), suggested that a high V/Ni ratio indicates marine organic matter input. This was also corroborated by Galarraga *et al.* (2008) who specifically reported that V/Ni ratios higher than 3 indicates marine organic material. It is not uncommon to have trace metals associated with organic matter fractions in shale. Matamoros-Veloza *et al.* (2011), reported that 90% of bulk Selenium in sampled shale from Yutangba, China where associated with the sulphide and the organic matter fraction. By investigating V/Ni ratios (Figure 4.6b) from data compiled from the Edale Derbyshire formation, a strong correlation was observed between V and Ni, rightly indicating the presence and association of some traces with organic matter composition. A V/Ni correlation ( $r = 0.94$ ) is also observed in sampled black shale from the Cleveland basins (Figure 4.7a). These are bituminous shales almost jet black in appearance and it is only expected that a V/Ni ratio will be indicative of organic matter occurrences. Cr association with calcium is indicative of a carbonate association as calcite while dolomite observed from compiled mineralogical data represents the carbonate sink in the shale matrix.

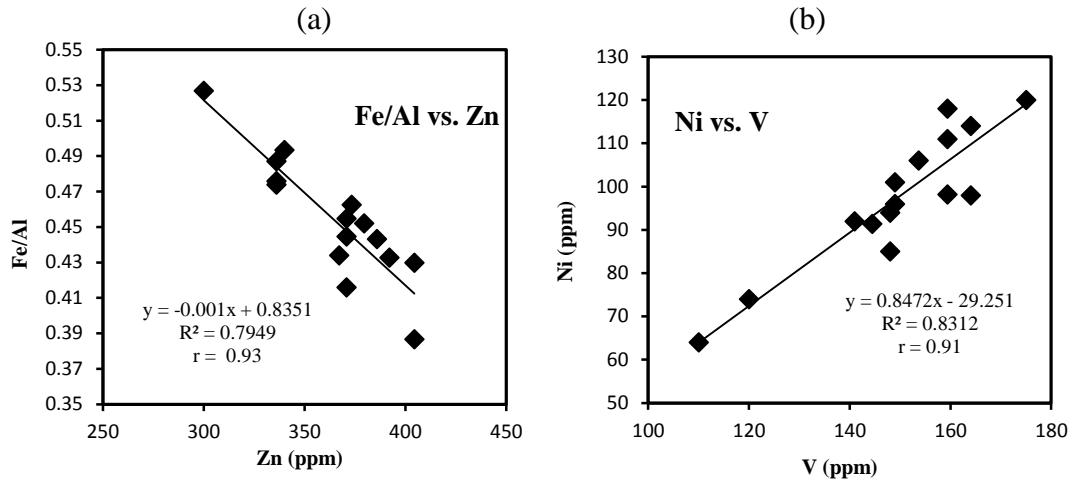


**Figure 4.6:** (a) Cross plot of Fe/Al ratio versus Zn (b) Cross plot of Ni versus V from the Edale shale formation at the Peak National District Park in Derbyshire (DRB).

Because dissolution of shale leads to the formation of other mineral compounds, the adsorption of trace elements onto their surfaces will vary depending on their affinity to these trace elements which is mostly controlled by their oxidation state. V from all three formations showed a very strong correlation to Fe and Zn while Cr showed strong positive correlation with Ca (Figure 4.7b) and Mg. However, it is important to note that the net available concentration of a substance or contaminant in a matrix like shale does not completely define what is releasable. The concept of metal mobility defines what is eventually labile and releasable.

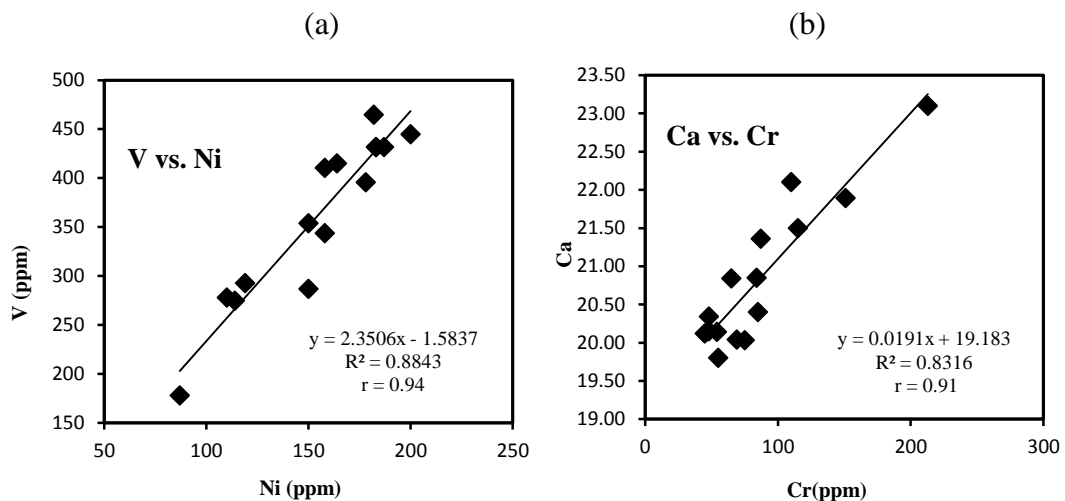


**Figure 4.7:** (a) Cross plot of V versus Ni (b) Cross plot of Ca versus Cr from the Edale shale formation at the Whitby Formation, Cleveland Basin (CLV).

Therefore, a geochemical evaluation of the mineralogical and elemental composition of the studied black shales only provides a qualitative assessment of the obvious

contaminant population. A proper assessment of the UK's shale gas development risk in terms of water contamination, should therefore involve the quantification of releasable concentrations of identified contaminants.

### 4.5.3 Acid Base Analysis

Mobility of trace elements in the environment, particularly in rocks is greatly influenced by the actions of weathering or degradation and this is a function of acid dissolution of the parent material by the rocks inherent ability to generate acids. As part of the research objectives (objectives 1) of determining the physical characteristics of sampled shales, the study assesses the potential for acid formation which are the prerequisite catalyst for rock degradation.

**Table 4.11:** Sulphur and Acid Potential (AP) Determination

<b>Samples Set</b>	<b>S (% , wt.)</b>	<b>AP (Kg/t)</b>
<b>LAN</b>	3.04 ( $\pm 0.31$ )	94.96 ( $\pm 9.91$ )
<b>DRB</b>	2.63 ( $\pm 0.07$ )	82.01 ( $\pm 9.96$ )
<b>CIV</b>	2.69 ( $\pm 0.10$ )	83.88 ( $\pm 9.37$ )

The method involves the assessment of the rock neutralization potential (NP), obtained from the amount of neutralizing bases (carbonates) present in the shale and the acid forming potential (AP), obtained from the total sulphur composition in the shale. Results obtained for sulphur analysis are displayed in Table 4.11. Three static acid base methods (Standard Sobek method, Modified Sobek method and the Modified Lawrence ABA method) are adopted because of the variability with these standard methods resulting in largely inconsistent results in practice. All results are displayed in Figure 4.8. Comparing the acid potential in all three shales Figure 4.8, the Lancashire formation appears the most susceptible to acid generation while the Edale formation and the Whitby formations have comparatively similar potentials. NP values determined by the Sobek method are comparatively larger than the modified Sobek method, thus indicating the dissolution of non-carbonate constituents such as silicates during the hot acid leaching adopted by the Standard Sobek method and the less aggressive use of ambient HCl acid in the modified Sobek test. Fizz ratings ranged from slight to moderate and indicated substantial carbonate content in all three shales. In addition, treatment with peroxide to remove siderite interferences as widely reported

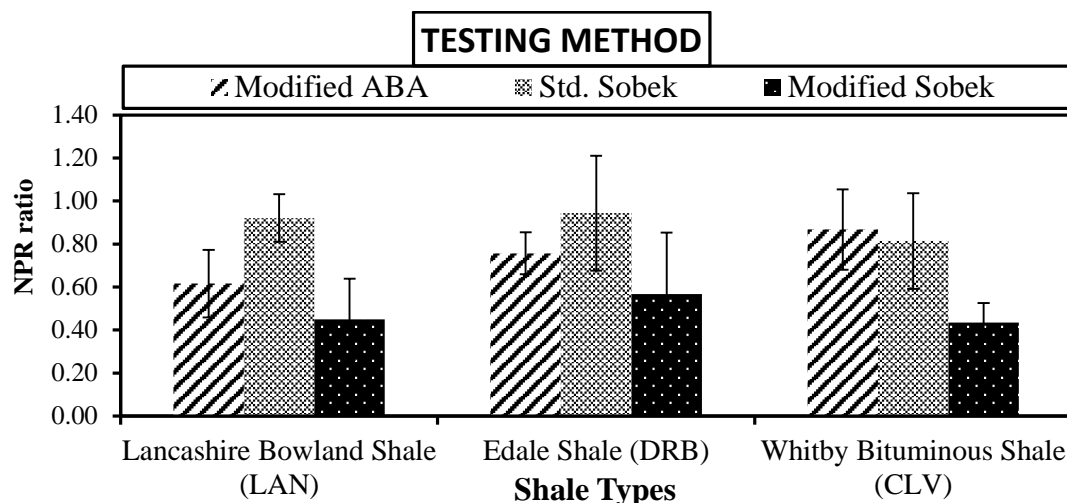


**Figure 4.8:** Plots of NPR test methods for mean Static ratios computed in all three investigated formations using three methodologies i.e. Standard Sobek method, modified Sobek method and the modified Lawrence ABA method

(Skousen et al. 1997, Haney *et al.* 2006) also account for the large differences. According to the modified ABA method, the Edale shale shows the least tendency to neutralise produced acid with an average NP value of 61.65 kg CaCO<sub>3</sub>/t ( $\pm 8.08$ ), while black shale from the Whitby formation showed the largest tendency to neutralize acids from its sulphide mineral with a mean NP value of 71.73kg CaCO<sub>3</sub>/t ( $\pm 12.28$ ). A ratio of NP to AP known as the neutralization potential ratio (NPR) or the acid/base account (ABA) is plotted in Figure 4.9 (a-c). All three static test methods predict potentially acid generating shales ( $NPR < 1$ ) with a few sample sets within the uncertainty region ( $1 < NPR < 2$ ) (Figure 4.9 a and b), when assessed by the modified Sobek and the modified ABA test method, both adopting siderite corrections and carbonating rating instead of the subjective fizz test. The modified ABA test method predicts NPR values of 0.62 ( $\pm 0.16$ ), 0.76 ( $\pm 0.10$ ) and 0.87 ( $\pm 0.19$ ) for the Lancashire, Edale and Whitby black shales respectively. Both Sobek methods tend to suggest the Whitby bituminous shale formation having the highest potential for acid generation with an average NPR value of 0.81 ( $\pm 0.22$ ) and 0.44 ( $\pm 0.09$ ) in the Standard Sobek and Modified Sobek methods respectively. These results seem to suggest that these UK formations are likely to produce acidic rock drainages (ARD) when disturbed and consequently provide the enabling conditions and catalyst for the release and mobility of heavy metals (assuming all heavy metals are mobilised under acid conditions).

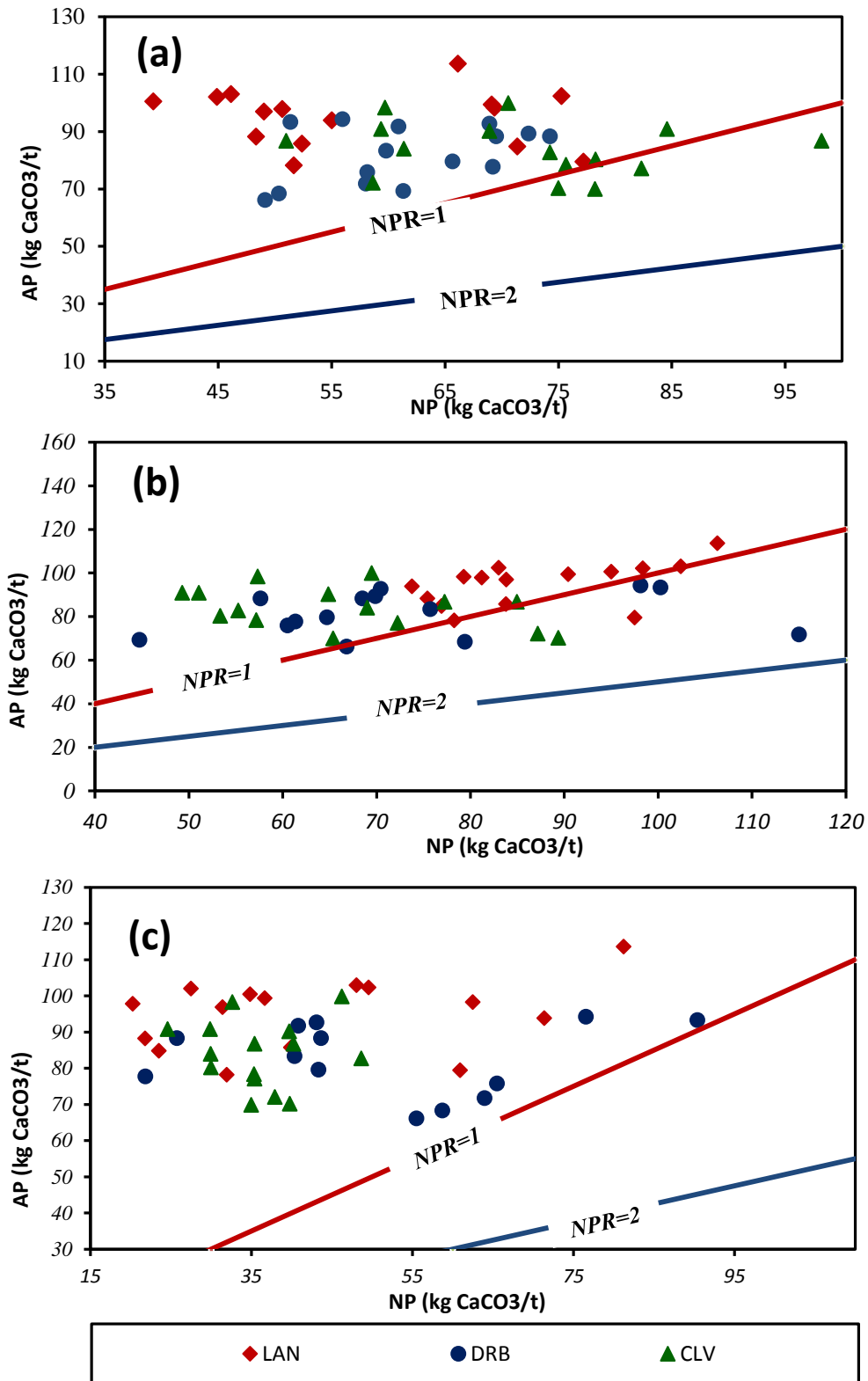


**Figure 4-9:** Plots of the Static ABA analysis for sampled shales (a) Modified Acid Base Method by (Lawrence and Wang 1997) (b) Standard Sobek Method by (Sobek et al. 1978) (c) Studies Modification to the Sobek Method.  
 NPR<1: Potentially Acid Producing  
 1<NPR<2: Uncertainty Zone  
 NPR>2: Non Acid Producing

#### 4.5.4 Sequential Batch Extraction

Having confirmed the likelihood of prerequisite processes for metal release and mobility such as acid formations in the sampled formations, the quantification of releasable concentrations of the selected toxicant indicators remains a question. At this stage of the study, since the bulk mineralogical and chemical compositions of these black shale formations are known, an assessment of releasable fractions of the bulk compositions can be determined. It is widely recognised that the distribution, mobility and release of heavy metals in the environment depends not only on their total concentrations but also on the associated form in the solid phase to which they are bound (Ure 1990, Filgueiras *et al.* 2002). As observed in the results, trace elements show association with certain phases such as organic matter, phyllosilicates, sulphides, etc. and this provides useful information on the release and mobility of these trace metals and in particular, those investigated in this study. To further achieve the chapter's objectives (objective 1), the experimental study evaluates the associated residing phases for the selected toxicant indicators in all three sampled formations and determination of the extent to which these metals could be mobilized. With this information, the likelihood of toxicant release following varying environmental changes such as major anthropogenic changes like fracturing was assessed.

Results show distinct differences in all three sets of black shales (Table 4.12). With the exception of Cu, the percentage recovery for the other heavy metals ranged between 96.5 – 100% suggesting a relatively effective extraction scheme. For Cu, net concentrations in each fraction may be affected by lower recovery factors, but the overall ratio or distribution between fractions is assumed to be relevant. Figure 4.10 shows the distribution of heavy metals from the sequential analysis, (A, B, C and D) showing the distribution by percentages while (E, F, G and H) show distributions by concentration.

**Table 4.12:** Distribution of PTE Indicators Extracted from the 6 Stage Sequential Extraction Protocols

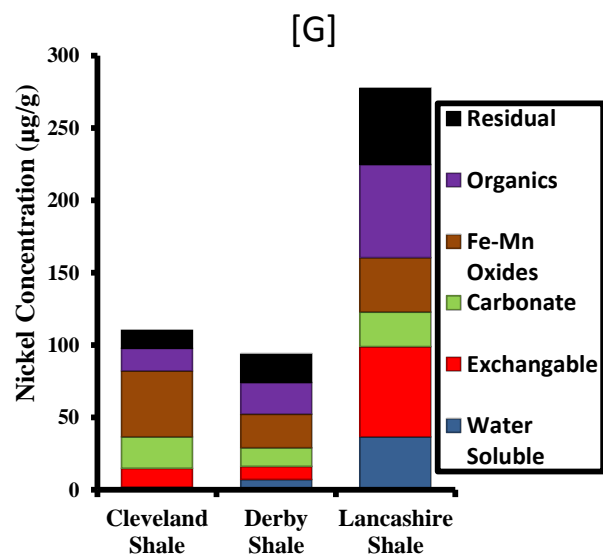
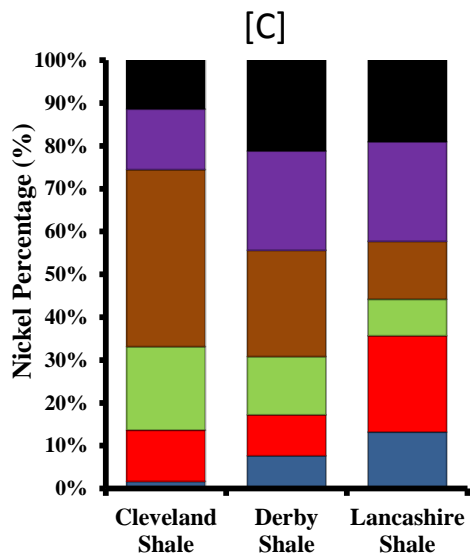
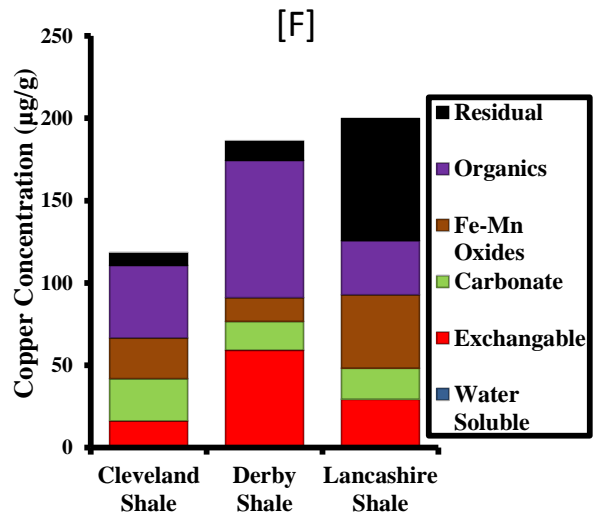
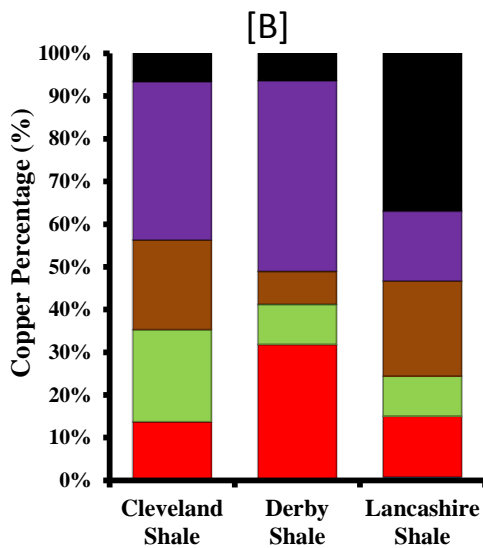
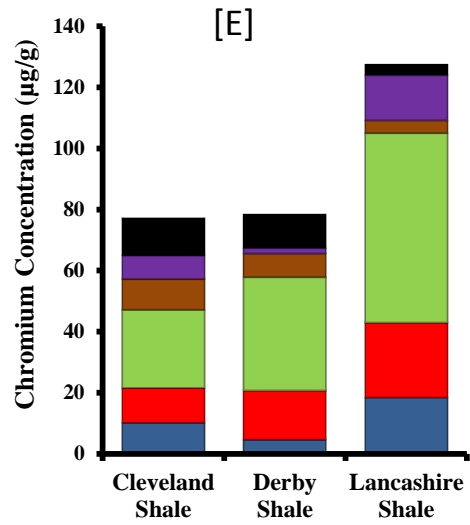
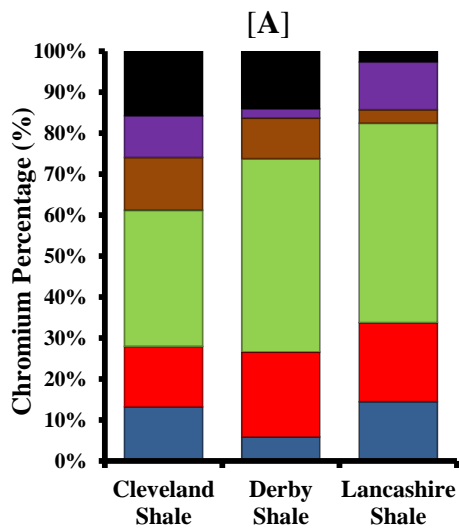
<i>Trace Metals</i>	<i>*Shale</i>	<i>XRF</i>	6 Stage Sequential Extraction (Tessier et al. 1979), modified						<b>Sum of all Fractions [1-6] (<math>\mu\text{g/g}</math>)</b>	<b>**% Recovery</b>
		<i>Bulk Concentration (<math>\mu\text{g/g}</math>)</i>	<i>Water Soluble (<math>\mu\text{g/g}</math>)</i>	<i>Exchangeable (<math>\mu\text{g/g}</math>)</i>	<i>Carbonate (<math>\mu\text{g/g}</math>)</i>	<i>Fe-Mn Oxides (<math>\mu\text{g/g}</math>)</i>	<i>Organics (<math>\mu\text{g/g}</math>)</i>	<i>Residual (<math>\mu\text{g/g}</math>)</i>		
			[1]	[2]	[3]	[4]	[5]	[6]		
<b>Cr</b>	LAN	131	18.40 $\pm$ 2.45	24.60 $\pm$ 2.46	62.00 $\pm$ 3.38	4.20 $\pm$ 0.75	14.80 $\pm$ 0.75	3.40 $\pm$ 0.92	127.40	97.25
	DRB	83	4.60 $\pm$ 1.62	16.20 $\pm$ 3.92	37.00 $\pm$ 4.71	7.80 $\pm$ 0.98	1.80 $\pm$ 0.60	11.00 $\pm$ 3.13	78.40	94.46
	CLV	79	10.00 $\pm$ 4.60	11.40 $\pm$ 5.35	25.60 $\pm$ 6.07	10.00 $\pm$ 1.34	7.80 $\pm$ 1.89	12.20 $\pm$ 2.04	77.00	97.47
<b>Cu</b>	LAN	285	0.80 $\pm$ 0.63	29.30 $\pm$ 4.62	18.80 $\pm$ 2.62	44.60 $\pm$ 1.26	32.80 $\pm$ 2.49	74.20 $\pm$ 1.93	200.50	70.35
	DRB	244	0.20 $\pm$ 0.42	59.10 $\pm$ 7.19	16.50 $\pm$ 9.20	14.40 $\pm$ 0.84	83.40 $\pm$ 6.93	11.80 $\pm$ 1.62	185.40	75.98
	CLV	140	0.20 $\pm$ 0.42	16.00 $\pm$ 2.58	25.60 $\pm$ 2.59	24.80 $\pm$ 2.15	44.00 $\pm$ 2.11	7.80 $\pm$ 1.23	118.40	84.57
<b>Ni</b>	LAN	291	36.60 $\pm$ 2.12	62.40 $\pm$ 1.71	23.80 $\pm$ 2.10	37.60 $\pm$ 1.78	64.40 $\pm$ 1.17	53.00 $\pm$ 1.94	277.80	95.46
	DRB	96	7.20 $\pm$ 0.79	9.00 $\pm$ 4.67	12.80 $\pm$ 1.75	23.40 $\pm$ 1.65	21.80 $\pm$ 1.40	20.00 $\pm$ 3.30	94.20	98.13
	CLV	115	1.80 $\pm$ 1.40	13.20 $\pm$ 1.62	21.60 $\pm$ 2.27	45.60 $\pm$ 1.71	15.60 $\pm$ 2.32	12.60 $\pm$ 1.65	110.40	96.00
<b>Zn</b>	LAN	378	5.24 $\pm$ 2.17	25.80 $\pm$ 3.01	100.60 $\pm$ 7.41	119.40 $\pm$ 5.80	49.60 $\pm$ 4.84	71.60 $\pm$ 2.76	372.24	98.48
	DRB	174	42.00 $\pm$ 1.94	23.80 $\pm$ 2.66	4.31 $\pm$ 1.35	74.40 $\pm$ 5.52	21.40 $\pm$ 0.70	7.00 $\pm$ 2.40	172.91	99.37
	CLV	138	21.40 $\pm$ 1.26	33.60 $\pm$ 1.90	9.60 $\pm$ 1.58	44.60 $\pm$ 2.32	11.80 $\pm$ 1.48	11.20 $\pm$ 0.79	132.20	95.80

\* LAN - Black shale from Bowland formation Lancashire

DRB - Black shale from the Edale formation Derbyshire

CLV - Bituminous Black shale from Whitby Coast

\*\* % Percentage Recovery = (sum of all fractions \* 100)/Bulk Concentration



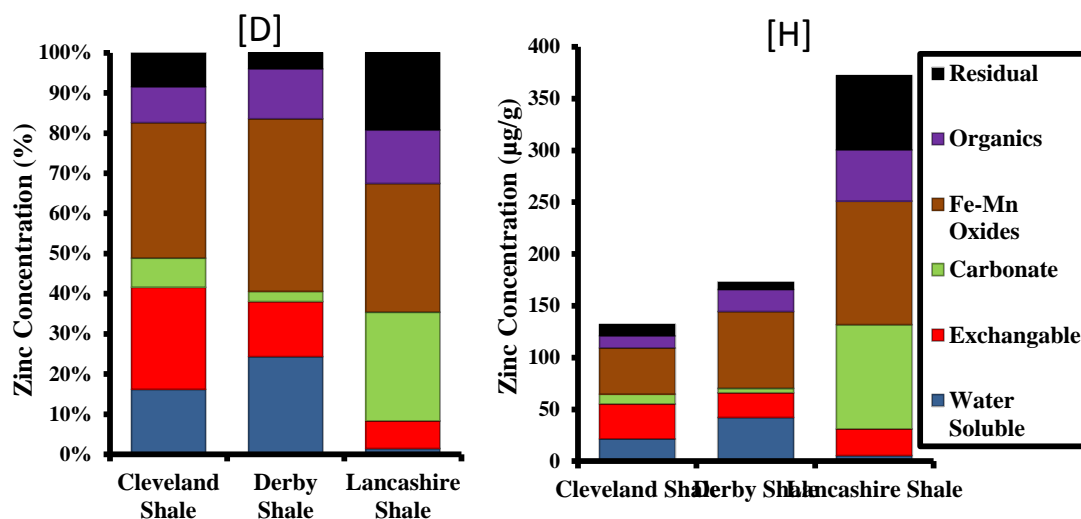


**Figure 4-10 [A-H]:** Distribution of indicator PTEs in the Sequential Extraction protocols applied, [A-D] in percentages, [E-H] in concentration ( $\mu\text{g/g}$ ).

Cr association to the carbonate fraction is highly pronounced, representing 33.2%, 47.2% and 48.7% in sampled set CLV, DRB and LAN shales respectively. Highly mobile water soluble and exchangeable fractions account for a combined 27.8% 26.6% and 33.7% in the sampled sets respectively. Apart from an observed relatively poor percentage recovery of Cu, results vary widely in all three investigated shale. Water soluble Cu is almost non-existent with mean extractible percentages at 0.4% (LAN), 0.1% (DRB) and 0.2% (CLV). Cu association to organic and sulphide fractions appears predominant in both Cleveland (37.2%) and Derby (44.8%) shales. Lancashire shale show a poor response to selectivity expected from the reagent used as 37.1% of Cu remain associated with residual fractions. Nickel association to the Fe-Mn oxide fraction is well pronounced in the Cleveland shale (41.3%) and maintains a fairly even distribution in both Derby and Lancashire shale. Mobile fractions account for 33%, 30.8% and 44.3% in the Cleveland, Derby and Lancashire shales respectively. Zn is clearly associated to large extent with the anhydrous Fe-Mn Oxide fractions in all three shales as shown in Figure 4.10, validating the results obtained from earlier trace element correlations. Immobile Zn averages at a mere 8.3% in the Lancashire shale. A summary of results received from the characterisation study for all sampled shale has been presented in Table 4.13. This has formed the basis of general results discussed.

**Table 4.13:** Summary of Characterisation Results for all Three Investigated Black Shale Formations

Sampled Shale	Lithology	Trace element population	Potentially Toxic Compositions	Total Sulphur Composition	Acid Potential (AP)	*Average Neutralization Potential (NP)	**ABA Static Analysis	Heavy metal (Cr, Cu, Ni & Zn) Mobility
Lancashire Carboniferous shale (LAN)	Dark grey shaly mudstone with occasional calcareous mudstones and siltstone.	Ba, Ce, Cr, Cu, Mo, Nb, Ni, Pb, Sr, Sb, Rb, V, Y, Zn & Zr	As, Cr, Cu, Ni, Sb, V, Y & Zn	3.04 (± 0.31)	94.96 (± 9.91)	62.50 (±22.52)	Potentially ARD generating with mean NPR ( 0.66 ±0.24)	Cu recovery was relatively poor recording a mobility factor of just 0.24 and a recovery efficiency of 70.1%. Zn relatively mobile with a combined 67.4% of extractible Zn associated with the water soluble, exchangeables and carbonate fractions.
Derbyshire Shale Carboniferous (DRB)	Very black laminated shale with prominent layers visible. Brownish colourations on weathered samples show indications of iron enrichment. Shale shows sequence of interbedded sandstone and siltstone.	Ba, Sr, Cr, P, Cu, V, Zn, Zr, Ni, Rb & Pb	Cr, Cu, Ni, V, Zn & Pb	2.63 (± 0.07)	82.01 (±9.96)	61.58 (±15.56)	Potentially ARD generating with mean NPR ( 0.76 ±0.19)	Cr found mostly associated with carbonates and exchangeables. Almost half extractible Cu compositions associated with the organic fraction. Largest Ni association found in hydrous Fe-Mn Oxides and organic matter. Zn resides predominate within the hydrous Fe-Mn Oxides phase.
Cleveland Jurassic Shale (CLV)	Grey to black shale with typical fissiled in nature, some evidenced of intermittent carbonate beds and silicate limestones	As, Ba, Cr, Cu, Sr, Nb, Ni, Rb, V, Y, Zr & Zn	As, Cr, Cu, Ni, V & Zn	2.69 (± 0.10)	83.88 (± 9.37)	58.21 (±19.36)	Potentially ARD generating with mean NPR ( 0.71 ±0.23)	61% of extracted Cr is of highly mobile residing in the water soluble, exchangeables and carbonate phases. Zn associated mainly with hydrous oxides and nearly half of Ni resides in the organic phase while very negligible Cu is mobile. Recovery efficiency ranged btw 84.6% - 97.5%

\*Average NP is average computed NP values for all 3 methods

\*\*ABA Static analysis computed the potential for ARD from the ratio of the NP to AP

## 4.6 General Discussion/Result Significance

The use of some form of standard procedures provides rock engineers the ability to determine the rock properties that have engineering implications to a design or model. Standard procedures have been adopted here with the aim of understanding those physical and geochemical properties with a cause and effect on toxicant release from the studied black shale formations. The dark lithological appearances of all three sampled shales suggest their development under anoxic conditions which is indicative of a reducing environment predominant with shales having more than 1% carbonaceous material. A common characteristic often associated with these shale types is their enrichment in several metals mostly precipitated or fixed into sulphide minerals and organic materials phases (Horan et al. 1994, Peng et al. 2005, Peng *et al.* 2009a, Peng et al. 2009b). Often, dark coloured shales are associated with high organic matter content which in petrological terms is also associated with an increased potential as a hydrocarbon source rock. Whether the darkened colouration in shales relates to its increased potential to house toxic contaminant has not been investigated. By virtue of the observed stratigraphy during sampling, it is not uncommon for these shales to have a wide variety of mineralogical phases. Sampled black shale from the Edale formation (DRB) showed evidence of iron enrichment observed by the brownish decolouration on weathered unit. With Fe being a notable sink for potentially toxic heavy metals, the association of trace metals with other major element composition was further investigated. The soft lustre of sampled black shale from the Forest of Bowland, Lancashire, revealed the possibility of easy degradation in comparison with the hard gritty textured bituminous shale from Whitby. If these observed lithological properties were to suggest the potential for toxicant mobility and release, the sampled black shale from the Whitby coast and the forest of Bowland, show more tendency to support heavy metal release due to their texture, colour and lustre.

From the mineralogical perspective, all three shales show variable compositional assays however, their potential to generate acid drainages have been investigated by examining the mineralogical data obtained. The relatively larger solubility of the Lancashire black shale has been attributed to the majorly (31.98%) Mica composition while a majorly quartz compositions (41.46%) accounts for the poor solubility a metal

releases observed in the CLV black shale. The potential for acid dissolution of the shale matrix has also been examined from the mineralogical data obtained. A suppression of the acid forming propensity can be achieved by a rich carbonate mineral phase. Interestingly, the Edale sampled black shale, with the largest observed carbonate mineral content (calcite-22.2%, dolomite-0.92% and siderite-0.93%) does not translate to an equally high NP value. NP for the DRB shale records an average 61.58 (kg CaCO<sub>3</sub>/t) with the LAN shale recording a slightly higher average of 62.50 (kg CaCO<sub>3</sub>/t). Pyrite composition in the LAN shale records the largest with an average (5.62%) explains the relatively larger release and mobility data obtained. If trace metals in these shales are associated with the most abundant mineral phase, then highly soluble LAN shale will release substantial trace metals in comparison with the less soluble CLV shale. Figure 4.11 shows that all studied lithologies exhibiting significant contents in clay minerals (>40%) as expected in most marine bands and calcareous mudstones. Also evident is the limited enrichments in the brittle carbonate phase as studied lithologies show largely phyllosilicate and quartz.

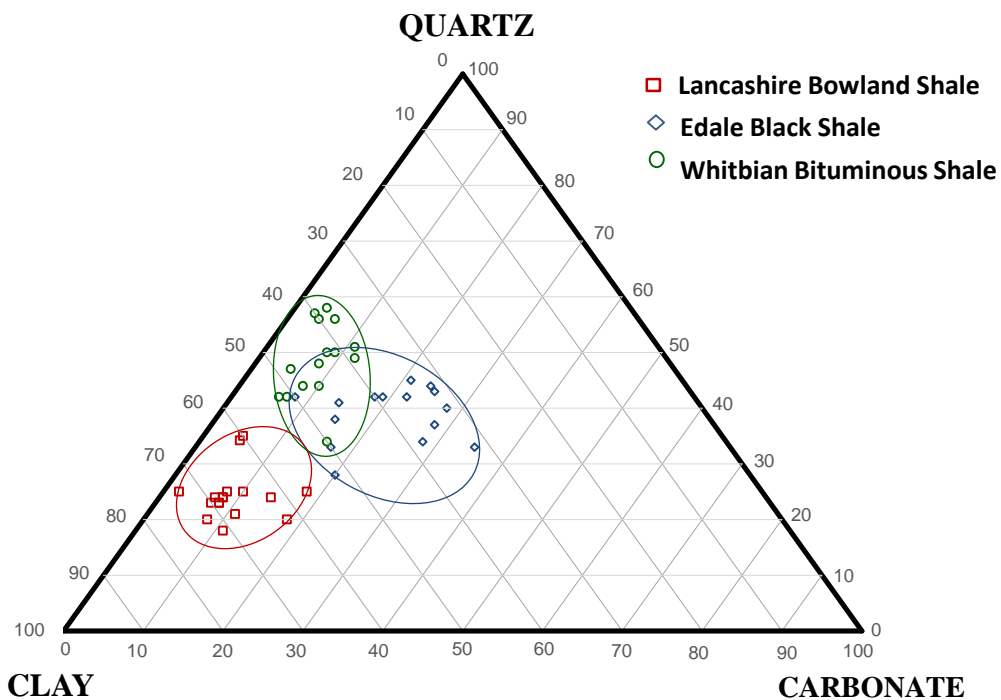


**Figure 4.11:** Mineralogical distribution of quartz, carbonate, and clay in all three investigated formations.

Trace metal association with major elements like Al and Fe and their ratios were examined with a correlation analysis as this reveals possible release trends that can give indications of toxicant release following release of residing host phase. With the investigated traces, a few observed association include Cu's positive correlation with the strongly bonded silicate fractions in the LAN black shale as well as Zn and Ni association with Fe. It is arguably possible that with Fe associated mostly with pyrite and siderite minerals, dissolution of these mineral phases will inevitably release the biophilic traces metals Zn and Ni. Similar trends are also observed in black shale from the Whitbian formation (DRB). V, Ni and Zn all show strong (>85%) correlations with Fe. It is not uncommon for bituminous shales particularly from the Whitbian formation to show increased compositions of heavy metals as widely reported by (Krauskopf and Bateman 1955, Dunham 1961, Gad *et al.* 1968).

An assessment of the acid generating potential of the sampled shales was investigated to assess the likelihood for metal mobility as this is a precursor for shale dissolution and eventual toxicant release. The study adopted a correction of the interference effect suffered from siderite following its identification in the mineralogical assessment. The resultant effect is a reduction in the additional alkalinity produced by the siderite composition during NP determination. Consequently, NP values as determined by modified Sobek method are generally lower as illustrated in Figure 4.12.

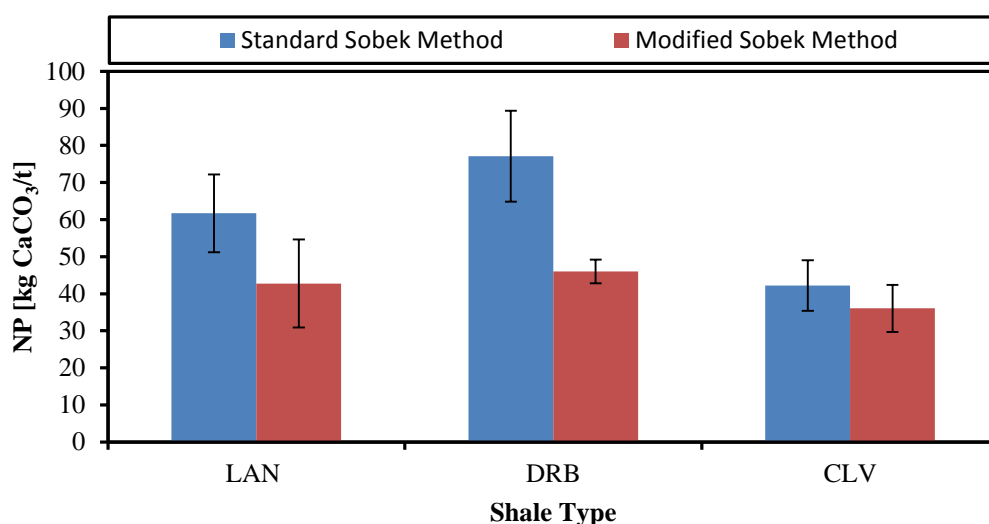


**Figure 4.12:** Comparison of Average NP values determined by the standard Sobek and the Modified Sobek Method

The results show that the carboniferous Edale black shale formations from Derbyshire have the highest potential to neutralize produced acid from its sulphide mineral. These results can also be seen in the mineralogical data where calcite composition reported for the DRB shale is averaged at 22.27% and the ternary plots which show a slight deviation towards the carbonate scale. In accounting for ABA, the data suggest as expect the DRB shale have the highest potential to produce ARD. In reality however, this does not equate to having the largest potential for heavy metal release as other factors such as the bulk concentration and mobility will jointly affect the release potential. What has however been achieved here is results on the potential for solubility by acid dissolution.

Data obtained from adopted batch extractions however reveals tangible information on mobility of identified PTEs. With shale being rich in organic matter, a keen interest was placed on heavy metals associated with the oxidisable organic and sulphides fraction. It is believed that the water soluble and acid soluble traces are readily labile following fluid rock interactions. Cr appeared to be readily mobile in all three formations, with a bulk of Cr associated with the Carbonates. Together with readily exchangeable and relatively labile water soluble fraction hold up to 60% of bulk Cr LAN (82.4%), DRB (73.8%) and CLV (61%). The largest non-labile Cr represents a small average of 15.8% (residual) in the CLV shale with the LAN shale showing a negligible 2.7%. Cu's poor recovery was anticipated following positive correlation with the strongly bonded silicate phases observed during the elemental analysis. Despites minimal recoveries, Cu in the Edale shale and Whitbian shale are predominantly (DRB-45%, CLV-37.2%) associated with the organic matter fractions while a bulk of Cu in the Lancashire shale (37%) are associated with the non- labile residual fractions. Ni appears to be hosted primarily by the Fe-Mn, organics and exchangeable fractions. Ni in the LAN formation reside primarily with the organics (23.2%) and exchangeable fraction (22.5%) with a reasonable percentage remaining non labile in the residual fraction. 41.3% of bulk Ni is associated with the hydrous oxides of manganese and iron (Fe-Mn Oxides) in the CLV shale and considering that this phase is thermodynamically unstable under anoxic circumstances as typical at fracture depths, substantial release of Ni is expected (Tokalioglu *et al.* 2000, Zorpas *et al.* 2000). It appears however; that Ni is appreciable mobile with average mobile

fractions estimated at 44.3%, 30.8% and 33.2% for LAN, DRB and CLV shales respectively. In terms of releasable concentration, Zn accounts for the largest releasable concentration in the LAN shale with a mean extracted concentration of just under 300mg/L. Data obtained show the a bulk of Zn is associated with the Fe-Mn oxide fraction (LAN-32.1%, DRB-43% and CLV 33.7%). Water soluble Zn is quite pronounced in the DRB and CLV shales at 24.3% and 16.2 % respectively, whilst the LAN shale records near negligible mean average of 1.4%. A significant proportion of Zn is mobile (associated with the readily releasable water soluble, exchangeable and carbonate fraction) as mobile Zn averaged at 35.3%, 40.6% and 48.9% in the LAN, DRB and CLV shales respectively. With the exception of Cu and Ni, significant proportions (< 45%) of the investigated traces are associated with the readily releasable and mobile water soluble, exchangeable and carbonate fraction. This is indicative of the increased direct risk of Cr and Zn contamination from the fractured formations as a result of mere fluid-rock interactions and acid development within the formation. Considering that an additional 38% (LAN), 52.8% (DRB) and 58.1% (CLV) of Cu and 36.7% (LAN), 47.9% (DRB) and 55.4% (CLV) are considerably mobile following microbial mediated degradation at fracture depths, it is very likely that an unprecedented release of mobile toxic trace metal composition is released following the fracturing of prospective shale gas formations.

#### **4.7 Limitations of Experimental Study**

Although the chapter objectives have been achieved, there are some unavoidable limitations. The use of non-core samples have been adopted to account for the typically random structure of shale in a prospective formation. Sampled shales have been disturbed from their preferred natural state by pulverisation and particle size reconstruction, in an attempt to simulate the effect of drilling during a shale formation development. The use of particle size reconstruction is unavoidable due to the proposed leaching methodology to be adopted. Sulphur component determination have been used to estimate the total pyrite composition rather than a direct quantification of pyrite composition in each sampled shale. This method have been adopted to account for the possible presence of other sulphide minerals which may contribute additional concentrations of sulphur. The use of Aquaregia for total digestion of shale was

adopted rather than hydrofluoric acid which is more efficient at completely digesting rock specimens. Hydrofluoric acid is however, prohibited for use in the research laboratory at the School of Civil Engineering and therefore, Aquaregia was adopted as an alternative.

#### **4.8 Summary and Conclusion**

In the presented study, the physical and geochemical characteristics of three sampled prospective UK shale gas formations have been investigated to assess the potential for toxicant release and mobility trends. Physical characteristic of the investigated shales have hinted on the ease of matrix solubility and increased weatherability or degradation following anthropogenic disturbances like fracturing. Geochemical characteristics have shown the possible occurrence of mobile and potentially toxic trace elements such as Cr, Cu, Ni, and Zn in potentially acid producing shale formations. Further investigation of release and mobility has revealed the possible release of unprecedented concentrations of the target trace metals following anthropogenic disturbances likened to fracturing these formations. It is understood from this investigative study the prospective gas formations returning wastewater generated from fluid rock interactions are likely to hold substantial concentrations of toxic inorganic compositions.

## Chapter 5. Column Kinetics: Natural Weathering Simulation

### 5.1 Introduction

Jared *et al.* (1999), stated that the unambiguous speciation of contaminant metals in soils requires an integrated approach, using both spectroscopic techniques and leaching tests. Several such studies have demonstrated the importance of an integrated investigative approach that employs a range of analytical techniques to evaluate toxic metal distribution and mobility. In terms of distribution, it has long been asserted that the chemical, physical and biological behaviour of trace and heavy metals in soils, rocks and the environment control their movement and fate (Forstner 1987, Hodson 2002, Roberts *et al.* 2005). Therefore, in a bid to understand contaminant distribution in the investigated formations, the previous Chapter's characterisation study helped to elucidate some of the properties that impact the fate of PTE. However, potentially toxic metals are rendered mobile and free to move within natural systems, and evidence for this introduction can be found in freshwater bodies, marine and lacustrine sediments, soils, ice, vegetation, human and animal populations. Once introduced into a particular environment, metals are not necessarily restricted to their initial host matrix as there is a dynamic cycle between all of the aforementioned phases (Roberts *et al.* 2005). Hence, a comprehensive investigation must in some way incorporate mobility into the risk assessment.

Several processes such as natural and even anthropogenic disturbances can influence mobility and consequently, their releases. For natural release in the case of black shale formations, this can occur by natural degradation or weathering and would contribute a small fraction of contaminant pollution to receiving waters. In the case of shale gas development however, contaminant release following anthropogenic processes may constitute a reasonably sizeable fraction and this can be used as a clear indication of contamination risk from an industrial process. So an integrated comprehensive risk assessment would require differentiating natural releases from anthropogenic releases caused by fracturing and shale gas development. Clearly, knowledge of the release potential under natural weathering conditions is required firstly as a benchmark for release potential. Subsequently, releases from anthropogenic processes can be compared to provide a view of the risk impact from fracturing these gas prospective

UK formations. There remains to date (Oct 2015) no comprehensive laboratory based risk assessment on the impact of shale gas development on water resources in the UK and the potential for contamination release following hydraulic fracturing. However, several publications in the past year have reviewed the potential risk impacts from proposed UK shale gas development (Wood et al. 2011, Mair *et al.* 2012, The Royal Society 2012). These and other studies have been criticized for not providing scientific data but drawing analogies with the US scenario.

One method of simulating releases from a heterogeneous material like shale is to adopt a kinetic leaching test that mimics fluid-rock interactions. By mimicking fluid rock interaction required for the release of contaminants into solution, potential influences on water resources can be investigated. Kinetic test methods have been adopted in several mobility studies (Stollenwerk and Runnels 1977, Chichester and Landsberger 1996, Reemtsma and Mehrtens 1997, Frostad *et al.* 2002, Falk *et al.* 2006, Shaw 2006, Lavergren *et al.* 2009a). It has also found use in addressing the ambiguous results for mines with low amounts of sulphur and carbonates, where it is difficult to predict whether water quality will be alkaline or acidic over time (Frostad et al. 2002, Sáinz *et al.* 2002, Akabzaa *et al.* 2007). Originally designed to provide information that can be used to predict mine drainage quality that may occur from mining operations and weathering, this kinetic method provides a useful means of assessing anthropogenic impact on prospective shale gas formations. The method is additionally designed to overcome the three main limitations of the static tests, the most important to this research being the determination and prediction of component concentrations. A kinetic leaching study on three prospective UK shale gas formations is therefore presented here and this method has been adopted in a fixed laboratory to predict water quality characteristics such as pH, alkalinity and the solubility of metals from disturbed sites discharges using observations from sample behaviour under simulated and controlled weathering conditions. The study experimentally simulates the natural weathering of all sampled shales to provide baseline data on natural release potentials void of anthropogenic disturbances for the studied formations. Contaminant release from the studied shales will involve the transfer of chemical elements from the shale matrix surface to the surrounding fluid.

## 5.2 Chapter Objectives

This study requires the knowledge of release patterns of the selected trace elements under prevailing natural environmental conditions. Understanding this release and its variation with time will provide a deeper understanding of the chemistry of the resulting products following fluid rock interaction. If weathering patterns are observed and have an influence on heavy metal releases, these metals concentration data could be indicative of the degradation of these rock samples under natural weathering conditions and the quality of drainage discharges that could be expected. Hence, the objectives of the experimental study in this chapter are as follows;

1. Using the studied shale lithologies, run a laboratory scale simulation of fluid rock interactions typically occurring during natural degradation and weathering, noting any observable weathering patterns and its influence on long term releases of trace heavy metal components.
2. Using the leaching data, observe the potential for the shales to produce acidic, circumneutral or alkaline drainages. This being a function of the relative weathering rates of the carbonates and pyrite compositions

This Chapter provides answers to the following questions;

1. Do the investigated UK prospective shale gas source rocks (already characterised as having high sulphur content and relatively low calcium carbonate equivalents NP values) follow a weathering pattern when degradation/weathering is simulated?
2. Can this weathering pattern translate to a release pattern for the investigated trace heavy metals used as indicators for contamination?
3. What is the potential drainage quality (i.e. acidic, circumneutral or alkaline) of the studied formations based on natural (non-anthropogenic) degradation or weathering?
4. Results obtained will serve as useful baseline data to compare anthropogenic influences (such as hydraulic fracturing) on degradation patterns and contamination release of the same studied lithologies.

## **5.3 Methodology**

The chosen method adopts a leaching column experimental setup that allows the accelerated weathering of the sampled shales. The method was design to mimicking the solubility and mobility of indicator heavy metals as would occur in nature if shales were exposed to weathering elements. To achieve the intended objective, the standardized leaching column protocol, EPA 1627: Kinetic test method for the prediction of mine drainage quality, formerly known as the Acid Drainage Technology Initiative's weathering procedure 2 (ADTI-WP2) is modified for this study.

### **5.3.1 Laboratory Simulation of Natural (Weathering) Releases**

Tap water was used as a leaching agent to simulate natural weathering of the sampled formation. A 12 week leaching run designed to simulate releases under natural weathering conditions commenced in July 2013 with 6 initial column flushes until relative standard deviations between conductivity readings were less than 20%. Laboratory supplied air at 4litres per min was supplied via a flow meter and bubbled through a carrier boy containing tap water. The saturated air rising to the top of the carrier boy is channelled to the leaching columns via a flowmeters designed to allow a flow of 1L/min into each column during the 7 days humidification cycle. The flow into each column is further regulated by a flow meters assigned to regulate flow to 1L/min ( $\pm 0.2$ ). A loading tube fitted with a funnel is attached to the inlet designed to supply leaching solvent. Leachates are collected following the 24hr saturation cycle via the water inlet tubing and immediately analysed for pH. Total water collected is measured and samples for trace metal determination are refrigerated until analysis. Week 12 analysis was completed in October 2013. Following the 12 weeks leaching run, samples in each leaching columns are removed dried, re-weighed, re-sieved and particle size distribution re-evaluated to determine the distribution after leaching. Surface area via the BET analysis was also re-determined following the end of the 12 week leaching. Leaching columns were cleaned out and prepared for the next batch of leaching experiment.

### **5.3.2 Justification of the Chosen Leaching Method**

The leaching column kinetic method was adopted to provide sample effluent chemistry. Although there are several kinetic test methods available, the leaching column method is the most flexible and easily redesigned to suit the experimental objectives. It is generally agreed that the major disadvantages of the leaching column method is its lack of an accepted standardised test method and the considerable number of variables in the setup, variety of test apparatus and operating procedures which prevents a unique interpretation of data and meaningful comparison with other studies or different lithological settings (Caruccio and Geidel 1978, Caruccio and Geidel 1986, Hornberger and Brady 2009). However, these disadvantages are of little significance to this study due to a number of reasons. Firstly, this study applies the principle and working conditions of the leaching kinetic test in achieving its aim of simulating fluid rock interactions and hence, considerable flexibility of the experimental method is required to achieve the research objective. Secondly, there are current standardised methods for leaching column test such as the EPA 1627 method (U.S. Environmental Protection Agency 2011) and these standard methods provide a stipulated test apparatus, setup and running operations that can be adopted or modified to achieve the experimental objectives. Finally, with the adoption of three sampling lithologies in this study, a meaningful comparison can be achieved.

In addition to this, the leaching column provides a wide range of models that can be experimentally defined such as downward displacement of mine waste pore water by supernatant water to simulate seepage to ground water or model mine waste behaviour under varying disposal conditions. This flexibility with the leaching column kinetic method makes it the preferred experimental method applicable to this study. With the added advantage of being a performance based method allowing for modification of the procedures to improve performance, overcome interferences and improve accuracy or precision of the results.

Column testwork may be undertaken to determine the kinetic behaviour of waste rock, ore or tailings stored on the surface and exposed to atmospheric weathering (sub-aerial storage), or stored under water cover (sub-aqueous storage). In either case, the experimental plan is to monitor water (leachate) quality with time by cyclic (weekly

or monthly) sampling. Unlike the humidity cell procedure, there is little, if any, standardization of column test work procedure, allowing considerable flexibility. This flexibility permits column operation to be highly site or material specific with regard to material particle size and size range (which for waste rock, ore or drill core is usually greater than that used for humidity cell tests, but still less than that of site conditions), sample mass, water infiltration or flow rate and degree of oxygenation. Because of the lack of standardization of the procedure some regulatory agencies view column testwork as supplementary to, or confirmation of, humidity cell testwork, rather than an alternative to humidity cell testwork. (Josh *et al.* 2012) states that trickle leach column tests have the following disadvantages (over humidity cells):

1. The primary weathering products may be retained and therefore leachate chemistry cannot be used as a measure of the relative rates of acid generation and neutralization, and of times to mineral depletion.
2. They are run at the laboratory temperature often with a reduced particle size, and without seasonal variations and the extremes of both temperature and precipitation. Consequently, they provide poor analogues for heterogeneous drainage and the secondary mineral precipitation and dissolution, the controlling factors for metal leaching under all but the most acidic pH values.

The first listed disadvantage appears to ignore the fact that humidity cell tests are intentionally accelerated and cannot be used to predict field rates of acid generation and neutralization; the second disadvantage is questionable, since column tests are invariably run on coarser material (except for tailings) than humidity cells and can be (and are) run with simulated site seasonal precipitation and temperature variations. Sub-aerial column (sometimes referred to as "trickle leaching") testwork is conducted to simulate the leaching effects of precipitation infiltration to, and drainage from, material stored at the surface and exposed to the atmosphere. Water addition rate to the column may be either fixed (i.e. a certain amount per cycle), or it may be varied to simulate the seasonal variations at the site. The column is open to the atmosphere so that there is no oxygen barrier, but there is usually no forced oxygenation as with a humidity cell. Similarly, the column is operated without aggressive flushing so that oxidation products may accumulate at particle surfaces in addition to being removed

in the leachate. This behaviour parallels field conditions and, as a result, leachate analyses from column testwork are a better indicator of expected water quality than leachate analyses from humidity cells - particularly if the column infiltration rate is varied to simulate site conditions. Column operational temperature can also be varied to simulate site conditions, although this is rarely done.

### **5.3.3 Sample Preparation**

Collected samples were reconstructed to particle sizes as described in sample preparation process discussed in Chapter 3. This ensures that the conditions of exposure are standardized for all sampled shale types, thereby facilitating the uniform exposure of samples to weathering conditions and collection of leachate. Details of sample collection and all preparations done to sample before leaching procedure are documented in Chapter 3.

### **5.3.4 Experimental Design and Setup**

A leaching column experiment was designed to assess investigated trace elements releases. Whereas in field studies, the objective is assessing the degradation of shale and the release of identified toxic elements over a specific time scale, in laboratory studies, the objectives include the additional task of mimicking realistic site/environmental conditions before trace metal releases can be assessed. There are no reported standardized leaching column experiments due to the varying nature of samples and materials that could be investigated i.e. (soil, rocks, waste, wood etc.), however the EPA developed the kinetic test method for the prediction of coal mine drainage quality (Method 1627) for the purpose of developing a standardized leaching column procedure. Although designed for the prediction of coal mine drainage quality, this research study has adopted the methodology for the assessment of PTEs from black shale. Fabrication of the leaching rig commenced in February 2013. The experimental setup comprised of three (3) clear rigid PVC pipe columns, 2 inches internal diameter and 76.2cm in height (Figure 5.1). Flow meters capable of measuring gas flows of up to 1.5L/min were connected to the thick walled latex inlet tubing.

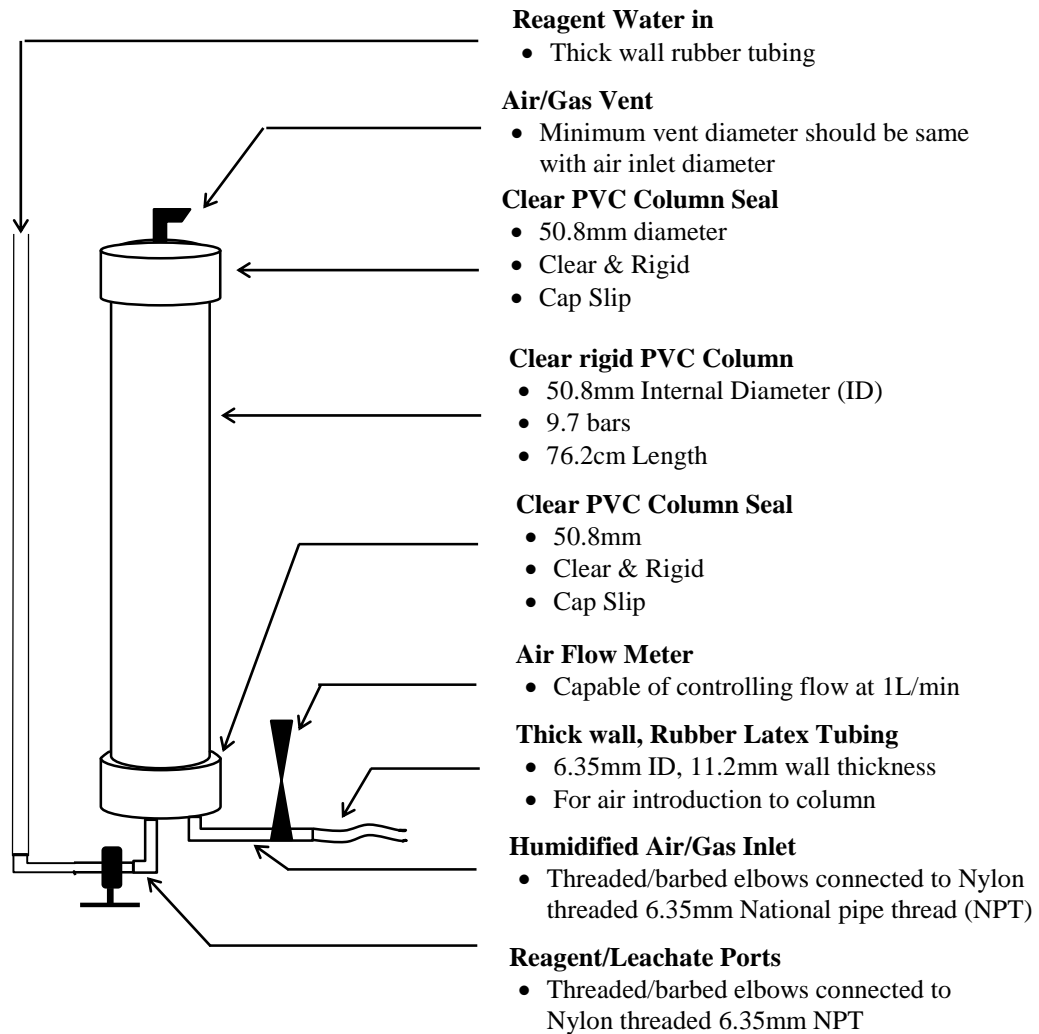


**Figure 5.1:** Schematic diagram of fabricated single leaching column

Columns were loaded with known weights of sampled black shale representing the investigated gas prospective shale formations and a fourth column, subjected to identical treatment, is loaded with uniform sized laboratory glass beads and served as control. Alternating cycles of 6 days humidification and 24 hours saturation were applied to each column following an initial flushing cycle (4cycles) to remove any oxidized components of the shale. Plate 5.2 shows the fabricated columns setup used for the leaching exercise. Controlled simulation of field weathering conditions involved some modifications to the leaching protocol and a number of procedures are implemented;

1. A carbon dioxide (CO<sub>2</sub>) and air mixture is added to the column and to the leaching fluid to maintain field conditions. Gases are mixed to a ratio of 90% air to 10% CO<sub>2</sub> using a two stage gas cylinder regulator.
2. A carboy is half filled with reagent water. The bottle is sealed with a rubber stopper containing inlet and outlet ports for the introduction and release of the mixed gases.
3. An initial column flush after the columns were loaded with samples was done to wash the shale samples of any oxidized materials accumulated during handling and storage. Flushing was terminated when the relative standard deviation between conductivity measurements of the collected flush water was  $\leq 20\%$ .



**Plate 5.2:** Fabricated Leaching Rig

A summary of each column design is presented in Table 5.1. Following each 24 hour saturation cycle, the leachate was drained from the column and collected for analysis. Leachate was collected through the water inlet tubing by disconnecting the tubing from the water source.

**Table 5.1: Summary Experimental Column Design**

<b>Parameter</b>	<b>Unit</b>	<b>Column 1 (LAN)</b>	<b>Column 2 (DRB)</b>	<b>Column 3 (CLV)</b>
Height of tailings in column	cm	65.2	64.4	63.1
Column diameter	cm	5.08	5.08	5.08
Column Height	cm	76.2	76.2	76.2
Surface area	cm <sup>2</sup>	1081.1	1068.3	1047.6
Volume of tailings	cm <sup>3</sup>	1321.5	1308.1	1285.2
Specific Gravity	-	2.43	2.4	2.57
Dry weight of tailing	kg	2.000	1.989	1.992
Leachant rate	L/week	0.269	0.268	0.323
Total leachant delivered	L	3.237	3.223	3.882
Ratio (leachant to mass of tailings)	L/kg	1.619	1.62	1.95

Care was taken to minimise carbon dioxide degassing, a process that drives the collected leachate towards equilibrium with the air outside the column and subsequently results in a sudden increase in pH. The total volume added to and collected from each column was measured and recorded prior to leachate analysis and all analytes determined are listed in Table 5.2 along with the analytical methods adopted. All glassware and Teflon vessels used were washed with detergent, rinsed in tap water, acid washed with Nitric acid, rinsed with tap water followed by a final rinse in ultrapure water. For sample preparation, dissolved analytes were determined in aqueous samples after suitable 0.45µm filtration and acid preservation. Samples for trace metal determinations were acidified following sampling and refrigerated below 4°C to prevent recrystallization.

**Table 5.2: Analysis and Appropriate Method Utilised**

<b>ANALYTE</b>	<b>METHOD</b>
pH	Std. Methods 4500-H (APHA 1998)
Alkalinity @ pH 4.5	Auto Titration (APHA 1998)
<i>Anions</i>	
Sulphate (SO <sub>4</sub> <sup>2-</sup> )	Ion Chromatography (IC) EPA Method 300.1
<i>Heavy Metals (PTEs)</i>	
Chromium (Cr)	
Copper (Cu)	GFAAS - EPA standard method 200.9 <sup>1</sup>
Nickel (Ni)	FAAS - EPA standard method 3111
Zinc (Zn)	
Calcium (Ca)	
Magnesium (Mg)	

### 5.3.5 Analysis and Spectrometric Determinations

The leachate was analysed for the target parameters using approved standard methods as listed in Table 5.2. A detailed description of this spectrometry instrumentation is provided in Section 3.2.1. The GFAAS holds a programmable sample dispenser (PSD) which allows the automatic delivery of measured volumes of sample to the furnace. A working detail of this spectrometric instrumentation, instrumentation setting and the furnace running parameters of all analytes measured are also provided in Section 3.2.1. The alkalinity of the leachate was determined via auto-Titration against a 0.02N sulphuric acid concentration to reach a pH end point of 4.5. Sulphate (SO<sub>4</sub><sup>2-</sup>) quantifications are determined via the Metrohm 850 Professional Ion Chromatography (IC). Details of the operating conditions and the instrumentation are summarised in Section 3.2.1 of the Chapter on materials and methods. Samples were filtered through a 0.45µm PTFE filter and a 20µL dilution of the filtered aliquots prepared in triplicate are injected during every determination. A total run time of 18.5 minutes for each sample presented was required for the analysis. Anions are identified based on their retention times compared to known standards. Quantification was accomplished by measuring the peak area and comparing it to a calibration curve generated from known standards.

### 5.3.6 Quality Control

The study adopts the EPA standard method 200.9<sup>1</sup> (Determinations of trace elements by stabilized temperature graphite furnace atomic absorption) in adherence to a formal quality control scheme that ensures results are reportable. Most analytical instruments produce a signal even when a matrix without analyte is analysed and this is often referred to as the instrument background level or noise. In addition, unwanted matrix components may interfere with quantification and it is necessary that these errors and interferences be accounted for. The standard requires that a characterisation of both instrument and laboratory performance be assessed prior to samples being analysed by the chosen analytical method, details provided in Table 5.3. This initial demonstration of both instrument and laboratory capability involves the determination of the IDL and MDL judged over a 5 point statistical check test (Table 5.3) as prescribed 40 CFR Part 136. The Laboratory fortified blank (LFB) and Laboratory reagent blank (LRB) are analysed at the start and intermittently during each batch of samples analysed to investigate matrix interferences. Recovery range are checked with values specified by the EPA standard method 200.9<sup>1</sup> (70-130%) and are computed as follows;

$$\text{LFB, R\%} = \frac{(\text{LFB})}{\text{Spike Level}} \times 100 \text{-----Eq. 5.1}$$

Where: R% = LFB Percentage recovery

LFB = LFB results, µg/L

Spike Level = LFB true value, µg/L

$$\text{Sample, R\%} = \frac{(\text{Avg. Spiked sample})}{(\text{Spike Level} + \text{Sample Test Result})} \times 100 \text{-----Eq. 5.2}$$

Where: Sample, R% = Sample Percentage recovery,

Avg. Spiked Sample = Average of spiked sample triplicate result, µg/L

Spike Level = LFB true value, µg/L

**Table 5.3:** Definition of Utilised Quality Control Parameters for GFAAS

Quality Control Parameter	Definition
Laboratory Reagent Blank ( <b>LRB</b> )	Milli-Q Water (18Ωm)
Method Detection Limit ( <b>MDL</b> ) (µg/L)	Cr(0.06), Cu(0.10), Ni(0.08) & Zn(0.13)
Quality Control Sample ( <b>QCS</b> )	NIST-1643e
Instrument Detection Limit ( <b>IDL</b> )	Cr(0.069), Cu(0.071), Ni(0.114), Zn(0.91)
Laboratory Fortified Blank ( <b>LFB</b> ) (µg/L) corresponding to 0.2Abs in 0.1% Nitric Acid matrix	Cr(7.5), Cu(30), Ni(24), Zn(75)

EPA standard method 3111 (Metals by flame atomic absorption spectrometry) was adopted in adherence to a formal quality control scheme for FAAS determinations. This standard requires the knowledge of the sensitivity detection levels (Table 5.4) and optimum concentration ranges stipulated in the manufacturer's manual, before sample analysis are performed. Milli-Q water which serves as the LRB, are spiked with known concentrations of standard solutions and serve as the LFB (Table 5.4). Intermittently during sample analysis, both LRB and LFB are analysed to verify baseline stability. Percentage recoveries were computed for the LFB and check against the stipulated 85 - 115% range recommended by the quality control standard. In adherence to a quality control protocol for determinations by Ion Chromatograph unit (IC), measurements are maintained by adopting the EPA Method 300.1 (Method for the determination of inorganic anions by ion chromatography).

**Table 5.4:** Definition of Utilised Quality Control Parameters for the FAAS

Quality Control Parameter	Definition
Sensitivity Value	Fe (0.12mg/L), Al (1mg/L), Ca (0.08mg/L), Mg (0.007mg/L), Cr(0.01 µg/L), Cu(0.1 µg/L), Ni(0.15 µg/L), Zn(0.2 µg/L)
Laboratory Reagent Blank (LRB)	Milli-Q Water (18Ωm)
Method Detection Limit (MDL) (µg/L)	Fe (1), Al (0.5), Ca (2), Mg (0.15), Cr(0.06), Cu(0.10), Ni(0.1), Zn(0.01)
Quality Control Sample (QCS)	NIST-1643e
Laboratory Fortified Blank (LFB) (mg/L) corresponding to 1Abs in 1:1 HCl matrix	Fe (30), Al (250), Ca (5), Mg (0.8), Cr(20), Cu(10), Ni(20) & Zn(2)

The standard requires that the analysis batch must include an initial calibration check standard, an end calibration check standard, laboratory reagent blank, and a laboratory fortified blank (Table 5.5). This initial demonstration of both instrument and laboratory capability involves the determination of the IDL and MDL judged over a 5 point statistical check test. The IDL is determined by computations from results obtained from 10 replicates of the LRB. Subsequently, MDL is obtained from computed IDL for all analytes investigated and reported with a 99% confidence. The standard also recommends a quality control sample in compliance with the initial demonstration of instrumentation performance and for this; the Fluka 69734 multi anion standard is used (Table 5.5). Analyses of these standards (in some cases, dilutions of standard concentrations) are compared with the certified true values to verify instrument performance.

**Table 5.5: Quality Control Parameters for IC Determinations**

<b>Quality Control Parameter</b>	<b>Definition</b>
Laboratory Reagent Blank ( <b>LRB</b> )	18Ωm Ultrapure Water (UPW)
Method Detection Limit ( <b>MDL</b> )	SO <sub>4</sub> <sup>2-</sup> (0.009mg/L)
Laboratory Fortified Blank ( <b>LFB</b> )	0.01 mg/L (SO <sub>4</sub> <sup>2-</sup> )
Calibration Standards	1mg/L combined anion standard
Initial Calibration Check Standard	1mg/L standard solution of SO <sub>4</sub> <sup>2-</sup>
End Calibration Check Standard	5mg/L standard solution of SO <sub>4</sub> <sup>2-</sup>
Instrument Performance Check Solution (IPC)	Two Separate standard solutions containing 5mg/L and 10mg/L of combined standard
Quality control Standard	Fluka/69734 Multi Anion Standard 1

Spiked blanks and calibration solutions are prepared from standard stock solutions. These standards include the 125mL Chromium, Copper, Nickel and Zinc standards solution for Atomic Absorption produced in a nitric acid matrix for stability. Calibration standards prepared for obtaining absorption calibration curves include Cr (150 µg/L), Cu (100 µg/L), Ni (240 µg/L) and Zn (5680µg/L) as specified by standard operating procedures (Variant Cookbook) for the detection of high concentrations in sampled matrix. Lower calibration standards Cr (8 µg/L), Cu (14 µg/L), Ni (25 µg/L) and Zn (0.7µg/L) were also prepared for determinations with smaller concentrations.

## 5.4 Results

A rather large data base of dissolve species for the investigated shale types was obtained from the analyses of all three column effluents. By extracting quantitative rates information for the various investigated species, a clear understanding of the release kinetics observed under the simulated weathering experiment can be evaluated. Subsequently, accurate prediction of release potentials for the investigated heavy metals in the respective investigated formations can be provided.

### 5.4.1 Presentation of Data

The following summarises the approach adopted for data presentation. The study employs two approaches to interpreting the data. Firstly, release trends are presented via time plots of data variation through time. This looks at the concentration data from the weekly leaching events and gives an exploratory view to the data collected. For this exploratory overview, the study adopts two methods of quantitatively expressing the heavy metals released into solvent;

1. Expressed as weighted concentrations that takes account of the specific weight of sample and volume of solution collected for each column. Numerically, the weighted concentrations can be expressed as;

$$\text{Weighted Conc.} = \frac{\text{Conc. } (\mu\text{g/L}) \times \text{Volume (mL)}}{\text{Sample mass (g)}} \text{----- Eq. 5.3}$$

2. Expressed as normalised elemental mass loss (as described by ASTM C1220 1998). This normalizes against the quantity of materials that has been removed from the specimen and can be expressed as

$$[\text{NL}]_i = C_{ij} \times \frac{V_j}{[f_i \times \text{SA}]} \text{----- Eq. 5.4}$$

Where:  $[\text{NL}]_i$  = Normalized mass loss of element  $i$

$C_{ij}$  = Concentration of element  $i$  in specimen  $j$  leachate

$V_j$  = Initial volume of leachate containing specimen  $j$

$f_i$  = the mass fraction of element  $i$  in the unleached specimen

$\text{SA}$  = Specimen Surface area ( $\text{mm}^2$ )

Hence data are presented adopting both methods as they serve varying purposes during result interpretation. Major and trace element data are plotted as an average of the analysis of samples from duplicate leachate analysis from each column. Plots are drawn to show comparison of all three investigated shales in terms of metal leaching rate, correlations of traces with and some major element components, sulphate leaching/depletion (Pyrite oxidation) rates and carbonate dissolution rate. Finally, geochemical equilibrium models were used to model the possible speciation of the investigated heavy metals. Curve fittings of data to deriving rates Equations are also presented. Plots of accumulated release give a better indication of the overall kinetics of the column leaching experiments hence each accumulated release curve is then fitted to either an exponential, power or linear function by regression analysis and the fitting parameters of the Equation are extracted. Data for each column (representing a shale type) are plotted to show an overview of individual column kinetics.

#### **5.4.2 Leachate Analysis**

Natural weathering laboratory simulation commenced on 16<sup>th</sup> July 2013 until 10<sup>th</sup> October 2013. Raw concentrations of weekly leachate were recorded against sampling volume collected and the weighted concentration was computed from Equation 5.3. Flush leachates are combined and concentrations were reported as week 0. Cumulative weighted concentrations are computed from the raw data and the weekly weathered mass in grams is also computed from the volume of leachate collected. Weekly analyses of alkalinity, temperature, sulphate, calcium and magnesium in addition to indicator trace heavy metals were useful in achieving the experimental plan.

##### ***5.4.2.1 Alkalinity, Conductivity and pH Effect on Metal Release***

Trends for pH determination are displayed in Figure 5.3. The average or median values of alkalinity for each week is shown in Figure 5.4, and  $\pm$ SD show the range in alkalinity concentrations of duplicate samples. Measuring alkalinity is important in determining the resulting leachate's ability to neutralize acid produced from oxidizing pyrite content and it accurately indicates the sensitivity of the stream to acid inputs. Although there appears to be scatter in the alkalinity data, the general trend show a gradual decrease in the leachate ability to neutralize acid produced from pyrite decomposition.

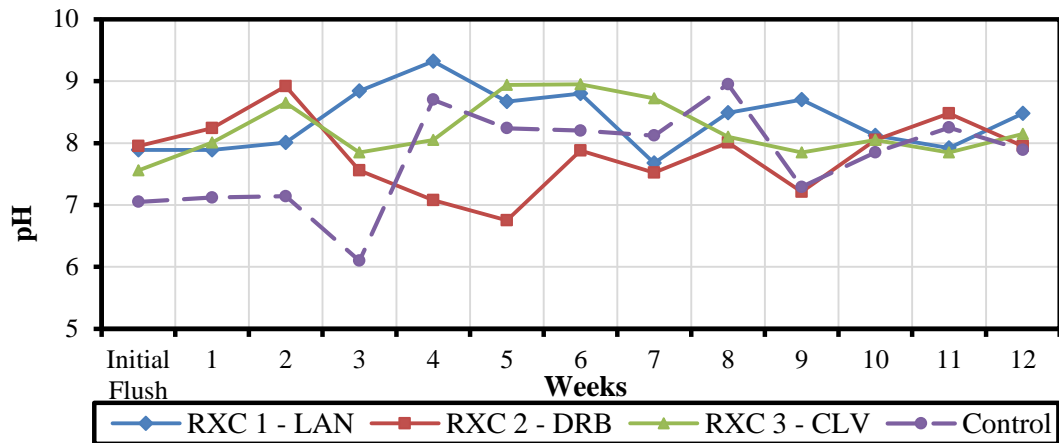


**Figure 5.3:** Weekly pH trend in Leachate

Whilst pH remains largely alkaline in nature, alkalinity measurements suggests a decrease in all three shales buffering capabilities. A possible explanation to this trend is the complete loss of carbonate buffering capacity ( $\text{CO}_3^{2-}$  and  $\text{HCO}_3^-$ ) in returning leachates. As more pyrite oxidation occurs, acidity increases and a further pH drop in alkalinity are expected from collected data and this could account for the intermittent pH drop observed. The observed drop in pH is consistent with the measure of dissolved ionic species in the leaching column effluent (conductivity) which show a rapid fall in conductivity between weeks 3 and week 4.

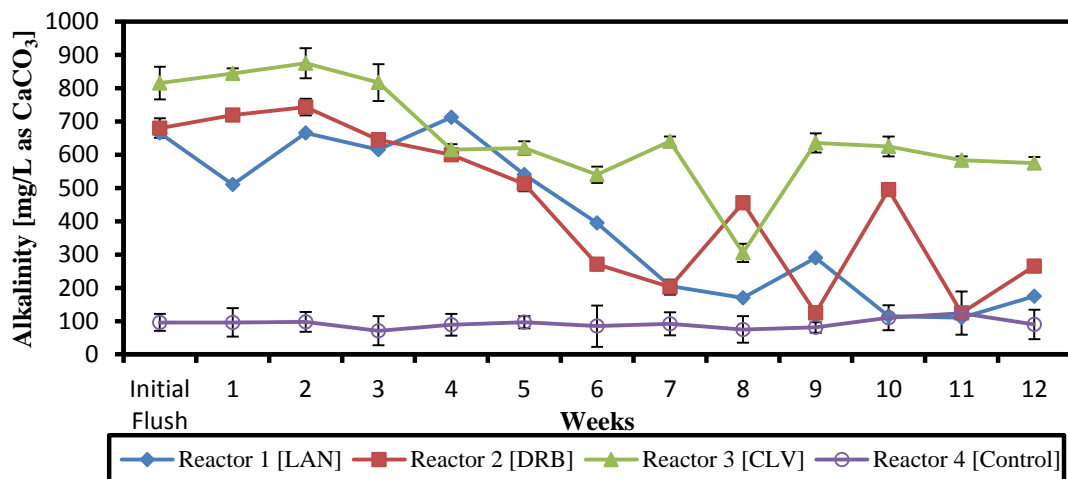


**Figure 5.4:** Alkalinity Concentrations for all Three Investigated Black Shales

Subsequently, conductivity measurements appear relatively constant until week 12 (Figure 5.5). With increased acidity the release of higher concentrations of heavy metals from all three black shales is highly likely. Overall, LAN shale leachates show a pH trend between 7.9 and 9.3. In the DRB shale leachate, pH dropped from pH 8.9

to just above pH 6.8 within weeks 2 and 5 whilst the CLV shale remained fairly constant between pH 7.5-8.9 suggesting minimal changes in alkalinity. A possible explanation to pH trend is the much quicker solubility of Calcite at the onset of the fluid interactions in comparison to pyrite solubility. A better understanding of this trend can be observed from the comparison of the relative weathering rates of the carbonates and pyrite compositions in all three investigated shales. By extracting quantitative rates information for the various investigated species, a clear understanding of the release kinetics observed under the simulated weathering experiment can be evaluated and a possible prediction of the trends can be deduced.

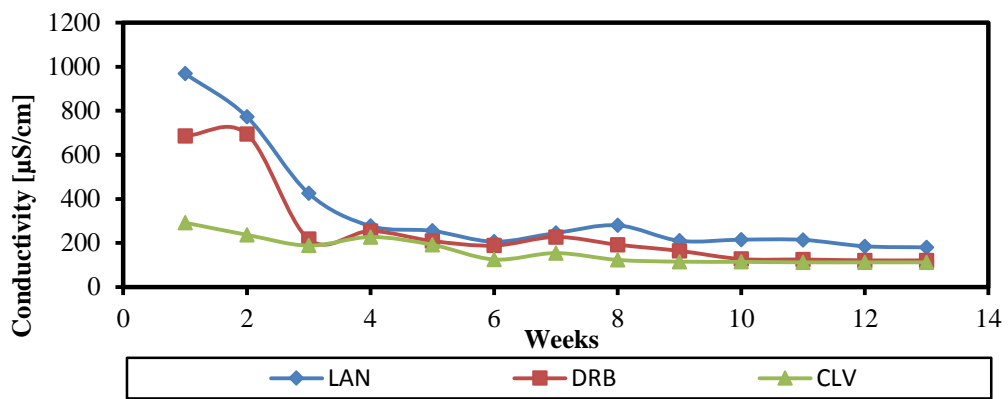


**Figure 5.5:** Conductivity Trends overtime for all Three Sampled Shales

#### 5.4.2.2 Dissolution and Contaminant Release Kinetics

Release quantification data obtained from the leaching test was used to evaluate weathering patterns in all three investigated formations and the overall heavy metal release kinetics. Firstly, a plot of leachate quality parameter through time, (Figure 5.6) is drawn to primarily explore patterns of variation or trends as stated in this Chapter's objective. Data for initial concentration (week 0) were excluded from the plots as these show concentrations in leachate without the addition of sampled shales. Hence, plots show an initial rise in concentrations from week 0 to week 1 before trends shown in weeks 1 to 12. Week 1 data represent the summation of release concentrations in flushing events and as expected, depict a sharp rise following accelerated releases from oxidised shale before the start of the leaching experiment. For major elements, trends show from week 10. Similar trend is observed in investigated traces, with a visible increase in release Cr, Cu, Ni and Zn observed from weeks 5, 6 3 and 5 respectively.

However, these plots do not provide the capability to understand the dissolution rates and the ensuing kinetics due to their representation as episodic releases. Cumulative plots (Figure 5.6) offer a better scenario of understanding the dissolution rates and ensuing kinetics. Therefore, for the purpose of this discussion, much attention is paid to cumulative releases of the investigated heavy metals as these plots of accumulated release give the best indication of the overall kinetics of the column leaching experiments (Hornberger and Brady 2009). Weekly releases expressed as weighted concentrations (Equation 5.3) were summed to give cumulative releases and plots of these weighted concentrations are used to determine the dissolution kinetics.

Theoretically, it is expected that as mineral compositions in the shale are impacted by fluid interactions, dissolution occurs until saturation of the surrounding fluid results in a decrease in release rate with increasing time. Several diffusion models are known to successfully model this relationships and it is generally thought to be the most likely controlling mechanism with metal releases. However, with all three investigated shales, a deviation from the theoretical occurs. Rather than the observed decreasing concentration as a function of time, all investigated heavy metals show leaching rates that increased through the end of the 12 week experimental period, showing an approximate exponential function with a positive coefficient. Eventually, the reaction rate will decrease as the limiting reactant is depleted. The rate of indicator heavy metals releases can be described by a linear function using the least square method. All computations were performed in Microsoft excel by designing programmed worksheet to perform individual computations. Integration of release concentrations data shows that the release of heavy metal indicators during the 12 week test follows a linear behaviour represented by the linear function;

$$C=At^n+K \text{ ----- Eq. 5.5}$$

Where A is an empirical rate constant, K is a constant that takes account of the observation that the extracted sulphur does not become zero at t = 0 and therefore is the term that refers to the cumulative measure of the initial flushes designed to

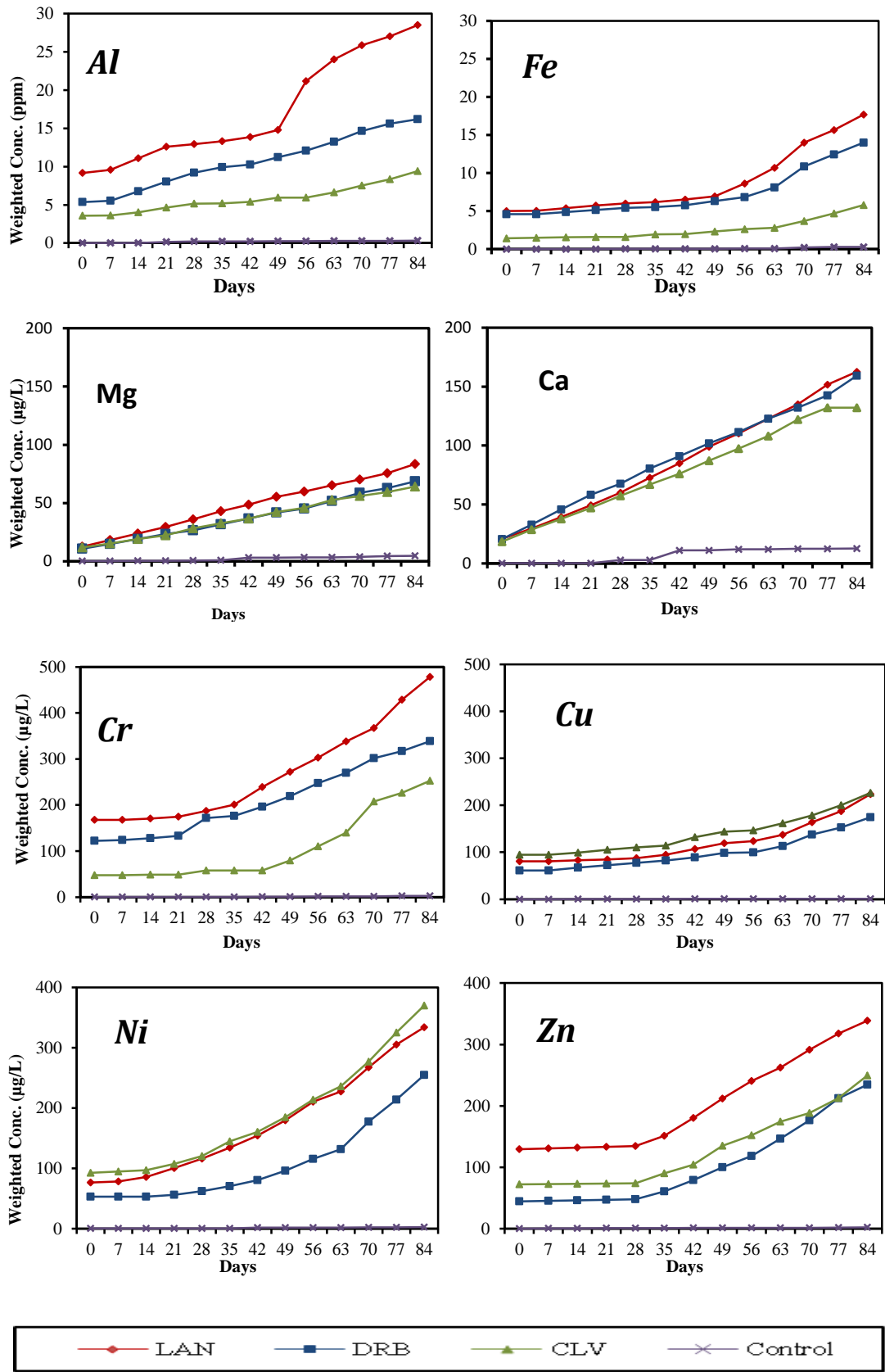


**Figure 5.6:** Cumulative Plots of Weighted Released Heavy Metal Concentrations Leached in tap water

remove oxidised components in the shales before leaching. The root of time dependency usually suggests a diffusion controlled reaction when the exponent ‘n’, is 0.5. A deviation from this ( $> \pm 0.1$ ) suggests the influence of other factors controlling the leaching process and can therefore not be regarded as fully diffusion controlled. In reality however, control by the rate of chemical reaction at the mineral surface will usually produce a linear reaction dependent on time if the reaction is first order ( $n = 1$ ) and second order if ( $n=2$ ). Table 5.6 summaries the statistics for these fits to the cumulative heavy metal data sets.

**Table 5.6:** Computation Result for Dissolution Rate and Goodness of Fit

Column	Fit Equation	A	n	k	R <sup>2</sup>
Cr (LAN)	$y=26.062x + 86.4$	26.062	1.000	86.400	0.9088
Cr (DRB)	$y=19.575x + 74.183$	19.575	1.000	74.183	0.9686
Cr (CLV)	$y=17.369x - 15.161$	17.369	1.000	-15.161	0.8017
Cu (LAN)	$y=10.814x + 45.248$	10.814	1.000	45.248	0.8495
Cu (DRB)	$y=8.79x + 37.532$	8.790	1.000	37.532	0.8984
Cu (CLV)	$y=10.443x + 65.934$	10.443	1.000	65.934	0.9209
Ni (LAN)	$y=22.092x + 19.801$	22.092	1.000	19.801	0.9560
Ni (DRB)	$y=15.790x - 1.514$	15.790	1.000	-1.514	0.8344
Ni (CLV)	$y=22.783x + 26.960$	22.783	1.000	26.960	0.9218
Zn (LAN)	$y=19.150x + 70.124$	19.150	1.000	70.124	0.9175
Zn (DRB)	$y=16.350x - 9.891$	16.350	1.000	-9.891	0.8805
Zn (CLV)	$y=14.996x + 23.696$	14.996	1.000	23.696	0.9005

However, this observed leach rates are an accurate result of the individual experiment but limited for use in extracting quantitative rates. Since quantitative rates provide us with a means to predict future heavy metal releases and compare releases across all investigated shales (one of the key objective of this Chapter) it is necessary to include the normalisation of the heavy metal leachate rate to the surface area, volume of

leachate and inventory of heavy metal leached from the rocks. This form of normalization takes the form of the elemental mass loss  $NL_i$  described in Equation 5.4. The value of  $NL_i$  is normalized to the weight fraction of individual elements in all three investigated formations, and is therefore suitable for a comparison with those of other elements within the sampled shale. This comparison is presented in Figure 5.7 showing a semi log plot of  $NL_i$  values for the investigated traces versus time.

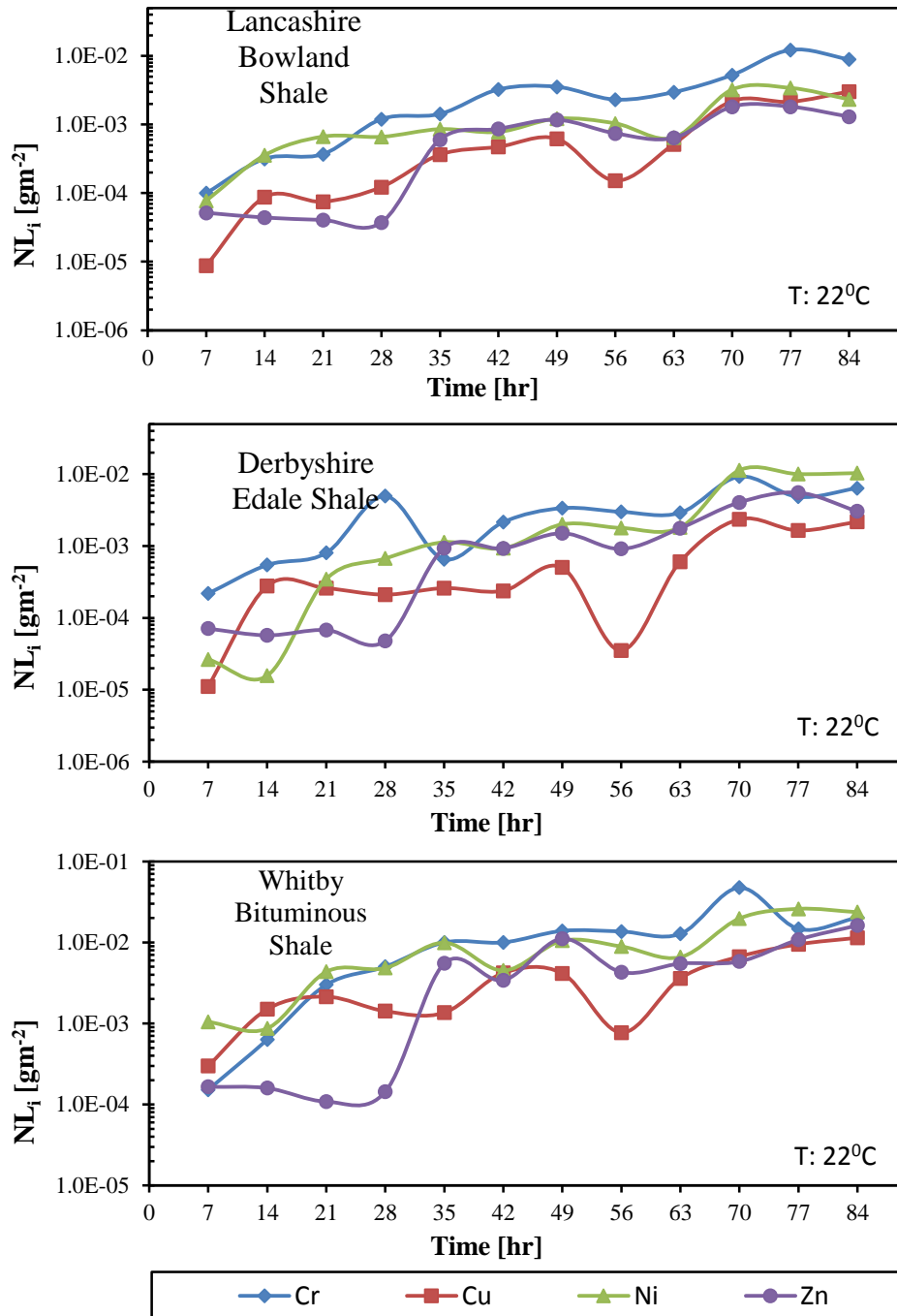


Figure 5.7: Comparison of Normalized Heavy metal Release from Sampled Shales

Average normalized release rates for each trace heavy metal is listed in Table 5.7. For the Lancashire black shale at average test temperature (22°C), these dissolution rate data show Cu with the slowest dissolution rate at day 7 and remaining mostly lower just until week 10 where it rates exceed Zn and at week 12 where rates exceed both Zn and Ni. Cr achieves the highest dissolution rate and remains steadily increasing over 2 orders of magnitude. By week 14, all 4 trace metals had release rates climbing 2 orders of magnitude from observed concentrations at week 1.

**Table 5.7:** Normalised Release Rates [mol/m<sup>2</sup>/day]

Traces	Reactor 1 (LAN)	Reactor 2 (DRB)	Reactor 3 (CLV)
Chromium (Cr)	9.31E-09	8.70E-09	2.86E-08
Copper (Cu)	1.78E-09	1.56E-09	8.51E-09
Nickel (Ni)	3.01E-09	7.98E-09	2.38E-08
Zinc (Zn)	1.62E-09	3.35E-09	1.12E-08

#### ***5.4.2.3 Predicting Long Term Leachate Composition***

With the computed dissolution rates, it is possible to estimate concentration values at different times, and provide some insight into longer term leachate composition. The curvilinear behaviour exhibited by the time series plots of chemical concentrations in each reaction column is common with many chemical and biological systems and can be described using an exponential growth function of the general form;

$$C_t = C_o \times e^{kt} \text{-----Eq. 5.6}$$

- Where:  $C_t$  = concentration at time t  
 $C_o$  = concentration at time zero  
 $e$  = base e, approximate value of 2.718  
 $k$  = Decay constant (rate of concentration change per unit time)  
 $t$  = Time

Hence, the constants (k) can be derived from a plot of the  $\ln(C_t / C_o)$  versus time and would represent the slope of plot determined by linear regression. A summary of the computed decay constant for all three shales in all 4 investigated traces are shown in Table 5.8 along with the  $R^2$  values computed from regression computations. Plots are presented in Figure 5.8 and 5.9 comparing release rates of changes of each trace element in all three reaction columns. Values closer to 1 represent strong relationships for estimating decay constants while lesser values indicate a weaker association.

**Table 5.8:** Estimated Decay (rate of change) Constants for Cr, Cu, Ni and Zn

Traces	Reactor 1 [ $\mu\text{g/L/day}$ ]	Variation ( $R^2$ )	Reactor 2 [ $\mu\text{g/L/day}$ ]	Variation ( $R^2$ )	Reactor 3 [ $\mu\text{g/L/day}$ ]	Variation ( $R^2$ )
Chromium (Cr)	1.36E-02	0.9543	1.36E-02	0.9815	2.23E-02	0.8874
Copper (Cu)	1.21E-02	0.9246	1.23E-02	0.9664	1.05E-02	0.9682
Nickel (Ni)	1.90E-02	0.9945	1.99E-02	0.9388	1.76E-02	0.9829
Zinc (Zn)	1.33E-02	0.9390	2.26E-02	0.9457	1.65E-02	0.9370

Chromium decay in column 1 and 2, like zinc in the Lancashire black shale (reactor 1) is on the order of  $1.36 \times 10^{-2}/\text{day}$  indicating similar leaching behaviour. All trace metals show increasing releases following leaching with a reduction in alkalinity as the shales ultimately produced acidic leachate. The above data suggest similarities in leaching behaviour for all traces investigated.

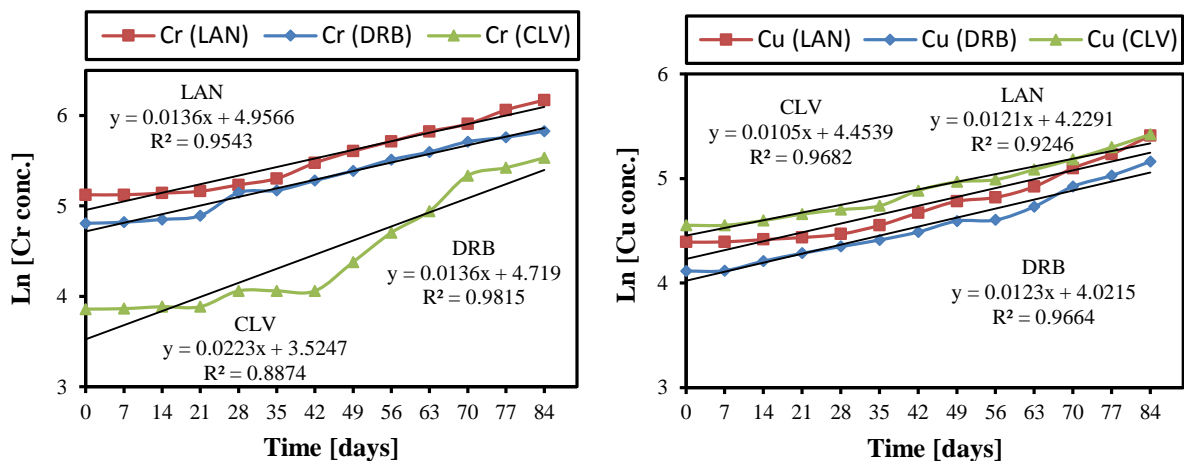


**Figure 5.8:** Curve fitting to flux computation

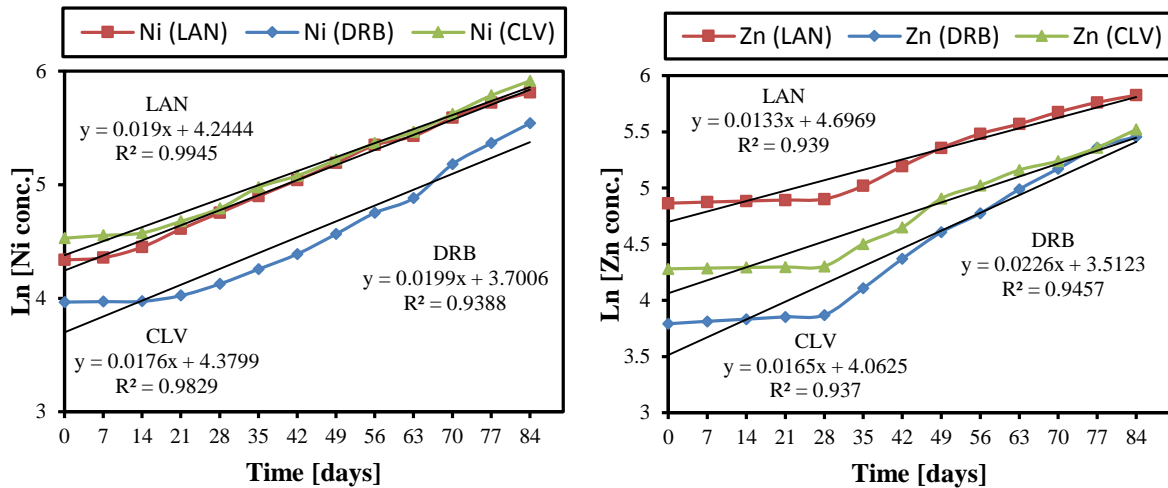


**Figure 5.9:** Curve fitting to flux computation (contd.)

The relatively high values of  $R^2$  values reported also suggested similar kinetics. By fitting these functions, time specific predictions of expected leachate quality can be obtained for trace metal concentrations. Figure 5.10 shows a 10 year prediction of trace metal concentrations. Data has been plotted on a semi logarithmic scale to accommodate for releases spanning over several orders of a magnitude. Nickel and copper in particular are predicted to reach concentrations in 7 orders of a magnitude. Results show that within 5 years of continuous degrading fluid interaction, released concentrations are estimated to increase by close to 1 order of magnitude. These results suggest that provided solubility control remains constant and sulphur compositions in the respective shales are not exhausted, potentially toxic trace metal compositions will be releases exponentially.

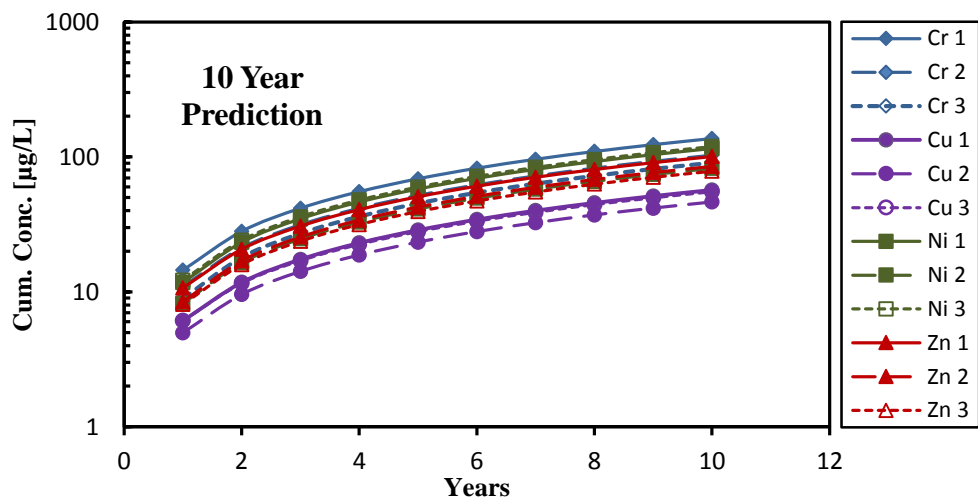


**Figure 5.10:** Ten year prediction of released heavy metal concentrations

#### ***5.4.2.4 Pyrite and Carbonate Weathering Rates***

A part of the shale leachate characteristic important to this study is the ability to predict the resultant nature (acidic, circumneutral or alkaline) of leachate produced following simulated fluid rock interactions. This information can be gathered by looking at the interplay of acid forming minerals (pyrite) and the neutralising potential (carbonates) within the formation. If the rate of pyrite proceeds at a faster rate allowing the quicker exhaustion in comparison to the neutralizing carbonate in the shale, then the leachate would eventually be alkaline. If the reverse is the case, then the leachate produced will eventually be acidic. Circumneutral leachate will however be produced if both pyrite and carbonate weathering rates proceed at fairly similar rates. Pyrite and carbonate oxidation rates have been assessed in this section to determine the long term nature of leachates produced.

Using average leached concentrations of sulphate from the analytical determinations, the weekly weathered mass of sulphur is computed from sulphur mass fraction from sulphate mass. This allows the computation of the cumulative percentage sulphur weathered mass in each column. The cumulative percentage carbonate weathered mass in each column is computed by adopting the cation approach which uses calcium and magnesium in computing the total carbonate contribution as they are mostly associated with acid neutralizing carbonates. This weekly mass of calcium and magnesium weathered is then used in computing the cumulative percentage  $\text{CaCO}_3$  weather each week. The method adopted here is based on the major assumptions that all Ca and Mg in solution are derived from carbonate dissolution only. However, results from XRD analysis (Table 4.8) suggest carbonate originates from calcite, dolomite and siderite but on closer inspection, dolomite and siderite contribute a negligible percentage (<2%) to overall carbonate contents in all three formations and hence the cation method was adopted. Hence, by obtaining cumulative percentages of sulphur and carbonate in all sampled shales, a comparison on the rates of acidification and neutralization in the respective shales can be plotted. A summary of the computed sulphur and carbonate weathering rates is shown in Table 5.9.

**Table 5.9:** Summary computation for Cumulative percentage of sulphur and carbonate weathered in all three investigated shales

Days	LAN		DRB		CLV	
	Sulphur (%)	Carbonate (%)	Sulphur (%)	Carbonate (%)	Sulphur (%)	Carbonate (%)
1	0.081	0.109	0.059	0.105	0.034	0.203
7	0.122	0.183	0.098	0.201	0.098	0.400
14	0.147	0.260	0.185	0.295	0.173	0.577
21	0.174	0.338	0.291	0.386	0.264	0.750
28	0.200	0.423	0.369	0.463	0.291	0.904
35	0.268	0.508	0.460	0.549	0.320	1.069
42	0.325	0.573	0.514	0.618	0.340	1.163
49	0.402	0.656	0.586	0.713	0.367	1.322
56	0.451	0.713	0.634	0.775	0.386	1.427
63	0.517	0.771	0.684	0.844	0.400	1.518
70	0.625	0.856	0.794	0.963	0.417	1.655
77	0.746	0.948	0.977	1.085	0.435	1.789
84	0.851	0.997	1.143	1.192	0.454	1.914

Following 12 weeks of leaching, 1% of the calcium carbonate in black shale from the Bowlands was released in comparison to a 0.85% sulphur composition weathered and released. Derbyshire Edale shale showed relatively close sulphur and carbonate weathering rates (S: 1.14%, CaCO<sub>3</sub>:1.16%) while the bituminous Whitby shale show faster carbonate dissolution rate (S:0.46%, CaCO<sub>3</sub>:1.90%) in comparison to sulphur (Table 5.9). Although all weathering rates depict a faster carbonate dissolution rate in comparison to the pyrite oxidation rate (Table 5.9), these rates are relatively similar within the short intervals of a twelve weeks leaching exercise to make a meaningful conclusion on the leachate characteristics. A better understanding of the long term leachate quality and characteristic nature of resulting leachate can be evaluated by fitting a function to the data as illustrated in Figure 5.11 and predicting the future nature of resulting leachate.

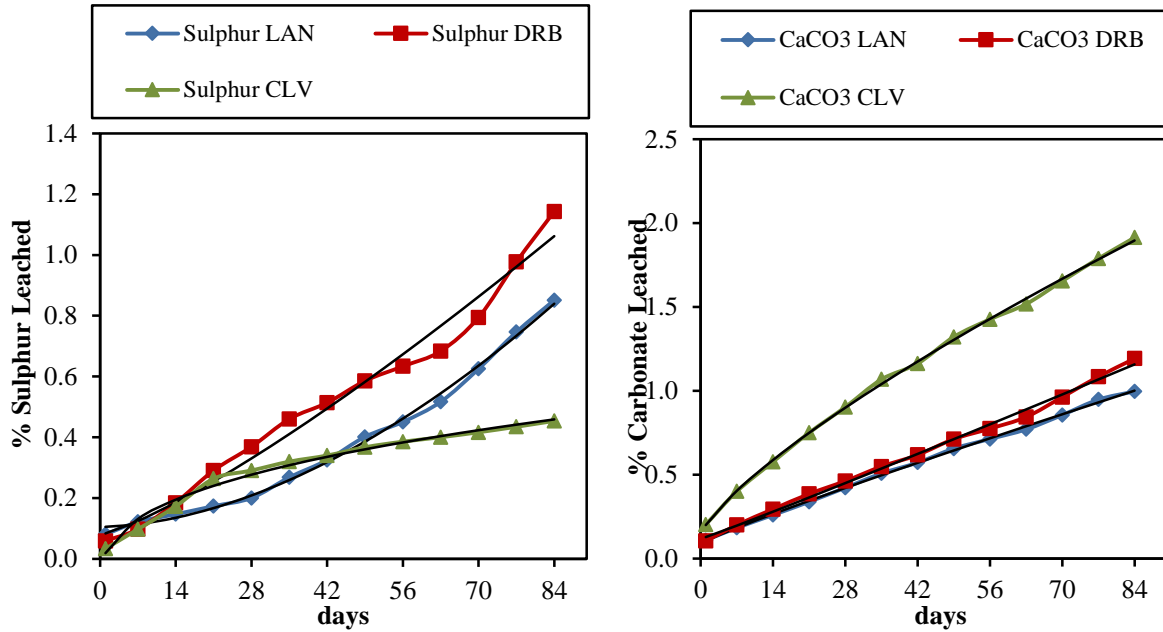


**Figure 5.11:** Curve fitting on cumulative percentage sulphur and carbonated data

The observed linear fit to the data of the form represented in Equation 5.5 is used in obtaining a linearization of the data collected (Table 5.10) and enabling a 10 year predictions of leachate characteristic computed in Table 5.11 and illustrated in Figure 5.12. This result indicate that provided the rates do not change, at the end of 10 years, black shale from the Bowland formation will leach approximately 31.85% of its sulphur content closely matched by a 38.2% neutralising carbonate content released within the same time scale (Table 5.11). This suggests a more likely circum-neutral leachate quality.

**Table 5.10:** Fitting Parameters of Sulphur and Carbonate Extraction for curves in Figure 5.10

Column	Description	Fit Equation	A	n	k	R <sup>2</sup>
RXC 1	Sulphur LAN	$y = 0.0089x + 0.001$	0.0089	1.0000	0.001	0.9519
RXC 2	Sulphur DRB	$y = 0.012x + 0.019$	0.0120	1.0000	0.019	0.9747
RXC 3	Sulphur CLV	$y = 0.0524x - 0.010$	0.0524	0.5000	-0.010	0.9797
RXC 1	Carbonate LAN	$y = 0.0107x + 0.114$	0.0107	1.0000	0.114	0.9982
RXC 2	Carbonate DRB	$y = 0.0124x + 0.106$	0.0124	1.0000	0.106	0.9955
RXC 3	Carbonate CLV	$y = 0.0198x + 0.297$	0.0198	1.0000	0.297	0.9903

**Table 5.11:** Computation of predicted percentage pyrite and carbonate rates

DURATION		LAN		DRB		CLV	
Days	Weeks /Years	Sulphate (%)	CaCO <sub>3</sub> (%)	Sulphate (%)	CaCO <sub>3</sub> (%)	Sulphate (%)	CaCO <sub>3</sub> (%)
70	10 weeks	0.63	0.86	0.86	0.98	0.43	1.68
77	11 weeks	0.69	0.94	0.94	1.06	0.45	1.82
84	12 weeks	0.75	1.01	1.02	1.15	0.47	1.96
365.2	1year	3.27	4.02	4.39	4.65	0.99	7.53
730.5	2years	6.53	7.93	8.76	9.20	1.41	14.76
1095.7	3years	9.80	11.83	13.13	13.74	1.72	21.99
2191.5	6years	19.59	23.55	26.24	27.38	2.44	43.69
3562.42	10years	31.85	38.21	42.65	44.45	3.12	70.83

Black shale from the Edale formation would have leached 42.65% acid producing sulphur required to be neutralised by an approximately equivalent 44.45% carbonate content and the Bituminous Whitby shale is predicted to leach 3.12% acid producing sulphur required to be neutralised by the 70.83% carbonate composition leached (Table 5.11). The significance of this is, while the leachate characteristics will appear to be acidic in both the Lancashire Bowland and Derbyshire Edale shales within the first few years (4years), the faster exhaustion of the pyrite compositions will eventually result in the production of alkaline drainage long into the future. For the bituminous Whitby shale however, the faster carbonate dissolutions ensures that the final leachate will eventually become acidic.

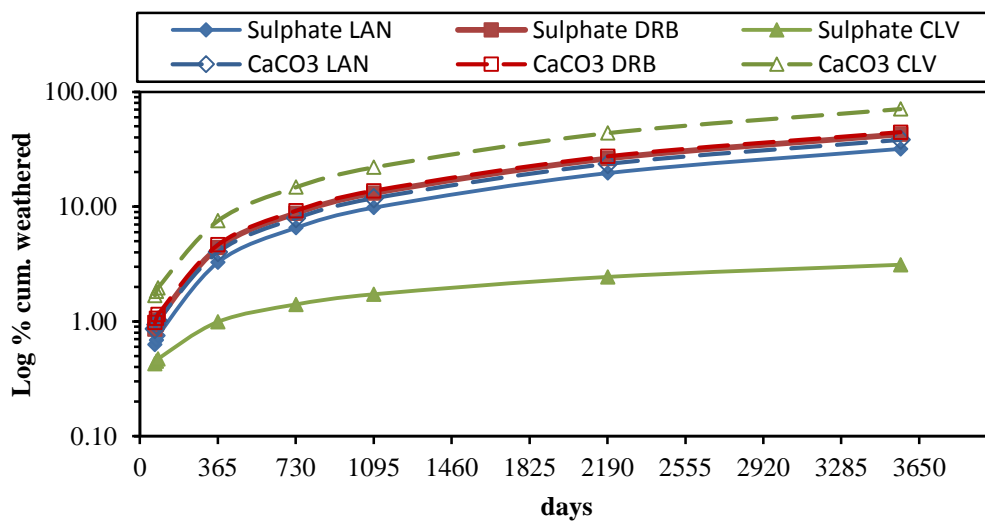


**Figure 5.12:** A 10 year Prediction of pyrite dissolution in comparison with carbonate dissolution rate

## 5.5 Geochemical Modelling for Metal Speciation

The chemical analytical techniques have so far reported total metal concentrations in the leachate without distinguishing metal speciation. It is general knowledge that metal toxicity is a function of the concentrations of specific metal species, not of the total metal and most often, best predicted by the free metal ion activity (Morel and Herring 1993, Stumm and Morgan 1996, Langmuir 1997, Jared et al. 1999). Therefore, with contamination monitoring, speciation of the metal provide a better understand of contaminant mobility and its effect on bioavailability and toxicity. For example with regards to toxicity, the valances state of Cr with the highest toxicity impact remains the trivalent and hexavalent chromium, while  $\text{Cu}^{2+}$ ,  $\text{Ni}^{2+}$  and  $\text{Zn}^{2+}$  are more potent contaminants than their total metal concentration. With the aid of geochemical modelling, the speciation of the selected indicator heavy metals were modelled using the Visual MINTEQ and PHREEQCI application (Parkhurst and Appelo 1999). Thermodynamic data adopted was the MINTEQ v4.0 database, which is derived from NIST databases (46.6 and 46.7).

Particular interest is paid to the complexation and chemical species of the indicator trace metals that provide the best prediction for metal toxicity (Table 5.12). Results for spectrometric and chromatographic analysis (Table 5.13) for weeks 5, 8 and 12, serve as model inputs in PHREEQCI. Ions were converted from milligram per litre to milli-equivalent per litre and anions balanced against cations as a control check of the reliability of the both the analyses and results. Generated output by the model include various metal ionic species whether free or complexed ions and a summary of modelled results is presented in Table 5.14 for all three sampled shales and Figure 5.13 illustrates the trends in selected toxic species.

**Table 5.12:** Dominant Chemical Species of Metals in Soils and Natural Waters

Metal	Soils	Waters	Best Predictor of Toxicity
Chromium (Cr)	$\text{Cr}^{3+}$	$\text{CrO}_4^{2-}$ , $\text{Cr}^{3+}$	$\text{CrO}_4^{2-}$
Copper (Cu)	$\text{Cu}^{2+}$ , Cu-OM <sup>1</sup>	$\text{Cu}^{2+}$ , -Fulvate	$\text{Cu}^{2+}$
Nickel (Ni)	$\text{Ni}^{2+}$	$\text{Ni}^{2+}$	$\text{Ni}^{2+}$
Zinc (Zn)	$\text{Zn}^{2+}$	$\text{Zn}^{2+}$	$\text{Zn}^{2+}$

<sup>1</sup>Cu-OM denotes copper complexed with organic matter

**Table 5.13:** Summary of Physiochemical Parameters from Selected Weekly Leachate

Parameter	(BOWLAND SHALE FORMATION)			DERBYSHIRE EDALE SHALE			WHITBY BITUMINOUS SHALE		
	Week 5	Week 8	Week 12	Week 5	Week 8	Week 12	Week 5	Week 8	Week 12
Ph	7.07 ( $\pm 1.02$ )	5.49 ( $\pm 0.15$ )	5.48 ( $\pm 1.10$ )	6.75 ( $\pm 0.84$ )	8.01 ( $\pm 0.93$ )	7.95 ( $\pm 1.20$ )	8.94( $\pm 0.58$ )	8.10( $\pm 0.87$ )	8.15( $\pm 1.31$ )
Alkalinity (mg/L)	540 ( $\pm 27.8$ )	170 ( $\pm 6.23$ )	175 ( $\pm 14.3$ )	512 ( $\pm 11.02$ )	455 ( $\pm 13.55$ )	265 ( $\pm 12.65$ )	620( $\pm 15.32$ )	305( $\pm 9.05$ )	575( $\pm 8.23$ )
Temp. ( $^{\circ}$ C)	24 ( $\pm 0.42$ )	25 ( $\pm 1.20$ )	23 ( $\pm 0.25$ )	24 ( $\pm 0.12$ )	25 ( $\pm 0.07$ )	23 ( $\pm 0.08$ )	24( $\pm 0.04$ )	25( $\pm 0.11$ )	23( $\pm 0.04$ )
Fluoride (mg/L)	6.22 ( $\pm 0.57$ )	5.98 ( $\pm 0.18$ )	5.1 ( $\pm 1.07$ )	5.216 ( $\pm 0.24$ )	4.81 ( $\pm 0.11$ )	4.1 ( $\pm 0.23$ )	6.10( $\pm 0.59$ )	2.45( $\pm 0.23$ )	1.08( $\pm 0.11$ )
Chloride (mg/L)	12.81 ( $\pm 1.24$ )	10.52 ( $\pm 0.65$ )	10.69 ( $\pm 1.32$ )	14.12 ( $\pm 0.71$ )	10.89 ( $\pm 0.56$ )	8.69 ( $\pm 0.58$ )	24.89( $\pm 1.21$ )	23.18( $\pm 1.78$ )	10.15( $\pm 1.05$ )
Nitrite (mg/L)	N.D	N.D	N.D	N.D	N.D	N.D	N.D	N.D	N.D
Bromide (mg/L)	N.D	12.65 ( $\pm 1.25$ )	9.21 ( $\pm 0.92$ )	N.D	N.D	N.D	18.14( $\pm 0.85$ )	8.98( $\pm 1.12$ )	8.05( $\pm 1.44$ )
Nitrate (mg/L)	1.5 ( $\pm 0.46$ )	1.69 ( $\pm 0.08$ )	1.32 ( $\pm 0.08$ )	2.5 ( $\pm 0.03$ )	0.69 ( $\pm 0.03$ )	0.32 ( $\pm 0.04$ )	2.14( $\pm 0.12$ )	1.69( $\pm 0.55$ )	1.50( $\pm 0.23$ )
Sulphate (mg/L)	171.20 ( $\pm 5.78$ )	337.59 ( $\pm 4.06$ )	702.91 ( $\pm 8.75$ )	72.25 ( $\pm 4.05$ )	37.78 ( $\pm 2.02$ )	130.78 ( $\pm 2.65$ )	23.56( $\pm 2.34$ )	14.75( $\pm 4.10$ )	15.62( $\pm 2.05$ )
Aluminium (mg/L)	0.39 ( $\pm 0.08$ )	6.37 ( $\pm 0.14$ )	1.46 ( $\pm 0.21$ )	0.74 ( $\pm 0.11$ )	0.84 ( $\pm 0.03$ )	0.59 ( $\pm 0.12$ )	0.03( $\pm 0.11$ )	0.03( $\pm 0.17$ )	1.05( $\pm 0.07$ )
Iron (mg/L)	0.19 ( $\pm 0.05$ )	1.71 ( $\pm 0.03$ )	2.03 ( $\pm 0.11$ )	0.11 ( $\pm 0.02$ )	0.52 ( $\pm 0.02$ )	1.56 ( $\pm 0.36$ )	0.33( $\pm 0.14$ )	0.29( $\pm 0.05$ )	1.09( $\pm 0.03$ )
Sodium (mg/L)	190.08 ( $\pm 4.65$ )	148.76 ( $\pm 2.55$ )	144.73 ( $\pm 12.05$ )	248.08 ( $\pm 7.10$ )	152.76 ( $\pm 5.61$ )	150.73 ( $\pm 4.75$ )	221.80( $\pm 2.06$ )	182.76( $\pm 4.09$ )	121.40( $\pm 5.16$ )
Calcium (mg/L)	11.17 ( $\pm 1.04$ )	7.52 ( $\pm 0.84$ )	5.62 ( $\pm 1.07$ )	11.51 ( $\pm 2.12$ )	7.92 ( $\pm 0.97$ )	13.98 ( $\pm 1.48$ )	15.48( $\pm 2.11$ )	10.71( $\pm 1.03$ )	11.40( $\pm 1.33$ )
Ammonium (mg/L)	2.1 ( $\pm 0.04$ )	1.84 ( $\pm 0.21$ )	1.68 ( $\pm 0.65$ )	1.10 ( $\pm 0.71$ )	0.84 ( $\pm 0.08$ )	0.68 ( $\pm 0.04$ )	3.10( $\pm 0.93$ )	2.84( $\pm 0.20$ )	2.05( $\pm 0.47$ )
Potassium (mg/L)	110.85 ( $\pm 14.55$ )	84.19 ( $\pm 1.15$ )	75.59 ( $\pm 2.15$ )	97.85 ( $\pm 0.95$ )	78.19 ( $\pm 1.36$ )	73.59 ( $\pm 2.69$ )	297.85( $\pm 5.21$ )	248.19( $\pm 8.14$ )	188.85( $\pm 4.03$ )
Magnesium (mg/L)	3.37 ( $\pm 0.47$ )	2.31 ( $\pm 0.52$ )	2.76 ( $\pm 0.45$ )	4.36 ( $\pm 0.24$ )	3.54 ( $\pm 0.85$ )	5.74 ( $\pm 0.96$ )	8.32( $\pm 0.54$ )	4.43( $\pm 0.78$ )	6.60( $\pm 0.92$ )
Chromium ( $\mu$ g/L)	13.73 ( $\pm 1.16$ )	30.80 ( $\pm 4.25$ )	49.4 ( $\pm 2.18$ )	4.30 ( $\pm 0.05$ )	28.58 ( $\pm 1.01$ )	21.92 ( $\pm 1.22$ )	N.D	30.62( $\pm 0.54$ )	26.36( $\pm 1.64$ )
Copper ( $\mu$ g/L)	7.63 ( $\pm 0.55$ )	4.4 ( $\pm 0.61$ )	36.4 ( $\pm 1.87$ )	5.02 ( $\pm 0.85$ )	0.99 ( $\pm 0.15$ )	21.92 ( $\pm 2.06$ )	4.07( $\pm 0.66$ )	3.06( $\pm 1.10$ )	26.36( $\pm 2.12$ )
Nickel ( $\mu$ g/L)	18.3 ( $\pm 1.13$ )	30.8 ( $\pm 1.17$ )	28.6 ( $\pm 0.57$ )	8.60 ( $\pm 0.55$ )	19.71 ( $\pm 0.35$ )	41.10 ( $\pm 1.56$ )	24.40( $\pm 1.28$ )	29.09( $\pm 2.06$ )	44.80( $\pm 1.05$ )
Zinc ( $\mu$ g/L)	16.78 ( $\pm 1.07$ )	28.6 ( $\pm 0.84$ )	20.8 ( $\pm 1.20$ )	12.90 ( $\pm 1.03$ )	18.23 ( $\pm 1.06$ )	21.92 ( $\pm 1.08$ )	16.27( $\pm 1.35$ )	16.84( $\pm 1.14$ )	36.90( $\pm 1.18$ )

**Table 5.14:** Result of PHREEQC output, containing predicted concentrations of selected ionic species

Days	Reactor LAN (Lancashire Black shale)					Reactor DRB (Edale Black shale)					Reactor CLV (Whitby Bituminous Shale)				
	Cr <sup>3+</sup> (µg/L)	CrO <sub>4</sub> <sup>2-</sup> (µg/L)	Cu <sup>2+</sup> (µg/L)	Ni <sup>2+</sup> (µg/L)	Zn <sup>2+</sup> (µg/L)	Cr <sup>3+</sup> (µg/L)	CrO <sub>4</sub> <sup>2-</sup> (µg/L)	Cu <sup>2+</sup> (µg/L)	Ni <sup>2+</sup> (µg/L)	Zn <sup>2+</sup> (µg/L)	Cr <sup>3+</sup> (µg/L)	CrO <sub>4</sub> <sup>2-</sup> (µg/L)	Cu <sup>2+</sup> (µg/L)	Ni <sup>2+</sup> (µg/L)	Zn <sup>2+</sup> (µg/L)
7	0.008 <b>(16.6%)</b>	0.174 <b>(82%)</b>	0.118 <b>(100%)</b>	1.040 <b>(98%)</b>	0.192 <b>(21%)</b>	0.572 <b>(99%)</b>	1.000 <b>(0.2%)</b>	0.188 <b>(99%)</b>	0.176 <b>(98%)</b>	0.467 <b>(54%)</b>	0.092 <b>(99%)</b>	1.000 <b>(0.01%)</b>	N.D	1.994 <b>(98%)</b>	0.233 <b>(61%)</b>
14	0.963 <b>(100%)</b>	0.0034 <b>(0.01%)</b>	1.289 <b>(99%)</b>	5.241 <b>(97%)</b>	0.573 <b>(67%)</b>	0.176 <b>(11%)</b>	6.122 <b>(87%)</b>	5.256 <b>(99%)</b>	0.112 <b>(97%)</b>	0.271 <b>(35%)</b>	0.309 <b>(74%)</b>	0.473 <b>(25%)</b>	3.916 <b>(99%)</b>	1.81 <b>(97%)</b>	0.121 <b>(30%)</b>
21	0.109 <b>(9.3%)</b>	4.668 <b>(90%)</b>	1.142 <b>(99%)</b>	9.995 <b>(96%)</b>	0.185 <b>(22%)</b>	2.200 <b>(100%)</b>	1.000 <b>(0.01%)</b>	4.664 <b>(99%)</b>	2.368 <b>(96%)</b>	0.641 <b>(74%)</b>	0.000 <b>(N.D)</b>	0.000 <b>(N.D)</b>	5.587 <b>(99%)</b>	9.039 <b>(97%)</b>	0.181 <b>(65%)</b>
28	0.007 <b>(0.2%)</b>	17.469 <b>(98%)</b>	1.973 <b>(99%)</b>	10.089 <b>(93%)</b>	0.054 <b>(6.8%)</b>	15.469 <b>(99%)</b>	1.000 <b>(0.01%)</b>	4.312 <b>(99%)</b>	5.239 <b>(97%)</b>	0.561 <b>(81%)</b>	3.722 <b>(99%)</b>	1.000 <b>(0.02%)</b>	4.147 <b>(99%)</b>	11.504 <b>(99%)</b>	0.268 <b>(65%)</b>
35	1.840 <b>(42.4%)</b>	11.026 <b>(57%)</b>	5.377 <b>(99%)</b>	12.026 <b>(93%)</b>	3.944 <b>(33%)</b>	1.723 <b>(99%)</b>	2.000 <b>(0.01%)</b>	4.474 <b>(99%)</b>	7.425 <b>(97%)</b>	9.467 <b>(82%)</b>	0.000 <b>(N.D)</b>	0.000 <b>(N.D)</b>	3.638 <b>(99%)</b>	21.47 <b>(98%)</b>	2.528 <b>(17%)</b>
42	0.982 <b>(8.2%)</b>	48.462 <b>(91%)</b>	8.433 <b>(99%)</b>	12.924 <b>(91%)</b>	5.451 <b>(27%)</b>	8.054 <b>(99%)</b>	1.000 <b>(0.01%)</b>	5.840 <b>(99%)</b>	8.781 <b>(98%)</b>	12.625 <b>(78%)</b>	0.000 <b>(N.D)</b>	0.000 <b>(N.D)</b>	15.982 <b>(99%)</b>	13.881 <b>(99%)</b>	2.166 <b>(17%)</b>
49	10.451 <b>(100%)</b>	0.021 <b>(1%)</b>	8.871 <b>(99%)</b>	15.753 <b>(89%)</b>	16.868 <b>(76%)</b>	9.021 <b>(99%)</b>	2.000 <b>(0.01%)</b>	8.788 <b>(99%)</b>	13.406 <b>(97%)</b>	16.142 <b>(86%)</b>	2.454 <b>(28%)</b>	27.769 <b>(71%)</b>	10.339 <b>(99%)</b>	21.212 <b>(99%)</b>	7.728 <b>(28%)</b>
56	7.628 <b>(78.4%)</b>	9.293 <b>(21.41%)</b>	3.100 <b>(99%)</b>	18.882 <b>(87%)</b>	10.402 <b>(52%)</b>	11.439 <b>(99%)</b>	2.000 <b>(0.06%)</b>	0.885 <b>(99%)</b>	17.250 <b>(98%)</b>	11.043 <b>(68%)</b>	12.240 <b>(99%)</b>	2.000 <b>(0.21%)</b>	2.734 <b>(99%)</b>	25.79 <b>(99%)</b>	10.69 <b>(71%)</b>
63	3.816 <b>(34%)</b>	32.710 <b>(65%)</b>	9.500 <b>(99%)</b>	10.354 <b>(86%)</b>	5.430 <b>(35%)</b>	8.876 <b>(99%)</b>	2.000 <b>(0.01%)</b>	12.061 <b>(99%)</b>	13.963 <b>(98%)</b>	23.020 <b>(91%)</b>	11.871 <b>(99%)</b>	0.000 <b>(N.D)</b>	13.237 <b>(99%)</b>	19.733 <b>(99%)</b>	13.926 <b>(70%)</b>
70	9.183 <b>(99.7%)</b>	2.110 <b>(0.27%)</b>	18.657 <b>(99%)</b>	4.737 <b>(16.9%)</b>	4.163 <b>(20%)</b>	12.916 <b>(99%)</b>	2.000 <b>(0.11%)</b>	21.631 <b>(99%)</b>	39.113 <b>(96%)</b>	17.012 <b>(64%)</b>	27.007 <b>(99%)</b>	0.017 <b>(0.11%)</b>	15.073 <b>(99%)</b>	36.366 <b>(99%)</b>	8.192 <b>(63%)</b>
77	19.405 <b>(100%)</b>	2.179 <b>(0.02%)</b>	16.471 <b>(99%)</b>	21.652 <b>(81%)</b>	12.357 <b>(67%)</b>	4.869 <b>(81%)</b>	5.178 <b>(19.2%)</b>	13.459 <b>(99%)</b>	29.934 <b>(93%)</b>	17.483 <b>(54%)</b>	7.534 <b>(99%)</b>	0.012 <b>(0.01%)</b>	19.204 <b>(99%)</b>	42.887 <b>(99%)</b>	15.325 <b>(71%)</b>
84	14.465 <b>(92.7%)</b>	5.041 <b>(7%)</b>	25.647 <b>(99%)</b>	4.212 <b>(20.9%)</b>	7.185 <b>(49%)</b>	8.777 <b>(99%)</b>	2.000 <b>(0.01%)</b>	19.559 <b>(99%)</b>	34.306 <b>(93%)</b>	14.357 <b>(73%)</b>	10.550 <b>(99%)</b>	4.000 <b>(0.12%)</b>	23.557 <b>(99%)</b>	39.706 <b>(99%)</b>	20.052 <b>(61%)</b>

N.D: Non detected

Bold values in parenthesis denote the equivalent percentage the reported value represent from the total concentration reported. (E.g. In column 1: 0.008µg/L is equivalent to 16.6% of total reported Cr<sup>3+</sup>)

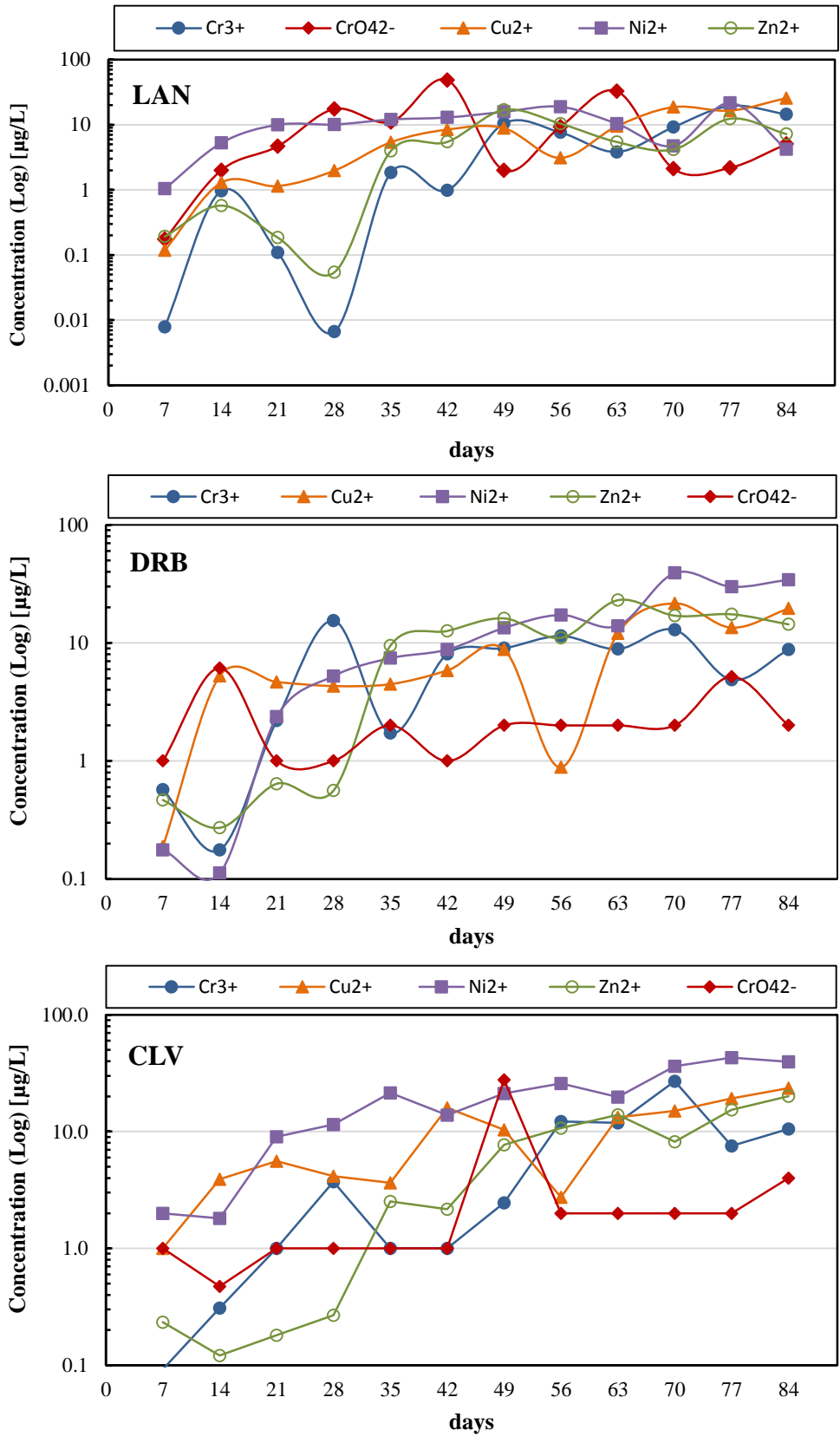


**Figure 5.13:** Heavy metal speciation in leachate from the Lancashire (LAN), Derbyshire (DRB) and Whitby (CLV) black shale formations.

## 5.6 General Discussion

Quality control and instrument performance checks allowed the conditioning of analytical techniques to suit the planned determinations. MDL and IDL provided the statistical means of assessing instrument capability and all three analytical techniques showed acceptable recoveries of spiked and certified standards (Table B.3, B.4 and B.5 in Appendix B). Weathering patterns observed from the 12 weeks leaching experiment are better explained from observed trends in alkalinity, conductivity and pH characteristics observed in weekly leachates analysed. Although, weekly pH trends depict a slightly circum-neutral to alkaline leachate (Figure 5.3), alkalinity measurements show a gradual decrease in the leachates ability to resist changes in pH from weeks 4 (Figure 5.4). Both LAN and DRB black shales show a rapid fall in alkalinity suggesting the build-up of sulphate concentrations in weekly leachates from week 5. Conductivity measurements show a rapid fall from week 1 to week 3 and remain fairly constant till week 12, suggesting a massive release of dissolved ionic species in the effluent leachate from flushing events till week 3 leachates. This would also suggest large dissolutions of oxidised shale released in the first weeks of leaching, typically expected following the removal of oxidised shale.

When dissolution patterns were investigated, all three shales showed gradual increases in reported analytes about week 5 and 6, with the exception of Ni at week 3. Subsequently, cumulative plots of releases designed to cater for the episodic releases from the experiment design, showed increases in the leaching rates with time over the 12 weeks period (Figure 5.6). In most cases, the limiting rate of reaction is controlled by the exhaustion of the limiting reactant. Although it is quite difficult at this stage to determine the limiting reactant, all indications point to sulphate production from available pyrite and the total exhaustion of the residing mineral phase. By fitting linear functions to the observed plots (Equation 5.5), the dissolution rates are computed to a fair degree of accuracy (Table 5.6). To extract comparable quantitative rates however, normalised leaching rates are computed using the SA/V ratio. Normalized plots of the investigated traces depict a rise over two to three orders of a magnitude within the 12 weeks leaching period in all three shales investigated. Significant releases are observed as summarised in Table 5.7, with the Whitby bituminous shale releasing trace metals at an order of a magnitude more in comparison to other black shales investigated.

Pyrite and carbonate weathering rates are used to predict the characteristics of releases leachates following fluid rock interactions simulated in the leaching column. As observed in the short term (Figure 5.11) leachates are characterised by closely similar sulphur and carbonate dissolution rates which accounts for the circum-neutral/alkaline characteristic observed during the pH monitoring (with exception of the Whitby bituminous shale). A linear fit to this data (Figure 5.11) allows a prediction of pyrite and carbonate dissolution rates reported in Table 5.11 and Figure 5.12. These results indicate that with the exception of the Whitby bituminous shale, a 10 year prediction of sulphur weathering rates far exceeds the carbonate weathering rates. This implies the possible generation of acidic leachates as significantly observed in most AMD mines. In addition, this dissolution rates provide the study with the capability to further predict the long term release concentration as intended in the studies objectives. By introducing a decay constant (Equation 5.6), predicted release concentrations can be evaluated as shown in Figure 5.10. These results illustrate a ten year release prediction and can be summaries in Table 5.15.

**Table 5.15:** Summarised concentration of a 10 years release prediction

<i>Trace Metals</i>	<b>5 Year Estimates</b>			<b>10 Year Estimates</b>		
	LAN (mg/L)	DRB (mg/L)	CLV (mg/L)	LAN (mg/L)	DRB (mg/L)	CLV (mg/L)
<b>Chromium</b>	6.89	5.18	4.52	13.68	10.29	9.05
<b>Nickel</b>	5.78	4.12	5.97	11.55	8.24	11.92
<b>Zinc</b>	5.07	4.26	3.94	10.06	8.52	7.85
<b>Copper</b>	2.87	2.33	2.79	5.69	4.62	5.52

To provide a clearer picture of release predictions, it is pertinent to compare these Figures with recommended maximum allowable concentrations and a summary of modelled percentages of toxic species summarised from Table 5.16. It is often acknowledged that total metal concentrations are not appropriate indicators of toxicity for contaminant risk monitoring, but rather the specific metal species give a better indication of possible risks. Therefore, a geochemical modelling exercise was

embarked on to assess possible trace metal species.  $\text{CrO}_4^{2-}$ ,  $\text{Cr}^{3+}$ ,  $\text{Cu}^{2+}$ ,  $\text{Ni}^{2+}$  and  $\text{Zn}^{2+}$ , where identified as best indicators for toxicity.

**Table 5.16:** Summarised mean percentages for identified toxic species from speciation results in Table 5.14

Sampled Shales	Cr(III)	Cr(IV)	Cu(2)	Ni <sup>+2</sup>	Zn <sup>+2</sup>
Lancashire Bowland Shale (LAN)	56.79%	42.71%	99.97%	79.06%	39.53%
Edale Carboniferous Shale (DRB)	90.95%	8.91%	99.92%	96.43%	69.97%
Whitby Bituminous Shale (CLV)	89.09%	12.13%	99.99%	98.62%	51.63%

Therefore in the following subsections, these standards are comparatively analysed with predicted concentrations for each investigated inorganic trace metal. Summarised results in Table 5.16 show that to a greater extent, a bulk of total Cr exist as insoluble Cr(III) ion and to a lesser extent as soluble Cr(IV) (explicit details can also be seen in Table 5.14), with the exception of LAN leachate from weeks 1, 3, 4, 5, 6, and 8 where hexavalent Cr concentrations exceeds trivalent chromium ionic concentrations, all other indicator species ( $\text{Cu}^{2+}$ ,  $\text{Ni}^{2+}$  and  $\text{Zn}^{2+}$ ) are modelled to exist in larger concentrations.

### 5.6.1 Chromium

The world health organisation as well as the European commission recognises the 0.05mg/L recommended maximum allowable concentration for Cr in drinking water. In terms of its ionic species, trivalent Chromium (Cr III), notable for its mild toxicity and its high solubility as well as the highly soluble hexavalent chromium (Cr VI), notable for its acute toxicity are good indicators of chromium toxicity. Computed five year release concentrations stand at 6.89mg/L, 5.18mg/L and 4.52mg/L in the LAN, DRB and CLV shales respectively, clearly exceeding recommended concentrations. Considering that a rise from 1 to 2 orders of magnitude is observed between 5 and 10 year predictions (Figure 5.10), this data provide the potential estimate of the likelihood of inorganic toxicity expected in returning wastewater. Considering discharges to the

environment in England, the environmental standard for annual mean concentration of dissolved hexavalent chromium is reported at 3.4µg/L in rivers and freshwater lakes and 0.6µg/L in transitional and coastal water (EA 2011). Modelled speciation results suggest averages of 42.7%, 8.91% and 12.13% of total chromium released occur as highly mobile hexavalent chromium Cr(VI) compounds (Table 5.16). These Figures suggest that mean released hexavalent chromium compounds stand at 2.94 mg/L, 0.46mg/L and 0.54mg/L in the LAN, DRB and CLV shales respectively. These predicted released concentrations clearly exceed permissible regulatory discharge values in rivers, freshwater lakes, transitional and coastal water and therefore, suggest that treatment for the removal of these inorganic compositions is required. Likewise, environmental standards for trivalent chromium in rivers and freshwater lakes are recommended as an annual mean concentration of 4.7µg/L (EA 2011). With speciation results showing means of 56.79%, 90.95% and 89.1% (Table 5.16) of total released chromium existing as Cr(III) species in the LAN, DRB and CLV shales respectively, mean predicted Cr(III) released stands at 3.91mg/L, 4.71mg/L and 4.03mg/L in these shales respectively. These figures show that released estimates of potentially toxic chromium species exceed both recommended permissible human and environmental limits.

## **5.6.2 Copper**

Copper, known to have an estimated daily intake from food at 1.0-1.3mg/day in adults, as recommended by the US EPA and WHO has a 0.01mg/kg/day minimum acceptable risk level following oral exposures stipulated in the UK. Drinking water toxicity limits for Cu is set at 2mg/L but an environmental standard for Cu concentrations in rivers and freshwater lakes are given 28µg/L at a reported maximum water hardness of >250 CaCO<sub>3</sub> mg/L (5µg/L for transitional and coastal waters). Comparing results for copper toxicity in humans, observed toxic species of free Cu<sup>+2</sup> ions are reported as close to 100% in all three shales and suggests that 5 year predicted results (2.87mg/L, 2.33mg/L and 2.79mg/L), just above drinking water permissible limits are released from LAN, DRB and CLV shales respectively. Of course these figures are all exceeded in the 10 year predictions and suggest long term risk from inorganic Cu contamination. Environmental discharge limits however, are well exceeded and suggest the potential for surface water contamination if discharged or insufficient treatment is offered.

### 5.6.3 Nickel

Classified as a possible carcinogenic (group 2B) element by the International Agency for Research on Cancer (IARC), Ni is also listed as a priority substance in the EA's environmental quality standard (EQS) and has an inland surface water permissible concentration of 20µg/L (EA 2011). In drinking water, toxicity limit is set at 0.02mg/L and the recommended daily intake of less than 1mg. Five year predictions of releasable concentrations are reported at 5.78mg/L, 4.12mg/L and 3.94mg/L in the LAN, DRB and CLV shales respectively, representing 289 times permissible concentrations in both inland surface waters and drinking water limits. Clearly constituting risk to both the environment and human health following exposures. The efficiency of the removal of inorganic Ni in most treatment works in the UK is therefore called to test. Speciation results suggest that 79.1%, 96.4% and 98.6% of total Ni released exist as the toxic free Ni<sup>+2</sup> ions in the LAN, DRB and CLV shales respectively. Even at this, Figures suggest that potential contamination risk could occur from Ni release.

### 5.6.4 Zinc

Zinc's 5 year predicted release concentration are reported as 5.07mg/L, 4.26mg/L and 3.94mg/L in the LAN, DRB and CLV shales respectively. With speciation results predicting a 39.5%, 69.97% and 51.6% of total Zn existing as the toxic Zn<sup>+2</sup> ion (Table 5.16), representing 2mg/L, 2.98mg/L and 2.03mg/L of toxic Zn species are releases from these shales respectively. This Figures all exceeding the recommended annual mean concentrations for total zinc at 125µg/L in rivers and freshwater lakes, recommended by the EA. With regards to human health however, a 3 mg/L toxicity limit is recommended in drinking water and this is exceeded by the 10 year release prediction summarised in Table 5.15. This data has shown that following natural (non-anthropogenic) releases, considerable toxic trace metals are released from all three investigated shale gas prospective formations to warrant considerations of treatment needs. Determining the effectiveness of the current treatment technologies in the removal of these concentrations require further studies however, what is not clear at this stage of the research is the contributions of anthropogenic influences on these trace metal releases.

## **5.7 Limitations of Experimental Study**

It is important to state a few limitations of the experimental study. The research study have been limited to the simulations of field conditions in a laboratory as against field experiments which are more representative of actual conditions and true reproductions of mobility effects. The constraints have been unavoidable due to the limited hydraulically fracture formations present in the UK. At the time of this study (2011-2014), access was denied to the sole fractured shale formation in the UK. The leaching column was adopted as the kinetic test method rather than more recent kinetic methods like the humidity cell tests. The decision to adopt the leaching column method was based on the robustness of the method and the cost efficiency to the project. The Atomic Absorption Spectrometer (AAS) was adopted rather than other efficient spectrometric devices like the Inductively Coupled Plasma Mass Spectrometry (ICP-MS). The choice of spectrometric device was solely based on ease of access to facility and cost of the experimental runs.

## **5.8 Summary & Conclusion**

All three gas prospective shales have been leached to assess the natural release characteristics of selected trace elements under prevailing natural environmental conditions void of anthropogenic interferences but characterised by fluid interactions. From the observed short term release kinetics, predictions on long term releases have also been evaluate. The expected drainage quality (leachate characteristics) following fluid interactions with theses formations have also been investigated with the aim of classifying expected drainage as either acidic, circumneutral or alkaline in nature, as this information was useful in determining pH control on mobility of the investigated trace metals. In addition, the speciation of investigated trace metals have been studied to observed the severity of contaminant risk and the likelihood of metal complexation that increases the risk impact from notably observed toxicant. The following were observed from the studied investigation;

1. Leachate analysed in all three investigated shales, show an increased leaching rates activated in the latter leaching stages (round weeks 3, 5 and 6) of the 12 week experimental period. These deviations suggest an approximate

exponential release rate dependent on the exhaustion of the limiting reactant(s) (possibly pyrite and trace metal residing mineral phase).

2. Predicted of the dissolution kinetics have showed increase in released rates of trace metals over two to three orders of a magnitude within 12 weeks of leaching in all three sampled shales
3. By introducing a decay constant, predictions on the possible 10 year release concentrations for all investigated trace metals in the sampled shale leachates have shown values exceeding EU permissible drinking water standards and UK Environmental quality standards for inland surface water disposal and transitional/ costal water environmental discharge standards.
4. Long term leachate characteristic predictions have shown the possible production of acidic leachates following fluid rock interactions over a ten year period in the Bowland black shale and the Whitby bituminous shale.
5. A geochemical model of possible speciation also reveal the release and solubility of  $\text{CrO}_4^{2-}$ ,  $\text{Cr}^{3+}$ ,  $\text{Cu}^{2+}$ ,  $\text{Ni}^{2+}$  and  $\text{Zn}^{2+}$ , all considered toxic species of the investigated trace metals.
6. The results of the study suggests that non-anthropogenic influences alone are capable of releasing toxic concentrations of the investigated trace metals in all three studied black shales.

## **Chapter 6. Column Kinetics: Fracture Simulated Releases**

### **6.1 Introduction**

Following the study on the release of PTEs from black shale samples retrieved from the investigated prospective shale gas formations, the study considered the influence of hydraulic fracturing (HDF) on these PTE releases and consequently, the possible risk contributions from shale gas development. To successfully evaluate HDF influences on heavy metal releases, assessing HDF industrial practices and simulating key characteristic in its operating conditions is fundamental to the research. This requires replicating as much as possible in the laboratory, key elements in the operational practice that could possibly have impacts on heavy metal release. Such influences such as temperature, pressure, carbon contents and other parameters that define fracturing and the environment must be reproduced. A few of the fundamental aspect of the operational fracturing, is the use of a fracturing fluid containing chemicals that serve different function during fracturing operations. From a contamination risk stand point, it is easy to identify chemical use having a substantial influence on the chemical composition of the returning flowback and the release of toxic components such as our heavy metal indicators.

Other conditions however, such as elevated CO<sub>2</sub> concentration typical in gas mining depths, fracture fluid pressure and temperature have to be considered during the laboratory simulation. In order to achieve comparably results with data obtained from the natural weathering kinetic study, similar experimental design is used for the planned experiment. A kinetic leaching study on three prospective UK shale gas formations is therefore presented here and this method has been adopted in a fixed laboratory to predict water quality characteristics such as pH, alkalinity and the solubility and release of investigated indicator metals using observations from sample behaviour under simulated fracture and weathering conditions. The study experimentally simulated the fracture influenced weathering of all sampled shales to provide data on anthropogenic release potentials for the studied formations. Released concentrations following the simulations of the fracturing conditions are targeted by the spectrometry analysis and thus enabling quantification. With the results obtained,

a comparison can be made between data from potential release concentration in the simulated natural weathering experiment reported in the previous Chapter.

## **6.2 Chapter Objectives**

In this experimental study, release patterns of the selected indicator trace elements under fractured induced weathering conditions are investigated. Data on the variation of PTE releases over time provides a deeper understanding of the leaching behaviour and the characteristic of resulting leachate following fracture simulations. The result should provide information on the characteristics of returning wastewater expected from the development of UK prospective shale gas formations. Hence, the objectives of the experimental study are as follows;

1. Using the studied shale lithologies, run a laboratory scale simulation of fluid rock interactions resulting from fracture induced weathering, noting observable weathering patterns and its influence on long term releases of indicator trace heavy metal compositions.
2. Observe the influence on the leachate quality and potential for the investigated shales to produce acidic, circumneutral or alkaline drainages.
3. Compare data with results obtained in the simulated natural weathering kinetic study in the previous Chapter.

## **6.3 Methodology**

The leaching column experimental setup (EPA 1627: Kinetic test method for the prediction of mine drainage quality) adopted in the previous natural weathering simulation is adopted for this investigation. The method aims at simulating the solubility and release of indicator heavy metals as would occur following a fracture induced weathering of the investigated prospective shales.

### **6.3.1 Composition and Preparation of Simulated Fracture Fluid**

An earlier review of chemical use during the sole fractured UK shale gas well, provided data on the chemical composition of fracture fluid used by the exploratory firm. Providing data necessary for the preparation of fracture fluid of similar

composition for the planned laboratory investigation is important for the experimental objectives set out in this chapter. Due to the stark difference in US reported chemical use with UK practises and the goal of the study to assess UK indigenous risks, only UK reported data of chemical use have been considered in the laboratory plan. The review revealed that of all five components highlighted by the exploratory firm, Hydrochloric acid (HCl) represents the sole constituent with a likely influence on heavy metal release. Other constituents such as the polyacrylamide friction reducer and the sand are used in negligible concentrations and are used in more of a mechanical capacity and deemed to have little or no effect on the chemical properties of the leachate produced. Based on data released by the exploratory firm (Table 2.3 Chapter 2), 99.75% of fracturing fluid contained water and sand with 0.125% representing Hydrochloric acid (HCl) and 0.075% representing Polyacrylamide oil based Friction Reducer (North Meols News, 2011; Cuadrilla Resources, 2012). A total 8399.2m<sup>3</sup> (8,399,200 litres) of fresh water was reported to have been used for all six stages with fracture fluid. This represents an equivalent volume of 8378.2m<sup>3</sup> (8,378,200 litres) of fresh water. From the percentage volume of acid used, a computed equivalent volume of food grade (E507) Hydrochloric acid represents 10.499m<sup>3</sup> (10499 litres). Assuming other fluids contribute negligible effect in diluting concentrated acid, a 10,499L 12.08M concentration of HCl acid, diluted in 8,378,200L will result in an empirical concentration of 0.02M concentration of HCl acid and quite rightly affirms the exploratory firm's claim that dilute concentration of the acid similar to stomach acids was used in the fracturing operation. Therefore, SFF serves as the leachant and is prepared by diluting a 12.08M concentration of HCl acid to a final concentration of 0.02M. A thorough determination of all quality control parameters was conducted before all analytical determinations and is similar to does documented in Chapter 5. This has not been documented here to avoid repetition.

### **6.3.2 Sample Preparation**

Collected sample were reconstructed to particle sizes as described in Table 4.1 to standardize the conditions of exposure for all sampled shale types and facilitate uniform expose of sample to weathering conditions and collection of leachate. Details of sample collection, preparation, determinations of surface area (BET) and all preparations to sample before leaching procedure are documented in the Chapter on

materials and methods. Similar dry sample weight of tailings (2000g) is prepared for all shale loaded leaching columns.

### **6.3.3 Experimental Design and Setup**

Leaching columns used in the natural leaching experiments are cleaned out and setup for this experiment. Four number columns, one for each sampled formation and a fourth to serve as control are setup. A simulated fracture fluid (SFF) containing 0.02M Hydrochloric Acid (HCl) and saturated with CO<sub>2</sub> was used as the leaching agent. A 12 weeks leaching exercise designed to simulate releases following the fracture of the formation commenced in December 2013 with 5 initial column flushes to attain a relative standard deviation of less than 20%. Tap water in the carrier boy is replaced by the SFF and laboratory supplied air at 8 litres per min (increase in flow rate to account for addition pressure during fracturing) is supplied via a flow meter and bubbled through a carrier boy containing SFF solution. In addition, a CO<sub>2</sub> gas cylinder is connected to the carrier boy and CO<sub>2</sub> is bubbled into the SFF solution. Gases are mixed to a ratio of 90% laboratory air to 10% CO<sub>2</sub> using flow valves (rotameter). Using a portable CO<sub>2</sub> meter, CO<sub>2</sub> released from the column exhaust is monitored. The CO<sub>2</sub> bubbled through the system accounts for the elevated CO<sub>2</sub> concentrations from oil and gas wells in comparison to atmospheric concentrations. The gas collected at the top of the carrier boy was channelled to the leaching columns via a series of flowmeters designed to allow a flow of 2L/min (increased flow rate to account for additional pressure during fracturing) into each column during the 7 day humidification cycle. Leachate are collected following the 24hr saturation cycle via the water inlet tubing and immediately analysed for pH. Total water collected was measured and samples for trace metal determination were refrigerated until analysis. Week 12 analysis was completed in March 2013. Again, following the 12 weeks leaching run, samples in each leaching columns were removed dried, re-weighed, re-sieved and particle size distribution re-evaluated to determine the distribution after leaching. Surface area via the BET analysis was also re-determined following the end of the 12 weeks leaching.

Columns were loaded with recorded masses of sampled black shale and a fourth column, subjected to identical treatment, was loaded with laboratory glass beads to serve as control. Alternating cycles of 6 days humidification and 24 hours saturation

were applied to each column following an initial flushing cycle (3Nos.) to remove any oxidized components of the shale. Leachates were analysed for major metals Al, Fe, Ca and Mg and indicator PTEs Cr, Cu, Ni and Zn. All glassware and Teflon vessels used were washed with detergent, rinsed in tap water, acid wash with Nitric acid, rinsed with tap water followed by a final rinse in ultrapure water. For sample preparation, dissolved analytes were determined in aqueous samples after suitable 0.45µm filtration and acid preservation. Samples for trace metal determinations are refrigerated below 4°C to prevent recrystallization. A summary of each loaded column characteristics is listed in Table 6.1 below.

**Table 6.1:** Summary Properties of Loaded Experimental Column

<b>Parameter</b>	<b>Unit</b>	<b>Column 1 (LAN)</b>	<b>Column 2 (DRB)</b>	<b>Column 3 (CLV)</b>
Height of tailings in column	cm	64.5	63.9	64.6
Column diameter	cm	5.08	5.08	5.08
Column Height	cm	76.2	76.2	76.2
Surface area	cm <sup>2</sup>	1081.1	1068.3	1047.6
Volume of tailings	cm <sup>3</sup>	1411.2	1388.1	1325.4
Specific Gravity	-	2.40	2.42	2.45
Dry weight of tailing	kg	2.000	2.000	2.000
Leachant rate /weeks	L/wk.	0.394	0.369	0.400
Total leachant delivered	L	4.730	4.430	4.795
Ratio (leachant to mass of tailings)	L/kg	2.365	2.215	2.398

## **6.4 Results**

A step wise presentation of results obtained is documented to set the stage for the discussion of result. A summary however, of the methodology adopted in the results presentation is provided in the section of presentation of data. Results presented here are solely representative of data obtained from the SFF leaching of all three investigated shale. Comparison between these and results obtained in the accelerated natural leaching experiment discussed in Chapter 5 are presented in Chapter 7.

### **6.4.1 Presentation of Data**

The general characteristics of the leachates collected from each column are presented with discussions on the pH, alkalinity and conductivity trends over the sampling period. As previously compiled in the previous leaching cycle, release trends are presented via time plots of analytical data obtained. Plots of accumulated release give a better indication of the overall kinetics of the column leaching experiments hence each accumulated release curve is then fitted to either an exponential, power or linear function by regression analysis and the fitting Equations Equation are extracted. A critical analysis of the data obtained is also reported by expressing release concentrations as normalised elemental mass loss by the introduction of the BET data gathered. This allows a comparative analysis of the releases in all three shales investigated. Plots are drawn to show comparisons of all three investigated shales in terms of metal leaching rate, sulphate leaching/depletion (Pyrite oxidation) rates and carbonate dissolution rate, allowing the determination of the acid mine drainage predictions for all three investigated shales. Geochemical modelling of the possible speciation of indicator heavy metals are also presented with emphasis on a selections best species for contamination monitoring. Predictions of potential metal releases are also made possible by extrapolations of the rates of reactions from the data obtained. Intra-column comparisons (comparison between columns) are also presented to visualise the characteristic behaviour between sampled black shales. Finally, release kinetics between the simulated natural weathering results and the fractured enhanced weathering are compared to aid our understanding of the influence of hydraulic fracturing on PTE releases and the possible impact of shale gas development on contamination release from prospective shale gas formations.

## 6.4.2 Leachate Analysis

The twelve weeks long laboratory simulation of fractured enhance weathering commenced on 9<sup>th</sup> December 2013 and was completed by 25<sup>th</sup> February 2014. Raw concentrations of weekly leachate were recorded against sampling volume collected and the weighted concentrations are computed. Flush leachates are combined and concentrations are reported as week 0. Subsequently, weekly releases are compiled as week 1 to weeks 12 releases. Cumulative weighted concentrations are computed from raw data and the weekly weathered mass in grams is also computed from volume of leachate collected. Weekly analyses of alkalinity, temperature, sulphate, calcium and magnesium in addition to indicator trace heavy metals were useful in achieving these Chapter objectives.

### 6.4.2.1 Leachate Characteristics

Prior to the leaching, the SFF recorded an average pH of 2.25 and it was expected that following fluid rock interactions and the dissolution of ionic compositions of the shale, an increase in pH would be observed. Hence, pH trends (Figure 6.1) show fluctuations between 5.45-7.3, 6.22-7.8 and 5.4-6.5 in the LAN, DRB and CLV shales respectively. Because of the low pH of the leachates, it is expected that common rock constituents considered as insoluble in neutral to alkaline environments may be leached by the low pH SFF resulting in changes in the metal chemistry within the columns.

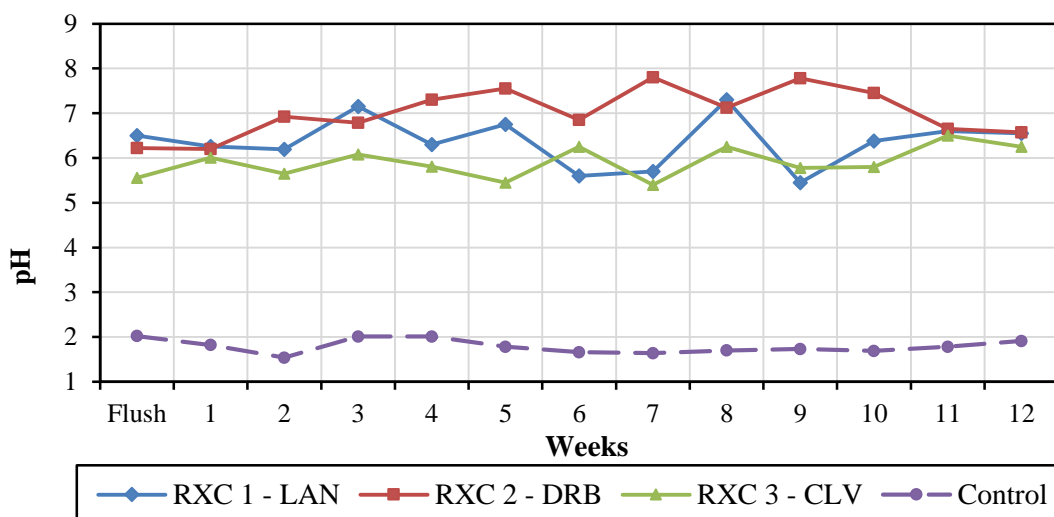


**Figure 6.1:** Weekly pH trend in Leachate

Constituents such as Al, Fe, Ca, Na, K are typically present as macro concentrations across all three shales. The DRB shale which produced the highest percentage carbonate content (22.27%) surprisingly did not produce the highest leachate alkalinity recorded but was slightly edged out by the CLV shale (Figure 6.2). Constant to slowly declining anions and cation concentrations were observed in all three shale with the exception of trace metal concentrations which rapidly increased from week 1 to week 12. This may suggest a prolonged trace metal dissolution even as the initially acidic SFF was neutralised by dissociating carbonates and other neutralizing elements. Alkalinity also declined gradually from week one as it appears was over-shadowed by sulphate production within the each column.

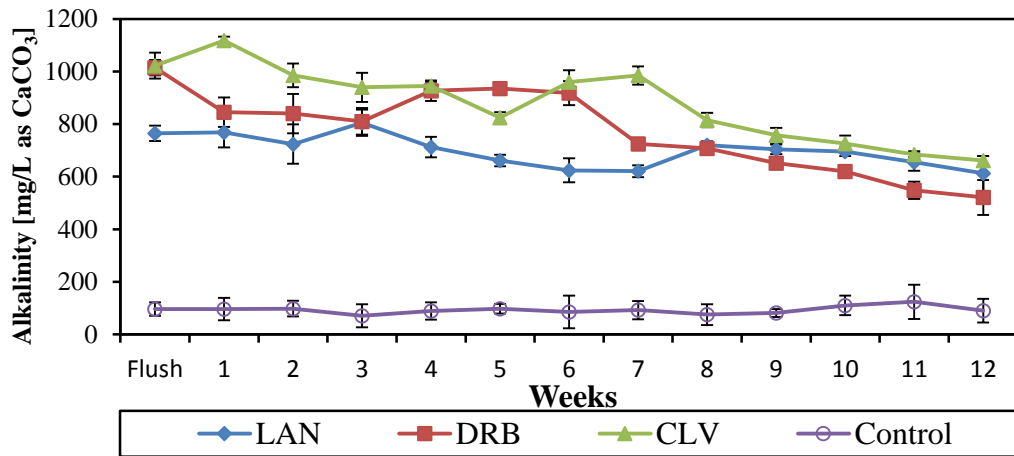


**Figure 6.2:** Alkalinity Concentrations for all Three Investigated Black Shales

The drop in conductivity between week 0 and 1 (with the exception of CLV shale) accounts for the loss oxidized shale following the initial flushing event. Leaching commences on week 1 and data show a gradual decrease in specific conductance from week 1 to 10 followed by a rapid increase from week 10 (Figure 6.3) in all three shales. Since conductance is a measure of the dissolved solids, the results are in agreement with results observed from the spectrometric chromatographic analysis which show increases in dissolved concentrations reported in the latter phases of the leaching. Similar trends have been reported in mine drainages in Canada and the US (Rose and Cravotta 1998, Hornberger and Brady 2009), where the low pH results in the solubility of minerals and elements. Eventually the dissolved constituents result in a high conductance reading during the latter phases of the weathering. Hornberger and Brady (2009), attributed this to reflects two phases of weathering; the first with circumneutral

leachate as alkalinity is generated; and the second, an acidification phase as pyrite oxidation dominates. DRB shale in column 2, records the lowest specific conductance lasting from week 1 till 10, however its rapid increase from week eleven superseding CLV conductance values in weeks 11, 12 and 14. The LAN shale records the largest conductance values with a minimum of 785 $\mu$ S/cm and highest recorded at 1814  $\mu$ S/cm. Leachates from the LAN shale also appear murky with larger dissolved particles when filter through a 0.45 micro filter and is indicative of the high conductance values obtained.

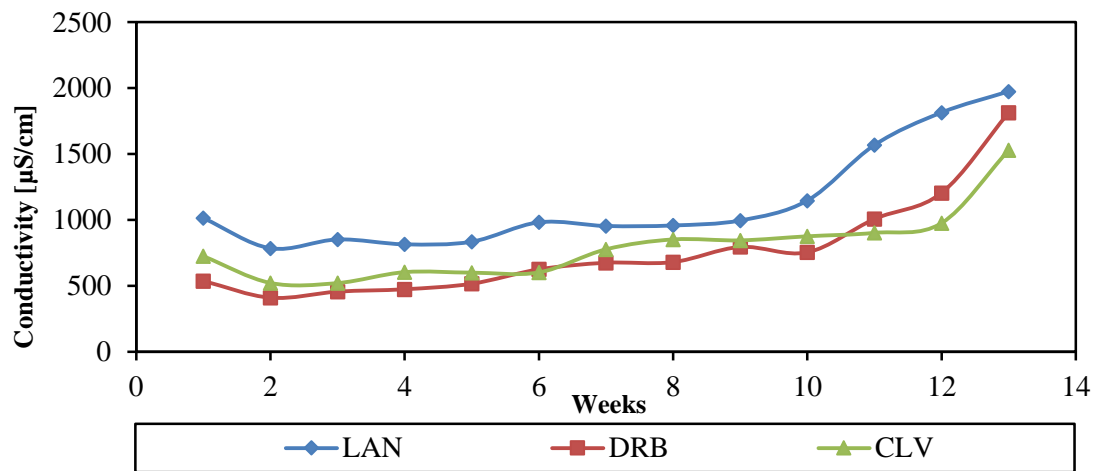


**Figure 6.3:** Weekly Conductivity Trends for all Three Sampled Shales

#### 6.4.2.2 Weathering Pattern

Weighted concentrations plots (episodic releases) are cumulatively plotted to show total releases over the leaching duration (Figure 6.4). Release for week 0 representing concentrations released during the initial column flush cycles have not been included in this plots. For trace metal concentrations (Figure 6.4), releases in the LAN shale are predominantly higher than both the DRB and CLV shales, with the exception of Cu. Release concentrations often start with an increase within the first 3 weeks followed by a gradual decline in releases. All trace metals follow this pattern with the exception of Cu in the DRB and CLV shales. Cumulative plots show a gradual flattening with each progressing week giving the indication of source depletion in the latter weeks of leaching.

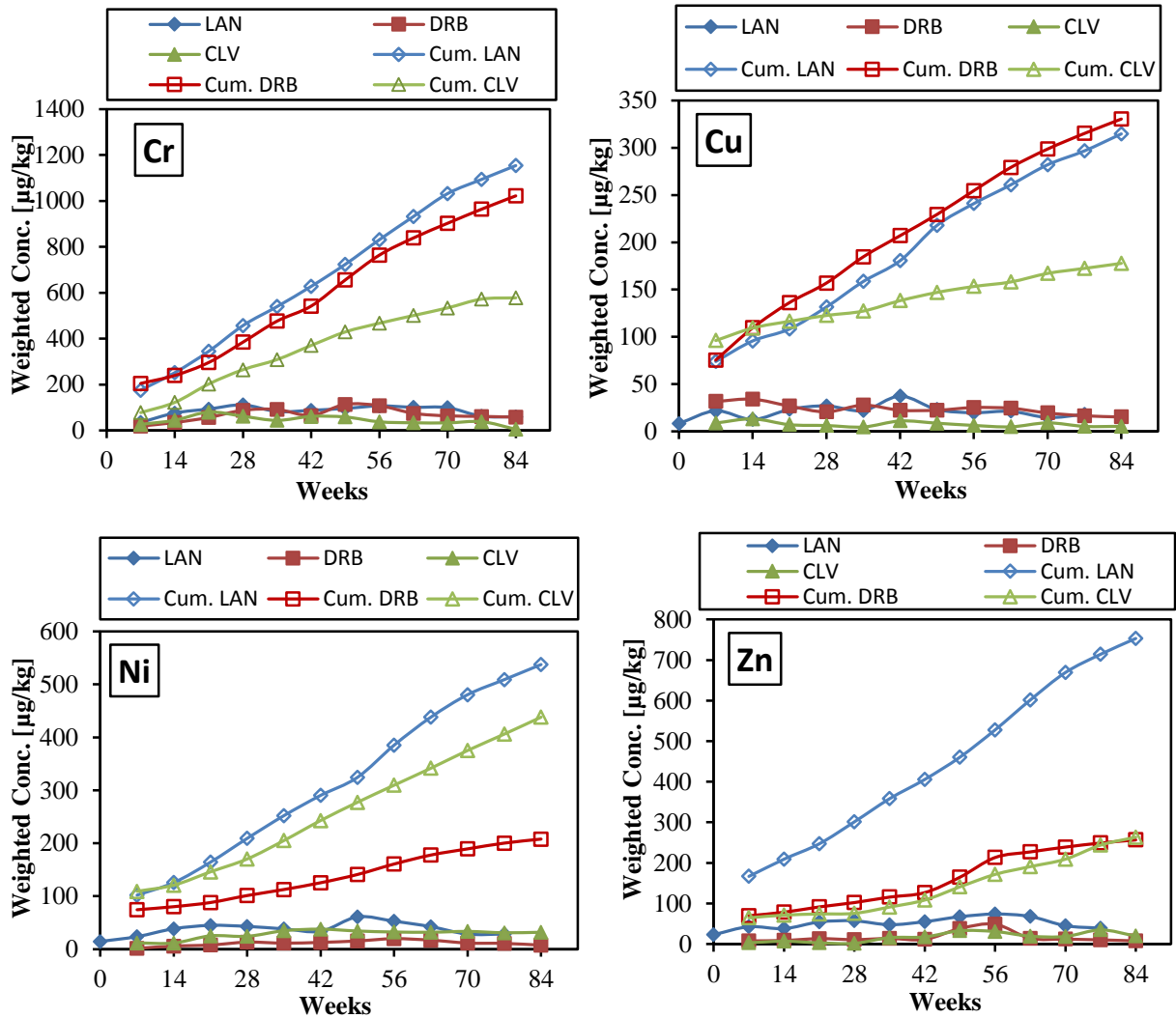


**Figure 6.4:** Leaching Data showing weighted Concentrations ■ and Cumulative Weighted concentrations □

Plots of cumulative releases of trace metal concentrations from all three shales show that the data can be best described by linear functions of the form;

$$C=At^n+K \text{ ----- Eq. 6.1}$$

Where A is the empirical rate constant in  $\mu\text{g}/\text{kg}\cdot\text{day}^{-1}$  and K is a constant that takes account of the observation that the extracted element does not become zero at time (t) = 0. Simply, K is the release concentrations recorded during the initial column flush. Details of observed linear fit to the cumulative data (Figure 6.5) are provided in Table 6.2 below. The regression coefficient,  $R_2$ , is a measure of the goodness of fit and is documented in Table 6.2.

**Table 6.2:** Computation for Dissolution Rates and Goodness of fit for the Cumulative Leaching Data

<b>Column</b>	<b>Fit Equation</b>	<b>A</b>	<b>n</b>	<b>k</b>	<b>R<sup>2</sup></b>
Cr (LAN)	$y=90.545x + 5.047$	90.545	1.000	5.047	0.9961
Cr (DRB)	$y=77.059x + 35.817$	77.059	1.000	35.817	0.9869
Cr (CLV)	$y=47.779x + 10.188$	47.779	1.000	10.188	0.9809
Cu (LAN)	$y=22.467x +29.407$	22.467	1.000	29.407	0.9916
Cu (DRB)	$y=23.870x -34.481$	23.870	1.000	34.481	0.9931
Cu (CLV)	$y=7.483x + 83.973$	7.483	1.000	83.973	0.9925
Ni (LAN)	$y=40.662x + 15.874$	40.662	1.000	15.874	0.992
Ni (DRB)	$y=12.596x + 45.079$	12.596	1.000	45.079	0.979
Ni (CLV)	$y=30.132x + 38.357$	30.132	1.000	38.357	0.989
Zn (LAN)	$y=54.145x + 48.445$	54.145	1.000	48.445	0.991
Zn (DRB)	$y=18.593x + 23.214$	18.593	1.000	23.214	0.956
Zn (CLV)	$y=17.855x + 10.752$	17.855	1.000	10.752	0.927

Hence, these results obtained suggest that Cr release in the LAN shale holds the largest dissolution rates at  $90.545\mu\text{g}/\text{kg}\cdot\text{day}^{-1}$ . The lowest rates are observed in Cu releases with a release rate of  $7.483\mu\text{g}/\text{kg}\cdot\text{day}^{-1}$ . Relatively large release rates are observed with Cr across all three sampled shales and although copper releases appeared to be low from the cumulative plots, dissolution rates are relatively high. Considering these linearized Equation however, important factors affecting the releases kinetics have been generalised by a single empirical rate expression ‘A’. These factors such as the effect of different particle sizes and surface reactivity (oxidation of species at the mineral/water interface) and the transport of dissolved species from the mineral surfaces to the bulk fluid, all play important roles that contribute to the leaching mechanism. It is therefore imperative that these factors be taken into account when determining the dissolution rates. A simple resolution to this challenge is to normalise the data to include a normalization of the leach rates based on a combination of these factors. These include properties such as SA/V and inventory of species leached. Therefore, specific details that contribute to the leaching mechanism are taken into

consideration and this approach allows a direct and quantitative comparison of elemental releases from all three shale samples. This form of normalization takes the form of the elemental mass loss (NL<sub>i</sub>).

### 6.4.2.3 Trace Metal Release Kinetics (Dissolution Rate)

These observed release patterns can be used to predict long term releases trends of selected PTE indicators if quantitative rates can be deduced. As discussed previously, a basis for comparison amongst all three sampled shales can be achieved if computed leaching rates can be normalised to the surface area, volume of leachate and quantitative inventory of heavy metals leached from the sampled rocks as described in Equation 6.2 below.

$$[NL]_i = C_{ij} \times \frac{V_j}{[f_i \times SA]} \text{----- Eq. 6.2}$$

- Where: **[NL]<sub>i</sub>** = Normalized mass loss of element *i*
- C<sub>ij</sub>** = Concentration of element *i* in specimen *j* leachate that was filtered through a 0.45 micron filter
- V<sub>j</sub>** = Initial volume of leachate containing specimen *j*
- f<sub>i</sub>** = the mass fraction of element *i* in the unleached specimen
- SA** = Specimen Surface area

Applying this normalization to the release data results in the dissolution rates listed in Table 6.3 and contains the average normalized release rates for each trace heavy metal investigated at an average test temperature of 20°C. In comparison to rates obtained in Table 6.2, a direct comparison base on the details contributing to the leaching mechanism reveal the largest being Cr dissolution in the Whitby Bituminous shale as against the Cr dissolution in the Lancashire Bowland shale. Results suggest that when these details are considered, Cu dissolution in the Edale shale which appears over three times rates in the other investigated shale is in fact closely similar (LAN-2.46E-09, DRB-2.99E-09 and CLV-4.42E-09 mol/m<sup>2</sup>/day) (Figure 6.5). Zinc release rates in the Lancashire Bowland shale reveal the slowest rates recorded with dissolution rate at 1.52E-09 mol/m<sup>2</sup>/day. Interestingly however, dissolution rates between weeks 1 and week 14 for Cr and Cu are relatively steady with only an order of a magnitude increase

and in some cases no observable increases in rates. In contrast to these, rates observed in Ni and Zn, show between one and two orders of a magnitude.

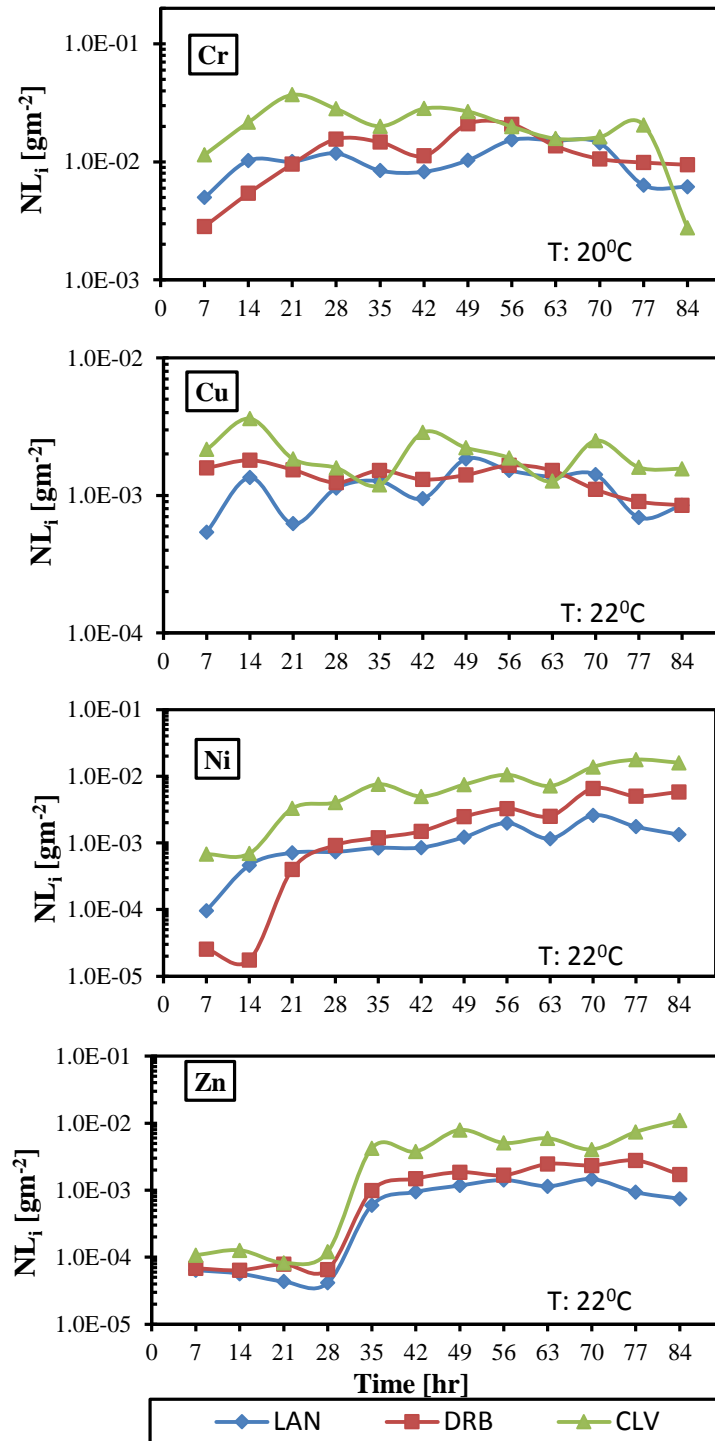


**Figure 6.5:** Comparison of Normalized Heavy metal Release from Sampled Shales

**Table 6.3:** Normalised Release Rates [mol/m<sup>2</sup>/day]

Traces	Reactor 1 (LAN)	Reactor 2 (DRB)	Reactor 3 (CLV)
Chromium (Cr)	2.70E-08	3.22E-08	5.52E-08
Copper (Cu)	2.46E-09	2.99E-09	4.42E-09
Nickel (Ni)	2.71E-09	5.85E-09	1.85E-08
Zinc (Zn)	1.52E-09	2.75E-09	8.81E-09

**6.4.2.4 Predicting Long term Leachate Composition**

As computed in the previous experimental analysis (Natural release kinetic), predictions of future leachate compositions can be obtained by adopting the relationship exhibited by the time series plots of released concentrations. This relationship describes the rate of chemical concentration change in column leachate and can be described as an exponential function expressed as;

$$C_t = C_o \times e^{kt} \text{-----Eq. 6.3}$$

Where: C<sub>t</sub> = concentration at time t, C<sub>o</sub> represents concentration at time zero, e is the base (approximate value of 2.718), k represents the rate of concentration change per unit time and t represents Time. Since this chemical changes follow a growth function similar to many chemical and biological systems, it is possible to predict long term concentrations, provided conditions do not change or there are very minimal condition variations (minimal changes in temperature). Hence by solving for the rate ‘k’, Equation 6.3 above can be rearranged as follows;

$$\ln (C_t/C_o) = \ln (e^{kt}) \text{-----Eq. 6.4}$$

$$\ln C_t - \ln C_o = kt \text{-----Eq. 6.5}$$

$$\ln C_t = kt + \ln C_o \text{-----Eq. 6.6}$$

$$k = (\ln C_t - \ln C_o) / t \text{-----Eq. 6.7}$$

$$k = \ln (C_t / C_o)/t \text{-----Eq. 6.8}$$

The rate of chemical change in column (or using a more conventional terms ‘growth constant’) can therefore be derived from a plot of the  $\ln (C_t / C_0)$  versus time (t) and would represent the slope of plot determined by linear regression. These computations are performed using a spread sheet and the summaries of results obtained are reported on Table 6.4 along with the  $R^2$  values computed from regression computations. The R squared ( $R^2$ ) values indicate a strong relationship for estimating the rate of change (growth constant) and suggest that the leachate characteristics completely follow a simple time-concentration function. As observed, all values exceeding 0.85 and thus shows the statistical significance of the results obtained (Table 6.4). The slowest rates of Cr change is observed in the Edale black shale but the values are relatively similar and show the effectiveness of the leaching protocol in providing similar leaching mechanisms. Cu in the Whitby formation however had the lowest rate of change at an order of magnitude slower than most rates observed while almost identical rates are observed for both Ni and Zn.

**Table 6.4:** Estimated rate of change (decay) constants for Cr, Cu, Ni and Zn

Traces	LAN Shale [ $\mu\text{g/L/day}$ ]	Variation ( $R^2$ )	DRB Shale [ $\mu\text{g/L/day}$ ]	Variation ( $R^2$ )	CLV Shale [ $\mu\text{g/L/day}$ ]	Variation ( $R^2$ )
Chromium (Cr)	+2.50E-02	0.9371	+2.21E-02	0.9683	+2.72E-02	0.8603
Copper (Cu)	+1.95E-02	0.9665	+2.09E-02	0.8807	+8.20E-03	0.9688
Nickel (Ni)	+2.25E-02	0.9656	+1.41E-02	0.9870	+1.91E-02	0.9843
Zinc (Zn)	+2.03E-02	0.9790	+1.88E-02	0.9729	+1.93E-02	0.9678

If results are compared with alkalinity trends, all trace metals show increasing releases following leaching with a corresponding increase in alkalinity. The above data suggest similarities in leaching behaviour for all traces investigated shales. Again the positive (+ve) values are an indication of an increase in rates (growth) rather than a decrease (decay). Plots of these relationships (Figure 6.6) show the similarity with all shales investigated. Trends show increasing rates but also give the indication of a drop in rates towards the latter stages of the leaching (week 11-12). Rates across all three shales for Cr, Ni and Zn are almost identical with Cr rates in the CLV shale, Cu, Ni and Zn rates in the LAN shale having a slight edge over other.

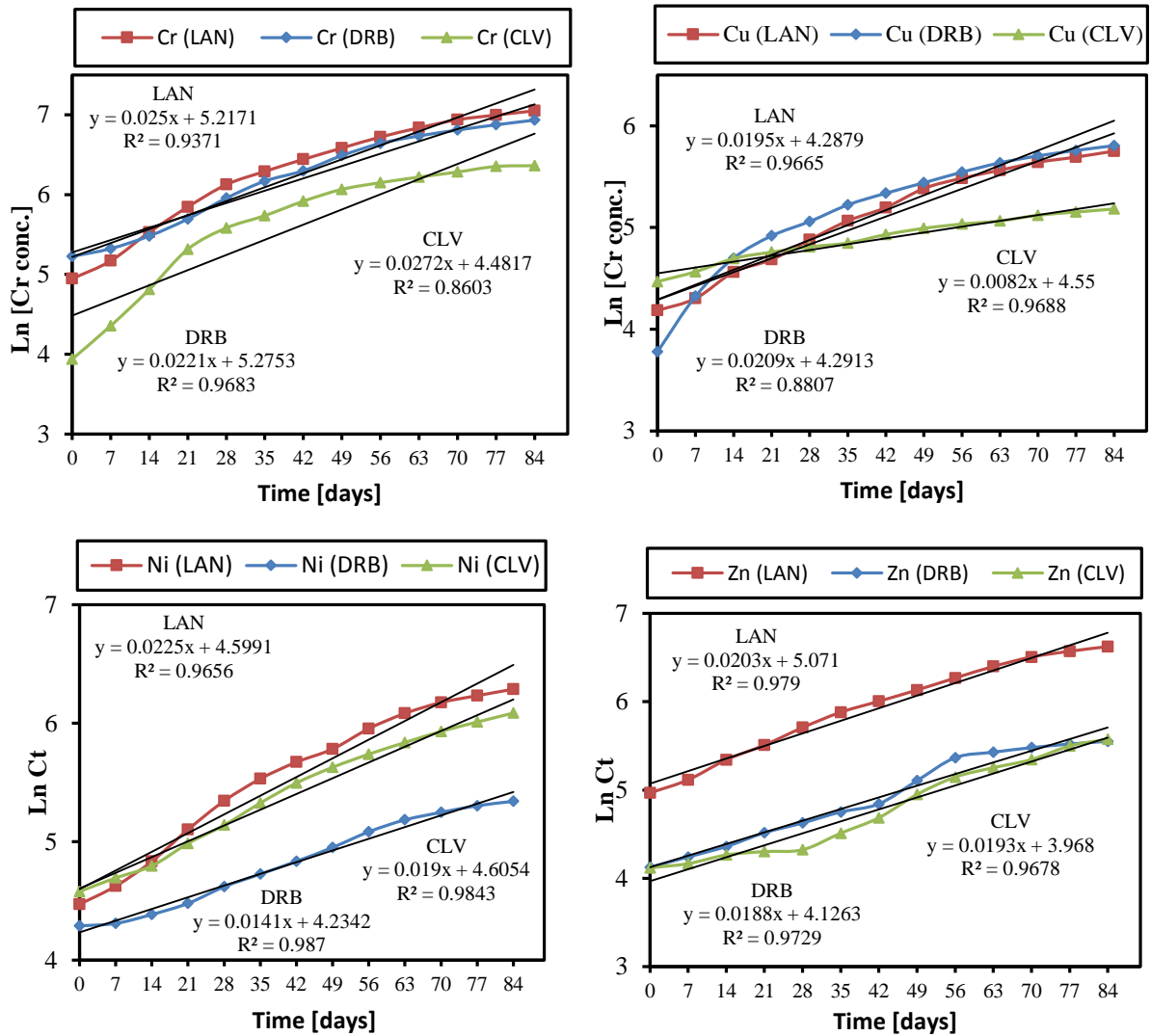


**Figure 6.6:** Curve fitting to flux computation

These rates can subsequently be useful as part of a collection of tools and techniques to estimate expected impacts and treatment needs however, for the intended study's objectives, a 10 year prediction (Figure 6.7) is evaluated showing time specific predictions of expected leachate quality. These data has been plotted on a semi logarithmic scale to accommodate for releases spanning over several orders of a magnitude. Results suggest that the largest observable releases are from Cr in the Lancashire Bowland shale and Whitby Bituminous shale. Both are predicted to reach concentrations in excess over 2 to 3 orders of a magnitude from initial concentrations. While most of the other investigated traces are predicted to rise above 1 to 2 orders of magnitude, Cu in the Whitby Bituminous shale show the least indication of mobility from modelled results (Figure 6.7).

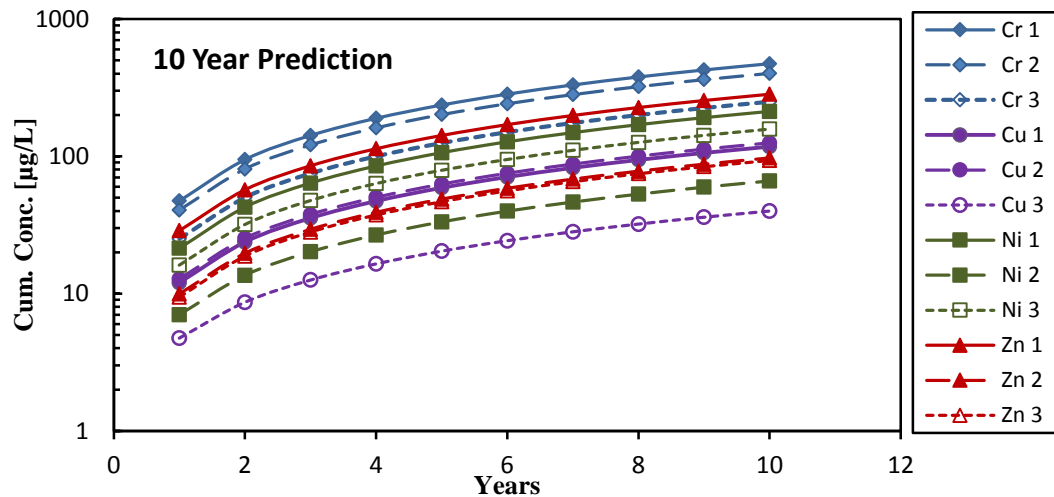


Figure 6.7: Ten year prediction of release concentrations

#### 6.4.2.5 Pyrite and Carbonate Weathering Rates

The nature of the resulting leachate is greatly dependent on the interplay of acid producing and base neutralising components. Hence, the advantages of predetermining the resultant nature of returning drainage from fractured formations can provide information on the possible risk impact. By obtaining the rates of acid formation in individual columns and comparing results with the corresponding neutralization potential, this objective can be achieved. Therefore in this section, pyrite and carbonate oxidation rates have been assessed to determine the long term nature of leachates produced. The methods adopted for this investigation have been described previously in similar analysis in Chapter 5 however it is essential to point out this method is based on the following key assumptions;

1. All Ca and Mg in solution are derived from carbonate dissolution only
2. Pyrite is the only sulphide mineral that contributes to acid formation.

Hence, by obtaining cumulative percentages of sulphur and carbonate in all sampled shales, a comparison on the rates of acidification and neutralization in the respective shales can be evaluated. After 12 weeks of leaching, results (Table 6.5) show that generally greater carbonate weather is achieved in comparison to pyrite dissolution and subsequent acid formation

**Table 6.5:** Summary computation for Cumulative percentage sulphur and carbonate weathered in all three investigated shales

Days	LAN		DRB		CLV	
	Sulphur (%)	Carbonate (%)	Sulphur (%)	Carbonate (%)	Sulphur (%)	Carbonate (%)
1	0.102	0.127	0.094	0.125	0.049	0.179
7	0.152	0.477	0.151	0.314	0.083	0.408
14	0.189	0.942	0.219	0.929	0.106	1.576
21	0.212	1.250	0.291	1.085	0.147	1.785
28	0.241	1.530	0.351	1.254	0.196	2.015
35	0.268	1.769	0.401	1.394	0.236	2.240
42	0.293	1.992	0.446	1.573	0.272	2.477
49	0.312	2.286	0.494	1.769	0.301	2.725
56	0.345	2.585	0.536	1.975	0.334	2.986
63	0.396	2.864	0.593	2.161	0.364	3.199
70	0.441	3.090	0.635	2.297	0.380	3.390
77	0.473	3.236	0.677	2.405	0.391	3.598
84	0.505	3.372	0.724	2.509	0.401	3.798

.Approximately 8 times more Carbonate is weathering in comparison to pyrite in both the LAN and CLV shales, enough to inhibit the generation of acids in the formation. In the Derbyshire Edale shale, 3.5 times more neutralising carbonates are released into solution (S:0.72%, CaCO<sub>3</sub>:2.54%) at the end of the 12 weeks leaching simulation while the bituminous Whitby shale show faster carbonate dissolution rate (S:0.401%, CaCO<sub>3</sub>:3.798%) in comparison to sulphur (Table 6.5). Although all weathering rates depict a faster carbonate dissolution rate in comparison to the pyrite oxidation rate (Figure 6.8), these rates are relatively similar within the twelve weeks leaching intervals to make a meaningful conclusion on the leachate characteristics. A better understanding of the long term leachate quality and characteristic nature of resulting leachate can be evaluated by fitting a function to the data as illustrated in Figure 6.8 and predicting the future nature of resulting leachate.

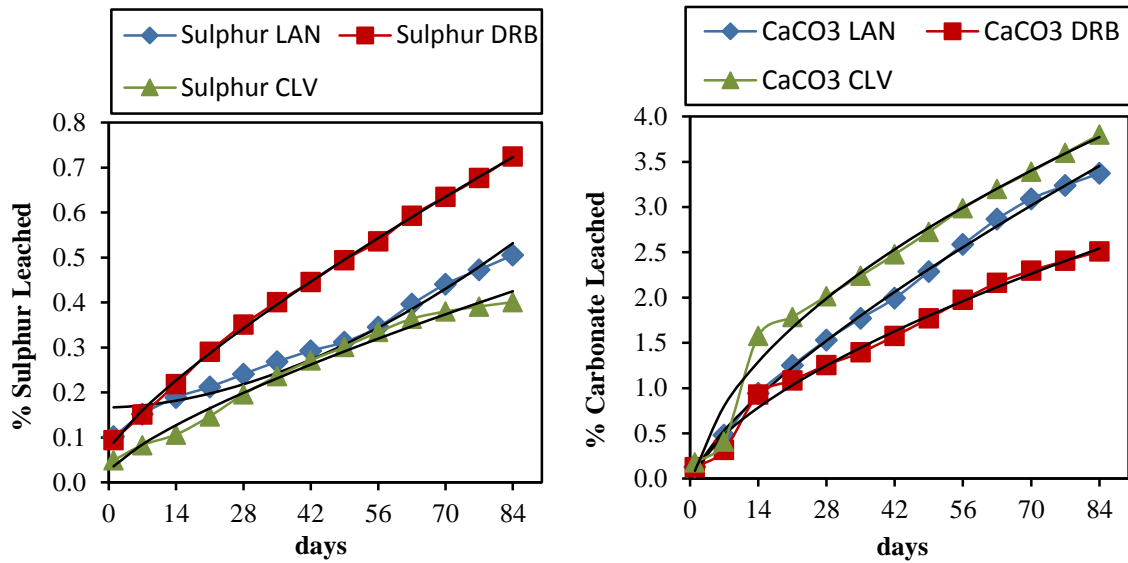


**Figure 6.8:** Curve fitting on cumulative percentage sulphur and carbonate data

The observed linear fit to the data is of the form represented in Equation 6.1 and was used in obtaining a linearization of the data collected (Table 6.6) and enabling a 10 year predictions of leachate characteristic shown in Figure 6.9. The results suggest that in the first year following fractured induced anthropogenic disturbances, provided the rates do not change, black shale from the Bowland formation will leach approximately 1.79% of its acid producing sulphur content and 14.52% of its acid neutralizing carbonate content.

**Table 6.6:** Curve Fitting Parameters for Sulphur and Carbonate plots in Figure 6.8

Column	Description	Fit Equation	A	n	k	R <sup>2</sup>
RXC 1	Sulphur LAN	$y = 0.005x + 0.109$	0.005	1.000	0.109	0.9901
RXC 2	Sulphur DRB	$y = 0.0074x + 0.118$	0.0074	1.000	0.118	0.9925
RXC 3	Sulphur CLV	$y = 0.0045x + 0.060$	0.0045	1.000	0.060	0.9754
RXC 1	Carbonate LAN	$y = 0.0389x - 0.328$	0.0389	1.000	0.328	0.9864
RXC 2	Carbonate DRB	$y = 0.0278x - 0.353$	0.0278	1.000	0.353	0.9647
RXC 3	Carbonate CLV	$y = 0.0406x - 0.627$	0.0406	1.000	0.627	0.9384

The same formation is projected to achieve double figures in 6 years, reaching approximately 10.20% of sulphur release and an equivalent 85.51% carbonate content

release (Table 6.7). Consequently, it is highly likely that return waste flow from the Bowland formation will be alkaline since rates of carbonate dissolution proceed much faster than sulphur dissolution. If solubility of any PTE of concern is encouraged by the acidic nature of the aqueous environment, mobility is very likely. These projections suggest that black shale from the Edale formation in Derbyshire will leach just 2.84% of its sulphur content in comparison to 10.50% of its carbonate content within its first year. This implies again that the waste stream will eventually become acidic as rates of carbonate dissolution occur much faster. These predictions suggest that waste flowback from the Whitby Bituminous formations will most likely give off acidic discharges.

**Table 6.7:** Computation of predicted percentage pyrite and carbonate rates

DURATION		LAN		DRB		CLV	
Days	Weeks /Years	Sulphate (%)	CaCO <sub>3</sub> (%)	Sulphate (%)	CaCO <sub>3</sub> (%)	Sulphate (%)	CaCO <sub>3</sub> (%)
70	10 weeks	0.43	3.05	0.64	2.30	0.38	3.47
77	11 weeks	0.46	3.32	0.69	2.49	0.41	3.76
84	12 weeks	0.50	3.59	0.74	2.69	0.44	4.04
365.2	1year	1.79	14.52	2.84	10.50	1.71	15.47
730.5	2years	3.47	28.72	5.56	20.65	3.37	30.30
1095.7	3years	5.15	42.92	8.28	30.80	5.02	45.14
2191.5	6years	10.20	85.51	16.44	61.25	9.97	89.66
3562.42	10years	16.51	138.79	26.64	99.35	16.18	145.36

Note: In less than 10 years all sulphur content in the LAN shale are exhausted (38.79% >100%, 145.36% > 100% available Carbonate).

However, if results obtained within the 12 weeks experimental leaching exercise are considering closely, the mobility of the investigated trace metals can be explained theoretically. In most of the weekly leachates obtained from leaching the LAN shale, percentage leached sulphur and carbonate contents are closely similar with sulphur at an average 0.48% leached in comparison to an average 0.68% leached carbonate content. The resulting leachate is therefore mostly characterised as either alkaline or circum-neutral in nature and hence could account for the pH trend observed from the resulting leachate. Corresponding data for the DRB and CLV shales suggest a predominantly alkaline characteristic and could account for the neutralizing effect on

the originally acid nature of the SFF (leachant). A 10 year prediction plot is illustrated in Figure 6.9

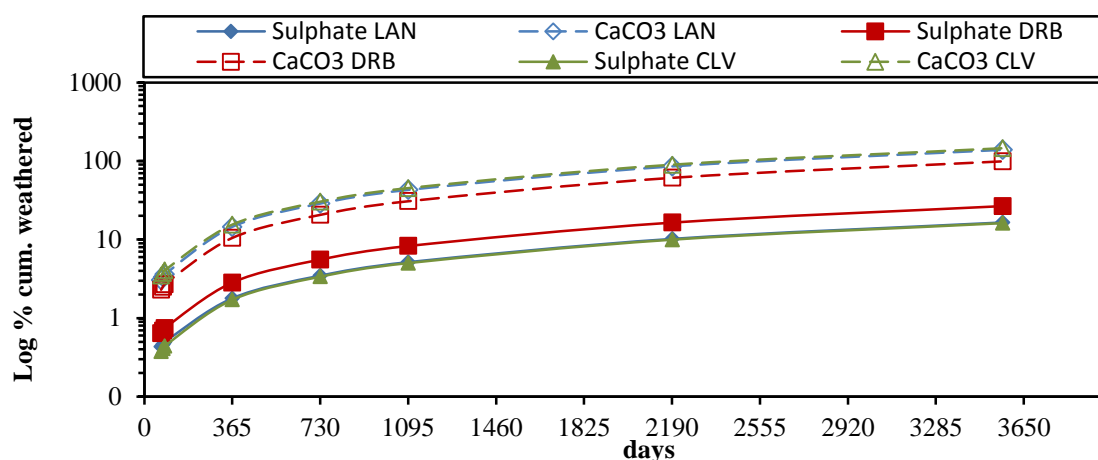


**Figure 6.9:** A 10 year Prediction of pyrite dissolution in comparison with carbonate dissolution rate

## 6.5 Geochemical Modelling for Metal Speciation

Therefore, with contamination monitoring, speciation of the metal provide a better understand of contaminant mobility and its effect on bioavailability and toxicity. For example with regards to toxicity, the valances state of Cr with the highest toxicity impact remains the trivalent and hexavalent chromium, while  $\text{Cu}^{2+}$ ,  $\text{Ni}^{2+}$  and  $\text{Zn}^{2+}$  are more potent contaminants than their total metal concentration. With the aid of geochemical modelling, the speciation of the selected indicator heavy metals were modelled using the PHREEQCI application (Parkhurst and Appelo 1999) with the Minteq v.4 database. One key shortcomings of the application is the inaccurate prediction of metal complexation by natural organic matter (NOM). It is important to state however that although considered inaccurate in predicting complexation by NOM, the application applies a competitive Gaussian model to estimate the complexation of metals by NOM. Alkalinity, pH, cation, anion and trace concentration that serve as inputs are obtained from spectrometric and chromatographic analysis of weekly leachate documented in Table 6.8. Again particular interest is paid to species such as  $\text{Cr}^{3+}$ ,  $\text{Cr}^{6+}$ ,  $\text{Cu}^{2+}$ ,  $\text{Ni}^{2+}$  and  $\text{Zn}^{2+}$  as they provide the best indicators for contamination. Generated output by the model include various metal ionic species whether free or complexed ions and a summary of modelled results is presented in Table 6.9 for Weeks 1, 5, 8 and 12 in all three sampled shales.

**Table 6.8:** Summary of Physiochemical Parameters from Selected Weekly Leachate

Parameter	(BOWLAND SHALE FORMATION)				DERBYSHIRE EDALE SHALE				WHITBY BITUMINOUS SHALE			
	Week 1	Week 5	Week 8	Week 12	Week 1	Week 5	Week 8	Week 12	Week 1	Week 5	Week 8	Week 12
pH	6.26	6.75	7.3	6.55	6.2	7.55	7.12	6.57	6.01	5.45	6.25	6.25
Alkalinity (mg/L)	768 ±9.1	661 ±3.4	720 ±10.3	612 ±5.8	845 ±7.1	935 ±14.6	708 ±9.8	521 ±14.2	1118 ±2.3	825 ±3.9	815 ±7.7	661 ±4.8
Temp. (°C)	20	20	20	20	20	20	20	20	20	20	18	20
Fluoride (F <sup>-</sup> ) (mg/L)	0.00	0.00	0.00	0.00	0.00	0.00	0.00	0.00	2.13	6.10	2.45	1.08
Chloride (Cl)	43.50	40.52	40.52	40.69	56.35	39.23	32.89	24.64	34.52	24.89	23.18	10.15
Nitrite (NO <sub>2</sub> <sup>-</sup> ) (mg/L)	0.00	0.00	1.11	1.63	0.00	0.00	0.00	0.00	N.D	N.D	N.D	N.D
Bromide (Br <sup>-</sup> ) (mg/L)	3.65	6.02	6.65	6.12	6.52	2.23	2.36	3.89	10.25	18.14	8.98	8.05
Nitrate (NO <sub>3</sub> <sup>-</sup> ) (mg/L)	0.00	0.54	1.12	2.20	0.89	1.12	1.68	1.32	2.75	2.14	1.69	1.50
Sulphate (SO <sub>4</sub> <sup>2-</sup> ) (mg/L)	45.18	25.15	30.24	29.66	44.88	39.58	33.11	37.53	38.63	31.66	31.03	6.76
Aluminium (Al) (mg/L)	1.90	3.95	6.26	2.74	0.70	1.74	2.02	1.82	0.31	2.64	3.86	2.84
Iron (Fe) (mg/L)	0.09	3.70	6.27	5.78	0.02	3.26	3.84	3.13	0.06	4.36	3.97	1.54
Sodium (Na <sup>+</sup> ) (mg/L)	221.00	189.15	188.21	184.20	255.10	352.20	335.60	192.45	198.34	221.80	182.76	121.40
Calcium (Ca <sup>2+</sup> ) (mg/L)	36.01	15.46	16.65	8.46	19.35	15.91	21.20	15.66	16.64	16.83	18.38	16.22
Ammonium (NH <sub>4</sub> <sup>+</sup> ) (mg/L)	0.00	4.15	3.85	3.14	1.12	2.10	0.88	0.80	2.24	3.10	2.84	2.05
Potassium (K <sup>+</sup> ) (mg/L)	141.00	131.80	104.56	99.35	95.25	88.60	70.30	66.40	336.18	305.64	298.21	251.60
Magnesium (Mg <sup>2+</sup> ) (mg/L)	23.86	25.45	34.56	14.79	15.13	9.62	16.48	3.48	16.42	15.58	19.22	12.64
Chromium (Cr) (µg/L)	35.28	82.50	107.10	60.00	19.25	91.50	108.00	57.95	26.55	44.18	37.80	5.33
Copper (Cu) (µg/L)	8.30	27.00	23.10	18.00	31.63	27.75	25.20	15.25	8.85	4.65	6.30	5.33
Nickel (Ni) (µg/L)	14.53	42.98	60.90	28.50	1.54	11.38	19.80	7.63	11.80	34.88	32.40	31.95
Zinc (Zn) (µg/L)	22.83	57.00	67.20	39.00	7.56	13.50	48.60	7.63	2.95	15.50	30.60	19.53

**Table 6.9:** Result of PHREEQC output file containing activities and concentrations of some ionic species

Days	Reactor LAN (Lancashire Black shale)					Reactor DRB (Edale Black shale)					Reactor CLV (Whitby Bituminous Shale)				
	Cr <sup>3+</sup> (µg/L)	CrO <sub>4</sub> <sup>2-</sup> (µg/L)	Cu <sup>2+</sup> (µg/L)	Ni <sup>2+</sup> (µg/L)	Zn <sup>2+</sup> (µg/L)	Cr <sup>3+</sup> (µg/L)	CrO <sub>4</sub> <sup>2-</sup> (µg/L)	Cu <sup>2+</sup> (µg/L)	Ni <sup>2+</sup> (µg/L)	Zn <sup>2+</sup> (µg/L)	Cr <sup>3+</sup> (µg/L)	CrO <sub>4</sub> <sup>2-</sup> (µg/L)	Cu <sup>2+</sup> (µg/L)	Ni <sup>2+</sup> (µg/L)	Zn <sup>2+</sup> (µg/L)
7	0.23 <b>(100%)</b>	N.G <b>(0%)</b>	N.D	2.284 <b>(40.2%)</b>	0.431 <b>(69.9%)</b>	19.275 <b>(100%)</b>	0.0001 <b>(0.0%)</b>	0.0001 <b>(98.1%)</b>	1.542 <b>(46.0%)</b>	7.751 <b>(73.8%)</b>	26.60 <b>(100%)</b>	N.G	1.92 <b>(22.00%)</b>	4.78 <b>(40.4%)</b>	2.08 <b>(70.37%)</b>
35	82.57 <b>(100%)</b>	N.G <b>(0%)</b>	26.842 <b>(99.3%)</b>	43.028 <b>(51.3%)</b>	57.057 <b>(74.7%)</b>	91.617 <b>(100%)</b>	N.D	27.77 <b>(99.9%)</b>	11.398 <b>(36.6%)</b>	13.521 <b>(46.8%)</b>	44.24 <b>(100%)</b>	N.G	2.10 <b>(46.19%)</b>	16.56 <b>(47.4%)</b>	11.88 <b>(76.54%)</b>
56	0.096 <b>(100%)</b>	N.G <b>(0%)</b>	1.289 <b>(99.8%)</b>	5.241 <b>(46.2%)</b>	0.573 <b>(62.2%)</b>	108.100 <b>(100%)</b>	N.D	25.139 <b>(99.7%)</b>	19.827 <b>(47.2%)</b>	48.649 <b>(66.3%)</b>	37.85 <b>(100%)</b>	N.G	1.19 <b>(19.10%)</b>	15.37 <b>(47.38%)</b>	23.01 <b>(75.10%)</b>
84	0.109 <b>(100%)</b>	4.668 <b>(0%)</b>	1.142 <b>(98.9%)</b>	9.995 <b>(52.7%)</b>	0.185 <b>(77.0%)</b>	57.976 <b>(100%)</b>	N.D	15.13 <b>(99.1%)</b>	7.636 <b>(55.6%)</b>	7.636 <b>(78.4%)</b>	5.33 <b>(100%)</b>	N.G	1.13 <b>(21.38%)</b>	16.50 <b>(51.58%)</b>	15.37 <b>(78.63%)</b>

N.D: Not detected

Bold values in parenthesis denote the equivalent percentage the reported value represent from the total concentration reported.

Chromium speciation results suggest it exists mainly in 2 oxidation states. Trivalent chromium ( $\text{Cr}^{3+}$ ) and hexavalent chromium Cr (VI). Trivalent chromium appears the most observed chromium species forming aqueous complexes with chlorides, carbonates but predominantly with hydroxides. Cr (VI) is seen however to form aqueous cations with Na and K but in rather negligible concentration (Table 6.9). Modelled results of chemical speciation of Cr revealed that 99.9% will exist as  $\text{Cr}^{3+}$  and less than 0.001% will exist as Cr (VI) in all weekly leachates analysed. In all three shales types leached, modelled results show that Cu will occur as free ion ( $\text{Cu}^{2+}$ ) with more than an average 99.8% of Cu concentrations detected. Ni on the other hand is predicted to occur up to 50% as free ion ( $\text{Ni}^{2+}$ ) in leachates analysed from all three shales. Predicted Zn speciation is projected to occur predominantly as ( $\text{Zn}^{2+}$ ) at an average of 75% across all leachate analysed.  $\text{CrO}_4^{2-}$  species are however, significantly absent from leachates sampled from the Whitby Bituminous shale and the Edale black shale.

From these results, it is clear that  $\text{CrO}_4^{2-}$  contamination are not likely a possible threat following anthropogenic disturbances as minute concentration of the toxic species are evident from the model results. With regards to Cu, as approximately 50% of existing Cu concentration occurs as toxic free ion, release of substantial Cu from the shale may result in potential risks. Perhaps the greatest risk identified in terms of predicted concentration is observed with  $\text{Cr}^{3+}$  with predicted concentrations reaching tops of  $82.57\mu\text{g/L}$ ,  $108.1\mu\text{g/L}$  and  $35.3\mu\text{g/L}$  in the LAN, DRB and CLV leachates respectively. Toxic  $\text{Ni}^{2+}$  species are predicted to occur in concentration ranging between  $11.4\mu\text{g/L}$  to  $44.9\mu\text{g/L}$  in leachate produced from the Edale black shale. Highest concentrations of toxic  $\text{Cu}^{2+}$  species records tops of  $26.84\mu\text{g/L}$ ,  $27.77\mu\text{g/L}$  and  $26.16\mu\text{g/L}$  in the LAN, DRB and CLV leachates respectively. Mobility of this toxic species is further encouraged by the higher proportion of hydrolysed metals species which are preferentially adsorbed compared to the free ionic metals. This is expected as it is generally agreed that the predominant forms of these metals in the environment are in fact the oxides, hydroxides and carbonates.

## **6.6 General Discussion**

The experiment was designed to evaluate the effect of hydraulic fracturing operations on selected PTEs release from black shale sampled from three shale gas prospective formations. In contrast to the natural weathering simulation (Experiment in Chapter 5), the leachant employed here is a SFF prepared from quantitative data on concentrations obtained from the sole hydraulically fractured shale gas well in the UK. Following the preparation of the SFF, slight modification in the procedure was adopted to mimic environmental conditions typified by the industrial operation. Similar analysis as conducted in the natural weathering experiment was undertaken to obtain data regarding the release of our indicator trace heavy metals. In this section, a thorough analysis of the results obtained during this simulated laboratory experiment is discussed here.

### **6.6.1 Column Leachate Chemistry**

Initial pH data on prepare leachant (SFF) recorded an average pH of 2.25 and therefore with the leachant already in an acid state, it was expected that pH trends following leaching would signify the extent of acid neutralization possible from shale samples leached. In response to the first week of leaching, pH spikes reported (Figure 6.1) are indicative of the ease in carbonate dissolution in contrast to the low solubility of pyrite attributed to its crystalline structure. The successive pH spikes observed in weeks in all three profiles are likely indicators of the magnitude and reactivity of acid neutralising minerals like siderite, dolomite and calcites detected during the shale characterisation phase. Along the profile there are obvious indications of acid generations within the column as observed in the intermittent drop in pH reported mostly in the LAN shale and latter weeks in the DRB shale. pH profile for the CLV shale reveal a thriving carbonate release as profile appears to maintain a steady range between 5.40 and 6.25. The DRB shale however, gives indications of a steadily increasing buffering capacity reaching tops of a circum-neutral pH 7.78.

Alkalinity profiles (Figure 6.2) are clearly in agreement with pH results as increased release of soluble ionic concentrations results in the initial spike in conductivity reported. Clearly, with increasing actions of an acidic leachant, more acid soluble

carbonate minerals are released into solution. Consequently, the observed fall in alkalinity can be attributed to the gradual increase in acidification within the leaching columns. In response to this, we observe a gradual rise in conductivity profiles for all three shales. The obvious tenet in support of this is the increased oxidation of sulphide mineral resulting in the build-up of acidic conditions within columns giving rise to elevated levels of trace metals and soluble salts.

### **6.6.2 Release Quantification**

The main purpose of the leaching test however, is to obtain aqueous phase concentrations of the selected PTEs indicators which are released from respective shale matrix. With identified weathering patterns observed from analytical quantification of released concentrations, useful data on long term releases can be obtained. Firstly, weekly weighted concentrations of trace indicator metals show initial rise in detected soluble concentration and a subsequent gradual drop usually around week 7 and 8. Since pH trends should play a role in the solubility of detectable analytes, an investigation of trends provided no significant correlation. Secondly, cumulative data of the release analytes however provide a view of the weathering patterns and computation of dissolution rates. Figure 6.5 depicts the trends and as reported earlier a slight dip in the cumulative plots can be observed towards the latter weeks of leaching. Exponential leaching trends are not uncommon and rather than indicate a decay rate/constant, a growth in released quantities is reported for all three investigated shales.

Considering the release rates, two rates have been computed and compared in Table 6.10. The first, show rates without the application of SA/V and other parameters that describe the leaching mechanism. With initial Cr rates in the LAN shale significantly greater than both the DRB and CLV shales however, normalized data show that in fact rates are relatively similar in all three shales. These normalised data can subsequently be used to provide accurate predictions of released concentrations. In Figures 6.8, trends for individual analytes across all three shales are compared. Cr rates show again an initial rise in the first few weeks as observed in cumulative data and similar trends are observed in the Cu rates. Ni however shows an increase over 2 orders of a magnitude in the LAN and CLV shales, and a 3 order magnitude increase in the DRB

shale. A 2 order magnitude increase is also observed in the Zn with a sharp spike in rates observed between weeks 4 and 5.

**Table 6.10:** Comparison of empirical rates with normalised dissolution rate constant for investigated traces heavy metals

Analytes	Dissolution Rate [ $\mu\text{g}/\text{kg}\cdot\text{day}^{-1}$ ]	Normalised Rate [ $\text{mol}/\text{m}^2/\text{day}$ ]
Cr (LAN)	75.20782	$2.70 \times 10^{-08}$
Cr (DRB)	42.6114	$3.22 \times 10^{-08}$
Cr (CLV)	58.62751	$5.52 \times 10^{-08}$
Cu (LAN)	17.04863	$2.46 \times 10^{-09}$
Cu (DRB)	51.19565	$2.99 \times 10^{-09}$
Cu (CLV)	14.59511	$4.42 \times 10^{-09}$
Ni (LAN)	23.42191	$2.71 \times 10^{-09}$
Ni (DRB)	4.464656	$5.85 \times 10^{-09}$
Ni (CLV)	12.22302	$1.85 \times 10^{-08}$
Zn (LAN)	25.20271	$1.52 \times 10^{-09}$
Zn (DRB)	7.031882	$2.75 \times 10^{-09}$
Zn (CLV)	1.191654	$8.81 \times 10^{-09}$

### 6.6.3 Release Predictions

The rate of chemical change in columns are derived from plots of the  $\ln(C_t / C_o)$  versus time (t) (Figure 6.7) and these linearized plots are used in making predictive plots (Figure 6.8) on the long term releases expected. An in-depth look at the predicted concentrations (Table 6.12) reveals concentrations in excess of permitted EA environmental quality standard (EQS) for discharge into rivers, freshwater lakes, transitional waters and coastal waters (EA 2011). For chromium, the EQS recommends an annual mean concentration of dissolved hexavalent chromium is reported at  $3.4\mu\text{g}/\text{L}$  in rivers and freshwater lakes and  $0.6\mu\text{g}/\text{L}$  in transitional and coastal water. Also, the world health organisation (WHO) as well as the European commission (EU) recognises the  $50\mu\text{g}/\text{L}$  recommended maximum allowable concentration for Cr in drinking water. Predicted 5 year Cr concentrations is estimated at  $236.3\text{mg}/\text{L}$ ,  $201.4\text{mg}/\text{L}$  and  $124.8\text{mg}/\text{L}$  in the LAN, DRB and CLV shales respectively, representing a 4000 fold increase from recommended drinking water limit. A 5 year

predicted copper, nickel and zinc concentration are well in excess of recommended EQS, WHO and EU standards and these Figures illustrate the scale of risk arising from anthropogenic disturbances of this pre-historic formations. These results have clearly shown larger than permissible releases capable of causing potential risk to human and environmental health, and as expected anthropogenic releases equally allow the release of potentially toxic contaminants from the studied shales. Considering however that total concentrations do not provided the best possible indication of potential risks but rather a quantification of identified toxic species, estimated percentages of toxic species ( $\text{CrO}_4^{2-}$ ,  $\text{Cr}^{3+}$ ,  $\text{Cu}^{2+}$ ,  $\text{Ni}^{2+}$  and  $\text{Zn}^{2+}$ ) obtained from speciation results (Table 6.11) together with the predicted 5 and 10 year releases from observed rates (Table 6.12) are assessed to obtain actually release estimates of the toxic species.

**Table 6.11:** Summarised mean percentages for identified toxic species from speciation results in Table 5.19

Sampled Shales	Cr(III)	Cr(IV)	$\text{Cu}^{+2}$	$\text{Ni}^{+2}$	$\text{Zn}^{+2}$
Lancashire Bowland Shale (LAN)	100.00%	N.G	75.00%	48.00%	70.95%
Edale Carboniferous Shale (DRB)	100.00%	N.G	99.20%	46.35%	66.33%
Whitby Bituminous Shale (CLV)	100.00%	N.G	27.20%	46.70%	75.20%

N.G: Negligible concentration

Data reported in Table 6.11 reveal that Cr (VI) is completely reduced to the mainly insoluble Cr (III) and consequently reducing chromium release and mobility. These results suggest that mean released concentrations of Cr will exist as mostly trivalent chromium compounds equivalent to 236.3mg/L, 201.4mg/L and 124.8mg/L in the LAN, DRB and CLV shales respectively. Even at low reported percentage (27.20%) for Cu in the DRB shale, a 5 year equivalent release stands at 5.55mg/L and clearly exceeds the drinking water toxicity limits set at 2mg/L and the EA recommended annual mean environmental discharge standard for rivers and freshwater lakes set at 28µg/L (for a maximum water hardness of >250 CaCO<sub>3</sub> mg/L)

and 5µg/L limits set for transitional and coastal waters. There also appears to be an exponential increase in reported data for the 10year release Figures in comparison with 5 year releases, indicating the deterioration of flowback quality over time. While these results have been painstakingly documented here, a thorough comparison between results obtained here and natural weathering simulated experiment is provided in Chapter 7.

**Table 6-12:** Summarised total concentration of a 10 years release prediction

Trace Metals	5 Year Estimates			10 Year Estimates		
	LAN (mg/L)	DRB (mg/L)	CLV (mg/L)	LAN (mg/L)	DRB (mg/L)	CLV (mg/L)
<b>Chromium</b>	236.3	201.4	124.8	472.5	402.4	249.4
<b>Nickel</b>	106.2	33.3	79.0	212.3	66.2	157.6
<b>Zinc</b>	141.7	48.7	46.7	283.0	97.2	93.3
<b>Copper</b>	58.9	62.6	20.4	117.5	124.9	39.9

#### 6.6.4 Predicting Flowback Quality (Acidity/Alkalinity Characteristics)

Adopting the principle of AMD, pyrite and carbonate weathering rates are useful in the prediction of the nature of returning flowback. As observed in the short term (Figure 6.9) leachates are characterised by closely similar sulphur and carbonate dissolution rates which accounts for the circum-neutral/alkaline characteristic observed during the pH monitoring. Linearization of the data obtained (Figure 6.8) allows the prediction of pyrite and carbonate dissolution rates reported in Table 6.7 and Figure 6.10. The results however begin to reveal quite glaring distinctions between sulphate and carbonate weathering rates being to appear from first year prediction data. By the first year following simulated anthropogenic disturbances in the LAN formation, pyrite weathering, which results in sulphuric acid generation have doubled carbonate weathered rates and by 10 years, sulphur weathering rates by over 22 folds. This results suggest the increasingly acidity of returning flowback from this formation consequently altering the dissolution and immobilization of PTE. The Edale shale formation on the other hand, releases more of its carbonate composition in excess of

the generated sulphuric acid production. A 10 year Figure show an eight (8) fold increase in weathered carbonate composition in comparison to sulphuric acid production (Table 6.7) and implies the alkaline characteristics of returning flowback. Flowback from the CLV formation is projected to be circum-neutral in nature following closely similar weathering rates for both acid forming sulphur and neutralising carbonates.

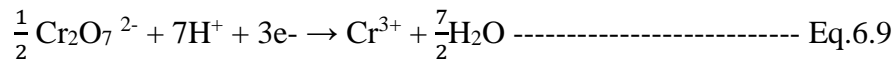
### **6.6.5 SFF Effects of Metal Mobility**

The acidic nature of the SFF is by far the most prominent characteristics of the leachant and it is expected that the acid soluble fraction of the shales, with contains metals mostly precipitated or co-precipitated with carbonate, are readily rendered labile. The carbonate phase is a loosely bound phase and liable to change with environmental conditions such as changes in pH. It is therefore right to conclude that the SFF leachant predominantly attacks heavy metals in association with the loosely bounded carbonate phase. As one of the general applications of sequential batch extraction is to provide an evaluation of metal mobility and release (Filgueiras et al. 2002), to fully comprehend the effects of SFF on the studied shales and offer a reasonable explanation to observed trend, we shall consider observed phase distribution of the metal pools from the sequential batch extraction (SBE) analysis (Chapter 4), which defines the phase distribution of the investigated traces within each sampled shale.

#### **6.6.5.1 Chromium**

SBE results provide a possible explanation to Cr releases following the SFF leaching. Approximately 82.45% of base metal concentrations of Cr in the LAN black shale were found associated with the acid soluble exchangeable and carbonate fractions and 48.7% of this fraction was released from the selective extraction of the carbonate phase. Similar results were obtained from in the DRB and CLV shales both recording 73.8% and 61% selectively released from the water soluble, exchangeable(s) and Carbonate fractions in the shales respectively. Therefore the dissolution this soluble fractions would account for the increased metal concentrations reported. Generally in aqueous systems at pH's between 6 and 12, Cr(III) is highly insoluble, existing predominantly as  $\text{Cr}(\text{OH})_3$  (Xiang-Rong *et al.* 2004, Whittleston 2009) but since

Cr(VI) species are highly soluble, chromium in solution is therefore mainly Cr(VI) and should accordingly exist as chromate ( $\text{CrO}_4^{2-}$ ) formed from acid dissociation however, from the modelled speciation results obtained (Table 6.9), it appears Cr(III) is prevalent due to the lowering of pH, a function of the SFF and further acid formation from oxidation of pyrite composition. This characteristic reduction of Cr(VI) to Cr(III) reported by (Lee et al. 1998, Lin 2002, Xiang-Rong et al. 2004, Moore et al. 2014) can be represented thus;



Organic matter enrichment typical with black shales is another factor that could account for the reduction of Cr(VI) to Cr(III). Therefore, a key effect of the SFF leaching is the lowering of pH which favours the production of Cr(III) due to increased reduction of Cr(VI).

### **6.6.5.2 Copper**

Copper was found liable (37%) with the residual fraction in the LAN shale, 45% associated with organic fraction in DRB and 37.2% similarly associated with the organic fraction in the CLV shale. These results suggest the poor mobility of Cu in all three shales and accounts for the poor quantitative releases (Figure 6.5) observed. Orem et al. (2014) reported significant correlation of copper with soil pH and organic matter and Vidic et al. (2013) also reported copper susceptibility to accumulation in surface soil layers due to strong bindings to organic matter (OM), clay minerals, and oxides of Fe, Al, and Mn. Normalised reaction rates remained fairly constant throughout the 12 weeks showing minimal rises and fall in rates. Acidic conditions often enhance the solubility of heavy metals and Cu is no different. The acidic nature of the SFF in conjunction with the oxidation of  $\text{FeS}_2$  causes a further fall in pH modifying the chemical speciation and relative distribution of chemical species of Cu. As observed pH was slightly acidic to near neutral (average pH 6.7), chemical speciation indicated that dissolved metal concentration in leachates were dominated by dissolved organic carbon metal complexes ( $\text{CuCO}_3$ ,  $\text{Cu}(\text{CO}_3)_2^{2-}$ ,  $\text{CuHCO}_3^+$ ), a trend widely reported (Gadd 2004, Murali Mohan et al. 2013, Elliott et al. 2014).

Consequently, released concentrations of Cu have increase in low pH environments owing to the chemical form in which these metals are present in the aqueous leachate.

#### **6.6.5.3 Nickel**

Nickel was found to be distributed almost evenly amongst the varying selective phases in the LAN shale. Organic and exchangeable fractions housed the largest at 23.2% and 22.5% respectively. Distributions in the DRB were predominantly associated with the Fe-Mn and organic matter and residual fractions recording 24.8%, 23.1% and 21.2% respectively while 41.3% of Ni from the base metal in the CLV shale was found associated with the Fe and Mn oxides fractions. These results suggested varying mobility trends in all three black shales with the most susceptible to acid dissolution being the LAN black shale with relatively high concentration of Ni association with the acid soluble exchangeable fraction. However, Nickel exhibited extensive mobility in acidic aqueous solutions in comparison to neutral conditions (Macaskie and Dean 1989). Like Cu, the acid nature of the SFF promotes the dissolution of residing phases, in particular associations with exchangeable and carbonate fractions. This accounts for increased releases in Ni concentration in the SFF simulated leaching experiment. Ni is capable of forming neutral or negatively charged complexes, making the metal highly mobile in relation to other trace elements. Results from the chemical speciation suggest it occurs primarily as free ions and with  $\text{Ni}^{+2}$ ,  $\text{NiHCO}_3^+$ ,  $\text{NiCO}_3$  and  $\text{NiSO}_4$  the predominant complexes. This formation of complexes helps to promote mobility.

#### **6.6.5.4 Zinc**

Zinc was discovered to be predominantly associated with the Fe-Mn oxides fractions with a relatively substantial percentage associated with the acid soluble carbonate phase in the LAN shale. Similar trends was discovered by (Southam 2000), who found that the greatest percentage of the total Zn in polluted soils and sediments was associated with Fe and Mn oxides. Higher associations were observed with the water soluble and exchangeable fractions for both DRB and CLV shales at 38.1% and 41.6% respectively and these results suggest more acid soluble Zn reside in the DRB and CLV shales. Column results however, suggest far greater mobility in the LAN shale in relation to both DRB and CLV shales. A possible explanation to this could be the

resultant dissolution of the predominant Fe-Mn phase in the LAN shale or the formation of soluble complexes promoting mobility. Chemical speciation results however suggest the predominance of free zinc ion ( $Zn^{+2}$ ) and the prevalence of dissolved organic carbon Zn complexes. Precipitation is not a major mechanism of retention of Zn in aqueous solutions because of the relatively high solubility of Zn compounds. As with all cationic metals, Zn adsorption increases with pH.

## **6.7 Limitations of Experimental Study**

Although the experimental objectives were achieved, a few unavoidable limitations exist. The simulation of fracturing fluids have totally relied on information released by operators of the sole hydraulically fractured site in the UK. Although, fracture fluid typically used have been found to contain more than experimentally simulated, the study was restricted to those used in order to mimic a typical UK scenario. Prior to the commencement of the leaching experiments, shales in each column were flushed with SFF rather than tap water in an attempt to avoid the leaching of shales oxidised during storage. Although tap water would have a limiting effect on shale dissolution in comparison to SFF, the study has considered that this effects on shale dissolution are negligible. The study have adopted the leaching column kinetic test method to mimic the fluid rock interactions that occur during the hydraulic fracturing of shale formations. Although this methods do not entirely mimic the exact dynamics of fluid rock interaction during the industrial process, the study has considered the method fit to represent as close as possible the true nature of fluid rock interactions.

## **6.8 Summary & Conclusion**

As an oxidation phenomenon, the low pH characteristic of the SSF in all shale filled columns exhibited increased metal mobility as a consequence of the increased solubility control on acid generating compositions within the shale. Consequently, metals are immobilized by two predominant processes. Firstly the higher number of negative sites for cation sorption and secondly the higher proportion of hydrolysed metals species which are preferentially adsorbed compared to the free ionic metals (Beveridge and Doyle 1989). All three gas prospective shales have been leached with the aim of determining natural release characteristics of selected trace elements under

prevailing natural environmental conditions without of anthropogenic interferences but characterised by fluid interactions. From observed short term release kinetics, predictions on long term releases have also been evaluate. The expected drainage quality (leachate characteristics) following fluid interactions with theses formations have also been investigated with the aim of classifying expected drainage as either acidic, circumneutral or alkaline in nature, as this information was useful in determining pH control on mobility of the investigated trace metals. In addition, the speciation of investigated trace metals have been studied to observed the severity of contaminant risk and the likelihood of metal complexation that increases the risk impact from notably observed toxicant. The following were observed from the studied investigation;

1. Leachate analysis showed progressively increased releases throughout the leaching period and a gradual fall in rates in the latter stages of leaching possibly indicating the exhaustion of the dissolved trace metal compositions. Overall, larger released concentrations are obtained with SFF simulated leaching
2. Following anthropogenic disturbances, predictions on the possible 10 year release concentrations for all investigated trace metals of the sampled shale leachates have shown values exceeding EU permissible drinking water standards and UK Environmental quality standards for inland surface water disposal and transitional/ costal water environmental discharge standards.
3. Long term pyrite and carbonate dissolution data designed to evaluate and predict long term leachate characteristic have shown the possible production of acidic leachates in the Lancashire formation, alkaline leachate in the Edale Derbyshire formation and circumneutral to alkaline leachates in the Whitby bituminous shale.
4. Chemical speciation analysis suggest the predominant reduction of Cr(VI) to Cr(III) following the acidic characteristics of the resulting leachate as Cr(III) remains the predominant Cr species.

5. All other trace metals exist predominantly as free ion  $\text{Cu}^{2+}$ ,  $\text{Ni}^{2+}$  and  $\text{Zn}^{2+}$  in the chemical speciation results obtained.

Results suggest the increased release of all investigated trace metal compositions following anthropogenic disturbances characterised by a simulated fracture fluid interaction with the studied shales.

## **Chapter 7. Comparative Analysis: Natural and Fracture Enhanced**

### **7.1 Introduction**

In the previous Chapters (6 and 7), the release of selected heavy metals through fluid-rock interactions have been studied with the aim to determine the extent to which these heavy metals could be mobilized, first, in their natural environment via natural weathering and degradation and secondly, during reactions that occur between fracturing fluids and the investigated prospective shales. The goals of both experiments were to leach the investigated prospective shale rocks under conditions likely to be encountered in natural weathering/degradation conditions and following hydraulic fracturing of the said formations. While experiments reporting the extraction and mobilization of heavy metals in the natural environment reported in Chapter 5 are considered to represent non-anthropogenic releases, fracture influenced heavy metal mobilization evaluated from experiments conducted and reported in Chapter 6, represented anthropogenic releases. Data regarding quantitative releases and release rates have been used in both experiments to assess the potential long term characteristics of returning wastewater, the potential generation of acidic drainage by fluid interactions with the formations and quantitative releases in both scenarios.

In this Chapter, a comparative analysis of both natural and fracture enhanced releases are evaluated to determine the risk contribution of shale gas development to contaminant mobility and consequently human and environmental health. As a frame of reference, variations to observed trends in metal releases and mobility resulting from observed changes in leaching trends, reaction rates, acidity/alkalinity characteristics of the effluent leachate, predicted resulting complexes and metal species and quantitative predictions of future releases are comparatively evaluated to observe the risk impacts of anthropogenic activities like Hydraulic fracturing or shale gas development on water resource. Particular attention is paid to quantitative releases from both simulated experiments as a precursor to the scale of contamination mobility possible from either natural weathering or non-disturbance and anthropogenic disturbances. The comparative analyses also provide time factored evaluations of the scale of contaminant mobility and release from data collected from both experimental kinetic studies.

## 7.2 Variations in pH, Conductivity and Alkalinity

A few characteristics such as pH, conductivity and alkalinity provide an understanding of the chemistry within each experimental column. Here, a statistical comparison between samples exposed to a natural weathering simulated leaching and those exposed to fracture enhanced simulated leaching were determined using paired t-tests. For these parameters the difference was calculated between the mean of the results for all three shale samples exposed to natural leaching simulation and the mean of the results for duplicate samples exposed to fracture enhanced leaching simulation. For a statistical evaluation of the significance of differences between both experimental data, a paired t-test that tests the statistical significance of dependent data was adopted (paired because in both experiments different treatment was performed on identical sample sets). The paired t-test allows the evaluation of our hypothesis that anthropogenic disturbances such hydraulic fracturing or shale gas development heightens the risk impact of contaminant release from the studied prospective shale gas formations. With respect to characteristic such as pH, alkalinity and conductivity, this statistical test proves that significant changes in the chemistry within experimental columns occur, which consequently affect the release and mobility of our indicator PTEs. Hence, to define our hypothesis

$H_0 : \mu d \leq 0$  (Null hypothesis: There is no significant difference in effects caused by simulated anthropogenic interferences)

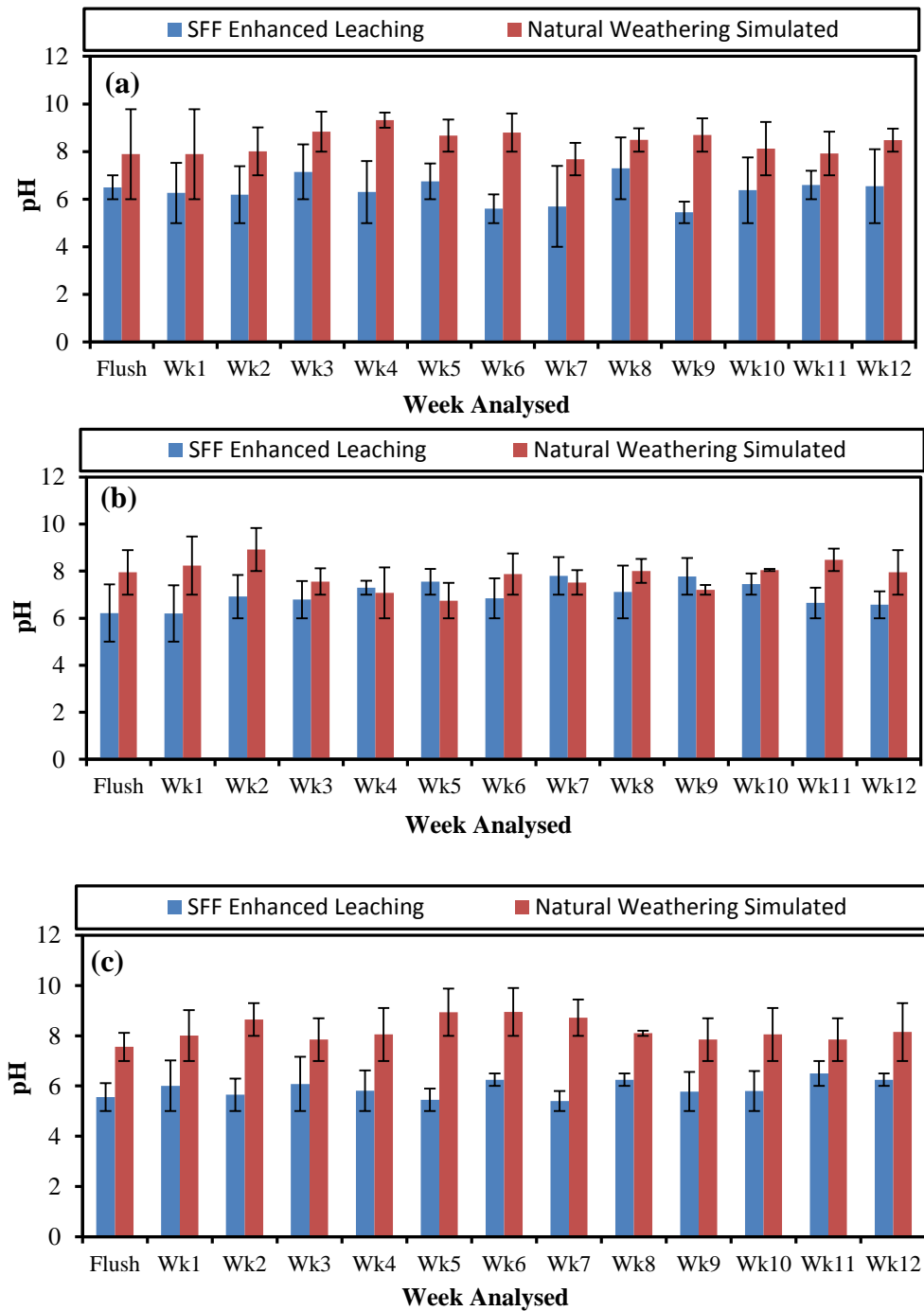
$H_A : \mu d > 0$  (Alternative hypothesis: There is significant difference in effect caused by simulated anthropogenic interferences)

Where;  $\mu d = (X_i - \bar{X}), \text{ and } (Y_i - \bar{Y})$  for two sampled

$$t = (X_i - \bar{Y}) \sqrt{\frac{n(n-1)}{\sum(x+a)^n = \sum_{i=0}^n (X_i - Y_i)^2}} \text{----- Eq. 7.1}$$

Sample results were evaluated strictly as normalized “weighted means” to account for variations in volume of sample in each experimental column and the weight of sample exposed to weathering. Comparisons were made on pH, alkalinity and conductivity data and results of the paired t-tests indicate that for all three shales, mean values were

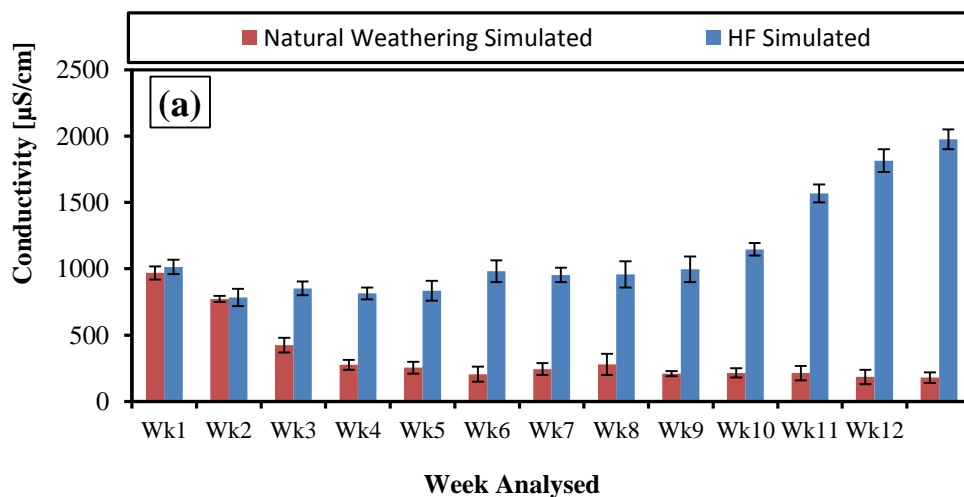
significantly greater in shales exposed to the fracture enhanced simulated leaching compared to those exposed to the natural degradation simulated leaching (i.e. significant at the 99% confidence interval). pH plots (Figure 7.1) depicting the comparisons between both experimental leaching simulation runs and quite easily seen is the lower pH observed in the fracture enhanced leaching simulation.

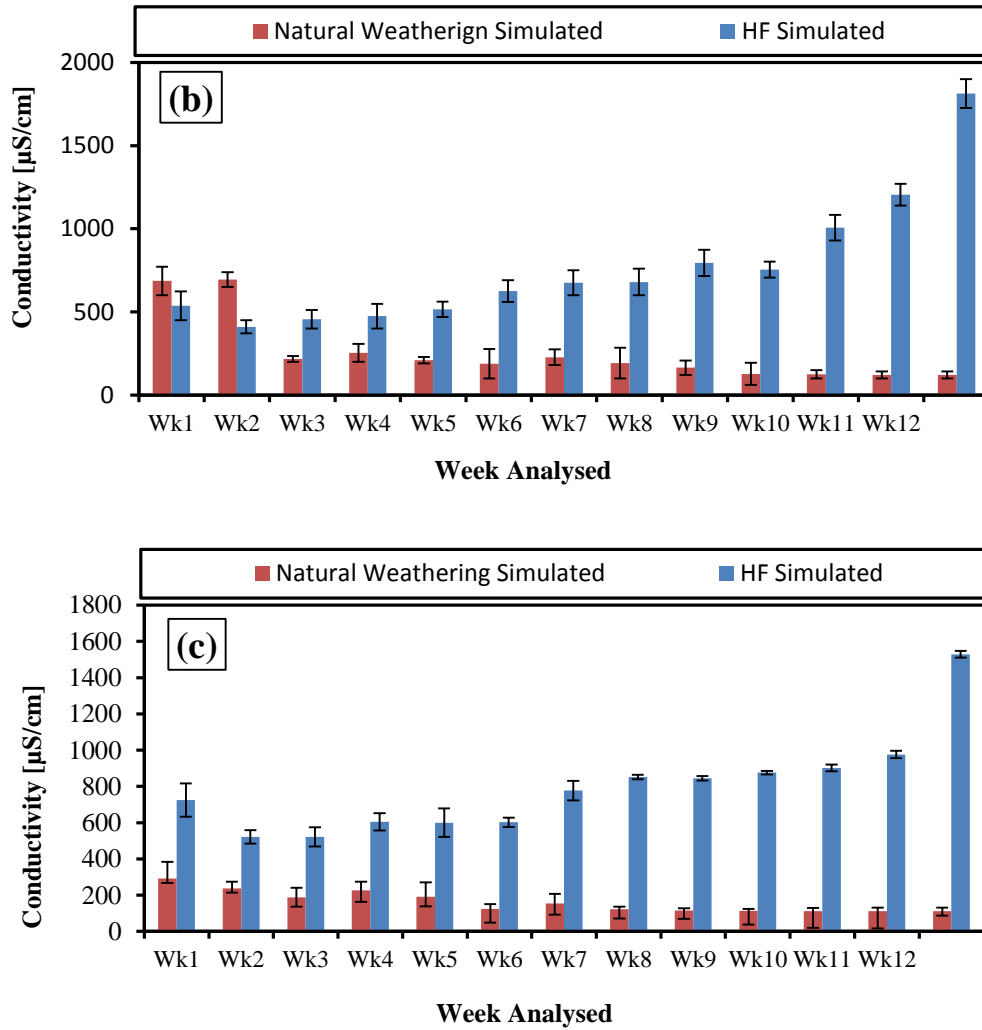


**Figure 7.1:** pH data for both simulated leaching scenarios in (a) Lancashire Bowland Shale (b) Derbyshire Edale shale (c) Whitby Bituminous Shale

There is a clear indication of the significantly acidic composition of leachates sampled from the fracture enhanced leaching simulation, a consequence of the acid nature of the simulated fracturing fluid (SFF) and possible the increased dissolution of poorly soluble pyrite composition. Which of these 2 effects provides the greatest influence is difficult to ascertain however, Figure 7.1b show very marginal differences in both leaching experiments to suggest that the Edale black shale contributes substantial carbonate neutralizing effect to cause such a marginal difference and this is in correlation with results obtained from all three neutralising potential test in Figure 4.8 of Chapter 4.

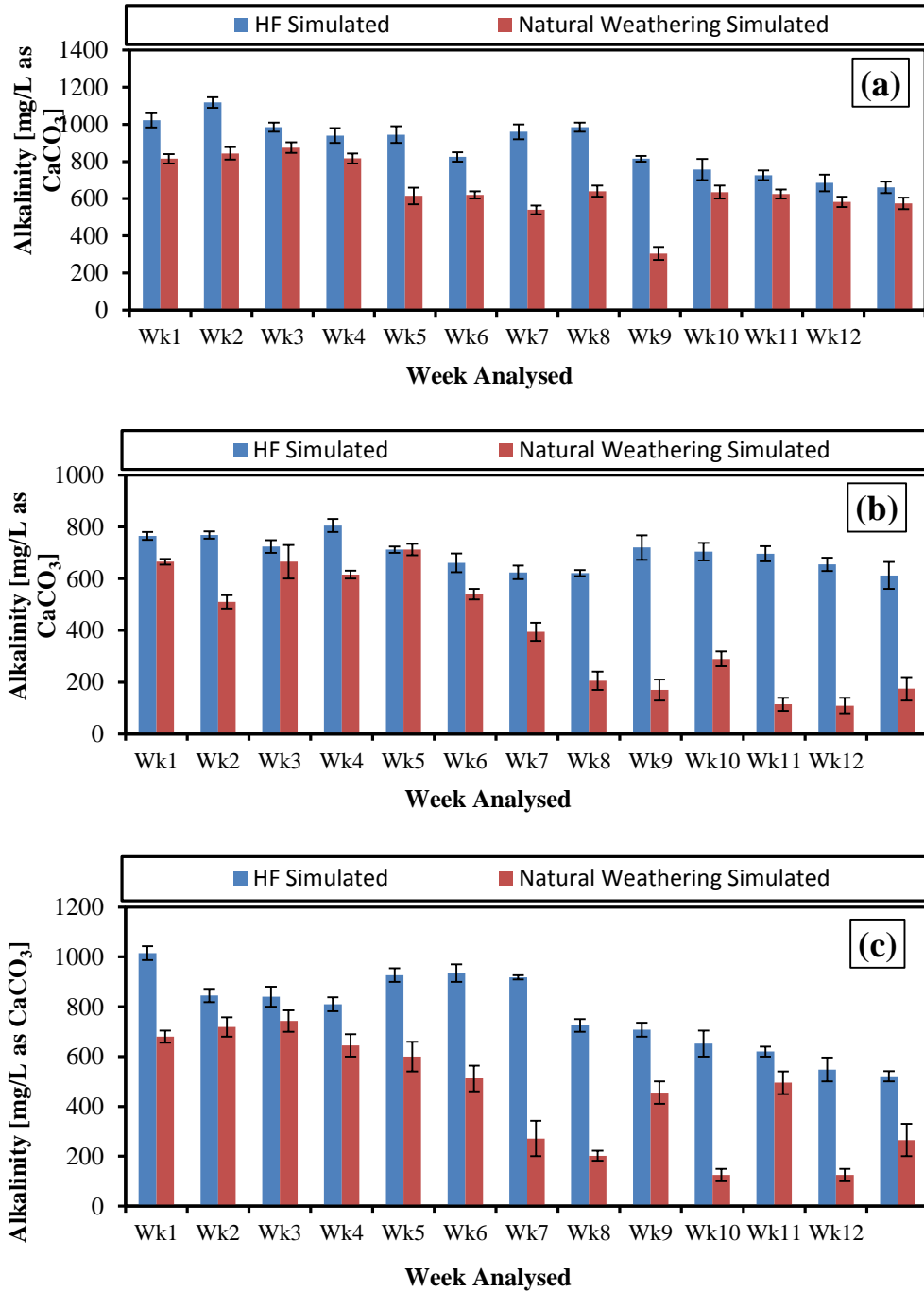
Conductivity of the leachate gives the indication of the amount of dissolved ionic species in the leaching column effluent. Data collected suggest a reversal of trends in both leaching simulations. A rise is observed in conductivity data in leachates from Figure 7.2, week 1 to weeks 12 for fractured enhanced simulated leaching while a fall in conductivity data is observed in the natural weathering simulated leaching. Paired t-test results provide sufficient evidence (paired t test:  $t = 5.29, 3.57$  and  $7.47$  for LAN, DRB and CLV shales respectively,  $D = 12$ ,  $P >, 0.0002, 0.001$  and  $0.000004$  respectively) at  $\alpha = 0.01$ , i.e. at a 99% confidence interval to conclude that there are significantly higher differences in effect caused by simulated anthropogenic interferences.





**Figure 7.2:** Conductivity data for both simulated leaching scenarios in (a) Lancashire Bowland Shale (b) Derbyshire Edale shale (c) Whitby Bituminous Shale

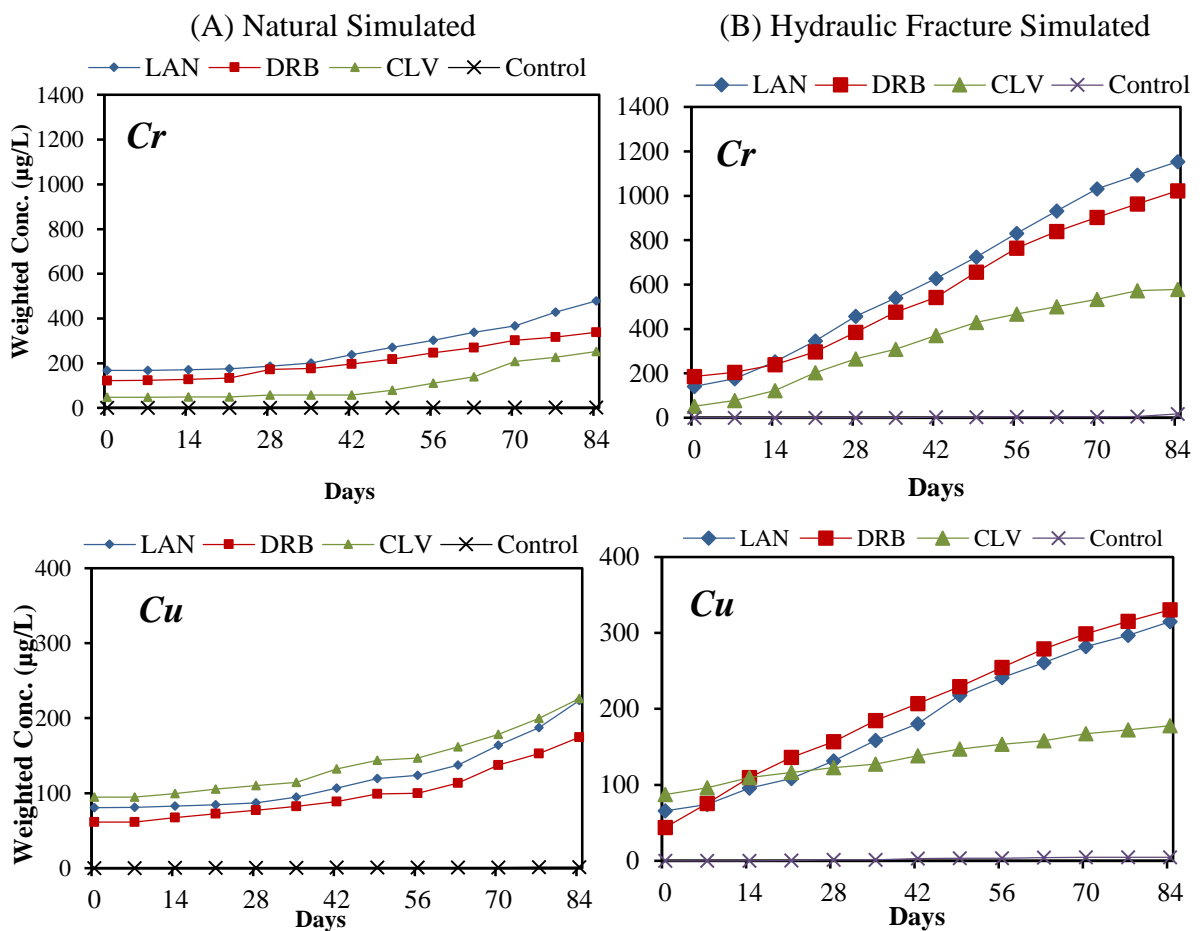
Theoretically, alkalinity produced from weathering these shale samples increased in proportion to increased  $\text{CO}_2$  content in the enhanced fracturing simulated leaching scenario and this accounts for the higher alkalinity shown in Figure 7.3. Results from paired t-test results provide sufficient evidence (paired t test:  $t = 10.33, 2.89$  and  $13.01$  for LAN, DRB and CLV shales respectively,  $DF = 12, P >, 2.50\text{E-}07, 0.014$  and  $1.96\text{E-}08$  respectively) at  $\alpha = 0.01$ , i.e. at a 99% confidence interval to conclude that there are significantly higher differences in effect on alkalinity caused by simulated anthropogenic interferences.



**Figure 7-3:** Alkalinity data for both simulated leaching scenarios in (a) Lancashire Bowland Shale (b) Derbyshire Edale shale (c) Whitby Bituminous Shale

### 7.3 PTEs Releases and Reaction Rate

Plots of cumulative heavy metal releases in both experiments are shown in Figure 7.4 and distinctly show the rise in heavy metal release in the fracture enhanced simulated leaching scenario (plots on column B). In the previous Chapters, the trends in individual leaching experiments have been discussed. The question however remains “are these observed increments in heavy metal releases from the fractured enhanced experimental simulations statistically significance to suggest the likelihood of heightened impact from anthropogenic interference such as hydraulic fracturing. Again, a paired t-test is therefore adopted to investigate statistical significance from the data obtained. Chromium, results in all three shales suggest that the differences are in fact extremely statistically significant ( $t_{LAN} = 5.05$ ,  $p < 0.001$ ), ( $t_{DRB} = 8.45$ ,  $p < 0.001$ ) and ( $t_{CLV} = 2.75$ ,  $p < 0.005$ ) and would suggest that with regards to Cr, simulated fracturing enhanced leaching does increase the release of trace metal from the studied formations.



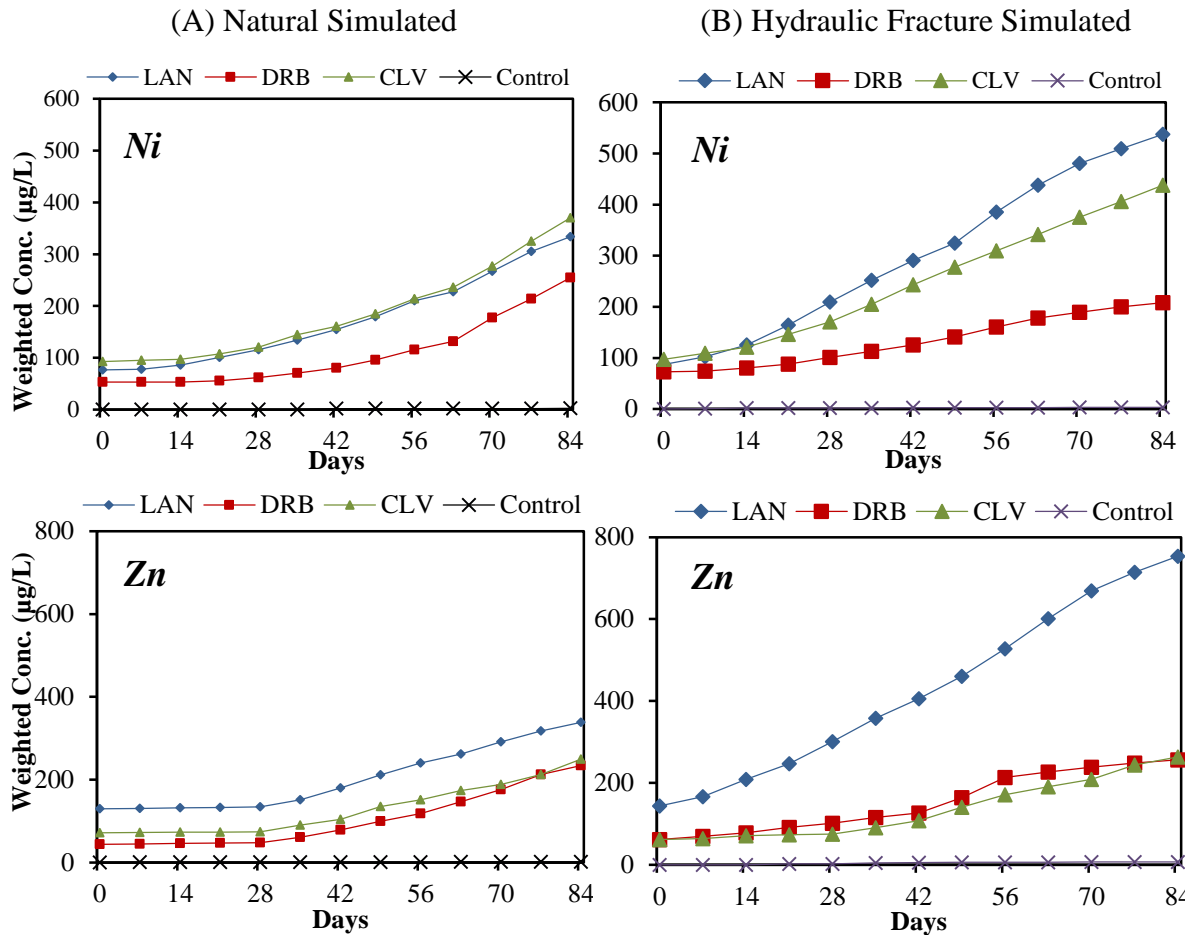


**Figure 7.4:** Leach curves for Cr, Cu, Ni and Zn in (A) Natural weathering simulated leaching experiment (B) Fracture Enhanced all other concentrations ate in µg/L.

Pair t-test results for Cu shows differences in release for both Lancashire and Derbyshire shales were statistically significant ( $t_{LAN} = 2.29$  at  $p < 0.005$  and  $t_{DRB} = 2.92$  at  $p < 0.001$ ). A test of statistical significance reveals only Ni in the Lancashire shale exhibiting any statistical significance ( $t_{LAN} = 4.06$  at  $p < 0.005$ ). Similar results was observed for the Zinc with both Edale shale and Whitby shales showing any significant difference while Lancashire shale show statistical significance at  $t_{LAN} = 8.59$ ,  $p < 0.001$ . If weatherability in both experimental scenarios is reviewed, results from the normalized experimental mass loss are considered for the comparison. The normalised elemental mass loss quantifies the release of ions into solution (leaching solvent). Results (Figures 7.5) show substantial incremental releases for Cr in all three shales leached by the SFF in comparison to simulated natural weathering release. All other indicator PTEs show relative similarities with the elemental mass loss with both leaching simulations. These results suggest the likely high mobility of Cr as a mobile

heavy metal in the sampled formations. In addition, the effect of SFF on the releases of ions can be evaluated. It appears that leaching with SFF have little effect on the mass loss for Ni and Zn in the Lancashire black shale as mass losses in the fracture enhanced and natural weathering scenarios are closely similar. (Ni:  $3.01\text{E-}09\text{ gm}^{-2}$  and  $2.71\text{E-}09\text{ gm}^{-2}$ , Zn:  $1.62\text{E-}09\text{ gm}^{-2}$  and  $1.52\text{E-}09\text{ gm}^{-2}$ ). In the Edale shale samples, HDF simulated leaching experiments have in fact reduced the mass loss of Ni and Zn (Figure 7.5b) into solution whilst Cu, Ni and Zn in the CLV shale have also suffered reductions in the mass loss of ions into solution following leaching with SFF. These results are in support of similar observations from paired t-test.

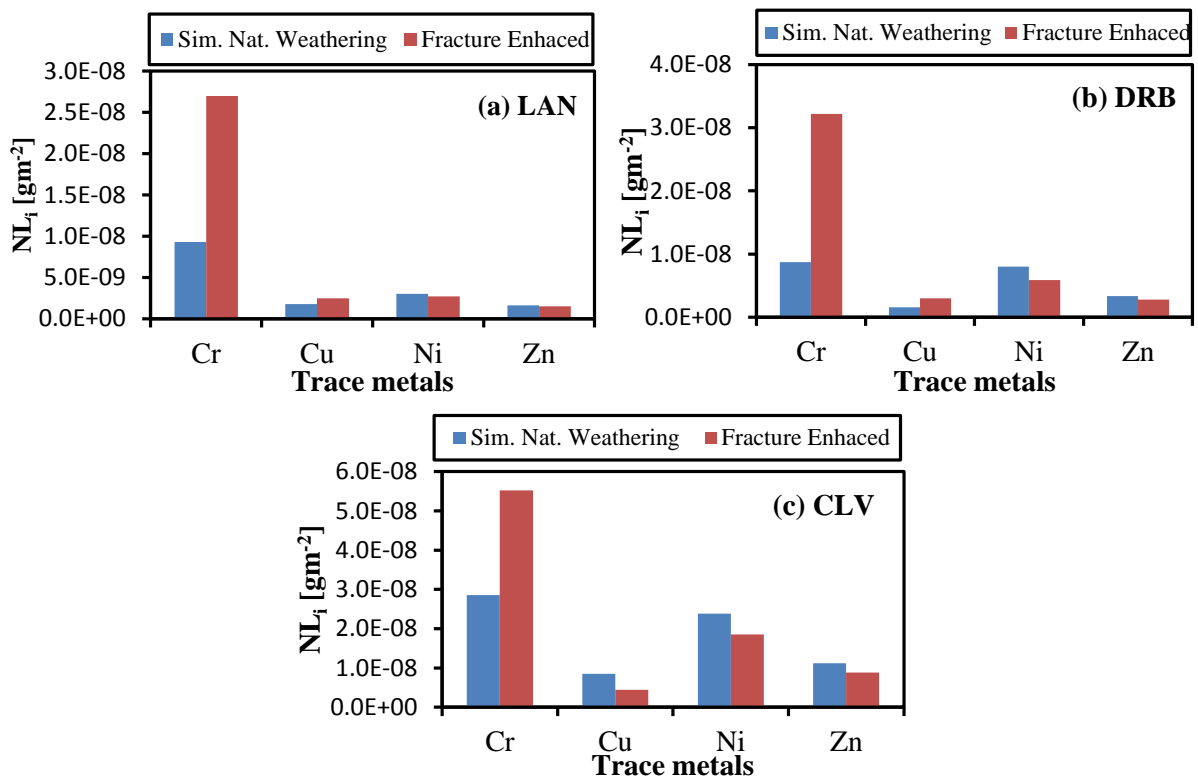


**Figure 7.5:** A comparison of mean computed elemental mass loss ( $NL_i$ ) in the natural weathering simulate leaching and the Fracture enhanced simulated leaching experiment

If rates are considered in terms of chemical flux (The amount of substance per unit volume, per unit time transformed into solution in the leaching column), a clearer picture of the column chemistry is observed (Figure 7.6). Ni and Zn which had previously shown low release rates following the SFF leaching simulation also show similar trends. In the Edale shale (DRB), more Zn and Ni ions were released into

solution per day during the natural weathering simulation in comparison to the fracture simulated leaching (Figure 7.6b). Similar observations were made for Cu (Figure 7.6c) in the Whitby Bituminous shale.

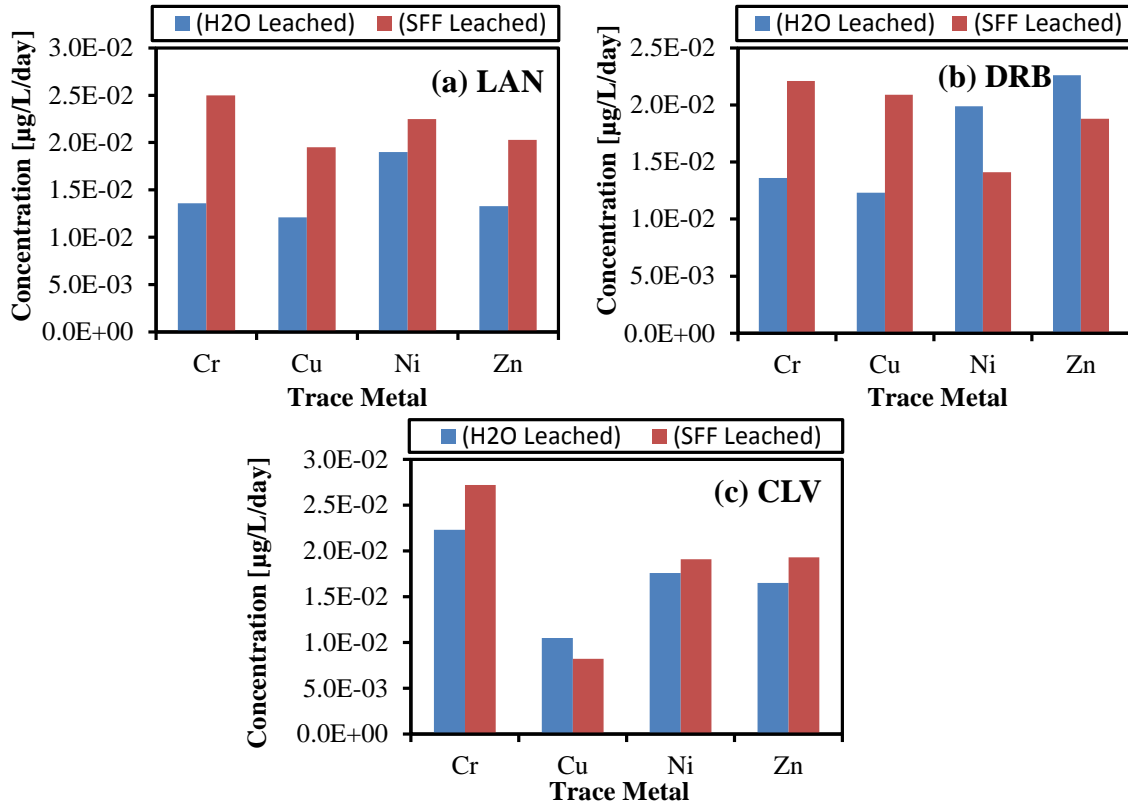


**Figure 7-6:** A comparison of chemical flux from the simulated natural weathering and fracture enhanced simulated leaching experiment

Immediately obvious is the slow flux in the natural weathering simulated leaching for Cu in all studied shales. Applying a fracture simulated leaching with the SFF however, significantly increases the solubility of trace metals with the exception of Cu in the CLV shale, Ni in the DRB shale and Zn also in the DRB shale. This implies that fracturing the formation has a significant effect on the solubility which in turn affects the mobility of these traces in the Whitby Bituminous shale formation and the Edale shale formation.

## 7.4 Flowback Quality

Weekly sampled leachates following each 12 weeks leaching simulation were analysed for sulphates, calcium and magnesium to assessing the interplay of acidity generation and carbonate neutralisation effect. From acid mine drainage (AMD), it has been established that both sulphur and carbonate content play a vital role in the eventual quality of returning wastewater. Cumulative percentages of sulphur and carbonate weathered in all three shales investigated were plotted to identify and predict trends in future releases. The percentage sulphur weathered is compared to the percentage carbonate weathered (Table 7.1) and depending on which of these two components is exhausted first, the characteristic nature of the leachate can be predicted. From data in Table 7.1, 3 year fracture simulated modelled results places soluble sulphur and carbonate in the Lancashire black shale at 5.15% and 85.51% equivalent to 3.13g of sulphur and 162.4g of calcite, and implies sufficient calcite is released to neutralise the acidic effect from 3.13g of sulphur, however, in terms of time scale, this suggest that calcite exhaustion will occur at a faster rate to sulphate exhaustion and eventually this shale would produce sulphur long into the exhaustion of available calcite composition. At 10 year fracture simulated modelled results for DRB a 99.35% of available calcite composition in comparison to a 26.64% dissolved sulphur composition suggest a similar conclusion.

**Table 7.1:** Comparing modelled 10 year predictions of Fracture and natural weathering simulated leaching of sampled shales

Time (yrs.)	Fracture Simulated						Natural Weathering Simulated					
	LAN		DRB		CLV		LAN		DRB		CLV	
	S (%)	CaCO <sub>3</sub> (%)	S (%)	CaCO <sub>3</sub> (%)	S (%)	CaCO <sub>3</sub> (%)	S (%)	CaCO <sub>3</sub> (%)	S (%)	CaCO <sub>3</sub> (%)	S (%)	CaCO <sub>3</sub> (%)
1	1.79	14.52	2.84	10.5	1.71	15.47	3.27	4.02	4.39	4.65	0.99	7.53
2	3.47	28.72	5.56	20.65	3.37	30.3	6.53	7.93	8.76	9.2	1.41	14.76
3	5.15	42.92	8.28	30.8	5.02	45.14	9.8	11.83	13.13	13.74	1.72	21.99
6	10.2	85.51	16.44	61.25	9.97	89.66	19.59	23.55	26.24	27.38	2.44	43.69
10	16.51	138.79	26.64	99.35	16.18	145.36	31.85	38.21	42.65	44.45	3.12	70.83

While similar observations and conclusions are noted for both natural and fracture simulated leaching results in all investigated shales, the distinguishing factor is that, calcite exhaustion occurs at a faster rate in the fracture simulated scenario in comparison to the natural weathering simulated scenario. Under the scenario where carbonates are exhausted before sulphur composition, the produced flowback quality will tend towards acidic. If the pyrite is exhausted before the exhaustion of the carbonate content, the sample will tend towards alkaline. These plots have been combined to visualise these percentages in relation to each other and provide the means to evaluate the acid base characteristic of final effluent. Natural weathering simulation results summarised in Figure 7.7(a) showed a clear distinction between carbonates and sulphur percentages in the Whitby Bituminous shale where 0.45% of pyrite had leached in comparison to a cumulative 1.91% weathered carbonate content.

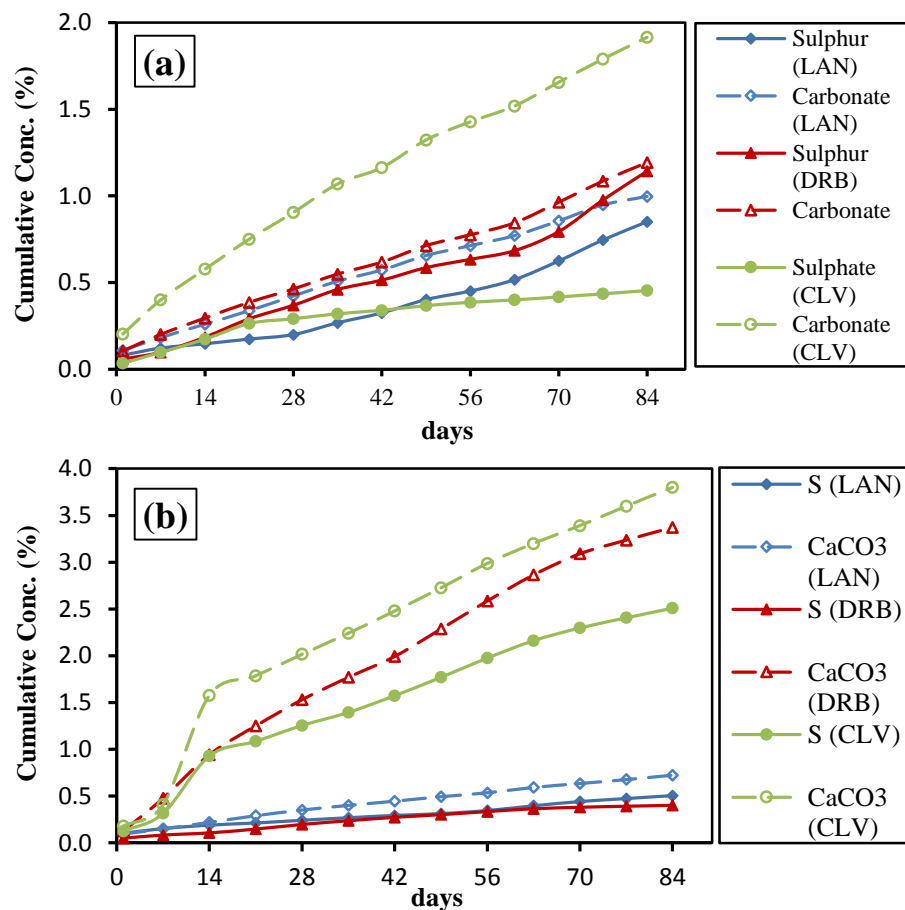


**Figure 7.7:** Combined plots of cumulative sulphur and CaCO<sub>3</sub> leaching rates in (a) Natural weathering leaching simulation (b) Fracture enhanced leaching simulation

Percentage for both LAN and DRB shales were closely matched with LAN shale weathering 0.851% of its pyrite content in comparison to 0.997% of its carbonate content and DRB shale weathering 1.14% of its pyrite content in comparison to 1.19% of its carbonate content. Observed trends in the fracture simulated leaching showed the dissolution of carbonate contents far exceeding sulphur dissolution. Evidently, the acidic characteristics of the leachant in the fracture simulated leaching experiment results in the heightened solubility of carbonate minerals and hence the increased weatherability of carbonate minerals in the studied shales.

A more direct way of obtaining the long term nature of the returning wastewater is to utilise the observed rates in predicting future leachate quality. Figures 5.11 and Figures 6.9 in the previous Chapters illustrated the results from modelled 10 year data. A better evaluation of the modelled results is obtainable if the quantification of sulphur and carbonates in each experimental column (Table 7.2) is reviewed.

**Table 7.2:** Summary of Sulphur and Carbonate content in experimental Column

<b>Parameter</b>	<b>Column 1 [LAN]</b>	<b>Column 2 [DRB]</b>	<b>Column 3 [CLV]</b>
<b>Dry weight of tailing (g)</b>	2000	1989	1992
<b>Sulphur (g)</b>	60.8	52.3	53.6
<b>CaCO<sub>3</sub> (grams CaCO<sub>3</sub> equivalent)</b>	189.92	163.12	167.09

Equivalent carbonate content (in grams) in each experimental column is approximately 3 times sulphur content as reported in Table 7.2, therefore the question is exactly what mass of carbonate is required to neutralise a gram of sulphur. According to Ward (2014), on a mass ratio basis, for each gram of sulphur present, 6.25 grams of calcite are required for acid neutralization. Therefore, for a reported 60.8g of sulphur present in the Lancashire would require 380g of calcite for a complete neutralisation of the generated acidic effect. Other factors however, play a role in determining the overall likelihood of an effluent acidic drainage other than the overall quantification of sulphur and carbonate content. In most cases, not all available sulphur and calcite will dissolve into solution and this change the dynamics of ABA evaluations.

## 7.5 Heavy Metal Speciation

Model results from speciation analysis show increased predicted concentrations of a majority of the investigated potentially toxic species in the fracture simulated leaching protocol in comparison to natural weathering simulated leaching protocol. Mean concentrations of all measured analytes in weekly leachates was used for the speciation modelling and the most dominant PTEs species are presented in Table 7.3 and an illustrative plot is provided in Figure 7.8a and b. This represents the mean summary of computed distribution of dissolved metal species including their complexes modelled from weekly leachates data from each experimental leaching column. At the observed leachate pH range of 5.5-8.9, speciation results indicates that predominate aqueous species are chiefly present as complexes in the form of hydroxides, carbonates and some free ions. The models also predicted that sulphate and fluoride complexes [ $\text{CrF}^{+2}$  and  $\text{Cr}^{+3}$ ] are additionally dominant in the fracture simulated leaching experiment. Because complexes that incorporate metals play a major role in controlling the availability and fate of metals in the environment, the increase in the fraction of a metal that is complexed consequently increases the solubility of the metal (Langmuir 1997) and this would suggest increased mobility.

**Table 7.3:** Computed percentages for toxic species from geochemical modelling of dissolved species

Shales	Natural Weathering Simulated Leaching					Fracture Simulated Leaching				
	$\text{Cr}^{3+}$	$\text{CrO}_4^{2-}$	$\text{Cu}^{+2}$	$\text{Ni}^{+2}$	$\text{Zn}^{+2}$	$\text{Cr}^{3+}$	$\text{CrO}_4^{2-}$	$\text{Cu}^{+2}$	$\text{Ni}^{+2}$	$\text{Zn}^{+2}$
<sup>1</sup> LAN	2E-6%	99.42%	0.81%	79.1%	39.5%	0.07%	72.4%	8.38%	50.1%	71.0%
<sup>2</sup> DRB	2E-4%	96.96%	0.26%	96.4%	68.5%	0.04%	77.8%	6.45%	48.8%	66.3%
<sup>3</sup> CLV	4E-5%	98.5%	2.22%	98.6%	51.6%	0.20%	64.6%	29.1%	46.7%	75.2%

- 1 LAN-Black shale from the Lancashire Bowland shale formation
- 2 DRB- Black shale from the Derbyshire Edale shale formation
- 3 CLV- Black shale from the Whitby Bituminous Shale formations

Modelled results show that trivalent chromium ions, free ions  $\text{Cu}^{+2}$ ,  $\text{Ni}^{+2}$  and  $\text{Zn}^{+2}$  occur at larger concentrations in the fracture simulated leaching protocol in comparison to the natural weathering simulated leaching protocol. It appears the pH

within the system plays a vital role in the predicted concentrations as a clear distinction is observed between trivalent and hexavalent chromium species. When overall predicted concentrations of both species are compared in relation to total chromium concentrations released in to the column, approximately 99.8% of total chromium in all three shales leached by the SFF are predicted to occur as trivalent chromium Cr (III) with a minute fraction (less than 1%) predicted to exist as hexavalent chromium. However, when the toxic species  $\text{CrO}_4^{2-}$  and  $\text{Cr}^{+3}$  are compared in relation to predicted total Cr(VI) and Cr(III) species from the modelled results, a reduction in the modelled  $\text{CrO}_4^{2-}$  concentrations in the fractured simulated leaching protocol in comparison to predicted values in the natural weathering simulated leaching protocol is observed. A possible explanation for this is the characteristic reduction of Cr(VI) to Cr(III) reported by (Lin 2002, Xiang-Rong et al. 2004, Whittleston 2009).

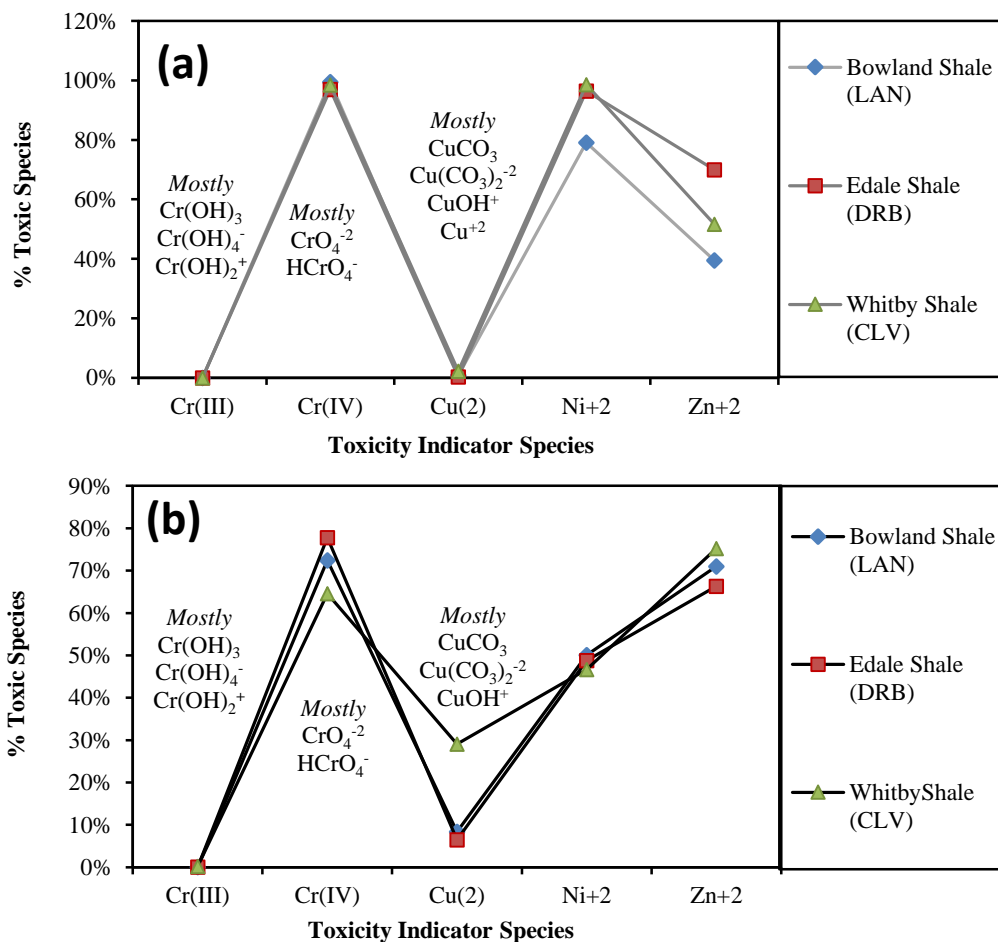


**Figure 7.8:** Results of aqueous PTE speciation for: (a) average natural weathering simulated leaching (b) average fractured enhanced weathering simulated leaching

This suggest that the release of highly toxic hexavalent chromium is encouraged by circum-neutral and alkaline condition within the formations and a possible consequence of pH control on the releases concentrations. Therefore, it appears that interactions within the acidic environment inhibit the release of hexavalent chromium. To further investigate the likely effect of pH on the predicted releases, the predicted concentrations of toxic species  $\text{Cr}^{+3}$ ,  $\text{CrO}_4^{2-}$ ,  $\text{Cu}^{+2}$ ,  $\text{Ni}^{+2}$  and  $\text{Zn}^{+2}$  are modelled as a function of pH ranging from 4 to 10 (Figure 7.9) using the same concentrations observed during the spectrometric and chromatograph analysis documented in Tables 5.13 and 6.8 in Chapters 5 and 6 respectively. As the alkalinity and thus pH content increases, these trace metals ions forms important complexes with anion and cations in the system. These trends in predicted concentrations within the pH range 4-10 are plotted for the dominant species and complexes observed from the modelled result.

Plot in Figure 7.9(a) show trends for a concentration range between  $2\text{E}-16\mu\text{g/L}$  up to  $231.99\mu\text{g/L}$  and shows the highly toxic hexavalent chromium species ( $\text{CrO}_4^{2-}$ ) spiking from a pH 6.2 to maximum at pH 10. Similar trend is observed in other dominant complexes such as  $\text{NaCrO}_4^-$ ,  $\text{KCrO}_4^-$  and  $\text{HCrO}_4^-$ , other species and complex also show spikes in predicted concentrations between pH 8 to 10 however in almost negligible concentrations. Trends in trivalent chromium species and in particular  $\text{Cr}^{+3}$  depict a decline as pH increases and leachate tends towards alkaline. The exception of the trivalent species  $\text{CrO}^{2-}$  which show an increase as an increase in pH is observed (Figure 7.9b). There is an observed fall in the concentration of Cu species as pH increases above pH 6, with the exception of  $\text{Cu}(\text{OH})_2$  species. The toxicity indicator species  $\text{Cu}^{+2}$  reduces in concentrations from  $6.35\mu\text{g/L}$  at pH 6 to  $0.006\mu\text{g/L}$  at pH 10 (Figure 7.9c). Predicted concentration of Ni species are fairly steady at acidic and circum-neutral pH however a gradual fall in predicted concentration is observed as pH rises from 8, with the exception of  $\text{NiCO}_3$  and  $\text{NiBr}^+$  (Figure 7.9d). Predicted Zn species gradually show a fall in concentration as pH tends towards alkalinity, with the exception of  $\text{ZnOH}^+$  and  $\text{ZnCO}_3$  which show a rise as pH increases till pH 9 and a subsequent fall in predicted concentration (Figure 7.9e). In general, this would suggest that provided conditions remain acidic, the these shales would leach more toxic compositions  $\text{Cr}^{+3}$ ,  $\text{Cu}^{+2}$ ,  $\text{Ni}^{+2}$  and  $\text{Zn}^{+2}$ , with the exception of  $\text{CrO}_4^{2-}$  which is evidently reduced to  $\text{Cr}^{+3}$  and other trivalent chromium species. Overall, predicted speciation

results have indicated that the fractured simulated leaching protocol provided a heightened risk of trace metal mobility.

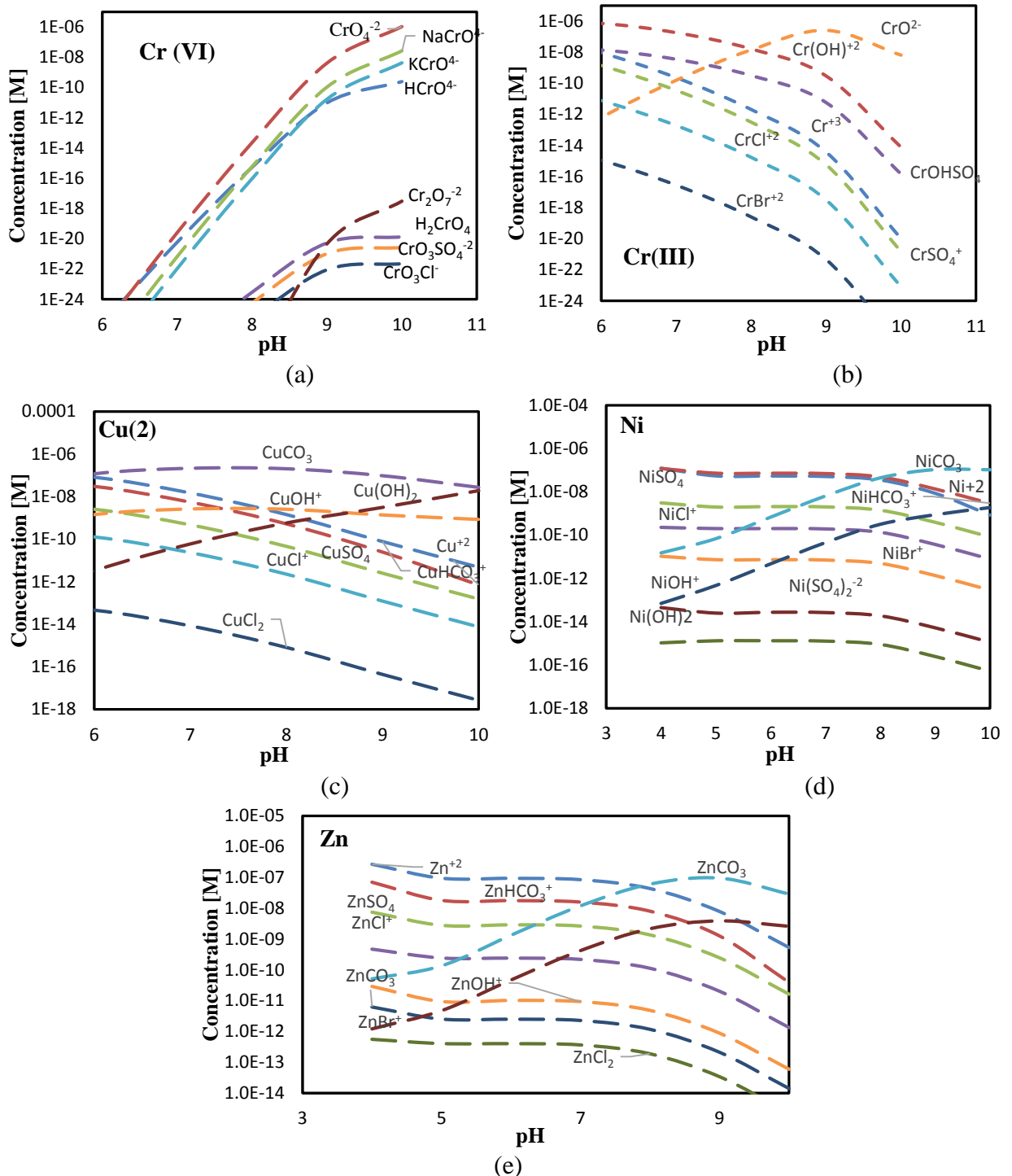


**Figure 7.9:** Speciation of (a) Cr(VI) ( $10^{-6}$  M) (b) Cr(III) ( $10^{-6}$  M) (c) Cu(2) ( $10^{-7}$  M) (d) Ni ( $10^{-7}$  M) and (e) Zn ( $10^{-6}$  M) from the Bowland black shale leached with SFF.

## 7.6 Chapter Summary

Two simulated kinetic leaching studies were conducted on shale samples from 3 prospective shale gas formations in the UK. The first kinetic study simulated the weathering of these shales in their natural environment and the second simulated the weatherability of the same shale samples influenced by hydraulically fracturing the formations. While the natural leaching kinetic study provided background concentration of a releasable and mobile metal PTEs indicators in the investigated shales as they existed before being affected by hydraulic fracturing, the fracture simulated leaching kinetic study provides a quantification on the releasable concentrations and overall impact from such anthropogenic activities. A comparative analysis of both simulated leaching kinetic was evaluated with the aim of determining the risk contribution of shale gas development to contaminant mobility and consequently human and environmental health. The comparative analyses discussed here also provided a time factored evaluations of the scale of contaminant mobility and release from data collected from both kinetic studies.

Using paired t-test, the effects of the two experimental treatments was assessed to identify if the difference observed was of any statistical significance. Results presented here have shown that there were significant differences in effects caused by anthropogenic interference simulated by the fractured enhanced leaching. Released concentration of the selected indicator trace metals in both experimental simulations was also comparatively analysed. Chromium results in all three shales were extremely statistically significant ( $t_{LAN} = 5.05$ ,  $p < 0.001$ ), ( $t_{DRB} = 8.45$ ,  $p < 0.001$ ) and ( $t_{CLV} = 2.75$ ,  $p < 0.005$ ) and therefore suggest that with regards to Cr, simulated fracturing enhanced leaching does increase the release of trace metal from the studied formations. Pair t-test results for Cu shows differences in release for both Lancashire and Derbyshire shales were statistically significant ( $t_{LAN} = 2.29$  at  $p < 0.005$  and  $t_{DRB} = 2.92$  at  $p < 0.001$ ). A test of statistical significance reveals only Ni in the Lancashire shale exhibiting any statistical significance ( $t_{LAN} = 4.06$  at  $p < 0.005$ ). Similar results was observed for the Zinc with both Edale shale and Whitby shales showing any significant difference while Lancashire shale show statistical significance at  $t_{LAN} = 8.59$ ,  $p < 0.001$ .

When the effect on reaction rates (elemental mass loss per exposed surface area in column) was evaluated for all three investigated shales, results suggest that applying a fracture simulated leaching significantly increases the solubility of trace metals with the exception of Cu in the CLV shale, Ni in the DRB shale and Zn also in the DRB shale. This implies that hydraulic fracturing may have little effect on the solubility of these traces in the Whitby Bituminous shale formation and the Edale shale formation. A time sensitive quantitative measure of rates (chemical flux) which measures the amount of substance per unit volume, per unit time transformed into solution in the leaching column also provide similar results that suggest the poor mobility of Cu relative to other trace heavy metals in all 3 shales. An assessment of the quality of the collected leachate provides a means to assess the nature of the resulting wastewater following both weathering scenarios. While both sulphur and carbonate weathered percentages were closely similar in the leaching protocols simulating natural weathering, observed trends in the fracture simulated leaching showed the dissolution of carbonate contents far exceeding sulphur dissolution and implying the late exhaustion of acid forming composition of the shales. Results showed that calcite exhaustion will occur at a faster rate to sulphate exhaustion and eventually these shales would produce sulphur long into the exhaustion of available carbonate composition. Consequently the release of mobile and potentially toxic elements from these formations is inevitable.

Because it has become apparent that metal toxicity is a function of the concentrations of specific metal species and not a direct function of the total metal concentration, an assessment of the likely distribution of species and complexes that could promote mobility and indicate the likelihood for toxicity was considered. Firstly, a shortlist of species that could be regarded as best predictors for toxicity from the selected PTEs investigated was selected. Then by obtaining data from the leachate analysis and adopting a thermodynamic database, the concentrations of individual species are computed using the geochemical equilibrium modelling application, PHREEQC (Parkhurst and Appelo 1999). Results show that at the recorded leachate pH range of 5.5-8.9 observed during both 12 week leaching tests, predominate aqueous species are chiefly present as complexes in the form of hydroxides, carbonates and some free ions. The models also predicted that sulphate and fluoride complexes [ $\text{CrF}^{+2}$  and  $\text{Cr}^{+3}$ ] are

additionally dominant in the fracture simulated leaching experiment. Modelled results also show that trivalent chromium ions, free ions  $\text{Cu}^{+2}$ ,  $\text{Ni}^{+2}$  and  $\text{Zn}^{+2}$  occur at larger concentrations in the fracture simulated leaching protocol in comparison to the natural weathering simulated leaching protocol and indicating some form of pH control. Therefore, the resultant effect of varying pH between 4 and 10 was investigated. The results obtained suggested that provided conditions remain acidic, the studied shales would leach more toxic compositions of  $\text{Cr}^{+3}$ ,  $\text{Cu}^{+2}$ ,  $\text{Ni}^{+2}$  and  $\text{Zn}^{+2}$ , with the exception of  $\text{CrO}_4^{2-}$  which is evidently reduced to  $\text{Cr}^{+3}$  and other trivalent chromium species. 5 year predicted concentrations in both kinetic studies are computed from obtained rates and are compared in all three investigated shales (Figure 7.10).

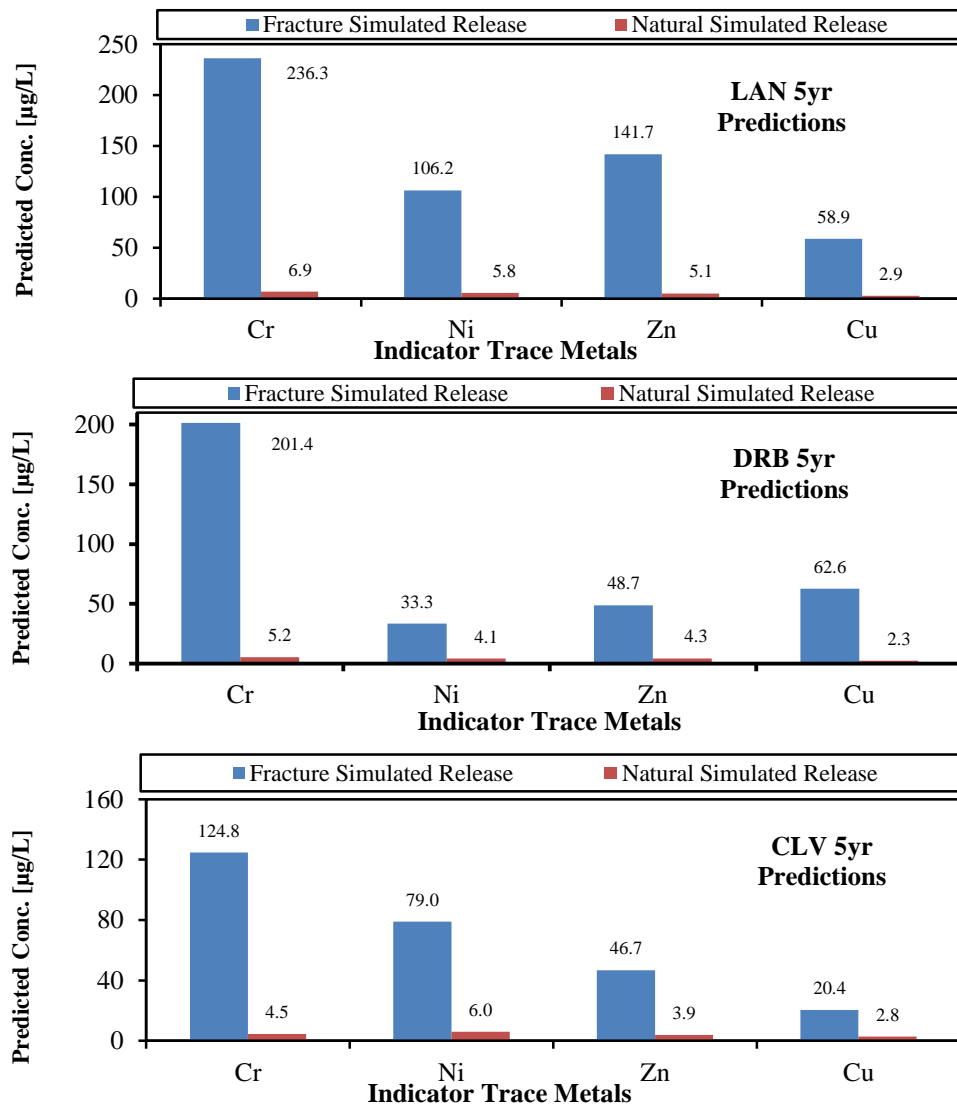


**Figure 7.10:** 5 year predicted release concentrations of investigated traces in the fractured simulated and natural weathering simulated leaching scenarios

A critical advantage of the adopted methodology is its predictive capability which allows the assessment of potential releases of the investigated traces. Cr was observed to have the highest predicted release, reaching concentrations of over 200µg/L in the LAN and DRB shales, and just approximately 125µg/L in the CLV shale. Overall, predicted concentrations trends suggest the deterioration of returning flowback with time and might suggest that need for a dynamic treatment system to cater for changes in contamination levels.

## **7.7 Conclusion**

In summary, the following were the observations made from this comparative analysis;

1. Significantly higher released concentrations of investigated PTEs were
2. Observed in the fractured simulated leaching kinetic experiment to suggest the increased risks from HDF and such anthropogenic activities.
3. A comparison of release rates and chemical fluxes suggest that fracturing the formation for gas has a significant effect on increasing the matrix surface area which in turn increases the tendency for mineral solubility and eventually an increase in the mobility of investigated traces in all three shales.
4. The qualities of returning wastewater from the fracture formation is severely influenced by the mineralogy of the geological terrain and simulated fracture leaching experiments have shown that there is significant deterioration of the returning wastewater over time. A consequence of the changing acidic or alkaline conditions in the brought about by the interplay of acid forming and carbonate neutralising components in the shale.
5. 5 year release predictions for both natural weathering and fracture simulated leaching releases produced most investigated traces well in excess of recommended EQS, WHO and EU standards and illustrates the scale of risk arising from fracture disturbances to these pre-historic formations

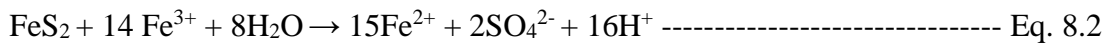
## Chapter 8. Microcosm Investigation of Biochemical Release Potential

### 8.1 Introduction

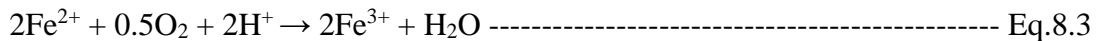
For the research study, assessing the potential for PTE release following anthropogenic interferences, in particular, hydraulic fracturing (HDF) is key. We hypothesised that hydraulic fracturing, as an operational technique during shale gas development, resulted in the accelerated release of PTEs from the studied shale. We therefore need to test releases impacted by prevailing environmental and operational conditions most common during fracturing operations. Reviewing downhole conditions at gas site in the US. suggest that anoxic conditions are quite predominant with temperatures in the range of 66°C -125°C (Salbu et al. 1998), little or no oxygen (Jorgensen et al. 2009), elevated CO<sub>2</sub> typical with most hydrocarbon wells (Wood et al. 2011, Marshall 2014) and abundance of acidophilic bacteria (Bosch *et al.* 2012 ). Hence, this laboratory assessment was focused extensively on mimicking realistic operational conditions typical to hydraulic fracturing of shale gas formations. The methodology adopted (leaching column kinetic) however, was inadequate in assessing the combined effect of certain environmental conditions such as the prevailing anoxic condition downhole and microbial effect on our investigated PTE releases and until the combined effect of both operational and environmental conditions are assessed, the scale of the HDF impact on PTE release is incomplete.

There is a paucity of data on the effect of acidic, oxygen depleted microbially infested environments on the release of heavy metals from black shale (Claus and Kutzner 1985, Beller 2005, ATCC 2013). On one hand, it is known, from previous experiments conducted in this study, that fluid rock interactions where the fluid is characterised by low pH increases the solubility of a majority of the binding sites for these heavy metal and consequently enhance the mobility of these heavy metals. On the other hand, it is also commonly known from literature that the rate controlling processes in sulphate rocks exposed to weathering is initiated by the oxidation of pyrite. When pyritic rocks are exposed to subsurface or surface water, the chemical and microbial oxidation of pyrite can release iron and sulphur from solid phases and produce a large amount of acid, which in turn results in the mobility of toxic metals in a process known as “acid

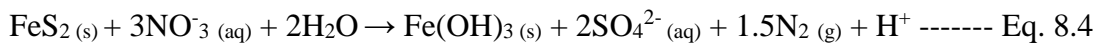
mine drain or acid rock drainage (AMD or ARD)”. In AMD, aerobic acidophilic microbes like the *Acidithiobacillus ferrooxidans* catalyses the breakdown of sulphide minerals forming sulphuric acid that further catalyses the release of metals (Whittleston 2009, DECC 2010, DECC 2014). A common sulphide mineral pyrite, will therefore oxidize chemically to ferrous iron or ferric iron in an aqueous solution in the presence of oxygen and these can typically be expressed as;



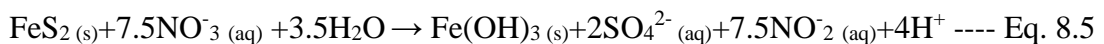
In a prolonged oxidisation, ferric iron can be sustained as shown in Equation 8.3 below;



Under anoxic conditions however, due to the absence of oxygen, a different electron acceptor is required. Studies in anoxic ground water environments (Beveridge and Doyle 1989, Macaskie and Dean 1989, Jorgensen et al. 2009) suggest that nitrate is a likely candidate and hence the process is mostly likely denitrification. Hence, with pyrite as the donor, the process can most typically be expressed as,

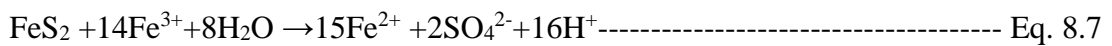
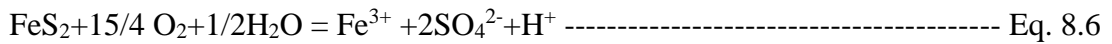


If the reduction of nitrate is complete, the end product is the release of gaseous nitrogen but in the case of an incomplete reduction, the intermediate ‘nitrite’ is produced in solution and these reaction can be expressed as;



Although there have been several attempts at providing evidence for the anaerobic nitrate dependent oxidation of several sulphide mineral, not until recently, have there been any breakthroughs (Bosch *et al.* 2010, Vidic et al. 2013, Bosch et al. 2012 ) and even at this success, several controversies still surround the evidence provided. Theoretically, the source of the controversy lies in the fact that pyrite has a crystalline structure well resistant to acid attack and therefore, there is a missing component

required to oxidise pyrite (Moore et al. 2014). A few literatures however, suggest that this process occurs in nature all the time (Lee et al. 1998, Jorgensen et al. 2009, Moore et al. 2014, Orem et al. 2014) and in fact, microbial oxidation of non-pyritic ferrous iron leads to the formation of ferric iron which is capable of oxidizing pyrite under acidic conditions (Lee et al. 1998, Xiang-Rong et al. 2004, Moore et al. 2014, Bosch et al. 2012 ).



Hence, the pathway is mostly characterised by an acidic aqueous environment as can be seen from Equation (7) where substantial  $\text{H}^+$  ions are released further lowering the pH of the system and this could have a profound influence on the release of heavy metals (Southam 2000). It is also suggested that acidophilic microbes such as *A.ferrooxidans*, catalyses the oxidation process (DECC 2010) but these microbes are known to respire aerobically. In an acidic, oxygen depleted environment however, acidophilic anaerobe would probably be responsible for this complex oxidation pathway and evidence of the reactions is found in products of the reaction such as the reduction of nitrate and the release of sulphate upon microbial incubation . Therefore, this Chapter attempts to simulate anaerobic microbial oxidation of the pyritic contents in the studied shales with the aim of investigates the combined effect of an acidic, oxygen depleted and microbial present environment on the release of selected PTEs investigated.

## 8.2 Chapter Objectives

In this study, microcosm experiments were used to investigate the combined effect of environmental and operational conditions on the release of selected PTEs. The experiments designed in this Chapter was therefore to evaluate the extent to which;

1. A solely chemically controlled oxidation can accelerate PTE release
2. A solely biological controlled oxidation can accelerate PTE release
3. A combination of chemical and biological oxidation can accelerate PTE release

The planned experimental objectives and a description of the microcosm setup are summarised in Table 8.1. It is important to the experimental study that reproduction of an anaerobic nitrate dependent oxidation of pyrite composition in the studied shales is achieved before investigating its resultant effect on the release of the investigated PTEs. Realistic fracturing operational conditions selected include the use of chemicals (simulated by adopting the prepared 0.02M concentration of hydrochloric acid (HCL) solution implemented in for the study) while realistic environmental conditions simulated is the anoxic conditions typical to drilled shale gas wells and the presence of proliferating anaerobic microorganisms.

**Table 8.1:** Matrix of proposed microcosm experiment to study the effect of environmental and operational condition on PTE releases

S/No	Experiment Title & Objective	Microcosm Setup
1	<p><b>Environmentally controlled - Bio-mediated Releases (with no SFF)</b></p> <p>To investigate a solely biological controlled heavy metal release from black shale under anoxic conditions mediated by microbial presence with no SFF influence.</p>	<p>Pulverised and sieved samples in tap water, flushed with Nitrogen to maintain anoxic conditions. Microcosm inoculated with sulphur reducing bacteria (<i>Thiobacillus denitrificans</i>)</p>
2	<p><b>Operational Controlled – Bio-mediated Releases (with SFF introduction)</b></p> <p>To investigate a combined chemical and biological controlled heavy metal release mimicking environmental and operational conditions (Bio-mediated with simulated fracturing fluid introduction)</p>	<p>Pulverised and sieved samples in prepared Simulated fracturing fluid (SFF) flushed with Nitrogen to maintain anoxic conditions and inoculated with bacteria (<i>Thiobacillus denitrificans</i>)</p>
3	<p><b>Operational Controlled – Non Bio-mediated Release (with SFF introduction)</b></p> <p>To investigate a solely chemically controlled heavy metal release mimicking operational conditions with no environmental influence</p>	<p>Pulverised and sieved samples in prepared Simulated fracturing fluid (SFF) flushed with Nitrogen to maintain anoxic conditions with no bacteria inoculation.</p>

Therefore, two operational conditions are evaluated. Firstly, anaerobic degradation/chemical weathering of black shale samples mimicking natural oxygen deprived environmental conditions and lastly anaerobic degradation/chemical weathering of black shale samples mimicking fracturing operational condition. Natural oxygen deprived environmental conditions as used in the former, represent the release of heavy metals from shale under anoxic conditions typical in buried formations undergoing biogenic weathering via natural groundwater ingress. Hence, the workflow for the experimental study can be summaries as follows;

1. Design of microcosm experiments that enable the test of laboratory realistic operational and environmental conditions, namely the microbial proliferation in oxygen depleted acidic environment.
2. Cultivation of microbial species capable of proliferating within the test conditions and verify the reproduction of a nitrate dependent anoxic oxidation reaction.
3. Run oxidation experiments with all three shale samples, verifying the denitrification process before quantifying the release of the selected PTE.

### **8.3 Design of Experiment**

The design details the microcosm vessel design, choice of inoculum and design of the analytical quantification. In this section all preliminary considerations and computations required to provide a robust experiment study are considered.

#### **8.3.1 Microcosm Design**

The developed microcosm was designed to allow sampling of leachate, introduction of gases and maintenance of anoxic conditions with no ingress of atmospheric conditions. Details of all criteria considered in the design are documented in Section 3.2.4.1 of Chapter 3. By adopting the “Standard guide for chemical fate in site specific sediment/water microcosms” ASTM E1624-94 (2008), a reaction vessel was assembled from components shown in Figure 8.1.

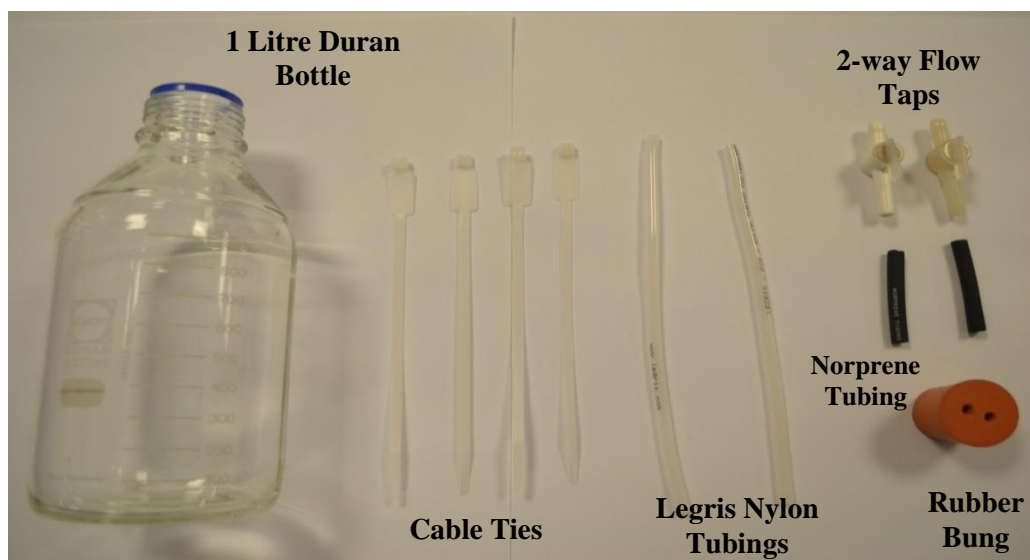


**Plate 8.1:** Laboratory Items and accessories use in designing the microcosm

The following assumptions are made to simplify the design of the microcosm experiment. Firstly, degradation/chemical weathering is the controlling mechanism responsible for metal release during the development of a shale gas play. Secondly, microbial population exist within the system to catalyse sufficient biodegradation and lastly down-hole environmental conditions during hydraulic fracturing are predominantly anaerobic.

### 8.3.2 The Choice of Inoculum

For the choice of inoculum, the study looked towards two unique sets of microbial communities. Firstly, notable microbial communities observed in oil and gas wells and secondly, microorganisms that populate AMD environments. These microbial communities are known to survive and proliferate despite the extreme acidity and heat and most are sulphur reducing bacteria. After an extensive review, the choice between two species, *Desulfovibrio desulfuricans*, with a working pH range of 5-9 and temperature range of 10°C-45°C and *Thiobacillus denitrificans* with an optimum condition for denitrification at pH 6.85 and 32.8°C were considered. These organisms can form a chemoautotrophically based biosphere in the subsurface, ultimately sustained by electron donors derived from sulphide minerals. From column experiments, a working pH range of 5 to 8 and a temperature range 25°C to 30°C are essentially the working conditions appropriate. *Thiobacillus denitrificans* was eventually selected due to wide reviews of its capability to perform nitrate dependent

pyrite oxidation (Gadd 2004, Moore et al. 2014, Bosch et al. 2012 ) however, the study resolved to running enrichment cultures, and developing communities specifically suitable for growth under experimental conditions.

### 8.3.3 Design of Oxidation Experiment

In this section, detailed plans of experiments conducted are reported with details on the results from design of experiments stage that determined the experimental runs. In addition, a check was necessary on the reactor configuration design to ensure that releasable concentrations are detectable by the analytical method and measurable based on the analytical detection limits.

#### 8.3.3.1 Statistical Design of Experiment Iteration

With all experimental design the statistical evaluation of the design was essential in determining possible iterations and aids with experiment randomization. Based on the planned experimental design, a full factorial 2<sup>\*\*</sup> (k-p) standard design with two replicates was adopted and inputs from a statistical application “Statistica (version 12)” was used to evaluate the factors that control the value of a parameter or group of parameters. Based on results obtained, iterations of the experiment setup required to achieve the study aim are tabulated in Table 8.2.

**Table 8.2:** Description of Experiment Runs

<b>Sample Description/I.D</b>	<b>Leaching Fluid</b>	<b>Bacterial Inoculation</b>	<b>Bacterial Type</b>
MRC 1 (LAN)	Tap Water + Growth Media	Yes	Ordinary Cultured
MRC 2 (LAN)	Simulated Fracture Fluid + Acidified Growth Media	Yes	Acid Cultured
MRC 3 (LAN)	Simulated Fracture Fluid	No	No Bacteria Introduction
MRC 4 (DRB)	Tap Water + Growth Media	Yes	Ordinary Cultured
MRC 5 (DRB)	Simulated Fracture Fluid + Acidified Growth Media	Yes	Acid Cultured
MRC 6 (DRB)	Simulated Fracture Fluid	No	No Bacteria Introduction
MRC 7 (CLV)	Tap Water + Growth Media	Yes	Ordinary Cultured
MRC 8 (CLV)	Simulated Fracture Fluid + Acidified Growth Media	Yes	Acid Cultured
MRC 9 (CLV)	Simulated Fracture Fluid	No	No Bacteria Introduction

### 8.3.3.2 Test of Quantifiable Concentrations

To ascertain that released concentrations are detectable with respect to the limits of detection of the analytical method, the estimated computation of releasable concentrations from the experimental setup was evaluated. Results from the leaching column kinetics (Chapters 5 and 6) enabled the computation of the approximate metal mass released per gram of rock for each investigated trace element. This enables the computation of the minimum mass of shale required per reactor for detectable concentrations measurable above detectable limit. Table 8.3 shows the computation of rock to fluid volumes required to achieve detectable concentrations of heavy metals based on the limits of detection specific to the adopted AA spectrometer.

**Table 8-3:** Computation of Reactor Configuration for Rock Fluid volume in Reactor

	1	2	3	4	5	6
<b>Metal</b>	<b>Analytical Detection Limit (ppm)</b>	<b>Minimum weekly mass weathered from column kinetics (g)</b>	<b>Expected mass (mg) release in 350g of rock</b>	<b>Aqueous Volume in Reactor (L)</b>	<b>Estimated conc. Detectable (mg/L)</b>	
Fe	0.001	7.05E-05	4.95E-02	0.450	110.0785	
Cr	0.001	4.22E-06	2.13E-03	0.450	4.7345	
Cu	0.0003	2.63E-06	1.37E-03	0.450	3.0547	
Ni	0.003	4.83E-06	2.55E-03	0.450	5.6684	
Zn	0.00001	3.84E-06	2.16E-03	0.450	4.8088	

Minimum releasable and measurable concentrations are computed as follows;

1. Column 2 shows the minimum detection limits for the AA spectrometer.
2. Column 3 shows the weekly mass weathered from the average of computed weekly weathered mass obtained from the leaching column analysis.
3. Column 4 computes the expected mass released from 350g shale rock proposed for the microcosm. (A product of column 3 and 350g shale rock)
4. Column 5 shows microcosm aqueous volume set at 450ml.
5. Column 6 is the estimated detectable release concentration for each investigated metal. These values are compared with the corresponding detection limits in column 2.

As the estimated detectable concentration exceed the analytical detection limits, measurable released concentrations of each analyte can be quantitatively measured by the chosen analytical method. However, an estimate of aqueous volume in the microcosm is further influenced by the analytical sampling volume required for each analysis listed in Table 8.4. The chosen methodology requires that a sampling volume of 15ml be extracted from any one reactor for the complete analysis of all parameters listed in Table 8.4. Hence, the total volume required for the 3 week duration should be greater than 315ml.

### 8.3.3.3 Analytical Determinations

In determining the duration of the experiment, a major consideration was the survival rate of the bacterium in the microcosm reactors. It is important that the bacteria survive considerably enough to influence the reaction kinetics in the reactors within the duration of the experiment. Although dependent on other factors such on the rate of reaction and duration till equilibrium is attained, a vital consideration is reviewed evidence on the growth and survival of *Thiobacillus denitrificans* undergoing nitrate dependent pyrite oxidation.

**Table 8.4:** Analysis and Appropriate Method

Analyte	Method
pH	Standard Method
Nitrate (NO <sub>3</sub> <sup>-</sup> ), Nitrite (NO <sub>2</sub> <sup>-</sup> ), Sulphate (SO <sub>4</sub> <sup>2-</sup> )	Ion Chromatography (IC)
Iron II (Fe <sup>2+</sup> ), Iron III (Fe <sup>3+</sup> )	Ferrozine Method (Spectrophotometer)
Chromium (Cr), Copper (Cu), Nickel (Ni) and Zinc (Zn)	A. Absorption Spectrometry (AAS)

A duration of 3 weeks is estimated for the experimental run, following an analytical study by Beller *et al.* (2013) that found no evidence of a Nitrate-dependent Fe (II) oxidation supporting the growth of *Thiobacillus denitrificans* in a liquid medium over a 20 day period. Another important test design consideration is the sample particle size for rock mass in the test reactor. The study adopts particle sizes less than 75µm as recent studies emphasised the general increased reactivity of nanosized minerals to microbial processes (Hochella *et al.* 2008, Bosch *et al.* 2010, Bosch *et al.* 2012 ).

## 8.4 Methodology

In this sections laboratory method are enumerated and this include the sample preparation, methods for cultivating *Thiobacillus denitrificans*.

### 8.4.1 Sample Preparation

At the laboratory, sampled were stored in sealed HDPE airtight containers under dark dry and cool conditions. These storage procedures were to prevent to the barest minimum the oxidation of pyrite resulting in the formation of soluble acid sulphate salts. Samples were retrieved from storage, pulverised in a ring type Gyro mill and sieved to  $<75\mu\text{m}$  in British standard sieve mesh No. 170. Crushed and sieved samples were stored in opaque Nalgene bottles and kept no longer than 6weeks before method implementation. Extreme care was taken to ensure all sieves were air pressure cleaned and contain no remnant of previously sieved materials that might contaminate the studied samples. Before method implementation, crushed and sieved samples were sterilized by autoclave to eliminate the influence of other bacterial community. Sterile samples were then incubated at  $121^{\circ}\text{C}$  for 30 minutes at 103KPa and subsequently incubated at  $30^{\circ}\text{C}$ . The impact of an incubation treatment of  $121^{\circ}\text{C}$  on the sampled shale was not considered and this was an observed limitation to the study.

### 8.4.2 Cultivation and Adaptation of Thiobacillus Denitrificans

Cultivation was done in six 150ml Wheaton borosilicate glass serum bottle sealed with 20mm crimp seals. Cultivation of potent *T.denitrificans* cells from freeze dry culture (Plate 8.2) was first achieved before cultivation of cells adapted to the SFF media was achieved. For cultivation, freeze dried ampoules vials of *T.denitrificans* ATCC©25259<sup>TM</sup> have obtained from the American type culture collection and cultivated under strictly anaerobic conditions. Pure cultures were grown in bicarbonate–buffered (30mM, pH 7.0) medium containing 25mM  $\text{Na}_2\text{S}_2\text{O}_3 \cdot 5\text{H}_2\text{O}$ , 23.4mM  $\text{NH}_4\text{Cl}$ , 24.7mM  $\text{KNO}_3$ , 18.4mM  $\text{KH}_2\text{PO}_4$ . The medium was supplemented with trace element solution containing Ethylenediaminetetraacetic acid (EDTA), Zinc sulphate ( $\text{ZnSO}_4$ ), Calcium chloride ( $\text{CaCl}_2$ ), Manganese (II) chloride ( $\text{MnCl}_2$ ), Iron (II) sulphate ( $\text{FeSO}_4$ ), Ammonium molybdate ( $\text{H}_8\text{MoN}_2\text{O}_4$ ), Copper (II) sulphate ( $\text{CuSO}_4$ ) and Cobalt (II) chloride ( $\text{CoCl}_2$ ).

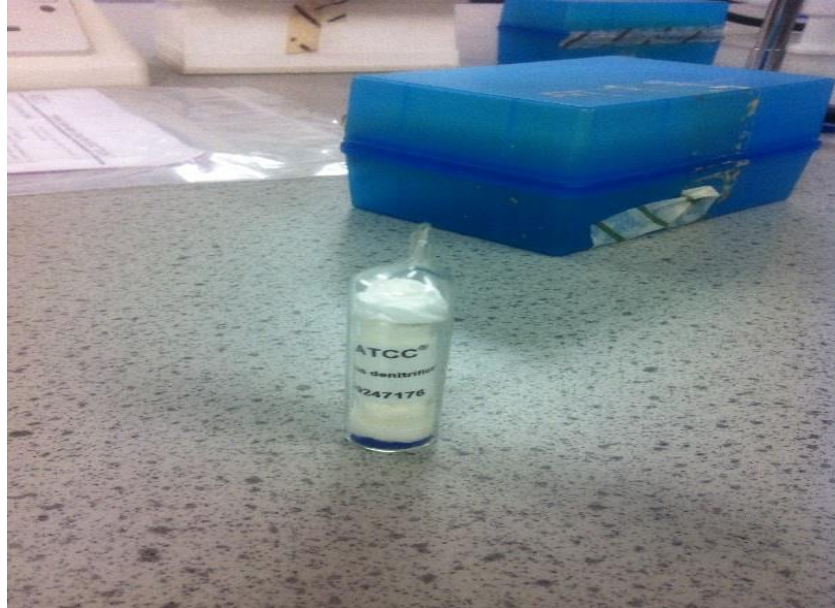


**Plate 8.2:** (a) Freeze dried ampoules vials of *Thiobacillus denitrificans* ATCC©25259TM

Potassium nitrate ( $\text{KNO}_3$ ) serves as electron acceptor and Sodium thiosulphate pentahydrate ( $\text{Na}_2\text{S}_2\text{O}_3 \cdot 5\text{H}_2\text{O}$ ) serves as electron donor. This bulk media solutions were prepared in conformity to ATCC T2 Medium #450 broth for *T.denitrificans* as detailed in the ATCC product information sheet. It was essential that the cultivating instructions were strictly adhered to as the growth of anaerobes could be altogether challenging. Table 8.5 below lists all four solutions, reagents and required reagent quantity for the preparation of the growth media. Extreme care was taken to ensure that solutions labelled A to D were sterilized before aesthetically combining all four solutions to make the recommended growth media. Extra solutions were prepared for subsequent cultivations of the bacteria. All growth media were refrigerated when not in use and re-sterilized before use. Before reused, it was important to visually inspect the growth media for visible particles or colloids, as this could give indication of contamination or growth of unwanted bacteria. After sterilization, each solution is allowed to cool before combining aesthetically. 30 mL of each solution was extracted and combined aesthetically in the 150mL borosilicate glass bottles. Three additional growth cells were prepared from the recommended broth in Table 8.5.

**Table 8-5:** ATCC medium: 450 T2 medium for Thiobacillus

	<b>Reagent</b>	<b>Quantity</b>	<b>Concentration</b>
<i>Solution A</i>	Na <sub>2</sub> S <sub>2</sub> O <sub>3</sub> .5H <sub>2</sub> O	5.0 g	80mM
	NH <sub>4</sub> Cl	1.0 g	75mM
	KNO <sub>3</sub>	2.0 g	79mM
	Distilled water	250.0 ml	-
<i>Solution B</i>	KH <sub>2</sub> PO <sub>4</sub>	2.0 g	59mM
	Distilled water	250.0 ml	-
<i>Solution C</i>	NaHCO <sub>3</sub>	2.0 g	95mM
	Distilled water	250.0 ml	-
<i>Solution D</i>	MgSO <sub>4</sub> .7H <sub>2</sub> O	0.8 g	3.25mM
	FeSO <sub>4</sub> .7H <sub>2</sub> O (2%, w/v, in N HCl)	1.0 ml	
	Trace Metals Solution	1.0 ml	-
	Distilled water	250.0 ml	-
<i>Trace Metal Solution</i>	EDTA	50.0 g	171.1mM
	ZnSO <sub>4</sub>	22.0 g	136mM
	CaCl <sub>2</sub>	5.54 g	49.9mM
	MnCl <sub>2</sub>	5.06 g	40.2mM
	FeSO <sub>4</sub>	4.99 g	32.8mM
	Ammonium molybdate	1.10 g	0.94mM
	CuSO <sub>4</sub>	1.57 g	9.84mM
	CoCl <sub>2</sub>	1.61 g	12.4mM
	Distilled water	1.0 L	-

However, all 250ml distil water prescribed in solution A to D was replaced by a 250mL solution of the prepared SFF (0.04M HCl solution). Under anaerobic conditions 0.5ml of the broth above was used in rehydrating the entire vial. The aliquot was aseptically transferred into the crimp bottles containing the recommended broth and incubated at 30<sup>0</sup>C. Cell growth was monitored at day 2, 3, 5 and 7 to ascertain the log phase of growth before harvesting to oxidation experiment.

For adaptation, following appreciable cell count of potent *T.denitrificans* cells, 1mL of potent cells were extracted and injected into 150mL borosilicate bottles containing modified SFF growth media. Incubation is done at 30<sup>0</sup>C until cloudiness was observed in the glass serum bottles indicating growth. The procedure was repeated until 3 growth cells cultivating *T.denitrificans* in the recommended growth media and another

3 growth cells cultivating *T.denitrificans* in the modified growth media were obtained. Growth cells are then incubated at 30°C for 7 days.

#### 8.4.2.1 Monitoring Bacterial Growth

Evidence of reproducing an anaerobic nitrate dependent oxidation reaction lies in monitoring the products of the reaction in Equation 8.4 and ensuring the growth of anaerobes. All cultivated cells are harvested within the log growth phase when cell growth is at maximum and ascertain the survival and potency of the inoculating bacterial before introduction to the oxidation experiment. Bacterial growth is monitored prior to inoculation in six separate growth cells labelled Cell A to F



**Plate 8.3:** (a) 150ml borosilicate glass serum bottle used as growth cells (b) Incubation of growth cells in a systematic rotary incubator at 37°C

Wheaton bottles labelled A, B and C represent cells grown in a non acidified broth (Strain A) while wheaton bottles labelled D, E and F represent cells grown in an acidified broth with the 0.04M HCL. This study adopts three methods for verifying cell growth;

1. Measuring the turnover of thiosulfate to sulphate and the depletion of Nitrate via ion chromatography (IC).
2. Measuring the optical density (OD600) of each growth cell at 12, 20, 28, 48, 72, 96, 120, 144 and 168hrs via a spectrophotometer.
3. Preparation of plates for counting of colony forming units at periodic intervals.

IC measurements of all monitored analytes involve the determination of background concentrations at start of cell cultivation. During the cultivation, analytical

determinations of sulphate ( $\text{SO}_4^{2-}$ ), Nitrate ( $\text{NO}_3^-$ ) and Nitrite ( $\text{NO}_2^-$ ) are performed for both recommended (Strain A) and the SFF modified broth bacteria (Strain B). On each sampling day, a 1ml aliquot of the growth broth is anaerobically redrawn from the cultivating crimp bottle for analyses; 1:100 dilutions are prepared from the 1ml aliquot for analysis in the IC. 1ppm standard solutions of Nitrate, Nitrite and Sulphate are prepared as calibration standards for the IC. Increased turbidity in a culture is another index of bacterial growth. The measurements of absorbance or optical density can therefore be used to indicate cell growth. Optical density at 600nm is measured periodically at 12, 20, 28, 48, 72, 96, 120, 144 and 168 hours via the Biomate 3 Thermo scientific spectrophotometer. Again, the analysis is performed for both the non-acid cultured bacteria (Strain A) and the acid cultured bacteria (Strain B). Lastly, a quantitative assessment of colony forming units is also adopted in monitoring the growth and survival of both bacterial strains. Cultivating media is prepared as previous described in Table 8.5, Oxoid's Agar Bacteriological (Agar No. 1), prescribed for the culture media is used to prepare agar plates for colony counting. Sterilization is done by autoclaving at  $121^\circ\text{C}$  in a LTE autoclave K150E manufactured by LTE scientific Ltd. 1mL Aliquots from each growth cell is serially diluted in 9ml ringer solutions to a maximum dilution factor of  $10^7$ . 0.1 mL of each dilute (in ringer solution) is then plated and incubated anaerobically at  $37^\circ\text{C}$ .

#### ***8.4.2.2 Maintaining Anoxic Conditions***

To ensure anaerobic conditions, plates are placed in a 7 litre Mitsubishi manufactured AnaeroPack Rectangular box as shown in Plate 8.3. The AnaeroPack jar is made to contain two 3.5 Litres AnaeroGen Packs capable of reducing oxygen levels to below 1% within 30 minutes with a resulting carbon dioxide level of between 9% and 13%. As an additional verification of anaerobic conditions, strips of anaerobic Indicator strips (BR0055B) manufactured by Oxoid, are placed in the jar to ascertain anaerobic conditions are attained.



**Plate 8.4:** 3.5L AnaeroPack Rectangular jar containing streaked plates

### ***8.4.2.3 Harvesting Cultivated Cells***

Strain A cells were harvested following the identification of peak log growth phase predominantly at day 3 while strain B cells have mostly harvested at day 4, also identified as the peak log growth phase. Cells were harvested anaerobically by centrifugation at 4000 rpm, 20°C for 15 min and subsequently re-suspension in the experiment reaction medium described in Table 8.5 without Potassium Nitrate ( $\text{KNO}_3$ ) and the Sodium thiosulphate ( $\text{Na}_2\text{S}_2\text{O}_3 \cdot 5\text{H}_2\text{O}$ ). This was immediately injected into the reaction vessels designed for the oxidation experiment. Only vessels assigned to have inoculums were injected with the harvested cells. Care was taken to ensure that the transfer process was anaerobic and exposure to external oxic environment was avoided.

### **8.4.3 Microbial Mediated Oxidation Experiment**

The oxidation experiment was performed in a 1 litre Duran bottle. The volumetric composition of the experimental reaction medium including the volume ratios of the electron acceptor and donor needs to be computed prior to the start of the experiment mainly to ensure the survival of bacteria for duration of the experiment.

#### ***8.4.3.1 Volumetric Composition of Oxidation Medium***

It was imperative that the sufficient  $\text{NO}_3^-$  and pyrite concentration are introduced to the experimental reaction medium to sustain survival and growth for the planned 3 weeks duration of the experiment. The study adopted depletion rates observed during

the cultivation experiment to compute the required  $\text{NO}_3^-$  concentration required for a 1 litre microcosm vessel. According to results, Nitrate depletion rate for both strain A and strain B growth cells monitored over a 72hr period is estimated at 15.96ppm hr<sup>-1</sup> and 13.53ppm hr<sup>-1</sup> respectively. Therefore, a planned 21days (504hr) oxidation experiment requires an estimated  $\text{NO}_3^-$  concentration of 8,043ppm (131.04mM) in the non-acid experimental reaction medium and 6,818ppm (109.96mM) in the acidified experimental reaction medium for survival of the inoculating bacteria during the experiment duration. Thus, for a 500mL aqueous reactor volume, 4.022g of  $\text{NO}_3^-$  in the form of Potassium Nitrate ( $\text{KNO}_3$ ) is added to the non-acidified experimental reaction medium to achieve a 131.04mM concentration of  $\text{NO}_3^-$  while, 4.409g of  $\text{KNO}_3$  is added to the acidified experimental reaction medium to achieve a final  $\text{NO}_3^-$  concentration of 109.96mM.

For Pyrite composition, designed estimates suggested the 350g of pyrite were sufficient to achieve measurable concentrations of analytes based on the minimum detection limits of the analytical techniques adopted. To confirm sufficiency as an electron donor, rates in the cultivation experiments were also considered. During the cultivation experiment, the electron donor (Thiosulphate) had a depletion rate of 0.28mMhr<sup>-1</sup> and 0.22mMhr<sup>-1</sup> for both strain A and strain B growth cells respectively, monitored over a 72hr period. When computed for 504hr experiment duration, 141.12mM (15.95g/L) of pyrite concentration must be available for the bacteria consumption in the non-acidified experimental reaction medium and 112mM (12.67g/L) in the acidified experimental reaction medium. Therefore, 7.975g and 6.335g of pyrite are required in both non-acidified and acidified reactor volumes respectively. Hence, of the 350g shale mass in each reactor, a maximum 2.28% and minimum of 1.81% must be available pyrite for the bacteria population to ensure growth and survival. XRD analyses on the all three shale types confirm available pyrite composition to ensure growth and survival. Hence, the bicarbonate buffered experimental reaction medium contained 35.5mM  $\text{NH}_4\text{CL}$ , 29.5mM  $\text{KH}_2\text{PO}_4$ , 40.5mM  $\text{NaHCO}_3$ , 1.63mM  $\text{MgSO}_4 \cdot 7\text{H}_2\text{O}$  and the pre-cultivation trace metal supplements listed in Table 8.5 but diluted in a 1:2 ratio. 131.04mM and 109.96mM  $\text{KNO}_3$  was used as electron acceptor for the non-acidified and acidified reaction medium respectively.

### 8.4.3.2 Oxidation Experiment

All 1 litre Duran bottle used as reactor vessels for the oxidation experiment were acid washed and autoclaved to ensure sterilization. 350g of each homogenized shale type was weighed in preparation for introduction into reaction vessels. Under anoxic conditions, homogenized and sterilized shale samples were then placed in the respective microcosm vessels and labelled appropriately as describe in Table 8.2.



**Plate 8.5:** Microcosm vessels filled with shale and reaction media.

500mL of the experimental reaction medium described above, inoculated with the assigned strain of bacteria was added to each reactor vessel and sealed with rubber stoppers/sampling tubing and tap combination. All reactor vessels were flushed with Nitrogen ( $N_2$ ) to drive out oxygen and maintain anaerobic conditions. All reactor vessels were subsequently incubated at  $37^{\circ}C$  with intermittent agitation. Sampling was done via the tubing just above the saturated shale in the reactor, the second tubing allows for the attachment of a nitrogen gas supply that prevents the introduction of oxygen and interactions with the external environment. Following sampling, pH readings were immediately taken before samples were stored for other analysis listed in Table 8.4. Determination of  $NO_3^-$ ,  $SO_4^{2-}$  and  $NO_2^-$  concentrations was measured via the IC following filtration through a  $0.25\ \mu m$  syringe filter. 1:100 dilutions of the sampled aliquot was prepared for this analysis. The study includes the determinations

of cations Ammonium (NH<sub>4</sub>), Sodium (Na), Calcium (Ca) and Potassium (K) for identification of any trends of important significance.

#### **8.4.4 Analytical Determinations**

This section details the method adopted for determinations listed in Table 8.4. Standard recommended test on quality control and matrix interference checks were conducted on determinations on the IC and details of similar procedures adopted are documented in Section 5.3.5 of Chapter and are not documented here to avoid repetition. Details of the analytical instrumentations are also provided in Section 3.2.1 in Chapter 3. A few standard operating conditions adopted are documented here.

##### ***8.4.4.1 Fe (II) and Total Fe Determination***

The choice of analytical technique is the spectrophotometric analyses of Fe(II)-ferrozine complex performed on a single aliquot before and after a reduction step with hydroxylamine. This method is used to measure Fe(II) and Fe(III) distribution during the bacteria cultivation period and in each reactor vessels to over the selected sampling period. The method is based on the Ferrozine (3-(2-pyridyl)-5,6-diphenyl-1,2,4-triazine-p,p'-disulfonic acid), reacting with divalent Fe to form a stable magenta complex with maximum absorbance recorded at 562nm. All solutions are prepared in good quality (18.2MΩm) ultrapure water (UPW).

Absorbance before the reduction step is recorded after 1mL of filtered sample and standard is inoculated with 100 μL of Ferrozine in a spectrophotometric cuvette. 50 μL of the 5M Ammonium Acetate buffer is added to the mixture and the mixture is left for 5 minutes for the magenta colour to fully develop. Absorbance is measured for both the standard and aliquots and the plot of absorbance against Fe<sup>2+</sup> concentration is completed. Due to the possible presence of organic matter in the sample aliquots, the possible formation of Fe (II) complexes may occur forming precipitate at acidic pH which inhibits the complete quantification of Fe (II). A careful observation of the formation of precipitates was implemented as a mitigation of this risk. Absorbance for the total Fe determination step is recorded after the reduction step where 200 μL of 1.4M hydroxylamine hydrochloride reducing agent is added to the mixture. A 50 μL addition of the buffer solution and 10 minutes read delay time completes the mixture

before absorbance readings are recorded. A Plot of absorbance against total Fe concentration allows the computation of observable Fe concentrations.

#### 8.4.4.2 Trace Metal Determination

Released concentrations of the investigated trace metals were determined in aqueous samples after suitable 0.45 $\mu$ m filtration and acid preservation. Analysis was via the Graphite Tube Atomizer GTA 120 furnace atomic absorption spectrometer and the Varian AA240FS Atomic Absorption Spectrometer manufactured by Agilent and located at the School of Process, Environmental and Materials Engineering.

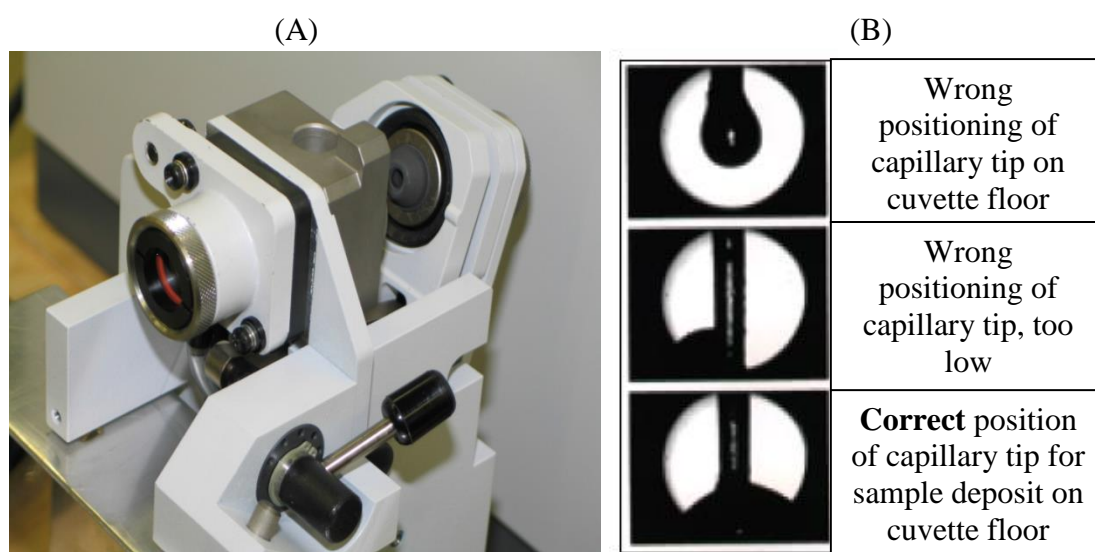


**Plate 8.6:** (A) The non-Zeeman Work-head (B) Capillary Tip Positioning

Analysis of the quality control sample was done following IDL and MDL determinations. The quality control sample, the National Institute of Standard and Technology's certified reference material (NIST-1643e) for trace elements in water was adopted in compliance to the documentation of initial demonstration of capability by the EPA standard method 200.9<sup>1</sup>. Duplicate analyses were compared with the certified true values to verify instrument performance and results were presented. Following leachate collection from the incubated reactor, 20ml leachate was redrawn from each reactor and analysed for the investigated trace metals listed in Table 8.4. Subsequently, daily analysis of 20ml leachates sampled from the incubated reactors was recorded.

### 8.4.4.3 Elemental Transformation Rate

Quantification of each analyte determined in the study takes into consideration the sampling technique. Because analyte determination during each sampling event must consider initial concentration in reactor or previous sampling events as experiment is a closed system, the cumulative amount of moles  $n$ , of element  $i$  released to the reactor solution over the duration of the experiment up to a sampling occasion  $k$  was calculated from the measured concentration ( $C_m$ ) and can be express as;

$$NL_i^k = [C_{i\text{ meas}}^k V_{total}^k + \sum_{s=1}^k C_{i\text{ meas}}^s V_{sample}^s](\text{moles}) \text{----- Eq. 8.8}$$

Where  $V_{total}^k$  is the total volume of the solution in the reactor the after removal of the  $k^{\text{th}}$  sample and  $V_{sample}^s$  is the volume of sample removed on sampling occasion  $k$  (Lovley and Coates 1997, Southam 2000, DECC 2010). Calculated concentrations changes over time are determined by linear regression using the Analysis Toolpak in Excel to a significant level of  $p < 0.05$ . Final concentrations for  $\text{SO}_4^{2-}$ ,  $\text{NO}_3^-$  and  $\text{NO}_2^-$  are expressed as millimoles (mM) while release concentrations for trace metals are expressed as  $\mu\text{mol kg}^{-1}$ .

## 8.5 Results and Discussion

In this section all results obtained are reported and discussed in a systematic manner commencing with bacteria cultivation and adaptation experiments and concluding with analytical results from each oxidation experiments. To ensure that each objective is thoroughly discussed with conclusions providing answers to the stated research question, a chronological approach to reporting the observed results is adopted. Therefore, for each experimental objective listed in Table 8.1, discussed results include leachate characterisation, survival of microbial population, a test of nitrate dependent anaerobic oxidation (which involves a check on  $\text{SO}_4^{2-}$ ,  $\text{NO}_3^-$  and  $\text{NO}_2^-$  trends in reactors) and quantification on the released of investigated indicator heavy metals.

### 8.5.1 Cultivation and Adaptation Results

Following cultivation and as a proof of nitrate dependent pyrite oxidation, all six growth cells are monitored by measuring the turnover of  $\text{S}_2\text{O}_3^{2-}$  to  $\text{SO}_4^{2-}$  and the

depletion of Nitrate via the IC (Figure 8.6). It was difficult to ascertain if nitrogen gas or aqueous nitrite is produced as an end product as shown in Equations 4 and 5 as the detection of gaseous diatomic nitrogen would introduce a challenge since reactors are flushed with nitrogen gas to drive off oxygen and maintain anoxic conditions. An increase in sulphate composition is observed in both growth media, with a 2 day lag in sulphate build-up in the SFF modified growth cell. Also noticeable is nitrate depletion almost immediately in aliquots sampled from the ordinary growth media whilst a 2 day lag is observed in the SFF modified growth cell. This lag is attributed to an inactive period where *T.denitrificans* remains dormant in reaction to the acidic environment (McLean et al. 2002, Struchtemeyer and Elshahed 2011). No nitrite was observed in solution in both media and this was considered a proof of complete oxidation to gaseous Nitrogen.

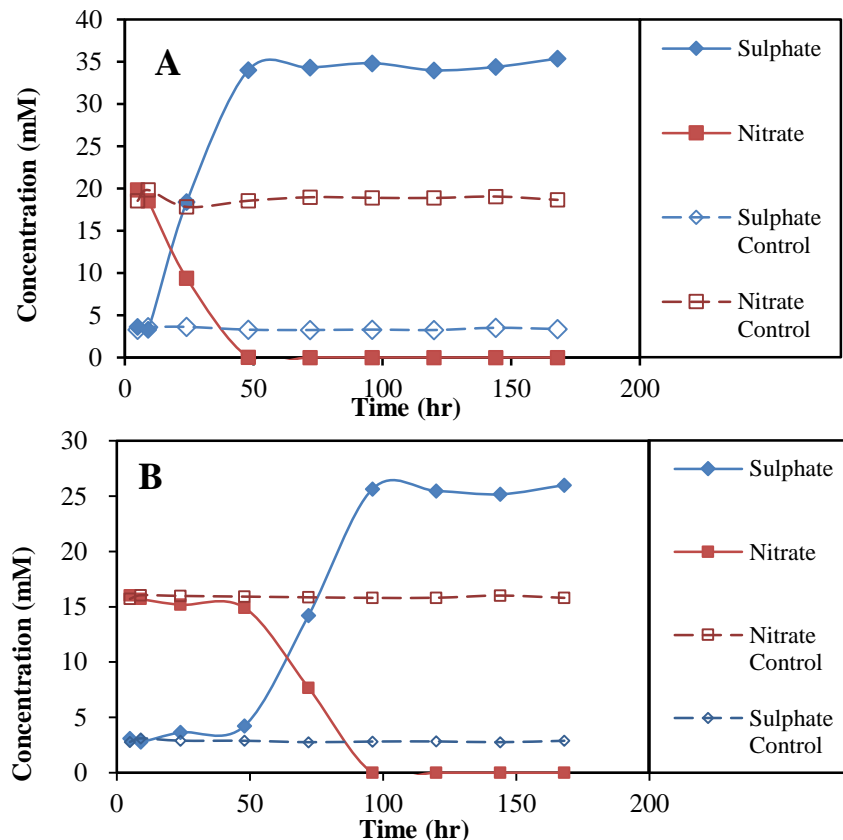


**Figure 8.7:** Mean concentrations of  $\text{SO}_4^{2-}$ ,  $\text{NO}_3^-$  and  $\text{NO}_2^-$  over sampling duration in both (A) Ordinary growth media and (B) SFF Modified growth media and evidence of nitrate dependent oxidation.

To ensure that viable *T.denitrificans* cells are harvested for the oxidation experiment, the study resolved to harvest growing cells at their growth peaks (log growth phase). Hence, using absorbance and CFU data, the peak growth stages during cultivation was determined. Results from a count of colony forming units per mL and measure of optical density for each growth cell is displayed in Table 8.6 and 8.7, a combined measurement of growth is plotted in Figure 8.7 showing count of colony forming unit and absorbance at OD600. Results from CFU plots show log phases in the recommended growth media (growth cells A, B and C) occurring between 10 and

**Table 8.6:** Computation of growth rate and generation time for both cultures

	Recommended Culture			SFF Modified Culture		
	CELL A	CELL B	CELL C	CELL D	CELL E	CELL F
<b>Highest Xt (CFU/MI)</b>	6.796	7.18	7.005	6.604	7.000	6.505
<b>Lowest Xt'(CFU/MI)</b>	2.412	2.29	2.603	4.063	4.657	4.135
<b>time (hr)</b>	28	28	28	116	116	92
<b>Growth Rate (k) (gen/hr)</b>	0.52	0.58	0.52	0.07	0.07	0.09
<b>Generation time (hrs)</b>	1.9	1.7	1.9	13.7	14.9	11.7

28hrs whilst a time lag of approximately 30hrs is observed in the SFF amended growth media (growth cells D, E and F). Results from the absorbance plots showed that the log growth phase cultured cells cultivated in the recommended growth media occurred between 28hr and 72hr whilst cultured cells in the amended growth media occurred between 48hr and 72hr of incubation.

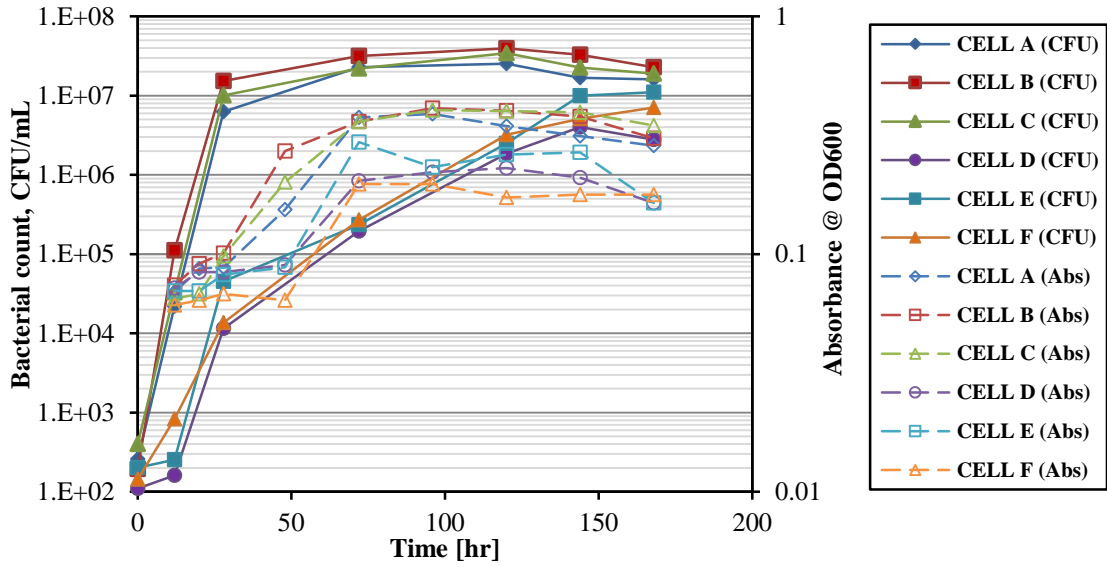


**Figure 8.8:** Count of cells in the cultivating growth cells

Generally, cultured cells in the SFF amended growth media showed a delayed growth rate clearly obvious from data presented in Table 8.6, where growth rates in both culture media have been computed from;

$$k = \frac{\log_{10}[X_t] - \log_{10}[X_{t'}]}{[0.301 \times t]} \text{-----Eq. 8.9}$$

Where  $X_t$  is the larger count of colony forming unit (CFU) in CFU/ML,  $X_{t'}$  is the smaller count of colony forming unit. The generation time  $t_{gen}$  is expressed as

$$t_{gen} = \frac{1}{k} \text{-----Eq. 8.10}$$

A summary of the count of colony forming units in the respective growth cells is presented in Table 8.7 and 8.8. Cells A, B and C contained *T.denitrificans* cells grown in the recommended ATCC broth while growth cells containing the SFF amended broth are cells D, E and F. This plots show an extended period of dormancy in cells cultivated in the amended broth. These cultivation exercises was repeated with acclimatised *T.denitrificans* cells until appreciable cells were obtained about day 3. Therefore, based on the results obtained the aggregate harvesting time for cultures grown in the recommended ATCC growth media was between 24hr and 48hr while cultures cultivated in the SFF amended growth media were harvested between 74hr and 80hr following incubation.

**Table 8.7:** Cultivation data showing count of CFU/mL and absorbance at OD600 for growth cells in recommended ATCC media

S/No.	<i>Growth Cell A</i>				<i>Growth Cell B</i>			<i>Growth Cell C</i>		
	Sampling Time (hr.)	Absorbance (A)	Log <sub>10</sub>	Cell count (CFU/mL)	Absorbance (A)	Log <sub>10</sub>	Cell count	Absorbance (A)	Log <sub>10</sub>	Cell count
1	0	0.069	-1.161	258	0.074	-1.131	195	0.065	-1.187	401
2	12	0.087	-1.060	21,841	0.091	-1.041	111,205	0.068	-1.167	32,902
3	28	0.088	-1.056	6,258,000	0.101	-0.996	15,255,849	0.098	-1.009	10,114,525
4	72	0.154	-0.812	22,750,000	0.271	-0.567	31,750,000	0.201	-0.697	21,950,000
5	120	0.376	-0.425	25,257,741	0.361	-0.442	39,523,585	0.361	-0.442	34,500,369
6	144	0.389	-0.410	16,854,523	0.411	-0.386	32,956,523	0.404	-0.394	22,580,006
7	168	0.346	-0.461	15,995,000	0.401	-0.397	22,773,333	0.400	-0.398	19,030,000

**Table 8.8:** Cultivation data showing count of CFU/mL and absorbance at OD600 for growth cells in SFF amended media

S/No.	<i>Growth Cell D</i>				<i>Growth Cell E</i>			<i>Growth Cell F</i>		
	Sampling Time (hr)	Absorbance (A)	Log <sub>10</sub>	Cell count	Absorbance (A)	Log <sub>10</sub>	Cell count	Absorbance (A)	Log <sub>10</sub>	Cell count
1	0	0.072	-1.143	110	0.070	-1.155	201	0.061	-1.215	144
2	12	0.084	-1.076	161	0.070	-1.155	255	0.064	-1.194	826
3	28	0.084	-1.076	11,558	0.082	-1.086	45,412	0.068	-1.167	13,651
4	72	0.090	-1.046	195,000	0.088	-1.056	235,000	0.064	-1.194	270,000
5	120	0.203	-0.693	1,845,225	0.296	-0.529	2,485,241	0.197	-0.706	3,200,512
6	144	0.221	-0.656	4,020,051	0.232	-0.635	10,003,612	0.197	-0.706	5,124,332
7	168	0.230	-0.638	2,800,000	0.262	-0.582	11,100,000	0.173	-0.762	7,100,000

## **8.5.2 Shale Oxidation Experiment: Proof of Nitrate Dependent Pyrite Oxidation**

During the oxidation experiment, the turnover of pyritic sulphur content in the shale to sulphate, depletion of Nitrate and the development of nitrite were investigated as proof of the denitrification reaction. pH data was monitored as a vital characteristic property of the system that could provide useful information on the chemistry within the reactors. Again the measure of the optical density and CFU are collected. In addition, Equation 8.4 suggests that the denitrification reaction involving pyrite will result in the oxidation of ferrous iron and the formation of ferric iron. Hence, data is also collected for the concentrations of ferrous and ferric iron in sampled aliquots from all reactors.

### ***8.5.2.1 pH and Bacterial Count***

pH data are compared with cell count data in each reactor in a bid to evaluate the response of *T.denitrificans* to changes in pH within the system. Theoretically, as oxidations of the pyrite contents in the shale progresses, the end products of the denitrification reaction alter the environment within the system. Firstly the build-up of  $\text{SO}_4^{2-}$  ensures that the environments become acidic as the pH is expected to fall. Secondly, provided there is a constant supply of nitrate source, denitrification produces the addition of nitrite ( $\text{NO}_2^-$ ) or Nitrogen gas which drives off any fugitive oxygen trapped in the aqueous environment ensure the system remains anoxic. Additionally if the study hypotheses are true, there is also the build-up of heavy metals released from the oxidizing shale. As expected the pH trends show a progressive acidification within the reaction. However, in almost all reactors there is noticeable increase in pH (Figure 8.8) suggesting the build-up of alkalinity in the reactors before a noticeable drop in pH is observed. A possible explanation to this is the initial dissolution of highly soluble carbonate compositions in the respective shale as sulphate production increases. Since these compositions are easily soluble in acid concentration, the products of the neutralization effect could account for the pH rise towards circum-neutral. Also observed is the response of *T.denitrificans* to the changing pH and chemistry within the system. In reactors representing the bioleaching of shales without SFF amendment (MRC 1, MRC 4 and MRC 7) shown in column A of Figure 8.8, it appears that

provided the pH in the systems remains neutral or about circum-neutral (pH range 6.5-7.5), there is an increase in growth rate however, as the pH drops below this range towards acidic, there is a reduced growth rate. In the bio-leaching SFF modified reactors however, even at pH lower than 6, noticeable increases in growth rates are still observed until a further drop below pH 5 before a noticeable decrease in growth rate. Obviously, this suggests that the adapted cultures are able to cope with a further drop in pH without noticeable inhibitions to their growth cycle.

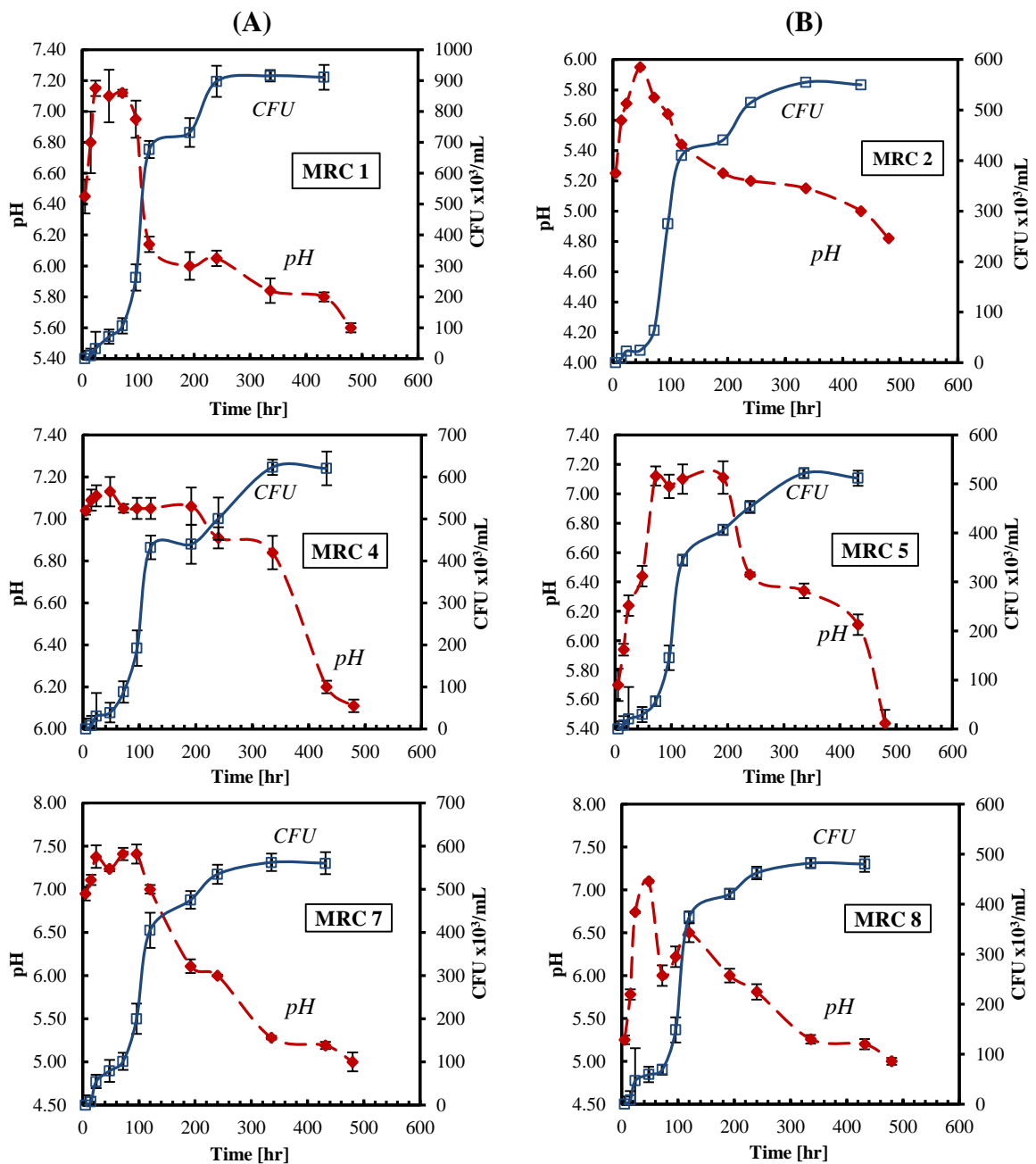


**Figure 8.9:** Plots of pH trends and counts of colony forming units (CFU)

### 8.5.2.2 Oxidation of $Fe^{2+}$ and Formation of $Fe^{3+}$

Additional proof of the denitrification reaction is the oxidation of ferrous iron to ferric iron as illustrated in Equation 8.4 and 8.5. Theoretically, soluble ferric iron will only occur at pH lower than 3.5 hence, ferric iron within the system would have to occur as a precipitate and this is most likely  $Fe(OH)_3$ . Therefore released ferric iron (from *T.denitrificans* accelerated oxidation) will exist as precipitates since no pH is reported below 3.5 during the oxidation experiment (Figure 8.9). From raw analytical concentrations obtained from iron determination experiment (ferroxine method), the elemental transformation rate  $NL_i^k$  are computed as expressed in Equation 8.8 (Table 8.9) based on the sampling technique.

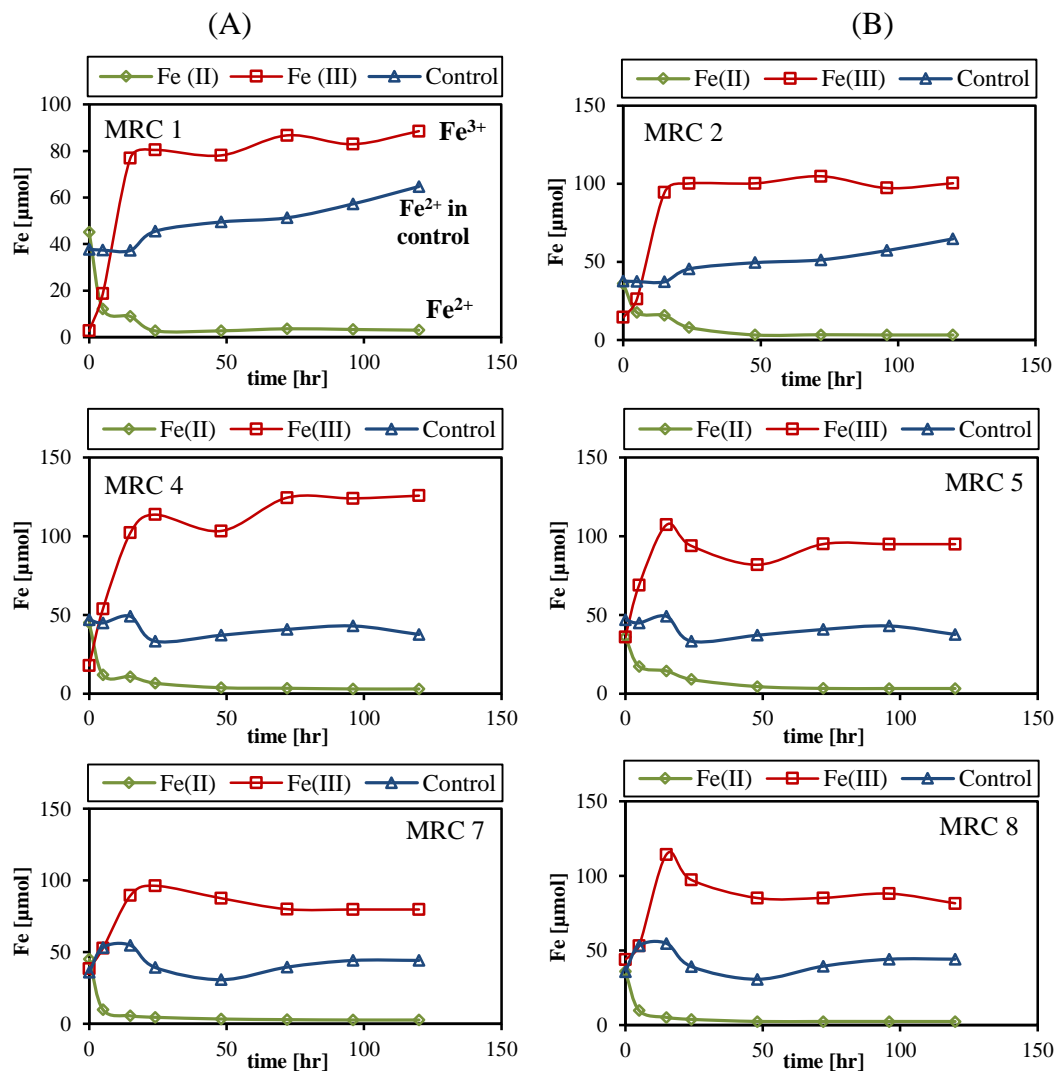


**Figure 8.10:** Proof of anaerobic, nitrate dependent oxidation of pyritic molecules from black shales by *T.denitrificans*. Plots shows the production of  $Fe^{3+}$  □ and oxidation of  $Fe^{2+}$  ◇ and  $Fe^{2+\Delta}$  in sterile controls (MRC 3, 6 and 9)

**Table 8.9:** Computation of Elemental transformation rate for Fe<sup>2+</sup>

Sampling Event	Time [days]	MRC1 ORD C <sub>s</sub> <sub>i</sub> (mg/L)	mol/L or M	Volume left V <sub>total</sub> (L)	Sample volume V <sub>s</sub> (L)	C <sup>k</sup> *V <sub>total</sub> (mol)	C <sub>s</sub> *V <sub>s</sub> (mol)	n (moles)	μmol	μmol/kg
<i>n</i> <sup>1</sup>	<i>0</i>	5.05	9.0E-05	0.480	0.020	4.34E-05	1.81E-06	4.52E-05	4.52E+01	129.12
<i>n</i> <sup>2</sup>	<i>5</i>	1.19	2.1E-05	0.460	0.020	9.82E-06	4.27E-07	1.21E-05	1.21E+01	34.45
<i>n</i> <sup>3</sup>	<i>15</i>	0.81	1.5E-05	0.440	0.020	6.38E-06	2.90E-07	8.91E-06	8.91E+00	25.45
<i>n</i> <sup>4</sup>	<i>24</i>	0.02	3.7E-07	0.420	0.020	1.55E-07	7.38E-09	2.69E-06	2.69E+00	7.68
<i>n</i> <sup>5</sup>	<i>48</i>	0.02	4.0E-07	0.400	0.020	1.61E-07	8.06E-09	2.70E-06	2.70E+00	7.72
<i>n</i> <sup>6</sup>	<i>72</i>	0.15	2.6E-06	0.380	0.020	9.95E-07	5.24E-08	3.59E-06	3.59E+00	10.25
<i>n</i> <sup>7</sup>	<i>96</i>	0.10	1.8E-06	0.360	0.020	6.49E-07	3.61E-08	3.28E-06	3.28E+00	9.37
<i>n</i> <sup>8</sup>	<i>120</i>	0.06	1.0E-06	0.340	0.020	3.39E-07	1.99E-08	2.99E-06	2.99E+00	8.54

N.B: Table represent elemental transformation rate computed using Equation 8.8 from raw concentration for Fe<sup>2+</sup>

**Table 8.10:** Computation of Elemental transformation rate for Fe<sup>3+</sup>

Sampling Event	Time [days]	MRC1 ORD C <sub>s</sub> <sub>i</sub> (mg/L)	mol/L or M	Volume left V <sub>total</sub> (L)	Sample volume V <sub>s</sub> (L)	C <sup>k</sup> *V <sub>total</sub> (mol)	C <sub>s</sub> *V <sub>s</sub> (mol)	n (moles)	μmol	μmol/kg
<i>n</i> <sup>1</sup>	<i>0</i>	0.30	5.37E-06	0.480	0.020	2.58E-06	1.07E-07	2.69E-06	2.69E+00	7.67
<i>n</i> <sup>2</sup>	<i>5</i>	2.17	3.89E-05	0.460	0.020	1.79E-05	7.77E-07	1.88E-05	1.88E+01	53.60
<i>n</i> <sup>3</sup>	<i>15</i>	9.23	1.65E-04	0.440	0.020	7.27E-05	3.31E-06	7.69E-05	7.69E+01	219.75
<i>n</i> <sup>4</sup>	<i>24</i>	9.68	1.73E-04	0.420	0.020	7.28E-05	3.47E-06	8.05E-05	8.05E+01	229.88
<i>n</i> <sup>5</sup>	<i>48</i>	9.37	1.68E-04	0.400	0.020	6.71E-05	3.35E-06	7.81E-05	7.81E+01	223.13
<i>n</i> <sup>6</sup>	<i>72</i>	10.57	1.89E-04	0.380	0.020	7.19E-05	3.79E-06	8.67E-05	8.67E+01	247.75
<i>n</i> <sup>7</sup>	<i>96</i>	10.01	1.79E-04	0.360	0.020	6.45E-05	3.59E-06	8.29E-05	8.29E+01	236.93
<i>n</i> <sup>8</sup>	<i>120</i>	10.88	1.95E-04	0.340	0.020	6.62E-05	3.90E-06	8.85E-05	8.85E+01	252.91

N.B: Table represent elemental transformation rate computed using Equation 8.8 from raw concentration for Fe<sup>3+</sup>

These results show the build-up of ferric iron following the oxidation of ferrous iron by *T.denitrificans*. This trend occurs in both SFF bioleaching oxidation experiments (MRC 2, 5 and 8) and the non-modified bioleaching oxidation experiments with no observable differences. Sterile controls which represent  $Fe^{2+}$  trends in the reactors MRC 3, 6 and 9 are also plotted to relatively minimal changes in concentrations. Ideally, it is expected that plots for sterile controls would remain constant during the sampling events however, slight increases and minimal decreases as observed in plots (Figure 8.9) might result from minimal errors during analytical determination.

### 8.5.2.3 Nitrate Reduction

According to Equations 8.4 and 8.5, the reduction of nitrate either to aqueous nitrite or gaseous nitrogen also provides evidence of the anaerobic nitrate dependent oxidation reaction. In results presented here (Figure 8.10A and B) and summarised in Tables 8.11-8.13, a gradual decline in Nitrate concentration while controls maintain a steady trend is observed.

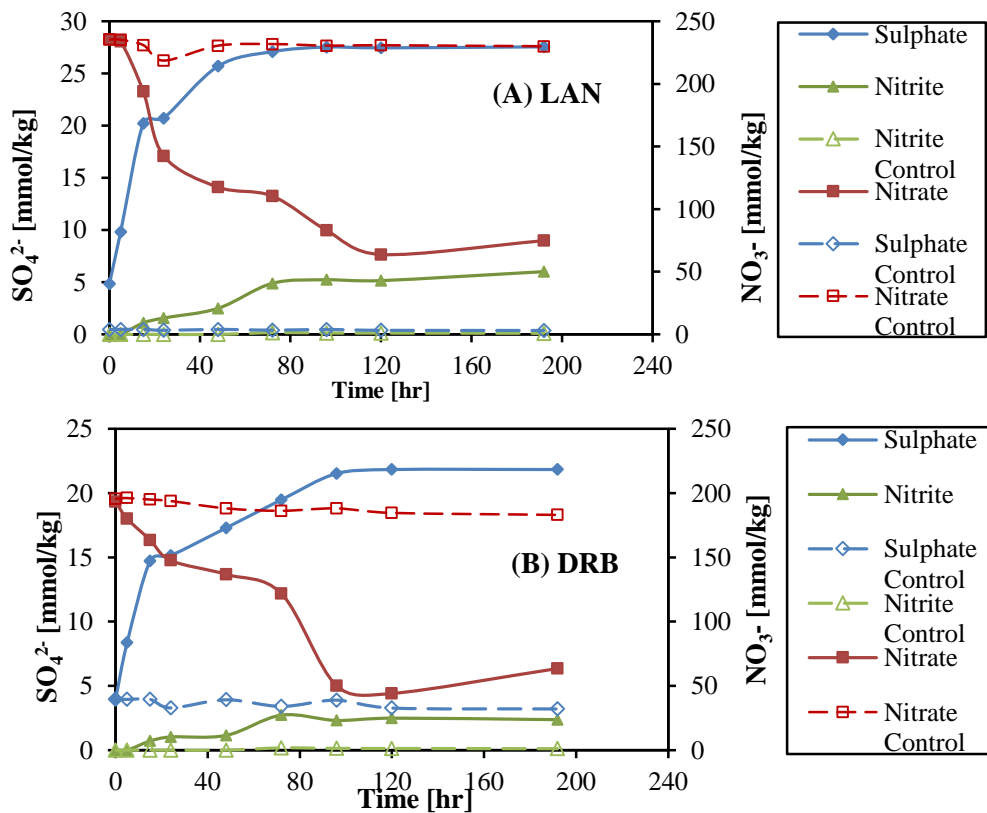


**Figure 8.11:** Sulphate ( $SO_4^{2-}$ ), Nitrate ( $NO_3^-$ ) and Nitrite ( $NO_2^-$ ) trends in reactors (A) MRC 1 (Bioleaching of LAN shale without SFF amendment) (B) MRC 5 (Bioleaching of LAN shale with SFF amendment) oxidation experiment.

**Table 8.11:** Computation of Elemental transformation rate Sulphate (SO<sub>4</sub><sup>2-</sup>) from raw concentration (ppm)

Sampling Event	Time [days]	MRC1 ORD C <sub>s</sub> <sub>i</sub> (mg/L)	mol/Lor M	Volume left V <sub>total</sub> (L)	Sample volume V <sub>s</sub> (L)	C <sup>k</sup> *V <sub>total</sub> (mol)	C <sub>s</sub> *V <sub>s</sub> (mol)	n (moles)	mmol/kg
<i>n</i> <sup>1</sup>	0	325.17	0.003	0.480	0.020	1.6E-03	6.8E-05	1.7E-03	4.84
<i>n</i> <sup>2</sup>	5	674.95	0.007	0.460	0.020	3.2E-03	1.4E-04	3.4E-03	9.83
<i>n</i> <sup>3</sup>	15	1435.08	0.015	0.440	0.020	6.6E-03	3.0E-04	7.1E-03	20.23
<i>n</i> <sup>4</sup>	24	1472.33	0.015	0.420	0.020	6.4E-03	3.1E-04	7.3E-03	20.72
<i>n</i> <sup>5</sup>	48	1870.52	0.019	0.400	0.020	7.8E-03	3.9E-04	9.0E-03	25.69
<i>n</i> <sup>6</sup>	72	1987.82	0.021	0.380	0.020	7.9E-03	4.1E-04	9.5E-03	27.09
<i>n</i> <sup>7</sup>	96	2026.60	0.021	0.360	0.020	7.6E-03	4.2E-04	9.6E-03	27.53
<i>n</i> <sup>8</sup>	120	2019.64	0.021	0.340	0.020	7.1E-03	4.2E-04	9.6E-03	27.45

**Table 8.12:** Computation of Elemental transformation rate Nitrate (NO<sub>3</sub><sup>-</sup>) from raw concentration (ppm)

Sampling Event	Time [days]	MRC1 ORD C <sub>s</sub> <sub>i</sub> (mg/L)	mol/L or M	Volume left V <sub>total</sub> (L)	Sample volume V <sub>s</sub> (L)	C <sup>k</sup> *V <sub>total</sub> (mol)	C <sub>s</sub> *V <sub>s</sub> (mol)	n (moles)	μmol
<i>n</i> <sup>1</sup>	0	10214.17	0.165	0.480	0.020	7.9E-02	3.3E-03	8.2E-02	235.35
<i>n</i> <sup>2</sup>	5	10143.90	0.164	0.460	0.020	7.5E-02	3.3E-03	8.2E-02	233.80
<i>n</i> <sup>3</sup>	15	8262.68	0.133	0.440	0.020	5.9E-02	2.7E-03	6.8E-02	193.92
<i>n</i> <sup>4</sup>	24	5724.65	0.092	0.420	0.020	3.9E-02	1.8E-03	5.0E-02	142.45
<i>n</i> <sup>6</sup>	72	4052.32	0.065	0.380	0.020	2.5E-02	1.3E-03	3.9E-02	110.44
<i>n</i> <sup>7</sup>	96	2488.28	0.040	0.360	0.020	1.4E-02	8.0E-04	2.9E-02	83.05
<i>n</i> <sup>8</sup>	120	1324.32	0.021	0.340	0.020	7.3E-03	4.3E-04	2.2E-02	63.74

**Table 8.13:** Computation of Elemental transformation rate Nitrite (NO<sub>2</sub><sup>-</sup>) from raw concentration (ppm)

Sampling Event	Time [days]	MRC1 ORD C <sub>s</sub> <sub>i</sub> (mg/L)	mol/L or M	Volume left V <sub>total</sub> (L)	Sample volume V <sub>s</sub> (L)	C <sup>k</sup> *V <sub>total</sub> (mol)	C <sub>s</sub> *V <sub>s</sub> (mol)	n (moles)	μmol
<i>n</i> <sup>1</sup>	0	ND	0.0E+00	0.480	0.020	0.0E+00	0.0E+00	0.0E+00	0.00
<i>n</i> <sup>2</sup>	5	ND	0.0E+00	0.460	0.020	0.0E+00	0.0E+00	0.0E+00	0.00
<i>n</i> <sup>3</sup>	15	38.65	8.4E-04	0.440	0.020	3.7E-04	1.7E-05	3.9E-04	1.10
<i>n</i> <sup>4</sup>	24	55.67	1.2E-03	0.420	0.020	5.1E-04	2.4E-05	5.5E-04	1.57
<i>n</i> <sup>6</sup>	72	187.63	4.1E-03	0.380	0.020	1.5E-03	8.2E-05	1.7E-03	4.89
<i>n</i> <sup>7</sup>	96	202.13	4.4E-03	0.360	0.020	1.6E-03	8.8E-05	1.8E-03	5.23
<i>n</i> <sup>8</sup>	120	198.50	4.3E-03	0.340	0.020	1.5E-03	8.6E-05	1.8E-03	5.15

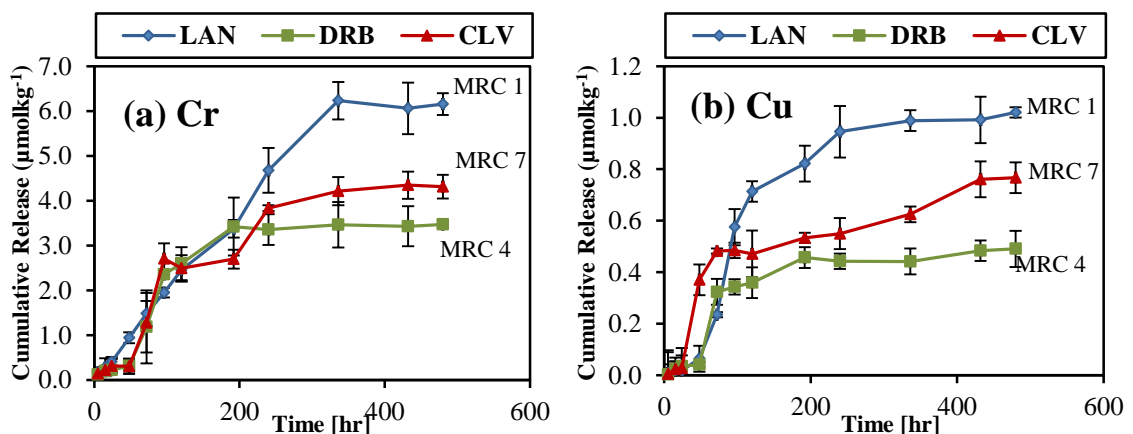
An increase in sulphate concentration (Table 8.11) can also be seen while sulphate control plots maintain a steady trend. The loss in sulphate observed in the sulphate control plots may be due to neutralisation by soluble calcite composition in the sterile control experiment. Very minimal nitrite is observed in the system (Table 8.13) which does not account entirely for the depleted nitrate however this was not further investigated as the possibility of complete reduction of nitrate is considered the case. Hence, two end products of the anaerobic nitrate dependent oxidation of pyrite expressed in Equations 8.4 and 8.5 have exhibited trends as expected from the denitrification reaction and this is sufficient proof required from the studies objectives.

### 8.5.3 Anaerobic Bio-mediated PTE Releases

In this section, results are presented and discussed on the influence of SFF amendment and non SFF amendments on the oxidation reaction. These reactors include the MRC 1 and 2 that contained black shale from the Bowland formation in Lancashire, reactors MRC 4 and 5 that contained black shales from the Edale shale formation in Derbyshire and reactors MRC 7 and 8 that contained black shale from the Whitbian Bituminous shale formation. Already results confirming the progression of a nitrate dependent oxidation reaction have been presented and at this stage the study proceeded to analyse the release of the investigated trace metals from each oxidation reactor.

#### 8.5.3.1 No SFF Amended Leachant

Released concentrations for most trace metals spiked within 24hr to 48hr hours following incubation and had achieved a steady release in most trace metals up to day 10 before a gradual decline in releases are observed.



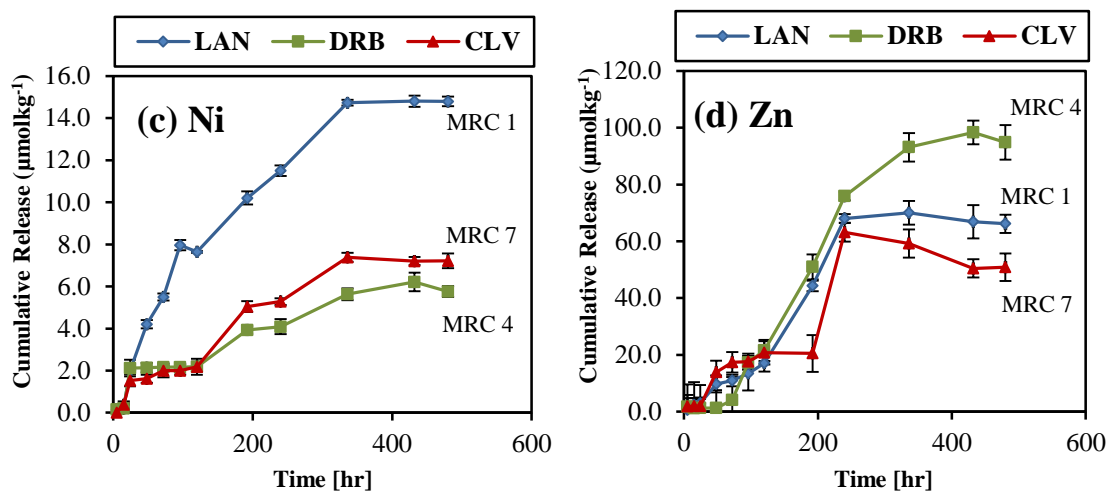


**Figure 8.12:** Release trends of investigated trace metals in the bio-mediated oxidation experiments with no introduction of SFF.

Zn attained the highest concentration with concentrations reaching  $66\mu\text{mol/kg}$ ,  $95\mu\text{mol/kg}$  and  $51\mu\text{mol/kg}$  in the Lancashire, Derbyshire and Whitby formations respectively (Figure 8.11a,b,c and d), and suggesting considerable releases of Zn from the studied formations under natural conditions of weathering mediated by microbes is a likely possibility. Cu releases are relatively minimal with tops of  $1.02\mu\text{mol/kg}$  (Figure 8.11b) observed in the Lancashire formation which had the highest Cu release. A general characteristic decline in release is observed around day 14 (day 10 for Cu) which coincides with the stationary phase reported from the plots of CFU (Figure 8.8) and as such suggest that *T.denitrificans* plays a pivotal part in the releases observed. With the exception Zn releases in the Derbyshire shale, the highest releases were observed in shale from the Lancashire formation.

### 8.5.3.2 With SFF Amended Leachant

Results presented here, discusses the observed release trend in experiments designed to investigate the influence of anoxic bio-mediated environments amended with SFF influence on PTE releases. At the onset of a confirmed anaerobic nitrate dependent pyrite oxidation, aliquots from the reactors were anaerobically withdrawn periodically and analysed for the studies investigated trace metals. Plotted results (Figure 8.12a-d) seem to show similar behaviour with non SFF amended releases (Figure 8.12a-d). The general trend shows the initial rise in concentrations followed by a decline in release till an almost stationary phase is observed.

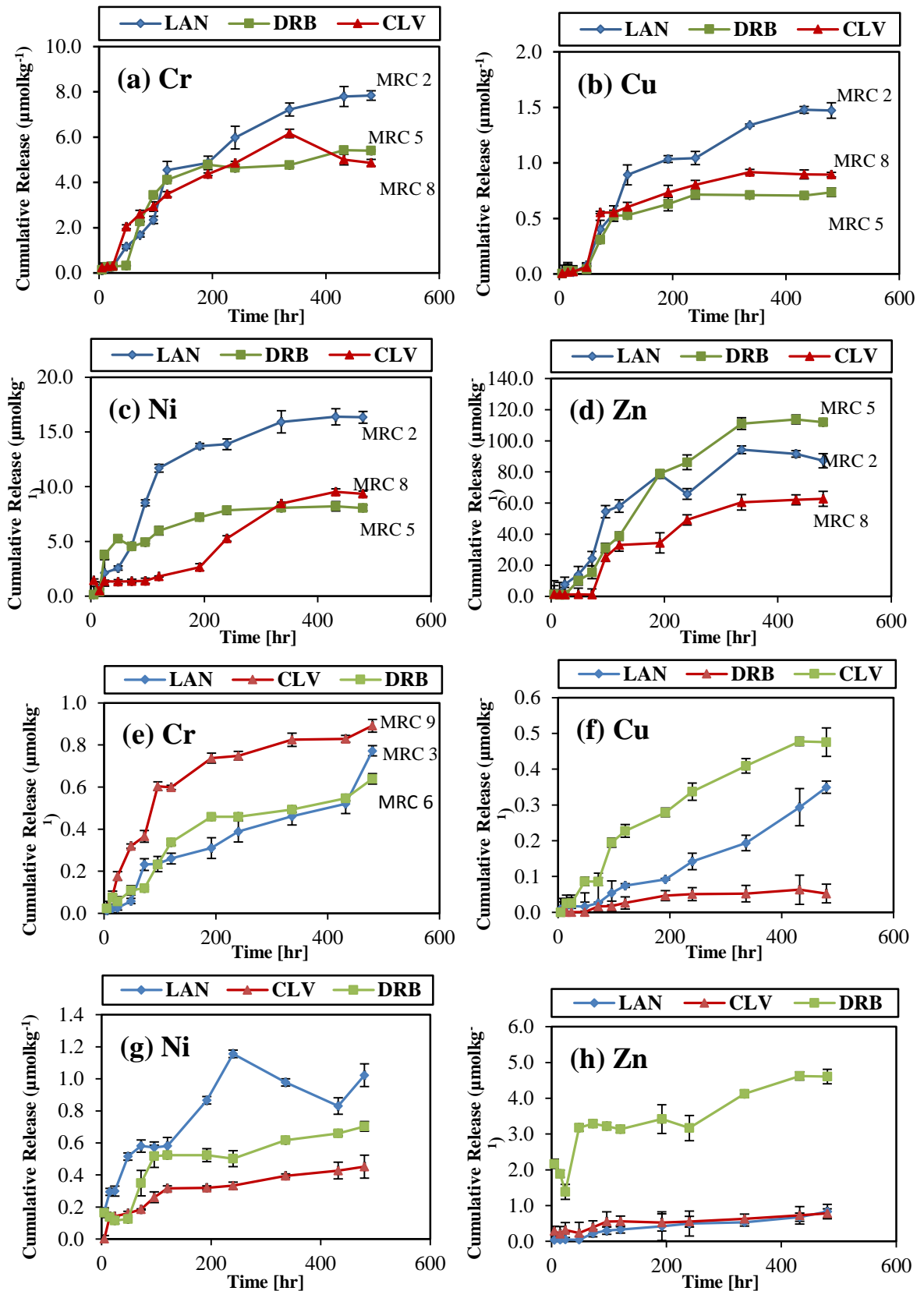


**Figure 8.13:** Release trends of investigated trace metals in the bio-mediated oxidation experiments with amended with SFF. Plots (a-d) represent bio-mediated oxidation results (e-h) represents non- bio-mediated oxidation results

#### **8.5.4 Anaerobic Non Bio-Mediated PTE Releases**

With non bio-mediated releases (Figure 8.12e-h) however, rates show an almost linear trend and in some cases clearly visible stationary phases. With the exception of Cr and Cu which show steady increases in releases (Figure 8.12e and f), other release plots depict fairly constant releases from day 8 (Figure 8.12g and h). These results suggest that the presence of both microbial populations in the reactors aids the accelerated release of trace metals from the sampled shales. However, when experiments are conducted to isolate influence of SFF without microbial mediation, minimal releases are observed. These are better illustrated in Figures 8.13a-c.

#### **8.5.5 Comparative Analysis of PTE Releases**

In this section, a comparative analysis between the solely chemically controlled batch oxidation experiments, the solely biologically controlled batch oxidation experiment and a combination of both chemical and biological controlled batch oxidation experiments is presented. The study was planned to evaluate the extent to which these simulated conditions controlled the release of the investigated heavy metals. A comparison of releases from the varying oxidation experiments is summaries in Figures 8.13. Results for Cr alone have been documented here as similar trend were observed for Cu, Ni and Zn releases. A computation of releases rates by linear regression is tabulated in Table 8.13. These results show that a solely chemically controlled oxidation produced substantially minimal impact on accelerating trace metal releases with rates ( $3.16\text{E-}06\text{mol/m}^2/\text{hr.}$ ,  $4.35\text{E-}06\text{mol/m}^2/\text{hr.}$  and  $1.86\text{E-}05\text{mol/m}^2/\text{hr.}$  in the Lancashire formation) at an order of a magnitude lower in comparison to both the biological ( $3.24\text{E-}05\text{mol/m}^2/\text{hr.}$ ,  $2.63\text{E-}05\text{mol/m}^2/\text{hr.}$  and  $1.08\text{E-}04\text{mol/m}^2/\text{hr.}$ ) and combined ( $4.09\text{E-}05\text{mol/m}^2/\text{hr.}$ ,  $3.96\text{E-}05\text{mol/m}^2/\text{hr.}$  and  $1.20\text{E-}04\text{mol/m}^2/\text{hr.}$ ) released rates. In the majority of plots (Figure 8.13a-f), a sharp rise in release rates are also observed within the first 100 hours which coincides with the log growth phase and a fall in pH show in Figure 8.8. The drop in pH was attributed to sulphate increase in the system as explained from Equation 8.4. Consequently, as cells proliferate, they oxidise more pyrite composition within the shale to sulphuric acid leading to a further drop in pH and this accounts for the sharp fall in pH observed. These results however, suggest that microbial presence plays a pivotal role in the

process as a solely biological controlled oxidation show a significant release rate closely related to the combined effect of both biological and chemical control

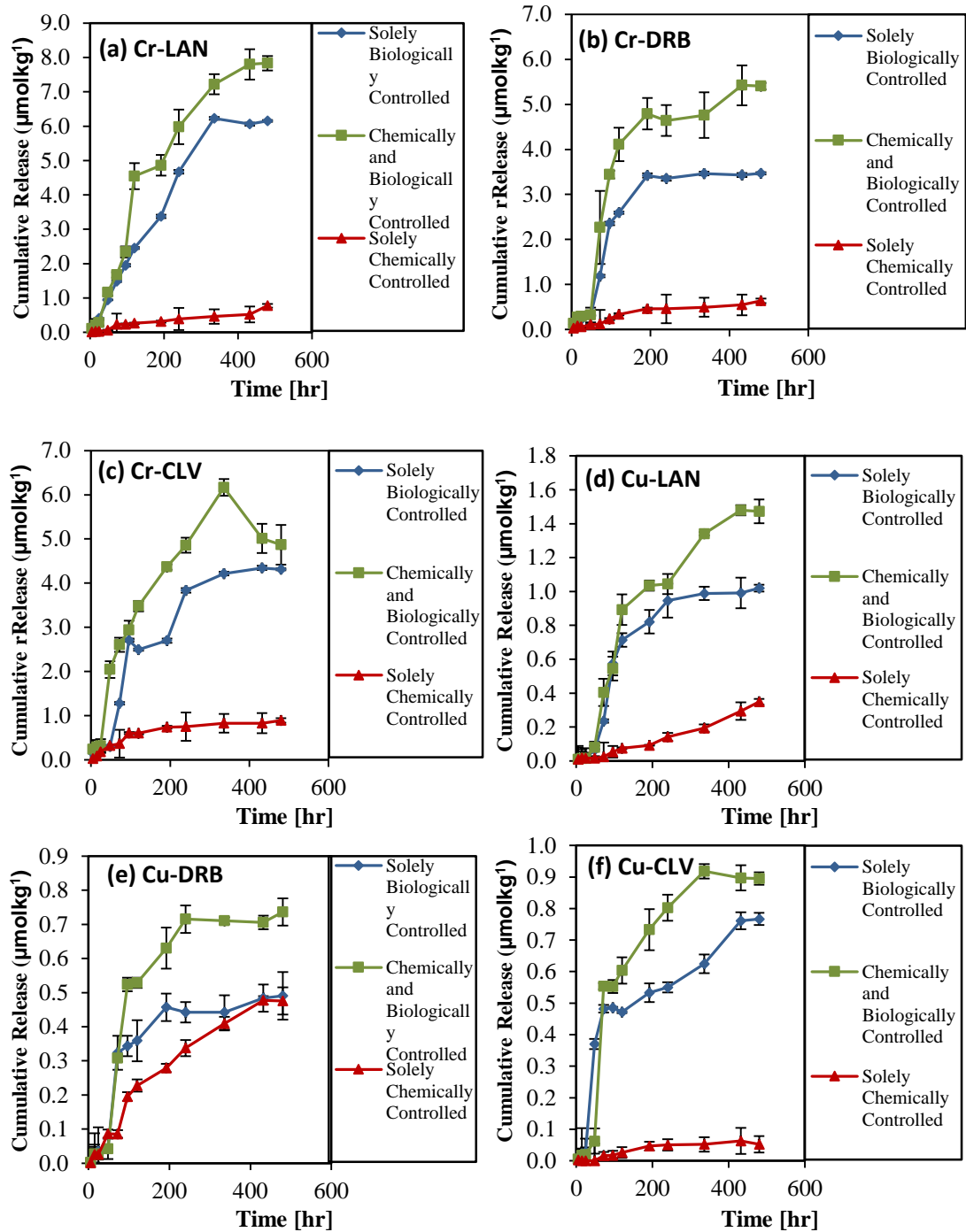


**Figure 8.14:** A comparison between results from varying simulated leaching configuration for releases of Cr from studies investigated shales.

Data on rates help to elucidate to a great detail the chemistry within the reactors. Rates in the biological and chemical controlled oxidation experiments are an order of magnitude higher than the chemically controlled oxidations rates, complimenting results obtained in Figure 8.14.

**Table 8.14:** Trace metal oxidation rates in ( $\text{mol m}^{-2} \text{hr}^{-1}$ ) computed from linear regression

Heavy Metals	MRC 1	MRC 2	MRC 3	MRC 4	MRC 6	MRC 7	MRC 8	MRC 9
<b>Cr</b> [ $\text{mol m}^{-2} \text{hr}^{-1}$ ]	3.24E-05	4.09E-05	3.16E-06	2.63E-05	4.35E-06	1.08E-04	1.20E-04	1.86E-05
<b>Cu</b> [ $\text{mol m}^{-2} \text{hr}^{-1}$ ]	2.46E-06	3.56E-06	7.36E-07	1.17E-06	1.23E-06	8.95E-06	1.25E-05	8.60E-07
<b>Ni</b> [ $\text{mol m}^{-2} \text{hr}^{-1}$ ]	3.25E-05	3.69E-05	1.64E-06	3.55E-05	3.52E-06	1.25E-04	1.59E-04	5.85E-06
<b>Zn</b> [ $\text{mol m}^{-2} \text{hr}^{-1}$ ]	1.32E-04	1.58E-04	1.26E-06	4.00E-04	8.80E-06	7.85E-04	9.66E-04	6.77E-06

To obtain a summarised and comparative view of releases from the leaching column results obtained in Chapter 5 and 6 and the microcosm leaching experiment obtained in this Chapter, a semi logarithm plot of these results is presented in Figure 8.14. Releases have been re-computed to show average daily releases as this provides a generalised basis for comparing all leaching experiments. These results provide a

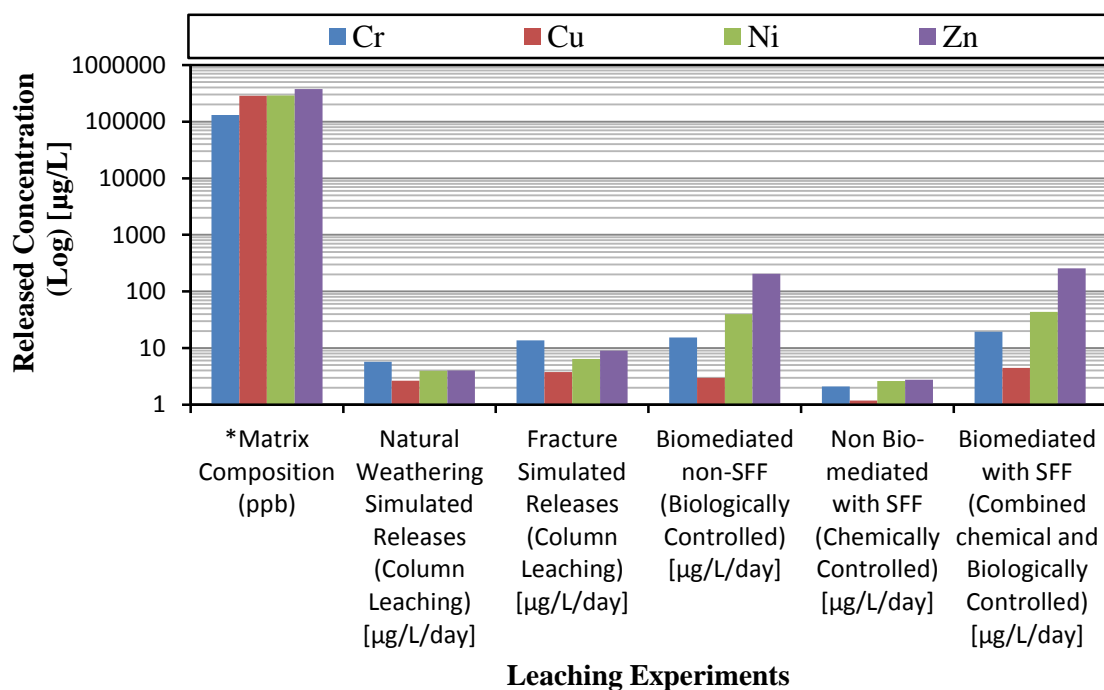


**Figure 8.15:** Semi Log plot comparing bulk matrix composition with average daily released concentrations from both leaching column and oxidation experiments

clearer view of the quantifiable releases in these leaching treatments and suggest that although these releases represent a fraction of the bulk compositions in sampled shales, bio-mediated releases and fracture simulated column releases show significant quantities in comparison to natural releases (simulated in the column experiments) and non-Bio-mediated release (solely chemically controlled oxidation). In the black shales sampled from the Trough of Bowland –Lancashire, characterisation by XRF analysis revealed a bulk composition estimated at 131mg/kg. Following a simulated natural weathering of this sampled shale over a 12 weeks accelerated leaching duration, 478.1µg/L an estimated 0.36% of bulk composition was released. A fractured simulated leaching over a similar 12 weeks leaching exercise, released 1153.8µg/L estimated at 0.88% of the bulk Cr composition in the sampled shale. Bio-mediated releases following a 20 day leaching experiment duration on the same shale released 0.23% in experiments conducted without SFF and 0.30% in experiments conducted in SFF. Similar trends are observed for all trace heavy metals investigated, bio-mediated Cu releases reported in the Lancashire shale are reported at 89.1µg/L (in SFF) and 59.5µg/L (non SFF) in comparison to 23.8µg/L released in the non-bio-mediated. Zn bio-mediated releases in the Whitbian bituminous shale are reported at 2.87% (in SFF) and 2.21% (non SFF) in comparison to the non-Bio-mediated (0.03%), natural weathering simulated (0.18%) and fracture simulated (0.19%) (Table 8.15). Ni bio-mediated releases in the Edale shale are reported at 0.42% (in SFF) and 0.33% (non SFF) in comparison to the non-bio-mediated (0.04%), natural weathering simulated (0.27%) and fracture simulated (0.22%) (Table 8.15).

With the aid of the microcosm experiment that allows the test of more operational and environmental conditions on these releases, these figures convincing show that operational condition during fracture such as the fracturing fluid composition as simulated in this study, environmental conditions such as microbial mediation, and anaerobic conditions do accelerate the release of the investigated trace metals. Mobilizations of these potentially toxic heavy metals from the sampled shales have been demonstrated here with the use of simulated fracturing condition in the laboratory using environmental samples from shale gas prospective formations in the UK. It is expected that wastewater and water industries in the UK will bear the brunt of this risk implications if offsite treatment methods are adopted.

**Table 8.15:** Comparative summary of bulk metal composition in sampled shales with cumulative releases from leaching column and microcosm oxidation experiments

Sampled Shale	Trace metals	<sup>1</sup> Matrix Composition (mg/kg)	<sup>2</sup> Natural Weathering Simulated Releases (Column Leaching) [µg/L]	<sup>3</sup> Fracture Simulated Releases (Column Leaching) [µg/L]	<sup>4</sup> Bio-mediated Non-SFF (Solely Biological) [µg/L]	<sup>5</sup> Non Bio-mediated with SFF (Solely Chemical) [µg/L]	<sup>6</sup> Bio-mediated with SFF (Combined Chemical and Biological) [µg/L]
<b>Lancashire (Carboniferous Bowland shale)</b>	<b>Cr</b>	131.0	478.1 (0.36%)	1153.8 (0.88%)	306.9 (0.23%)	42 (0.03%)	389.1 (0.3%)
	<b>Cu</b>	285.0	223.5 (0.08%)	314.7 (0.11%)	59.5 (0.02%)	23.8 (0.01%)	89.1 (0.03%)
	<b>Ni</b>	291.0	333.8 (0.11%)	537.5 (0.18%)	800.2 (0.27%)	52.2 (0.02%)	871.1 (0.3%)
	<b>Zn</b>	378.0	338.6 (0.09%)	753.2 (0.2%)	4096 (1.08%)	55.4 (0.01%)	5125.4 (1.36%)
<b>Edale shale basin (Peak district national park)</b>	<b>Cr</b>	83.0	338.9 (0.41%)	1022 (1.23%)	159.3 (0.19%)	32.2 (0.04%)	254.1 (0.31%)
	<b>Cu</b>	244.0	174.5 (0.07%)	330.4 (0.14%)	27.6 (0.01%)	29.1 (0.01%)	42 (0.02%)
	<b>Ni</b>	96.0	254.8 (0.27%)	207.9 (0.22%)	312 (0.33%)	34 (0.04%)	399.9 (0.42%)
	<b>Zn</b>	174.0	234.4 (0.13%)	256.5 (0.15%)	6115.4 (3.51%)	257.3 (0.15%)	7044.7 (4.05%)
<b>Whitby Bituminous Shale (Cleveland Basin)</b>	<b>Cr</b>	79.0	252.7 (0.32%)	577.8 (0.73%)	207 (0.26%)	41.6 (0.05%)	214.6 (0.27%)
	<b>Cu</b>	140.0	226.3 (0.16%)	177.7 (0.13%)	44.6 (0.03%)	3.02 (0.002%)	50.9 (0.04%)
	<b>Ni</b>	115.0	370 (0.32%)	438.2 (0.38%)	401.9 (0.35%)	24 (0.02%)	553.3 (0.48%)
	<b>Zn</b>	138.0	249.7 (0.18%)	263.2 (0.19%)	3043.1 (2.21%)	45.7 (0.03%)	3960.1 (2.87%)

N.B Equivalent percentages of the matrix composition are placed in parenthesis

<sup>1</sup> Bulk weighted concentrations (adopting Equation 5.3 in Chapter 5) computed from XRF analyses (refer to Table 4.7 in Chapter 4)

<sup>2</sup> Cumulative release concentrations from leaching column experiment reported in Chapter 5. Average daily (divided by duration of leaching) concentration is adopted to provide a basis for comparison with oxidation experiment)

<sup>3</sup> Cumulative release concentrations from leaching column experiment reported in Chapter 5. Average daily (divided by duration of leaching) concentration is adopted to provide a basis for comparison with oxidation experiment)

<sup>4</sup> Cumulative release concentrations from oxidation experiment investigating metal release without SFF and solely mediated by *T.denitrificans*

<sup>5</sup> Cumulative release concentrations from oxidation experiment investigating metal release in SFF without inoculation with *T.denitrificans*

<sup>6</sup> Cumulative released concentrations from oxidation experiment investigating metal release in SFF and mediated by *T.denitrificans*

## 8.6 Limitations of Experimental Study

It is important to highlight a few limitations of the experimental study presented here. The microcosm experiment attempts the simulation of field conditions but is limited in its capability to mimic all field conditions typical to the industrial extraction of shale gas. The study is limited in its use of one of many possible sulphur reducing bacteria for the simulation of contaminant release. Although there are evidences of other bacterial species in shale formations and their presence could play a vital role in contaminant mobility within the formation, only the impact of the anaerobes like *Thiobacillus denitrificans* have been assessed. The study regarded the effect of autoclaving the shale samples at 121°C, on degradation and enhanced weathering has negligible. All treatments and cultivation techniques used in ensuring bacteria survival have also been considered to have negligible effect contaminant mobility but necessary to achieve as replicable as possible, all field conditions.

## 8.7 Summary and Conclusion

The Chapter objective was to evaluate the effect of a solely biological controlled oxidation experiment, solely chemically controlled oxidation experiment and a combination of both oxidation types on trace metal release from the investigated shales. A series of oxidation experiment were conducted under anaerobic conditions to mimic first and foremost, the nitrate dependent oxidation of pyrite from the sampled shale, having ascertained and quantified sufficient compositions of pyrite in each shale matrix sampled for the study. Subsequently, the releases of the investigated trace metals were obtained and a comparative assessment of release quantification was present. The following summarises the conclusions from the investigative study;

1. The chemolithrophic bacterium, *Thiobacillus denitrificans* is capable of anaerobic nitrate dependent pyrite oxidation and if present during fracture conditions can play a role in heavy metal mobility during fluid rock interaction.
2. Mobilization and release of potentially toxic trace metals such as investigated in the study, is accelerated by operational fracturing conditions such as chemical use and environmental factors such as the anaerobic conditions and bacteria proliferation in fracture wells.

3. Data collected has shown that a significant immobilization of heavy metals can be achieved by the eradication of bacteria in fracture wells and during drilling operations.

## Chapter 9. Conclusion and Recommendations

This thesis investigated the possible risks of contaminant release from UK prospective shale gas formations by quantifying the release and mobilisation of toxic trace elements from the source rock, black shale. Potentially toxic heavy metals chromium, copper, nickel and zinc have been used as contaminant indicators and a quantifications of their releases following simulated hydraulic fracturing conditions and well downhole environmental conditions have been evaluated. Environmental samples used for the investigation were obtained from three UK prospective shale gas formations, the Carboniferous Bowland shale formation in Lancashire, the Edale shale basin in Derbyshire and the Whitbian bituminous shale formation. The study's aim was to ascertain if hydraulic fracture operations accelerated the release of toxic contaminants from the source rock and the scale of risk implications. The key conclusions from the study can be summarised as follows;

Characterisation study on these prospective formations revealed the potential for decomposition and ease of contaminant mobility following fluid rock interactions. Prospective UK shale gas formations have a characteristic fissile lithology and can be characterised as commonly laminated, sub fissile, very dark grey to black shale with most intercalated with calcareous sandstone and mudstones, and these lithological features suggest their decomposition ease. Mineralogically, all three shales are mainly composed of physiosilicates and silicate minerals, mostly quartz, kaolinite and fine grained micas. They are all commonly rich in pyrite and a host of trace heavy metals with some indicating the potential presence of naturally occurring radioactive materials. A quantification of trace metal populations reveal the presence of PTEs of notable toxicity such as Cr(131ppm), Cu(285ppm), Ni(291ppm) and Zn(378ppm), all in excess of reported world shale averages. An assessment of the acid generating potential predicted all three shales to be potentially acid generating following the standard modified ABA static test (Skousen et al. 1997, Haney et al. 2006) which report NPR values of 0.62 ( $\pm 0.16$ ), 0.76 ( $\pm 0.10$ ) and 0.87 ( $\pm 0.19$ ) for the Lancashire, Edale and Whitby black shales respectively. Sequential batch extractions revealed the increased mobility of trace heavy metals Cr, Ni and Zn with mobile fractions associated with the

water soluble, exchangeable and carbonate fractions accounting for larger than average 33%, 30.8% and 44.3% in the Lancashire, Edale and Whitby black shales respectively.

The laboratory simulation of both environmentally controlled natural weathering and fracture influenced releases of PTE in the studied shales suggests that non-anthropogenic influences alone are capable of releasing toxic concentrations of the investigated trace metals in all three studied black shales. Significantly higher released concentrations of monitored heavy metals were observed in the fractured simulated leaching kinetic experiment to suggest the increased risks from HDF influenced anthropogenic activities. A comparison of release rates and chemical fluxes suggest that fracturing the formation for gas has a significant ( $t_{LAN} = 5.05$ ,  $p < 0.001$ ), ( $t_{DRB} = 8.45$ ,  $p < 0.001$ ) and ( $t_{CLV} = 2.75$ ,  $p < 0.005$ ) effect on increasing the matrix surface area which in turn increases the tendency for mineral solubility and eventually an increase in the mobility of investigated traces in all three shales. The qualities of returning wastewater from the fracture formation is severely influenced by the mineralogy of the geological terrain and simulated fracture leaching experiments have shown that there is significant deterioration of the returning wastewater over time, a consequence of the changing acidic or alkaline conditions brought about by the interplay of acid forming and carbonate neutralising components in the shale. 5 year release predictions for both natural weathering and fracture simulated leaching releases produced most investigated traces well in excess of recommended EQS, WHO and EU standards and illustrates the scale of risk arising from fracture disturbances to these pre-historic formations.

An investigation into the release of PTE under prevailing environmental and operational conditions typical to fracturing shale gas wells accelerated the release of the investigated heavy metals. The chemolithrophic bacterium, *Thiobacillus denitrificans*, is capable of anaerobic nitrate dependent pyrite oxidation and if present during fracture conditions can play a role in heavy metal mobility during fluid rock interaction. Mobilization and release of potentially toxic trace metals such as investigated in the study, is accelerated by operational fracturing conditions such as chemical use and environmental factors such as the anaerobic conditions and bacteria proliferation in fracture wells. Data collected has shown that a significant

immobilization of heavy metals can be achieved by the eradication of bacteria in fracture wells and during drilling operations.

These findings suggest that significant risk of contaminant release is an eminent possibility from shale gas development activities. Returning flowback will contain potentially toxic contaminants, mostly inorganics. The threat of inorganic contamination to receiving treatment plants is well known. They are the most widely common threats to modern treatment works, as they require additional upgrades in methods of detection as well as treatments. NORMs are just examples of modern treatment concerns from inorganic contaminants for water and wastewater treatment facilities. This thesis has provided in quantitative terms the extent of releases expected. While it is clear that both the water and wastewater industries in the UK will bear the brunt of these risk implications if offsite treatment methods are adopted, the consequence to human and environmental health is too large to fathom and opens the investigation to further research work.

From this thesis, the following recommendation can be suggested for future work;

1. Three prospective UK formations have been investigated however, there are more prospective formations recently reported and similar risk identifications of their potential for contaminant release is as important.
2. The acquisition of direct flowback and produced water from currently fractured shale gas wells in the UK provide the greatest avenue to risk investigation. The recommendation is that a collaboration between drilling firms and academia be sought that provides access to sites for the purpose of conducting similar investigation, would be beneficial to the sustainability shale gas development in the UK.
3. This thesis has identified risks to water resources in the UK without addressing the mitigation or treatment needs involved. Future research should include in detail, the implications of identified risks to the water and wastewater industries in terms of cost and treatment needs. Obtaining access to site specific wastes would allow investigations into treatment needs that could reduce costs and promote sustainability.

4. A few environmental and operational factors that were realistic to the study based on time frame and facility availability have been investigated. Future research should look into investigating more site specific environmental and operational factors such as pressure application and temperature effects on releases and mobility.
5. A number of critical PTE, such as NORMs and hydrocarbon by-products common with oil and gas activities, have not been investigated in this thesis. Future research should look into incorporating a wide range of contaminants into the risk identification.

This thesis has adopted laboratory style simulations in assessing the potential risks due to the difficulty with gaining onsite access. A comprehensive risk investigation may need to consider onsite investigations. Where simulations have been adopted, results obtained are only as close to real life occurrences as the simulations allow.

## Reference

- Acharya, Henderson, C., Matis, H., Kommepalli, H., Moore, B. and Wang, H., (2011). *Cost Effective Recovery of Low-TDS Frac Flowback Water for Re-use*. New York: GE Global Research. Retrieved from: [http://www.gwpc.org/sites/default/files/event-sessions/3Acharya\\_Haris.pdf](http://www.gwpc.org/sites/default/files/event-sessions/3Acharya_Haris.pdf) [Accessed 2nd Feb 2012]
- Adriano, D.C., (2001). *Trace Elements in Terrestrial Environments: Biogeochemistry, Bioavailability, and Risks of Metals*. New-York, Springer-Verlag.
- Akabzaa, T.M., Armah, T.E.K. and Baneong-Yakubo, B.K., (2007). "Prediction of acid mine drainage generation potential in selected mines in the Ashanti Metallogenic Belt using static geochemical methods." *Environmental Geology*, **52**,(5): 957-964.
- Alexander, T., Baihly, J., Boyer, C., Clark, B., Waters, G., Jochen, V., Le Calvez, J., Lewis, R., Miller, C.K., Thaeler, J. and Toelle, B.E., (2011). "Shale gas revolution." *Schlumberger Oilfield Review*, **23**,(Autumn): 40–55.
- Andrews, I.J. (2013). *The Carboniferous Bowland Shale gas study: geology and resource estimation*. British Geological Survey for Department of Energy and Climate Change. Department of Energy and Climate Change. London, UK, DECC.
- APHA, (1998). *Standard methods for the determination of water and wastewater*. Washington, DC, American Public Health Association & Water Environmental Federation.
- Armstrong, J.P., Smith, J., D'Elia, V.A.A. and Trueblood, S.P. (1997). The occurrence and correlation of oils and Namurian source rocks in the Liverpool Bay–North Wales area. *Petroleum Geology of the Irish Sea and Adjacent Areas*. N.S. Meadows, S.P. Trueblood, M. Hardman and G. Cowan. London, Geological Society Special Publications, **124**: 195-211.
- Arthur, J.D., Langhus, B. and Alleman, D., (2008). *An overview of modern shale gas development in the United States*. New York: All Consulting. Retrieved from: <http://www.all-llc.com/publicdownloads/ALLShaleOverviewFINAL.pdf> [Accessed
- ATCC (2013). *Thiobacillus denitrificans (ATCC® 25259™)*. American Type Culture Collection.
- Audibert, A., Lecourtier, J. and Du Petrole, F., (1992). "Compatibility of Hydrosoluble Polymers With Corrodible Materials." *SPE Production Engineering*, **7**,(2): 193-198.
- Bank, T., Malizia, T. and Andresky, L. (2010). Uranium Geochemistry In the Marcellus shale: Effects on metal mobilization. GSA Annual Meeting, Colorado, The Geological Society of America.
- Bank, T.L. (2011). Trace metal chemistry and mobility in the Marcellus shale. Technical Workshops for the Hydraulic Fracturing Study, U.S.

Barwise, A.J.G., (1990). "Role of nickel and vanadium in petroleum classification." *Energy Fuels*, **4**: 647-652.

Basu, S. (2011). A Review of the Chemical Characteristics of Frac/Flowback/Produced Water. AAEE/NJWEA Industrial Waste Preconference Workshop, Atlantic City, NJ, AECOM.

Beller, H.R., (2005). "Anaerobic, Nitrate-Dependent Oxidation of U(IV) Oxide Minerals by the Chemolithoautotrophic Bacterium *Thiobacillus denitrificans*." *Appl. Environ. Microbiol.*, **71**,(4): 2170-2174.

Beller, H.R., P., Z., Legler, T.C., Chakicherla, A., Kane, S., Letain, T.E. and O'Day, P.A., (2013). "Genome-enabled studies of anaerobic, nitrate-dependent iron oxidation in the chemolithoautotrophic bacterium *Thiobacillus denitrificans*." *Frontiers in Microbiology* **4**: 249., **4**: 249.

Berrow, M.L. and Stein, W.M., (1983). "Extraction of metals from soils and sewage by refluxing with aqua regia." *Analyst*, **108**: 277-285.

Beveridge, T.J. and Doyle, R.J., (1989). *Metal Ions and Bacteria*. New York, Wiley.

Bhattacharya, S. and Parkin, G.F. (1988). Modelling toxicity kinetics in complete-mix anaerobic systems. Proc. Joint CSCE-ASCE Natl Conf. Envir. Eng., University of British Columbia, Vancouver.

Blauch, M.E., Myers, R.R., Moore, T.R., Lipinski, B.A. and Houston, N.A. (2009). Marcellus Shale Post-Frac Flowback Waters: Where is All the Salt Coming from and What are the Implications? SPE Eastern Regional Meeting, Society of Petroleum Engineers

Bosch, J., Heister, K., Hofmann, T. and Meckenstock, R.U., (2010). "Nanosized iron oxides collides strongly enhances microbial iron reduction." *Appl. Environ. Microbiol.*, **76**,(1): 184-189.

Bosch, J., Lee, K., Jordan, G., Kim, K. and Meckenstock, R.U., ( 2012 ). "Anaerobic, Nitrate-Dependent Oxidation of Pyrite Nanoparticles by *Thiobacillus denitrificans*." *Environ. Sci. Technol.*, **46**: 2095–2101.

Bowens, S. (2014). Consultation on Rathlin Energy West Newton Site-Environment Agency's consultation on EPR/BB3001FT/A001 and EPR/PB3030DJ/A001. Environment Agency:Permitting & Support Centre. UK, Friends of the Earth.

Brown, L. and Rhead, M.M., (1979). "Liquid chromatographic determination of acrylamide monomer in natural and polluted aqueous environments." *Analyst*, **104**: 391-399.

Bruner, K.R. and Smosna, R. (2011). A comparative study of the Mississippian Barnett shale, Fort Worth Basin, and Devonian Marcellus shale, Appalachian Basin. U.S Department of Energy. U.S, NETL.

Bull, R.J., Robinson, M., Laurie, R.D., Stoner, G.D., Greisiger, E., Meier, J.R.J. and Stober, J., (1984). "Carcinogenic effects of acrylamide in Sencar and A/J mice. ." *Cancer Research*, **44**: 107-111.

Calvert, S.E. and Pedersen, T.F., (1993). "Geochemistry of Recent oxic and anoxic marine sediments: Implications for the geological record." *Marine Geology*, **113**: 67-88.

Caruccio, F. and Geidel, G. (1978). Geochemical factors affecting coal mine drainage quality. Reclamation of Drastically Disturbed Lands. American Society of Agronomy. Madison, WI.: 129-148.

Caruccio, F.T. and Geidel, G. (1986). An evaluation of mine waste - overburden analytical techniques. National Symposium on Mining, Hydrology, Sedimentology, and Reclamation, Lexington, Kentucky, University of Kentucky.

Chen, Y., Cheng, J.J. and Creamer, K.S., (2008). "Inhibition of anaerobic digestion process: A review." *Bioresource Technology*, **99**,(10): 4044–4064.

Chichester, D.L. and Landsberger, S., (1996). "Determination of the Leaching Dynamics of Metals from Municipal Solid Waste Incinerator Fly Ash Using a Column Test." *Journal of the Air & Waste Management Association*, **46**,(7): 643-649.

CIEH, (2012). *CIEH Briefing Note-Hydraulic Fracturing: Impacts on the environment and human health* CIEH Northern Ireland. Retrieved from: <http://www.cieh.org/assets/0/72/1126/1212/1216/1218/08316171-c668-41d1-8d85-8af09f3d2193.pdf> [Accessed 22nd Feb 2012]

Claus, G. and Kutzner, H.J., (1985). "Physiology and kinetics of autotrophic denitrification by *Thiobacillus denitrificans* " *Appl. Microbiol. Biotechnol.*, **22**: 283-288.

Considine, T., Watson, R., Considine, N. and Martin, J. (2012). Environmental Impacts during Marcellus Shale Gas Drilling: Causes, Impacts, and Remedies Shale Resources and Society Institute.

Consulting Regeneris, (2011). *Economic Impact of Shale Gas Exploration & Production in Lancashire and the UK*. Cheshire, UK: Cuadrilla Resources. Retrieved [Accessed 2nd Nov 2011]

Cuadrilla Resources (2011). Shale Gas Parliamentary Inquiry: Written Evidence from Cuadrilla Resources Holdings Limited Energy and Climate Change Committee. UK, Cuadrilla Resources Holdings Limited,.

Cuadrilla Resources (2012). "Composition of components in Bowland shale hydraulic fracturing fluid for Preese Hall-1 well." Retrieved 14th April 2012, from <http://www.cuadrillaresources.com/wp-content/uploads/2012/02/Chemical-Disclosure-PH-1.jpg>.

DECC (2010). Strategic Environmental Assessment for Further Onshore Oil & Gas Licensing Department of Energy and Climate Change. London, AMEC Environment & Infrastructure UK Limited.

DECC, (2011). *The Unconventional Hydrocarbon Resources of Britain's Onshore Basins - Shale Gas*. United Kingdom: Department of Energy and Climate Change. Retrieved [Accessed 2nd Nov 2011]

DECC (2014). Energy Consumption in the UK (2014). Department of Energy & Climate Change. London, DECC.

DTI (2003). Energy White Paper: Our energy future creating a low carbon economy. Department for Transport. London, The stationary office (TSO).

Dunham, K.C., (1961). "Black shale, oil and sulphide ore." *The Advancement of Science*, **18**,(73): 284-299.

EA (2004). The determination of acrylamide in waters using chromatography with mass spectrometric detection- Methods for the examination of Waters and Associated Materials. Environment Agency. United Kingdom, Environment Agency: 1-14.

EA (2011). Environment Agency: H1 Annex D-Basic Surface water discharges Appendix A – Environmental Quality Standards. UK, Environment Agency.

EA (2012). "Exploratory drilling in Lancashire." Retrieved 2nd May 2012, 2012, from <http://ea-transactions.gov.uk/business/topics/134511.aspx>.

Ebukanson, E.J. and Kinghorn, R.R.F., (1986). "Oil and gas accumulations and their possible source rocks in southern England." *Journal of Petroleum Geology*, **9**,(4): 413-428.

EIA, (2011). *World Shale Gas Resources: An Initial Assessment of 14 Regions Outside the United States* U.S. Department of Energy. Retrieved from: <http://eia.gov/analysis/studies/worldshalegas/pdf/fullreport.pdf> [Accessed 2nd September 2011]

El Kammar, A.M. and El Kammar, M.M., (1996). "Potentiality of chemical weathering under arid conditions of black shales from Egypt." *Journal of Arid Environments*, **33**,(2): 179-199.

Elliott, A.S., Suri, N.K., An, D., Voordouw, G., Kaert, K. and Langille, D.L. (2014). Analysis of Microbes in Hydraulic Fracturing of Montney Tight Gas Formations in

Western Canada. SPE/CSUR Unconventional Resources Conference. Canada, Society of Petroleum Engineers.

Environment Agency (2006). The state of groundwater in England and Wales UK, Environment Agency, : 11.

Environment Agency (2009a). Soil Guideline Values for nickel in soil. Science Report SC050021 / Nickel SGV. I. Martin, H. Morgan, C. Jones, E. Waterfall and J. Jeffries.

Environment Agency, (2009b). *Water for People and the Environment: Water Resources Strategy for England and Wales*. UK. Retrieved from: <http://webarchive.nationalarchives.gov.uk/20140328084622/http://cdn.environment-agency.gov.uk/geho0309bpx-e-e.pdf> [Accessed December 2011]

EPA, (2011). *Draft plan to study the potential impacts of hydraulic fracturing on drinking water resources*. Washington, D.C. Retrieved from: <http://o.aolcdn.com/os/industry/energy/photos/EPA-Hydraulic-Fracturing-Draft-Plan.pdf> [Accessed 2nd Nov 2011]

Ethridge, E.C., Clark, D.E. and Hench, L.L., (1979). *J. Phys. Chem.*, **25**,(2): 35.

Ewbank, G., Manning, D.A.C. and Abbott, G.D., (1993). "An organic geochemical study of bitumens and their potential source rocks from the South Pennine Orefield, central England." *Organic Geochemistry*, **20**,(5): 579-598.

Falk, H., Lavergren, U. and Bergbäck, B., (2006). "Metal mobility in alum shale from Öland, Sweden." *Journal of Geochemical Exploration*, **90**,(3): 157-165.

Ferguson, M.L. and Johnson, M.A., (2009). "Comparing Friction Reducers' Performance in Produced Water from Tight Gas Shales." *Journal of Petroleum Technology*.

Filgueiras, A.V., Lavilla, I. and Bendicho, C., (2002). "Chemical sequential extraction for metal partitioning in environmental solid samples." *Journal of Environmental Monitoring*, **4**: 823-857.

Fisher, Q.J., Raiswell, R. and Marshall, J.D., (1998). "Siderite Concretions from Nonmarine Shales (Westphalian A) of the Pennines, England: Controls on Their Growth and Composition." *Journal of Sedimentary Research*, **68**,(5): 1034-1045.

Forstner, U. (1987). *Metal speciation in solid wastes: Factors affecting mobility. Speciation of metals in water, sediment, and soil systems*. S. Bhattacharji and L. Landner, Springer-Verlag, Berlin: 237-256.

Friedman, M., (2003). "Chemistry, Biochemistry, and Safety of Acrylamide. A Review." *Journal of Agricultural and food chemistry*, **51** 4504–4526.

Frostad, S., Klein, B. and Lawrence, R.W., (2002). "Evaluation of Laboratory Kinetic Test Methods for Measuring Rates of Weathering." *Mine Water and the Environment*, **21**,(4): 183-192.

FSA (2012). "Current EU approved additives ". Retrieved 2nd February, 2011, from <http://www.food.gov.uk/science/additives/enumberlist#.U9EBjPldV8E>.

Fu, X., Wang, J., Zeng, Y., Cheng, J. and Tano, F., (2011). "Origin and mode of occurrence of trace elements in marine oil shale from the Shengli River Area, Northern Tibet, China." *Oil Shale*, **28**: 487-506.

Gad, M.A., Catt, J.A. and Le Riche, H.H. (1968). Geochemistry of the Whitbian (Upper Lias) sediments of the Yorkshire coast. Proceedings of the Yorkshire Geological Society, Hull, UK, Yorkshire Geological Society.

Gadd, G.M., (2004). "Microbial influence on metal mobility and application for bioremediation." *Geoderma*, **122**: 109 - 119.

Galarraga, F., Reategui, K., Martínez, A., Martínez, M., Llamas, J.F. and Márquez, G., (2008). "V/Ni ratio as a parameter in palaeoenvironmental characterisation of non mature medium-crude oils from several Latin American basins." *J. Petrol. Sci. Eng.*,(61): 9-14.

Goldschmidt, V.M., (1958). V.M. Goldschmidt, Oxford University Press.

Green, C.A., Styles, P. and Baptie, B.J., (2011). *Preese Hall Shale Gas Fracturing Review and Recommendations for Induced Seismic Mitigation* DECC. Retrieved from: <http://og.decc.gov.uk/assets/og/ep/onshore/5075-preese-hall-shale-gas-fracturing-review.pdf> [Accessed

Halliburton, (2008). *U.S. Shale Gas: An Unconventional Resource. Unconventional Challenges (white paper)*. Retrieved from: [http://www.halliburton.com/public/solutions/contents/shale/related\\_docs/H063771.pdf](http://www.halliburton.com/public/solutions/contents/shale/related_docs/H063771.pdf) [Accessed 12th Feb 2012]

Haney, E.B., Haney, R.L., Hossner, L.R. and White, G.N., (2006). "Neutralization potential determination of siderite (FeCO<sub>3</sub>) using selected oxidants." *J. Environ. Qual.*, **35**,(3): 871-879.

Hayes, T., (2009). *Sampling and analysis of water stream associated with the development of Marcellus shale gas* Illinois, United States: Marcellus Shale Coalition. Retrieved from: [http://catskillcitizens.org/learnmore/20100916IOGAResponsetoDECChesapeake\\_IOGAResponsetoDEC.pdf](http://catskillcitizens.org/learnmore/20100916IOGAResponsetoDECChesapeake_IOGAResponsetoDEC.pdf) [Accessed 22nd Feb 2012]

Hayes, T., (2011). *Characterization of Marcellus Shale and Barnett Shale Flowback Waters and Technology Development for Water Reuse*. Retrieved from:

[http://www.epa.gov/hfstudy/12\\_Hayes - Marcellus Flowback Reuse 508.pdf](http://www.epa.gov/hfstudy/12_Hayes_-_Marcellus_Flowback_Reuse_508.pdf)  
[Accessed 2nd Feb 2012]

Hayes, T. and Severin, B.F., (2012). *Barnett and Appalachian shale water management and reuse technologies*. U.S: Research Partnership to Secure Energy for America. Retrieved from: <http://www.netl.doe.gov/technologies/oil-gas/publications/EPact/08122-05-final-report.pdf> [Accessed 1st Sept 2012]

Hillier, S., (2006). "Appendix A. Mineralogical and chemical data." *Geological Society of London*, **21**: 449-459.

Hlavay, J., Prohaska, T., Weisz, M., Wenzel, W.W. and Stinger, G.J., (2004). "Determination of Trace Elements Bound to Soils and Sediment Fractions." *Pure Appl. Chem.*, **76**,(2): 415-442.

Hochella, M.F., Lower, S.K., Maurice, P.A., Penn, R.L., Sahai, N., Sparks, D.L. and Twining, B.S., (2008). "Nanominerals, mineral nanoparticles, and earth systems " *Science of the Total Environment*, **319**,(5870): 1631-1635.

Hodson, M.E., (2002). "Siegel, F.R. Environmental Geochemistry of Potentially Toxic Metals.: Berlin (Springer), 2002, 218 pp. Hardback £35. ISBN 3 540 42030 4." *Mineralogical Magazine*, **66**,(4): 622-623.

Horan, M.F., Morgan, J.W., Grauch, R.L., Coveney, R.M., Murowchick, J.B. and Hulbert, L.J., (1994). "Rhenium and osmium isotopes in black shales and Ni-Mo-PEG-rich sulfide layers, Yukon Territory, Canada, and Hunan and Guizhou province, China." *Geochimica et Cosmochimica Acta.*, **58**: 257-265.

Hornberger, R.J., Brady, K.B., Cuddeback, J.E., White, W.B., Scheetz, B.E., Telliard, W.A., Parsons, S.C., Loop, C.M., Bergstresser, T. and McCracken, C. (2004a). Refinement of ADTI-WP2 standard weathering procedures, and evaluation of particle size and surface area effects upon leaching rates: Part 1: Laboratory evaluation of method performance. Proceedings of 2004 National Meeting of the American Society for Mining and Reclamation and the.

Hornberger, R.J., Brady, K.B., Scheetz, B.E., White, W.B. and Parsons, S.C. (2005 ). ADTI-WP2 Leaching Column Method for Overburden Analysis and Prediction of Weathering Rates. Proceedings of 26th West Virginia Surface Mine Drainage Task Force Symposium, Morgantown, WV.

Hornberger, R.J. and Brady, K.B.C., (2009). *Development and Interpretation of the ADTI-WP2 Leaching Column Method*. Washington D.C. Retrieved [Accessed 1st October 2012]

Hornberger, R.J., Brady, K.B.C., Cuddeback, J.E., White, W.B., Scheetz, B.E., Telliard, W.A., Parsons, S.C., Loop, C.M., Bergstresser, T.W., McCracken Jr., C.R. and Wood, D. (2004b). Refinement of ADTI-WP2 Standard Weathering Procedures, and Evaluation of Particle Size and Surface Area Effects upon Leaching Rates: Part 1:

Laboratory Evaluation of Method Performance. Proceedings of 2004 National Meeting of the American Society for Mining and Reclamation and the 25th West Virginia Surface Mine Drainage Task Force, Lexington, KY, ASMR.

iGas (2012). "Results presentation and shale update [online presentation]." Retrieved 1st September 2013, from [www.igasplc.com/uploads/analystpresentationjune2012final.pdf](http://www.igasplc.com/uploads/analystpresentationjune2012final.pdf)

IOD, (2013). *Infrastructure for Business: Getting shale gas working*. UK. Retrieved from: <http://www.iod.com/influencing/policy-papers/infrastructure/infrastructure-for-business-getting-shale-gas-working> [Accessed 2nd February 2014]

Jared, W.L., Stewart, D.I., Duxbury, J.R. and Richard, J.S., (1999). "Toxic metal mobility and retention at industrially contaminated sites." *Geological Society Special Publications*, **157**: 241-264.

Jeng, A.S., (1991). "Weathering of some Norwegian alum shales: I. Laboratory simulations to study acid generation and the release of sulphate and metal cations (Ca, Mg & K)." *Acta Agriculturae Scandinavica, Section B - Soil & Plant Science*, **41**: 13-35.

Jones, D.G. and Plant, J.A., (1989). "Metallogenic models and exploration criteria for buried carbonate-hosted ore deposits – a multidisciplinary study in eastern England." 65-94.

Jorgensen, C.J., Jacobsen, O.S., Elberling, B. and Aamand, J., (2009). "Microbial Oxidation of Pyrite Coupled to Nitrate Reduction in Anoxic Groundwater Sediment." *Environ. Sci. Technol.*, **43**,(13): 4851–4857.

Josh, M., Esteban, L., Delle Piane, C., Sarout, J., Dewhurst, D.N. and Clennell, M.B., (2012). "Laboratory characterisation of shale properties." *Journal of Petroleum Science and Engineering*, **88–89**,(0): 107-124.

Kaufman, P., Penny, G.S. and Paktinat, J. (2008). Critical Evaluation of Additives Used in Shale Slickwater Fracs. SPE Shale Gas Production Conference. Fort Worth, Texas U.S.A, Society of Petroleum Engineers.

Kelley, K.D. and Taylor, C.D., (1997). "Environmental geochemistry of shale-hosted AgPbZn massive sulfide deposits in northwest Alaska: natural background concentrations of metals in water from mineralized areas." *Applied Geochemistry*, **12**,(4): 397-409.

Krauskopf, K.B. and Bateman, A.M., (1955). "Sedimentary deposits of rare metals: in Economic Geology." *Econ. Geol.*, **50th Anniversary Volume**: 411-463.

Langmuir, D., (1997). *Aqueous Environmental Geochemistry*. New Jersey, Prentice-Hall.

Lavergren, U., Åström, M.E., Bergbäck, B. and Holmström, H., (2009a). "Mobility of trace elements in black shale assessed by leaching tests and sequential chemical extraction." *Geochemistry: Exploration, Environment, Analysis*, **9**,(1): 71-79.

Lavergren, U., Åström, M.E., Falk, H. and Bergbäck, B., (2009b). "Metal dispersion in groundwater in an area with natural and processed black shale - Nationwide perspective and comparison with acid sulfate soils." *Applied Geochemistry*, **24**,(3): 359-369.

Lawrence, R.W. and Wang, Y. (1997). Determination of Neutralization Potential in the Prediction of Acid Rock Drainage. Proceedings of 4th International Conference on Acid Rock Drainage Vancouver, BC.

Lee, J., Chon, H.-T. and Kim, K.-W., (1998). "Migration and dispersion of trace elements in the rock-soil-plant system in areas underlain by black shales and slates of the Okchon Zone, Korea." *Journal of Geochemical Exploration*, **65**: 61-78.

Leggett, J.K., (1980). "British Lower Palaeozoic black shales and their palaeo-oceanographic significance." *Journal of the Geological Society*, **2**: 139-156.

Leung, W.M., Axelson, D.E. and Van Dyke, J.D., (1987). "Thermal degradation of polyacrylamide and poly(acrylamide-co-acrylate)." *Polymer Science*, **25**,(7): 1825-1846.

Li, Y.-H. and Schoonmaker, J.E. (2005a). Chemical composition and mineralogy of marine sediments. *Sediments, Diagenesis, and Sedimentary Rocks*. F.T. Mackenzie, Treatise on Geochemistry, Holland, H.D., Turekian, K.K., Executive Directors. **7**: 1-35.

Li, Y.H. and Schoonmaker, J.E. (2005b). Chemical composition and mineralogy of marine sediments. *Sediment, Diagenesis and Sedimentary Rocks*. F.T. Mackenzie. Oxford, Elsevier-Pergamon. **7**: 1-35.

Lieber, M.A., (1991). "Final Report on the Safety Assessment of Polyacrylamide." *International Journal of Toxicology*, **10**: 193-203.

Lin, C., (2002). "The chemical transformations of chromium in natural waters - a model study." *Water, Air, and Soil Pollution*, **139**: 137-158.

Lopez, P., Navarro, E., Marce, R., Ordoñez, J., Caputo, L. and Armengol, J., (2006). "Elemental ratios in sediments as indicators of ecological processes in Spanish reservoirs." *Limnetica*, **25**,(1-2): 499-512.

Loukola-Ruskeeniemi, K., Uutela, A., Tenhola, M. and Paukola, T., (1998). "Environmental impact of metalliferous black shales at Talvivaara in Finland, with

indication of lake acidification 9000 years ago." *Journal of Geochemical Exploration*, **64**,(1-3).

Lovley, D.R. and Coates, J.D., (1997). "Bioremediation of metal contamination." *Curr. Opin. Biotechnol.*, **8**: 285 - 289.

Macaskie, L.E. and Dean, A.C.R. (1989). Microbial metabolism, desolubilization and deposition of heavy metals: uptake by immobilized cells and application to the treatment of liquid wastes. *Biological Waste Treatment*. A. Mizrahi. New York, Alan R. Liss: 150 - 201.

Mair, R., Bickle, M., Roberts, J., Goodman, D., Selley, R., Shipton, Z., Thomas, H. and Younger, P., (2012). *Shale Gas Extraction in the UK: A Review of Hydraulic Fracturing*. London. Retrieved from: <http://eprints.gla.ac.uk/69554/1/PY-Shale-gas-2012-06-28-.pdf> [Accessed 12th Dec 2012]

Marshall, J., (2014). *Water UK response to the DCLG Consultation on statutory consultee arrangements in the planning process*. London, UK. Retrieved from: <https://dl.dropboxusercontent.com/u/299993612/Publications/Policy%20positions%20%2B%20briefings/Shale%20gas%20fracking/Water%20Uk%20Response%20to%20DCLG%20planning%20consultation%20Dec%202014.pdf> [Accessed Jan 2014]

Matamoros-Veloza, A., Newton, R.J. and Benning, L.G., (2011). "What controls selenium release during shale weathering." *Applied Geochemistry*, **26**: 222-226.

Maynard, J.R., Wignall, P.B. and Varker, W.G., (1991). "A hot new shale facies from the Upper Carboniferous of Northern England." *Journal of the Geological Society*, **148**: 805-808.

McGraw, S. (2011). *Pennsylvania Fracking Accident: What Went Wrong*. Popular Mechanic. U.S., Hearst Magazines Division.

McLean, J.S., Lee, J.U.-. and Beveridge, T.J. (2002). Interactions of bacteria and environmental metals, fine-grained mineral development, and bioremediation strategies. *Interactions Between Soil Particles and Microorganisms*. P.M. Huang, J.-M. Bollag and N. Senesi. New York, Wiley: 227 - 261.

Mohialdeen, M.J. and Raza, S.M., (2013). "Inorganic geochemical evidence for the depositional facies associations of the Upper Jurassic Chia Gara Formation in NE Iraq." *Arab. J. Geosci.*, **6**: 4755-4770.

Moore, V., Beresford, A. and Gove, B., (2014). *Hydraulic fracturing for shale gas in the UK: Examining the evidence for potential environmental impacts*. Bedfordshire, UK. Retrieved from: [rspb.org.uk/fracking](http://rspb.org.uk/fracking) [Accessed 2nd December 2014]

Mor, S., Ravindra, K., Dahiyaa, R.P. and Chandra, A., (2006). "Leachate Characterization and assessment of groundwater pollution near municipal solid waste landfill site." *Environmental Monitoring and Assessment*, **118** 435-456.

Morel, F.M.M. and Herring, J.G., (1993). Principles and applications of aquatic chemistry. New York, John Wiley & Sons, Inc.

Moulton, S. and Plagakis, S., (2012). *The right to know, the responsibility to protect*. Washington D.C: OMB Watch. Retrieved from: [http://www.ombwatch.org/files/info/naturalgasfrackingdisclosure\\_highres.pdf](http://www.ombwatch.org/files/info/naturalgasfrackingdisclosure_highres.pdf) [Accessed 3rd Aug 2012]

Murali Mohan, A., Hartsock, A., Bibby, K.J., Hammack, R.W., Vidic, R.D. and Gregory, K.B., (2013). "Microbial community changes in hydraulic fracturing fluids and produced water from shale gas extraction." *Environmental science & technology*, **47**,(22): 13141-13150.

Myers, J. and Macun, I., (1991). "Acrylamide neuropathy in a South African factory: an epidemiologic investigation." *American Journal of Industrial Medicine*, **19**,(4): 487-493.

NHMRC (1996). Australian drinking water guideline. Fact Sheet No. 78, National Health and Medical Research Council.

Niskavaara, H., Reimann, C., Chekushin, V. and Kashulina, G., (1997). "Seasonal variability of total and easily leachable element contents in topsoils (0-5 cm) from eight catchments in the European Arctic (Finland, Norway and Russia)." *Environ Pollut.*, **96**,(2): 261-274.

North Meols News (2011). "Fracking Fluid Explained " Fracking. , from [http://www.northmeols.com/2011\\_news\\_archive.html](http://www.northmeols.com/2011_news_archive.html).

Nyahay, R., Leone, J., Smith, L., Martin, J. and Jarvie, D., (2014). "Update on the Regional Assessment of Gas Potential in the Devonian Marcellus and Ordovician Utica Shales in New York." *Online Journal for E&P Geoscientists*.

OGP, (2012). *Shale gas in Europe*. Retrieved from: [www.ogp.org.uk/index.php/download\\_file/view/252/2855/](http://www.ogp.org.uk/index.php/download_file/view/252/2855/) [Accessed 25th April 2012]

Orem, W., Tatu, C., Varonka, M., Lerch, H., Bates, A., Engle, M., Crosby, L. and McIntosh, J., (2014). "Organic substances in produced and formation water from unconventional natural gas extraction in coal and shale." *International Journal of Coal Geology*, **126**: 20-31.

Parkhurst, D.L. and Appelo, C.A.J., (1999). *User's guide to PHREEQC (version 2) A computer program for speciation, batch-reaction, one-dimensional transport, and inverse geochemical calculations*. U.S. Retrieved [Accessed 12 December 2013]

Pederson, L.R., Buckwalter, C.Q., McVay, G.L. and Riddle, B.L. (1983). Glass surface area to solution volume ratio and its implications to accelerated leach testing. Materials

Research Society Symposium Proceedings, New York: Elsevier Science Publishing Co.

Peng, B., Song, Z., Tu, X., Xiao, M., Wu, F. and Lv, H., (2004). "Release of Heavy metals during weathering of the Lower Cambrian black shales in Western Hunan, China." *Environmental Geology*, **45**: 1137-1147.

Peng, B., Tang, X.Y., Yu, C.X., Xie, S.R., Xiao, M.L. and Song, Z., (2009a). "Heavy metal geochemistry of the acid mine drainage discharged from the Hejiacun uranium mine in central Hunan, China." *Environmental Geology*, **57**,(8): 421-434.

Peng, B., Tang, X.Y., Yu, C.X., Xu, L.S., Xie, S.R. and Yang, G., (2009b). "Geochemical study of heavy metal contamination of soils derived from black shales at the HJC uranium mine in Central Hunan, China." *Acta Geologica Sinica*, **83**,(1): 89-106.

Peng, B., Wu, F.C., Xiao, M.L., Xie, S.R., Lu, H.Z. and Dai, Y.N., (2005). "The resource functions and environmental effects of black shales." *Bulletin of Mineralogy Petrology and Geochemistry*, **24**,(2): 153-158.

Philippe & Partners, (2011). *Final report on unconventional gas in Europe*. Brussels: European Union. Retrieved from: [http://ec.europa.eu/energy/studies/doc/2012\\_unconventional\\_gas\\_in\\_europe.pdf](http://ec.europa.eu/energy/studies/doc/2012_unconventional_gas_in_europe.pdf) [Accessed 2nd April 2012]

Plant, J.A., Baldock, J.W. and Smith, B. (1996). The role of geochemistry in environmental and epidemiological studies in developing countries: a review Environmental geochemistry and health with special reference to developing countries. J.D. Appleton, R. Fuge and G.J.H. McCall. London, Geological Society. **113**: 7-22.

Puura, E., Neretnieks, I. and Kirsimäe, K., (1999). "Atmospheric oxidation of the pyritic waste rock in Maardu, Estonia. 1: field study and modelling." *Environmental Geology*, **39**: 1-19.

Pye, K. and Krinsley, D.H., (1986). "Microfabric, mineralogy and early diagenetic history of the Whitby Mudstone Formation (Toarcian), Cleveland Basin, U.K." *Geological Magazine*, **123**: 191-203.

Rabus, R., Hansen, T.A. and Widdel, F., (2006). "Dissimilatory sulphate and sulfur reducing prokaryotes " *Prokaryotes*, **2**: 659-768.

Reemtsma, T. and Mehrrens, J., (1997). "Determination of polycyclic aromatic hydrocarbon (PAH) leaching from contaminated soil by a column test with on-line solid phase extraction." *Chemosphere*, **35**,(11): 2491-2501.

Roberts, D., Nachtegaal, M. and Sparks, D.L. (2005). Speciation of Metals in Soils. Chemical Processes in Soils. M.A. Tabatabai and D.L. Sparks, Soil Science Society of America: 619-654.

Rose, A.W. and Cravotta, C.A. (1998). Geochemistry of Coal Mine Drainage. Coal Mine Drainage Prediction and Pollution Prevention in Pennsylvania. Harrisburg, Pennsylvania Department of Environmental Protection,.

Sáinz, A., Grande, J.A., de la Torre, M.L. and Sánchez-Rodas, D., (2002). "Characterisation of sequential leachate discharges of mining waste rock dumps in the Tinto and Odiel rivers." *Journal of Environmental Management*, **64**,(4): 345-353.

Salbu, B., Krekling, T. and Oughton, D.H., (1998). "Characterisation of radioactive particles in the environment." *Analyst*, **123**: 843-849.

Scheetz, B.E., Freeborn, W.P., Komarneni, S., Atkinson, S.D. and White, W.B., (1981). "Comparative study of hydrothermal stability experiments: Application to Simulated Nuclear Waste Forms." *Nuclear and Chemical Waste Management*, **2**: 229 - 236.

Scotney, P.M., Joseph, J.B., Marshall, J.E.A., Lowe, M.J., Croudace, I.W. and Milton, J.A., (2012). "Geochemical and mineralogical properties of the Lower Callovian (Jurassic) Kellaways Sand, variations in trace element concentrations and implications for hydrogeological risk assessment." *Quarterly Journal of Engineering Geology and Hydrogeology*, **45**: 45-60.

Selley, R.C., (1987). "British shale gas potential scrutinized." *Oil and Gas Journal*: 62-64.

Selley, R.C. (2005a). UK Shale-Gas Resources. Petroleum Geology Conference. London, The Geological Society **6**: 707-714.

Selley, R.C. (2005b). UK shale-gas resources In: Dore, A. G. & Vining, B. A. (Eds). Petroleum geology: Northwest Europe and global perspectives. Proceedings of the 6th Petroleum Geology Conference, London, Geological Society.

Shaw, D., (2006). "Mobility of arsenic in saturated, laboratory test sediments under varying pH conditions." *Engineering Geology*, **85**,(1-2): 158-164.

Skoryna, S.C., Paul, T.M. and Edward, D.W., (1964). "Studies on Inhibition of Intestinal Absorption of Radioactive Strontium." *Can. Med. Assoc. J.*, **91**,(6): 285-288.

Skousen, J.A., Renton, J., Brown, H., Evans, P., Leavitt, B., Brady, K. and Cohen, L., (1997). "Neutralization potential of overburden samples containing siderite." *Jour. Environmental Quality*, **26**: 673-681.

Smith, E.A., Prues, S.L. and Oehme, F.W., (1996). "Environmental degradation of polyacrylamides - Effects of artificial environmental conditions: temperature, light, and pH." *Ecotoxicology and Environmental Safety*, **35**: 121-135.

Smith, J.W. and Young, N.B., (1967). "Organic composition of Kentucky's New Albany Shale: Determination and uses." *Chemical Geology*, **2**: 157-170.

Smith, N., Turner, P. and Williams, G. (2010). UK data and analysis for shale gas prospectivity. Petroleum Geology Conference London, Geological Society of London. **7**: 1087-1098.

Sobek, A.A., Shchuller, W.A., Freeman, J.R. and Smith, R.M., (1978). Field and laboratory methods applicable to overburdens and minesoils Cincinnati, Ohio, EPA.

Southam, G. (2000). Bacterial surface-mediated mineral formation. Environmental Microbe -Metal Interactions. D.R. Lovley. Washington, Am. Soc. Microbiol: 257 - 276.

Spears, D.A. and Amin, M.A., (1981a). "Geochemistry and mineralogy of marine and non-marine Namurian black shales from the Tansley borehole." *Sedimentology*, **28**: 407-417.

Spears, D.A. and Amin, M.A., (1981b). "A mineralogical and geochemical study turbidite sandstones and interbedded shales, mam tor, derbyshire, uk." *Clay Minerals*, **16**: 333-345.

Stollenwerk, K.G. and Runnels, D.D., (1977). Leachability of arsenic, selenium, molybdenum, boron, and fluoride from retorted oil shale.

Struchtemeyer, C.G. and Elshahed, M.S., (2011). "Bacterial communities associated with hydraulic fracturing fluids in thermogenic natural gas wells in North Central Texas, USA." *FEMS Microbial Ecology*, **81**: 13-25.

Stumm, W. and Morgan, J.J., (1996). Aquatic chemistry. New York, John Wiley & Sons, Inc.

Tessier, A., Campbell, P.G.C. and Bisson, M., (1979). "Sequential Extraction Procedure for the Speciation of Particulate Trace Metals." *Analytical Chemistry*, **51**,(7).

The Royal Society, (2012). *Shale gas extraction in the UK: a review of hydraulic fracturing* London. Retrieved from: [royalsociety.org/policy/projects/shale-gas-extraction](http://royalsociety.org/policy/projects/shale-gas-extraction) and [raeng.org.uk/shale](http://raeng.org.uk/shale) [Accessed 2 July 2012]

Tokalioglu, S., Kartal, S. and Elçi, L., (2000). "Determination of heavy metals and their speciation in lake sediments by flame atomic absorption spectrometry after a four-stage sequential extraction procedure." *Analytica Chimica Acta*, **413**: 33-40.

Tourtlot, H.A., (1979). "Black shale: Its deposition and diagenesis " *Clays and Clay Minerals*, **27**,(5): 313-321.

Turekian, K.K. and Wedepohl, K.H., (1961). "Distribution of the Elements in some major units of the Earth's crust." *Geological Society of America Bulletin*, **72**: 175-192.

U.S. Environmental Protection Agency (2011). Method 1627: Kinetic Test Method for the Prediction of Mine Drainage Quality. Washington, DC, U.S. Environmental Protection Agency.

U.S. Nuclear Regulatory Commission (2000). Consolidated guidance about materials licenses: Program-specific guidance about well logging, tracer, and field flood study licenses. Washington, DC, Office of Nuclear Material Safety and Safeguards,.

Urbina, I. (2011). Regulation Lax as Gas Wells' Tainted Water Hits Rivers. The New York Times. New York.

Ure, A.M., (1990). "Trace elements in soil: Their determination and speciation." *Fresenius' Journal of Analytical Chemistry*, **337** (5): 577-581.

USEPA (2012). "Radiation Protection: Strontium." Retrieved Jan 2012, from <http://www.epa.gov/radiation/radionuclides/strontium.html>.

Van Hamme, J.D., Sing, A. and Ward, O.P., (2003). "Recent Advances in Petroleum Microbiology." *Molecular and Microbiology Reviews*, **67**: 503-549.

Vidic, R.D., Brantley, S.L., Vandenbossche, J.M., Yoxtheimer, D. and Abad, J.D., (2013). "Impact of Shale Gas Development on Regional Water Quality." *Science*, **340**.

Vinogradov, A.P., (1967). "Introduction to the geochemistry of the oceans -Vvedenie v geokhimiya okeana (In Russian)."

Ward, R., (2014). *Shale gas and water: An independent review of shale gas exploration and exploitation in the UK with a particular focus on the implications for the water environment*. Retrieved from: <http://nora.nerc.ac.uk/id/eprint/504726> [Accessed

White, W.M., (2013). *Geochemistry*, John Wiley & Sons Ltd.

Whittleston, R.A., (2009). "Chromium Contamination: Processes Affecting Subsurface Contaminant Mobility." *Earth & Environment*, **4**: 83-113.

WHO, (2011). *Acrylamide in drinking-water-Background document for development of WHO guidelines for drinking-water quality*. Geneva. Retrieved from: [http://www.who.int/water\\_sanitation\\_health/dwq/chemicals/acrylamide.pdf](http://www.who.int/water_sanitation_health/dwq/chemicals/acrylamide.pdf) [Accessed 13 Aug 2012]

Woo, N.C., Choi, M.J. and Lee, K.S., (2002). "Assessment of Groundwater Quality and Contamination from Uranium-Bearing Black Shale in Goesan–Boeun Areas, Korea." *Environmental Geochemistry and Health*, **24** (3): 264-273.

Wood, R., Gilbert, P., Sharmina, M. and Anderson, K., (2011). *Tyndall Centre Report: An updated assessment of environmental and climate change impacts* Manchester: The Co-operative. Retrieved [Accessed 17th Dec 2011]

Woodrow, J.E., Seiber, J.N. and Miller, G.C., (2008). "Acrylamide release resulting from sunlight irradiation of aqueous polyacrylamide/Iron mixtures." *Journal of Agricultural and food chemistry*, **56**,(8): 2773-2779.

Xiang-Rong, X., Hua-bin, L., Xiao-Yan, L. and Ji-Dong, G., (2004). "Reduction of hexavalent chromium by ascorbic acid in aqueous solutions." *Chemosphere*, **57**: 609-613.

Yanga, H., Leea, S., Jina, Y., Choia, J., Hanb, D., Chaeb, C. and Leea, M.C., (2005). "Toxicological effects of acrylamide on rat testicular gene expression profile." *Reproductive Toxicology*, **19**,(4): 527–534.

Yitagesu, F.A., Van der Meer, F., Van der Werff, H. and Zigterman, W., (2009). "Quantifying engineering parameters of expansive soils from their reflectance spectra." *Engineering Geology*, **105**,(3-4): 151-160.

Yu, C., Lavergren, U., Peltola, P., Drake, H., Bergbäck, B. and Åströma, M.E., (2014). "Retention and transport of arsenic, uranium and nickel in a black shale setting revealed by a long-term humidity cell test and sequential chemical extractions." *Chemical Geology*, **363** 134-144.

Yu, C., Peng, B., Peltola, P., Tang, X. and Xie, S., (2010). "Effect of weathering on abundance and release of potentially toxic elements in soils developed on Lower Cambrian black shales, P. R. China." *Environmental & Geochemical Health*, **34**,(3): 375-390.

Zhao, H., Givens, N.B. and Curtis, B., (2007). "Thermal maturity of the Barnett Shale determined from well-log analysis." *American Association of Petroleum Geologists*, **91**: 535-549.

Ziegler, K., Daines, S.R. and Turner, P., (1997). *Petroleum Geology of the Southern North Sea: Future Potential*, Geological Society of London.

Zorpas, A.A., Constantinides, T., Vlyssides, A.G., Haralambous, I. and Loizidou, M., (2000). "Heavy metal uptake by natural zeolite and metals partitioning in sewage sludge compost." *Bioresource Technology*, **72**: 113-119.

## APPENDIX A: Shale Characterisation Data

**Table A-1:** Correlation Matrix for Black Shale Sampled from the Bowland Lancashire Formation (Coefficient of R<sup>2</sup> values for Majors, Minors and Traces)

	<i>SiO<sub>2</sub></i>	<i>CaO</i>	<i>Al<sub>2</sub>O<sub>3</sub></i>	<i>Fe<sub>2</sub>O<sub>3</sub></i>	<i>K<sub>2</sub>O</i>	<i>MgO</i>	<i>Na<sub>2</sub>O</i>	<i>TiO<sub>2</sub></i>	<i>MnO</i>	<i>Sr</i>	<i>Cr</i>	<i>V</i>	<i>Zr</i>	<i>Rb</i>	<i>Ni</i>	<i>Zn</i>	<i>Cu</i>	<i>Ba</i>	<i>Pb</i>	<i>Fe/Al</i>	<i>Al/Fe</i>	
SiO <sub>2</sub> (% Wt.)	1.00																					
CaO (% Wt.)	-0.27	1.00																				
Al <sub>2</sub> O <sub>3</sub> (% Wt.)	0.21	-0.32	1.00																			
Fe <sub>2</sub> O <sub>3</sub> (% Wt.)	-0.37	0.00	0.42	1.00																		
K <sub>2</sub> O (% Wt.)	0.02	0.28	-0.11	-0.42	1.00																	
MgO (% Wt.)	-0.65	0.11	0.01	0.39	-0.07	1.00																
Na <sub>2</sub> O (% Wt.)	0.03	-0.15	0.08	-0.21	-0.25	0.05	1.00															
TiO <sub>2</sub> (% Wt.)	-0.17	0.04	0.25	0.60	-0.55	0.11	-0.41	1.00														
MnO (ppm)	-0.16	0.16	0.28	-0.05	0.15	0.26	0.25	-0.14	1.00													
Sr (ppm)	-0.17	-0.29	0.15	-0.01	-0.24	-0.05	0.42	-0.34	-0.17	1.00												
Cr (ppm)	-0.23	-0.20	-0.04	0.08	0.00	-0.06	-0.21	-0.04	-0.35	0.48	1.00											
V (ppm)	† <b>0.90</b>	-0.02	0.11	-0.44	0.09	-0.63	0.11	-0.27	0.01	-0.12	-0.20	1.00										
Zr (ppm)	-0.34	0.16	-0.22	0.36	-0.52	0.47	0.47	-0.01	0.04	0.32	-0.04	-0.17	1.00									
Rb (ppm)	-0.15	0.10	-0.10	-0.12	0.31	-0.31	-0.19	-0.16	-0.28	0.38	0.59	-0.07	-0.11	1.00								
Ni (ppm)	-0.48	0.11	0.11	† <b>0.94</b>	-0.45	0.41	-0.20	0.54	-0.26	0.02	0.15	-0.53	0.48	-0.08	1.00							
Zn (ppm)	-0.39	0.10	0.27	† <b>0.95</b>	-0.47	0.33	-0.16	0.52	-0.05	0.09	0.05	-0.42	0.49	-0.07	<b>0.94</b>	1.00						
Cu (ppm)	† <b>0.97</b>	-0.16	0.24	-0.37	0.09	-0.68	-0.04	-0.17	-0.15	-0.12	-0.11	† <b>0.94</b>	-0.38	-0.08	-0.48	-0.41	1.00					
Ba (ppm)	0.29	0.30	0.15	-0.02	0.15	-0.49	-0.29	0.27	-0.01	-0.17	0.12	0.42	-0.38	0.04	-0.09	-0.02	0.45	1.00				
Pb (ppm)	-0.37	-0.10	0.11	0.23	-0.11	0.18	-0.31	0.15	0.09	0.26	0.49	-0.27	0.12	0.44	0.19	0.18	-0.27	-0.29	1.00			
*Fe/Al	-0.49	0.12	0.07	<b>0.94</b>	-0.42	0.43	-0.26	0.56	-0.17	-0.07	0.10	-0.53	0.48	-0.09	† <b>0.98</b>	† <b>0.94</b>	-0.50	-0.09	0.21	1.00		
*Al/Fe	0.50	-0.14	-0.07	<b>-0.93</b>	0.40	-0.46	0.27	-0.56	0.13	0.11	-0.06	0.54	-0.48	0.11	<b>-0.98</b>	<b>-0.94</b>	0.52	0.10	-0.19	-1.00	1.00	

Note: Strongly correlated R<sup>2</sup> values are in bold font

\*Ratios of Iron and Aluminium oxides have been included to limit the constant sum effect that may lead to spurious correlations.

† Strong to very strong correlations according to Hatva's Scale

**Table A-2:** Correlation Matrix for Black Shale Sampled from the Edale formation (Coefficient of R<sup>2</sup> values for Majors, Minors and Traces)

	SiO <sub>2</sub>	CaO	Al <sub>2</sub> O <sub>3</sub>	Fe <sub>2</sub> O <sub>3</sub>	K <sub>2</sub> O	MgO	Na <sub>2</sub> O	TiO <sub>2</sub>	SO <sub>3</sub>	MnO	P <sub>2</sub> O <sub>5</sub>	Sr	Cr	V	Zr	Rb	Ni	Zn	Cu	Ba	Pb	Fe/Al	Al/Fe	
SiO <sub>2</sub> (% Wt.)	1.00																							
CaO (% Wt.)	0.16	1.00																						
Al <sub>2</sub> O <sub>3</sub> (% Wt.)	0.06	0.22	1.00																					
Fe <sub>2</sub> O <sub>3</sub> (% Wt.)	-0.02	-0.23	0.09	1.00																				
K <sub>2</sub> O (% Wt.)	-0.02	0.19	0.21	0.23	1.00																			
MgO (% Wt.)	-0.55	-0.06	0.17	-0.15	-0.47	1.00																		
Na <sub>2</sub> O (% Wt.)	0.31	0.33	0.02	0.03	0.54	-0.66	1.00																	
TiO <sub>2</sub> (% Wt.)	0.26	-0.50	0.22	-0.09	0.10	-0.17	-0.12	1.00																
SO <sub>3</sub> (% Wt.)	0.48	0.23	-0.51	-0.28	0.07	-0.48	0.14	-0.12	1.00															
MnO (% Wt.)	-0.24	0.45	0.44	0.19	-0.26	0.36	-0.13	-0.38	-0.54	1.00														
P <sub>2</sub> O <sub>5</sub> (% Wt.)	0.32	-0.55	-0.10	-0.18	0.21	-0.32	-0.01	† <b>0.86</b>	0.25	-0.79	1.00													
Sr (ppm)	-0.41	0.25	0.29	0.17	-0.46	0.64	-0.54	-0.43	-0.50	† <b>0.88</b>	-0.76	1.00												
Cr (ppm)	-0.30	-0.16	0.24	-0.14	-0.62	† <b>0.88</b>	-0.72	0.10	-0.49	0.41	-0.17	0.64	1.00											
V (ppm)	-0.31	0.23	-0.15	0.53	0.06	-0.12	-0.05	-0.48	-0.16	0.57	-0.63	0.54	-0.18	1.00										
Zr (ppm)	0.14	-0.50	0.18	0.01	0.39	-0.31	0.35	† <b>0.78</b>	-0.27	-0.50	<b>0.77</b>	-0.66	-0.20	-0.51	1.00									
Rb (ppm)	-0.15	-0.68	0.01	0.06	0.28	-0.02	0.12	0.53	-0.34	-0.60	0.64	-0.56	-0.07	-0.49	† <b>0.85</b>	1.00								
Ni (ppm)	-0.20	0.25	-0.06	0.64	0.20	-0.15	0.05	-0.33	-0.25	0.53	-0.51	0.44	-0.20	† <b>0.91</b>	-0.31	-0.34	1.00							
Zn (ppm)	-0.04	-0.17	-0.08	† <b>0.92</b>	0.40	-0.37	0.17	-0.12	-0.04	0.06	-0.11	-0.01	-0.40	0.60	-0.01	-0.01	0.67	1.00						
Cu (ppm)	-0.23	-0.05	-0.67	-0.01	0.38	-0.18	0.15	0.04	0.19	-0.40	0.24	-0.37	-0.32	0.17	0.19	0.27	0.28	0.16	1.00					
Ba (ppm)	-0.37	0.10	-0.05	-0.27	0.53	0.09	-0.15	0.20	0.24	-0.43	0.37	-0.29	-0.12	-0.17	0.14	0.23	-0.12	-0.09	0.51	1.00				
Pb (ppm)	0.30	0.38	0.49	0.25	0.25	-0.03	0.20	-0.46	-0.03	0.19	-0.41	0.15	-0.13	0.02	-0.26	-0.16	0.06	0.11	-0.44	-0.21	1.00			
Fe/Al	-0.03	-0.27	-0.08	0.99	0.19	-0.17	0.03	-0.13	-0.20	0.12	-0.16	0.12	-0.17	0.54	-0.02	0.06	0.64	† <b>0.93</b>	0.11	-0.26	0.17	1.00		
Al/Fe	0.12	0.29	0.05	-0.98	-0.26	0.14	-0.02	0.06	0.24	-0.10	0.10	-0.09	0.15	-0.52	-0.05	-0.12	-0.64	† <b>-0.94</b>	-0.16	0.14	-0.10	-0.99	1.00	

Note: Strongly correlated R<sup>2</sup> values are in bold font

\*Ratios of Iron and Aluminium oxides have been included to limit the constant sum effect that may lead to spurious correlations.

† Strong to very strong correlations according to Hatva's Scale

**Table A-3:** Correlation Matrix for Black Shale Sampled from the Toarcian Whitby formation ( $R^2$  values for Majors, Minors and Traces)

	SiO <sub>2</sub>	CaO	Al <sub>2</sub> O <sub>3</sub>	Fe <sub>2</sub> O <sub>3</sub>	K <sub>2</sub> O	MgO	Na <sub>2</sub> O	TiO <sub>2</sub>	SO <sub>3</sub>	Mn	Sr	Cr	V	Zr	Rb	Ni	Zn	Cu	Ba	Pb	Fe <sub>2</sub> O <sub>3</sub> / Al <sub>2</sub> O <sub>3</sub>	Al <sub>2</sub> O <sub>3</sub> / Fe <sub>2</sub> O <sub>3</sub>	
SiO <sub>2</sub> (%Wt.)	1.00																						
CaO (%Wt.)	0.09	1.00																					
Al <sub>2</sub> O <sub>3</sub> (%Wt.)	0.34	-0.52	1.00																				
Fe <sub>2</sub> O <sub>3</sub> (%Wt.)	-0.37	0.30	-0.61	1.00																			
K <sub>2</sub> O (%Wt.)	-0.02	-0.59	0.11	-0.39	1.00																		
MgO (%Wt.)	0.38	0.08	-0.17	0.20	-0.21	1.00																	
Na <sub>2</sub> O (%Wt.)	-0.21	-0.17	0.24	0.27	-0.09	-0.21	1.00																
TiO <sub>2</sub> (%Wt.)	0.10	-0.01	0.21	-0.18	0.40	-0.30	0.03	1.00															
SO <sub>3</sub> (%Wt.)	-0.12	-0.24	0.49	-0.29	0.09	-0.21	0.18	0.07	1.00														
Mn (%Wt.)	-0.04	0.08	0.13	-0.20	-0.12	0.04	-0.37	0.28	0.14	1.00													
Sr (ppm)	-0.03	-0.36	0.29	0.02	0.20	0.14	0.46	-0.19	0.32	-0.62	1.00												
Cr (ppm)	-0.11	† <b>0.91</b>	-0.60	0.19	-0.38	-0.14	-0.20	0.10	-0.25	0.07	-0.42	1.00											
V (ppm)	-0.40	0.34	<b>-0.70</b>	† <b>0.93</b>	-0.24	0.18	0.28	-0.20	-0.32	-0.33	0.17	0.25	1.00										
Zr (ppm)	0.06	0.47	-0.14	0.19	-0.41	-0.25	-0.15	0.17	-0.40	0.52	-0.65	0.36	0.13	1.00									
Rb (ppm)	-0.08	0.17	0.04	0.59	-0.53	0.05	0.60	0.04	0.13	-0.26	0.23	0.06	0.43	-0.03	1.00								
Ni (ppm)	-0.30	0.24	-0.60	† <b>0.94</b>	-0.32	0.33	0.32	-0.28	-0.29	-0.26	0.09	0.09	† <b>0.94</b>	0.13	0.51	1.00							
Zn (ppm)	0.34	-0.38	† <b>0.89</b>	-0.71	0.09	-0.04	-0.07	0.30	0.40	0.26	0.14	-0.45	† <b>-0.76</b>	-0.09	-0.11	-0.67	1.00						
Cu (ppm)	-0.37	0.18	0.00	-0.14	-0.07	-0.14	0.08	-0.16	0.60	0.06	0.03	0.27	-0.15	-0.35	0.01	-0.14	-0.01	1.00					
Ba (ppm)	0.25	-0.22	0.39	-0.08	0.23	-0.39	-0.03	0.44	-0.06	-0.02	-0.09	-0.18	-0.24	0.17	0.18	-0.25	0.28	-0.36	1.00				
Pb (ppm)	0.04	0.12	0.19	0.08	-0.47	0.33	0.07	-0.20	0.04	0.21	0.11	0.04	-0.09	-0.07	0.24	-0.09	0.08	0.06	0.02	1.00			
Fe <sub>2</sub> O <sub>3</sub> / Al <sub>2</sub> O <sub>3</sub>	-0.39	0.46	-0.89	0.91	-0.30	0.20	0.04	-0.23	-0.45	-0.18	-0.16	0.44	† <b>0.91</b>	0.20	0.34	† <b>0.86</b>	† <b>-0.89</b>	-0.08	-0.24	-0.03	1.00		
Al <sub>2</sub> O <sub>3</sub> / Fe <sub>2</sub> O <sub>3</sub>	0.39	-0.45	0.87	-0.92	0.28	-0.22	-0.03	0.20	0.41	0.18	0.13	-0.41	<b>-0.93</b>	-0.19	-0.34	† <b>-0.88</b>	† <b>0.87</b>	0.09	0.25	0.07	-0.99	1.00	

Note: Strongly correlated  $R^2$  values are in bold font

\*Ratios of Iron and Aluminium oxides have been included to limit the constant sum effect that may lead to spurious correlations.

† Strong to very strong correlations according to Hatva's Scale

**Table A-4** Computed Neutralization Potential for All Three Investigated Formations

Method	Shale	<i>Black Shale Sample sets (n=15)</i>															*AVG.	**S.D
		1	2	3	4	5	6	7	8	9	10	11	12	13	14	15		
<b>Sobek NP (kg CaCO3/t)</b>	<i>LAN</i>	59.27	73.81	96.30	73.00	66.92	65.40	65.00	51.19	50.40	58.28	53.78	57.50	43.75	52.41	58.35	61.69	10.50
	<i>DRB</i>	57.62	69.88	61.35	66.80	64.69	70.44	60.50	44.74	68.48	75.71	79.39	100.25	115.00	98.13	123.59	77.10	22.30
	<i>CLV</i>	35.27	44.94	39.27	35.35	39.34	31.05	47.16	39.00	37.23	42.22	57.19	43.35	47.32	44.86	49.48	42.20	13.25
<b>Modified Sobek NP (kg CaCO3/t)</b>	<i>LAN</i>	62.50	31.39	81.25	49.57	23.50	21.80	34.85	20.26	36.64	31.94	39.89	60.94	71.38	48.05	27.50	42.76	18.90
	<i>DRB</i>	25.75	10.08	21.82	55.51	43.33	43.10	65.49	10.38	43.66	40.37	58.71	90.40	63.95	76.55	40.81	45.99	23.13
	<i>CLV</i>	48.65	35.38	29.88	34.97	39.76	24.57	37.92	29.95	40.23	35.40	35.31	29.96	32.62	39.70	46.22	36.04	6.37
<b>Modified ABA NP (kg CaCO3/t)</b>	<i>LAN</i>	69.35	49.01	66.12	75.25	71.36	48.33	39.25	50.64	69.11	51.66	52.36	77.20	54.99	46.10	44.87	57.71	12.35
	<i>DRB</i>	74.23	72.36	69.21	49.11	65.66	68.91	58.12	61.30	69.50	59.79	50.32	51.36	58.01	55.95	60.89	61.65	8.08
	<i>CLV</i>	74.23	98.21	84.56	78.21	74.99	59.35	58.63	61.36	50.99	82.31	75.66	78.25	59.68	68.9	70.56	71.73	12.28

\*Avg. - Average of (n=15) sample sets

\*\* S.D – Standard Deviations

## **APPENDIX B: Quality Control Results**

### **9.1 GFAAS Quality Control Results**

Computations for the MDL determined from 10 replicates of the LRB are summarised in Table B.1. Results from the 5 point statistical check test for GFAAS determinations are summarised in Table B.2 and include checks on signal – noise ratio (S/N). A student's t value (2.821) for a 99% confidence level and a standard deviation estimate with n-1 degrees of freedom for 10 replicates was adopted (Table B.1). Check test 3 has been ignored as there are no predetermined requirements expected for MDL based on the analytical methods used and the nature of the leachates produced. Since MDL is a function of the spike concentration, the quality control method stipulates the use of appropriate spikes that range between 2 to 5 times the estimated detection limit as utilised in Table B.1 below.

**Table B-1:** Computation of MDL for GFAAS from spiked LRB

Sample	<sup>2</sup> Results for Cr Spiked Conc. (0.14µg/L)	<sup>1</sup> % Recovery	<sup>2</sup> Results for Cu Spiked Conc. (0.36µg/L)	<sup>1</sup> % Recovery	<sup>2</sup> Results for Ni Spiked Conc. (0.29µg/L)	<sup>1</sup> % Recovery	<sup>2</sup> Results for Zn Spiked Conc. (0.46µg/L)	<sup>1</sup> % Recovery
1	0.10	72.2	0.36	101.3	0.24	82.8	0.49	107.2
2	0.16	115.5	0.38	106.9	0.28	96.6	0.44	96.2
3	0.12	86.6	0.32	90.1	0.20	69.0	0.49	107.2
4	0.11	79.4	0.29	81.6	0.27	93.1	0.41	89.7
5	0.16	115.5	0.38	106.9	0.27	93.1	0.39	85.3
6	0.13	93.8	0.38	106.9	0.25	86.2	0.39	85.3
7	0.11	79.4	0.31	87.2	0.24	82.8	0.36	78.7
8	0.12	86.6	0.35	98.5	0.25	86.2	0.46	100.6
9	0.14	101.0	0.36	101.3	0.21	72.4	0.39	85.3
10	0.15	108.3	0.30	84.4	0.27	93.1	0.44	96.2
Mean	0.13	93.8	0.34	96.5	0.25	85.5	0.43	93.2
STD DEV	0.022		0.035		0.027		0.045	
<sup>3</sup> t value	2.82		2.82		2.82		2.82	
<sup>4</sup> MDL	0.061		0.099		0.075		0.127	

**1** % Recovery computed from Equation 5.1.

**2** Spike derived from multiples of MDL i.e. Cr ( $2 \times \text{MDL}$ ), Cu ( $5 \times \text{MDL}$ ), Ni ( $2.5 \times \text{MDL}$ ) and Zn ( $5 \times \text{MDL}$ )

**3** Student's t value = 2.821 for a 99% confidence level and a standard deviation estimate with n-1 degrees of freedom for 10 replicates

**4** MDL = Std. Dev.  $\times$  Student's t value

**Table B-2:** Results for adopted 5 point statistical Check test for GFAAS Determinations

	<b>Criteria</b>	<b>Cr</b>	<b>Cu</b>	<b>Ni</b>	<b>Zn</b>	<b>Status</b>
Test 1	$(MDL \times 10) > \text{Spike}$	0.61 > 0.14	0.99 > 0.36	0.88 > 0.29	1.14 > 0.46	TRUE
Test 2	MDL < Spike	0.06 < 0.14	0.10 < 0.36	0.09 < 0.29	0.11 < 0.46	TRUE
Test 3	MDL < Requirement (70%-130%)	N/A	N/A	N/A	N/A	N/A
Test 4	$2.5 \leq \left(\frac{Avg}{Std.D}\right) \leq 10$	$2.5 \leq \frac{6.0}{10} \leq$	$2.5 \leq 9.81 \leq 10$	$2.5 \leq 9.33 \leq 10$	$2.5 \leq 9.46 \leq 10$	OK
Test 5	$70\% \leq \text{Avg. \% Recovery} \leq 130\%$	95.26	96.53	92.30	126.15	OK

## 9.2 FAAS Quality Control Results

Instrument and laboratory performance checks for the FAAS also involved the computation of the IDL, MDL and statistical test instrument capability. Results are summaries in Table B.3 below. With reported spikes corresponding to 1Abs in 1:1 HCl matrix, the laboratory fortified blanks are analysed and reported mean ( $n=3$ ) and percentage recoveries are listed in Table B.4.

**Table B-3:** Summary results for MDL determinations

<b>Parameters</b>	<b>Cr</b>	<b>Cu</b>	<b>Ni</b>	<b>Zn</b>	<b>Al</b>	<b>Fe</b>	<b>Ca</b>	<b>Mg</b>
Mean ( $n=10$ )	7.54	6.72	8.53	6.83	0.034	0.021	0.067	0.056
Mean (% Recovery)	94.25	95.97	94.78	85.33	91.08	88.75	88.67	91.48
STD DEV	0.30	0.30	0.36	0.32	0.00	0.01	0.04	0.05
t value	2.82	2.82	2.82	2.82	2.82	2.82	2.82	2.82
MDL( $\mu\text{g/L}$ )	0.85	0.836	1.002	0.904	0.008	0.014	0.012	0.015

### 9.3 IC Quality Control Results

Sulphate, the only anion determination in the leaching column analysis is completed via the IC. Results in Table B.5 show the percentages recoveries following the determination of a certified value for sulphate in the Fluka/69734 Multi Anion Standard 1 via the IC. All recoveries show greater than 85% recovery of the corresponding spiked concentrations utilised while sulphate recoveries show better than 98% recoveries. These determinations along with intermittent analysis of both LRB and LFB ensure the analytes quantification is reportable and measured with the laboratory and instrument contributed errors accounted for.

**Table B-4:** Sample and LFB recoveries and percentage differences of triplicate spikes adopted for FAAS determinations

Analytes	Spiked Conc. (mg/L)	<sup>1</sup> Lab Reagent Blank (µg/L)	<sup>2</sup> Lab Fortified Blank (LFB) (µg/L)	<sup>3</sup> % Recovery of LFB
Al	250	<MDL	238.1 ±6.05	95.2
Fe	30	<MDL	26.8 ±2.14	89.3
Ca	5	<MDL	4.29 ±0.56	85.8
Mg	0.8	<MDL	0.72 ±0.56	89.8
Cr	20	<MDL	19.6 ±2.08	98.0
Cu	10	<MDL	8.9 ±1.04	89.4
Ni	20	<MDL	17.2 ±3.78	88.7
Zn	2	<MDL	1.77 ±0.68	88.5

<sup>1</sup> LRB is Ultrapure (Milli-Q) water defined in Table B.1

<sup>2</sup> LFB is LRB spiked with known concentration of standards and defined in Table B.1

<sup>3</sup> % Recovery of LFB computed from Equation 5.1

**Table B-5:** Quality Control Test with a Certified Multi Anion Standard for IC

Metals	<sup>1</sup> Certified Values (mg/L)	Laboratory Determined (mg/L)	Standard Deviation (n=4)	<sup>2</sup> % Recovery	<sup>3</sup> Requirement
	20.00	20.002 ± 1.08		100.0	
SO <sub>4</sub> <sup>2-</sup>	20.00	19.695 ± 0.74	0.13	98.5	Passed
	20.00	19.896 ± 0.88		99.5	
	20.00	19.785 ± 1.01		98.9	

<sup>1</sup> Certified Values for the Fluka/69734 Multi Anion Standard 1 containing SO<sub>4</sub> (20mg/L)

<sup>2</sup> % Recovery computed from Equation 5.1

<sup>3</sup> Standard requires recoveries should be 85% ≤ Recovery ≤ 115%

## APPENDIX C: Leachate Characteristics

**Table C-1:** Reactor 1 (LAN) Weekly Monitoring Report for Natural Weathering Simulation

Week	Water In (L)	Water Out (L)	pH	Conductivity ( $\mu\text{S}/\text{cm}$ )	Alkalinity (to pH 4.5) mg/L as $\text{CaCO}_3$
Initial Flush	0.75	0.535	7.89	8695	665 $\pm$ 29.3
Week 1	0.44	0.335	7.89	6730	510 $\pm$ 17.2
Week 2	0.363	0.305	8.01	4250	665 $\pm$ 25.2
Week 3	0.37	0.295	8.84	2770	615 $\pm$ 10.5
Week 4	0.335	0.28	9.32	2550	712 $\pm$ 8.1
Week 5	0.367	0.305	7.07	2065	540 $\pm$ 22.2
Week 6	0.278	0.252	6.80	2450	395 $\pm$ 5.5
Week 7	0.426	0.315	5.68	2800	205 $\pm$ 12.6
Week 8	0.28	0.22	5.49	2100	170 $\pm$ 14.7
Week 9	0.303	0.245	5.70	2150	290 $\pm$ 18.4
Week 10	0.585	0.53	5.12	2148	115 $\pm$ 18.1
Week 11	0.625	0.585	5.12	1855	110 $\pm$ 12.5
Week 12	0.65	0.52	5.48	1800	175 $\pm$ 17.6

**Table C-2:** Reactor 2 (DRB) Weekly Monitoring Report for Natural Weathering Simulation

Week	Water In (L)	Water Out (L)	pH	Conductivity ( $\mu\text{S}/\text{cm}$ )	Alkalinity (to pH 4.5) mg/L as $\text{CaCO}_3$
Initial Flush	0.605	0.470	7.95	6860	680 $\pm$ 18.1
Week 1	0.372	0.285	8.24	6940	719 $\pm$ 8.23
Week 2	0.329	0.260	8.92	2179	743 $\pm$ 5.21
Week 3	0.346	0.273	7.56	2540	645 $\pm$ 3.65
Week 4	0.3	0.240	7.08	2095	600 $\pm$ 3.50
Week 5	0.342	0.285	6.75	1880	512 $\pm$ 12.5
Week 6	0.21	0.200	5.88	2275	271 $\pm$ 15.5
Week 7	0.413	0.2800	5.52	1925	202 $\pm$ 11.2
Week 8	0.238	0.196	6.01	1645	455 $\pm$ 11.6
Week 9	0.31	0.245	5.21	1274	125 $\pm$ 10.4
Week 10	0.695	0.535	6.05	1256	495 $\pm$ 12.2
Week 11	0.65	0.600	5.48	1210	125 $\pm$ 9.25
Week 12	0.625	0.545	5.95	1210	265 $\pm$ 6.43

**Table C-3: Reactor 3 (CLV) Weekly Monitoring Report for Natural Weathering Simulation**

<b>Week</b>	<b>Water In (L)</b>	<b>Water Out (L)</b>	<b>pH</b>	<b>Conductivity (<math>\mu\text{S}/\text{cm}</math>)</b>	<b>Alkalinity (to pH 4.5) mg/L as <math>\text{CaCO}_3</math></b>
Initial Flush	0.975	0.511	7.56	2929	815 $\pm$ 9.3
Week 1	0.615	0.455	8.01	2376	844 $\pm$ 5.2
Week 2	0.499	0.415	8.65	1880	875 $\pm$ 15.2
Week 3	0.515	0.415	7.85	2275	817 $\pm$ 11.5
Week 4	0.43	0.37	6.81	1925	615 $\pm$ 6.2
Week 5	0.46	0.405	6.64	1254	620 $\pm$ 10.1
Week 6	0.305	0.285	6.01	1542	540 $\pm$ 4.6
Week 7	0.56	0.435	6.52	1233	640 $\pm$ 4.5
Week 8	0.405	0.305	5.00	1158	305 $\pm$ 7.4
Week 9	0.325	0.295	6.45	1140	635 $\pm$ 8.9
Week 10	0.675	0.48	6.38	1125	625 $\pm$ 10.0
Week 11	0.65	0.535	6.21	1120	583 $\pm$ 11.9
Week 12	0.65	0.525	6.12	1122	575 $\pm$ 12.4

**TableC-4: Summary Computation of Weathered Mass**

Analytes	Reactors	WK 1	WK 2	WK 3	WK 4	WK 5	WK 6	WK 7	WK 8	WK 9	WK 10	WK 11	WK 12	Total Mass Weathered	Average Mass Weathered
<b>Al (mg)</b>	<b>RXC 1</b>	0.140	0.457	0.451	0.094	0.118	0.135	0.294	1.402	0.695	0.982	0.688	0.761	6.216	0.518
	<b>RXC 2</b>	0.053	0.320	0.342	0.280	0.209	0.065	0.273	0.165	0.291	0.750	0.567	0.321	3.637	0.303
	<b>RXC 3</b>	0.010	0.177	0.258	0.182	0.012	0.067	0.225	0.010	0.199	0.422	0.445	0.551	2.559	0.213
	<b>RXC 4</b>	0.002	0.003	0.068	0.029	0.008	0.002	0.009	0.011	0.004	0.001	0.000	0.019	0.157	0.013
<b>Fe (mg)</b>	<b>RXC 1</b>	0.011	0.101	0.102	0.077	0.058	0.085	0.129	0.375	0.601	1.756	0.972	1.055	5.322	0.444
	<b>RXC 2</b>	0.000	0.072	0.075	0.066	0.031	0.049	0.157	0.102	0.310	1.475	0.948	0.848	4.132	0.344
	<b>RXC 3</b>	0.021	0.025	0.019	0.007	0.014	0.007	0.010	0.007	0.055	0.427	0.537	0.570	1.698	0.142
	<b>RXC 4</b>	0.000	0.006	0.004	0.001	0.000	0.000	0.012	0.005	0.000	0.066	0.044	0.008	0.148	0.012
<b>Ca (mg)</b>	<b>RXC 1</b>	2.907	0.000	0.000	0.210	0.542	3.319	2.745	0.563	0.759	6.580	9.719	5.692	33.035	2.753
	<b>RXC 2</b>	3.451	0.000	0.000	0.155	0.448	1.769	2.067	0.572	0.872	4.950	6.244	9.117	29.645	2.470
	<b>RXC 3</b>	4.661	0.000	0.000	0.623	1.336	5.448	4.335	0.859	1.800	6.708	5.281	0.095	31.146	2.595
	<b>RXC 4</b>	0.002	0.000	0.000	0.264	0.924	0.836	0.311	0.079	0.003	0.147	0.106	0.097	2.770	0.231
<b>Mg (mg)</b>	<b>RXC 1</b>	1.895	0.000	0.000	0.187	0.255	2.329	2.253	1.547	1.474	2.625	3.136	4.141	19.843	1.654
	<b>RXC 2</b>	1.117	0.000	0.000	0.103	0.246	1.258	2.061	0.899	1.540	3.734	2.541	3.127	16.628	1.386
	<b>RXC 3</b>	1.543	0.000	0.000	0.349	0.574	1.122	2.018	1.644	1.730	1.613	1.776	2.495	14.864	1.239
	<b>RXC 4</b>	0.001	0.000	0.000	0.037	0.025	0.497	0.231	0.033	0.008	0.129	0.426	0.122	1.508	0.126
<b>Cr (µg)</b>	<b>RXC 1</b>	0.000	0.930	1.088	3.528	4.186	9.526	10.419	6.776	8.704	15.450	35.934	25.688	122.227	10.186
	<b>RXC 2</b>	0.408	1.020	1.499	9.267	1.225	4.022	6.307	5.601	5.432	17.268	9.050	11.947	73.046	6.087
	<b>RXC 3</b>	0.104	0.432	0.000	3.436	0.000	0.000	9.499	9.340	8.737	32.386	10.058	13.837	87.829	7.319
	<b>RXC 4</b>	0.022	0.032	0.073	0.027	0.000	0.145	0.014	0.467	0.003	0.015	0.355	0.000	1.153	0.096
<b>Cu (µg)</b>	<b>RXC 1</b>	0.056	0.558	0.479	0.784	2.326	3.016	3.969	0.968	3.301	14.045	13.689	18.928	62.119	5.177
	<b>RXC 2</b>	0.061	1.529	1.424	1.158	1.429	1.307	2.759	0.193	3.320	12.951	9.050	11.947	47.129	3.927
	<b>RXC 3</b>	0.000	1.816	2.594	1.718	1.647	5.097	5.035	0.934	4.369	8.096	11.495	13.837	56.637	4.720
	<b>RXC 4</b>	0.000	0.092	0.036	0.001	0.015	0.217	0.000	0.000	0.002	0.000	0.213	0.000	0.576	0.048
<b>Ni (µg)</b>	<b>RXC 1</b>	0.505	2.326	4.351	4.312	5.582	5.080	7.938	6.776	4.202	21.068	22.245	14.872	99.256	8.271
	<b>RXC 2</b>	0.057	0.034	0.749	1.448	2.450	2.011	4.336	3.863	3.923	24.464	21.719	22.400	87.455	7.288
	<b>RXC 3</b>	1.039	0.865	4.323	4.811	9.881	4.485	10.449	8.873	6.553	19.663	25.864	23.522	120.328	10.027
	<b>RXC 4</b>	0.000	0.016	0.003	0.008	0.000	0.723	0.000	0.067	0.016	0.123	0.000	0.162	1.117	0.093
<b>Zn (µg)</b>	<b>RXC 1</b>	0.438	0.372	0.344	0.318	5.116	7.303	9.923	6.292	5.402	15.450	15.400	10.816	77.173	6.431
	<b>RXC 2</b>	0.278	0.224	0.266	0.187	3.675	3.640	5.913	3.573	6.941	15.829	21.719	11.947	74.192	6.183
	<b>RXC 3</b>	0.197	0.190	0.130	0.172	6.587	4.078	13.299	5.137	6.553	6.940	12.932	19.371	75.586	6.299
	<b>RXC 4</b>	0.355	0.065	0.073	0.034	0.000	0.145	0.000	0.048	0.042	0.000	0.213	0.162	1.136	0.095

**Table C-5: Raw Concentration of Major Elements**

Week	Al (ppm)				Fe (ppm)				Ca (ppm)				Mg (ppm)			
	LAN	DRB	CLV	Control	LAN	DRB	CLV	Control	LAN	DRB	CLV	Control	LAN	DRB	CLV	Control
Week 0	9.165	5.355	3.583	<MDL	5.007	4.578	1.434	<MDL	20.893	20.715	18.434	<MDL	12.667	10.845	11.837	<MDL
Week 1	<MDL	0.186	<MDL	<MDL	<MDL	<MDL	<MDL	<MDL	8.677	12.108	10.244	<MDL	5.658	3.920	3.392	<MDL
Week 2	1.498	1.233	<MDL	<MDL	<MDL	<MDL	<MDL	<MDL	9.669	12.863	9.000	<MDL	5.591	4.412	3.975	<MDL
Week 3	1.528	1.255	0.621	<MDL	<MDL	<MDL	<MDL	<MDL	10.067	12.600	9.333	<MDL	5.549	4.179	3.119	<MDL
Week 4	<MDL	1.167	0.492	<MDL	<MDL	<MDL	<MDL	<MDL	10.752	9.255	10.411	2.668	6.468	3.131	6.130	0.223
Week 5	<MDL	0.735	<MDL	<MDL	<MDL	<MDL	<MDL	<MDL	12.696	12.903	9.383	<MDL	7.027	5.223	4.251	<MDL
Week 6	0.536	<MDL	<MDL	<MDL	<MDL	<MDL	<MDL	<MDL	12.228	10.563	9.114	8.195	5.674	4.902	4.017	2.363
Week 7	0.932	0.976	0.516	<MDL	<MDL	<MDL	<MDL	<MDL	13.852	10.811	11.192	<MDL	6.667	5.173	5.614	<MDL
Week 8	6.373	0.840	<MDL	<MDL	1.707	<MDL	<MDL	<MDL	11.501	9.669	10.251	<MDL	4.514	3.542	3.514	0.204
Week 9	2.836	1.189	0.675	<MDL	2.043	1.264	<MDL	<MDL	12.317	11.308	10.781	<MDL	5.465	6.323	6.771	0.050
Week 10	1.852	1.401	0.880	<MDL	3.313	2.757	<MDL	<MDL	12.415	9.253	13.976	<MDL	4.953	6.980	3.361	0.274
Week 11	1.176	0.944	0.833	<MDL	1.661	1.581	1.004	<MDL	16.614	10.407	9.870	<MDL	5.362	4.235	3.320	0.753
Week 12	1.464	0.589	1.049	<MDL	2.028	1.556	1.086	<MDL	10.946	16.728	<MDL	<MDL	7.964	5.738	4.752	0.225

**Table C-6: Raw Concentration of Minor (Trace) Elements**

Week	Cr (ppb)				Cu (ppb)				Ni (ppb)				Zn (ppb)			
	LAN	DRB	CLV	Control	LAN	DRB	CLV	Control	LAN	DRB	CLV	Control	LAN	DRB	CLV	Control
Week 0	167.875	122.474	47.440	0.181	80.750	61.237	94.880	<MDL	76.500	52.790	92.620	0.181	129.625	44.344	72.289	<MDL
Week 1	<MDL	1.433	0.228	<MDL	0.168	0.215	<MDL	<MDL	1.508	0.201	2.284	<MDL	1.307	0.974	0.434	0.612
Week 2	3.050	3.922	1.042	<MDL	1.830	5.882	4.375	0.171	7.625	0.131	2.083	<MDL	1.220	0.863	0.458	0.120
Week 3	3.688	5.490	0.000	0.142	1.623	5.216	6.250	<MDL	14.750	2.745	10.417	<MDL	1.165	0.975	0.313	0.142
Week 4	12.600	38.612	9.287	<MDL	2.800	4.827	4.644	<MDL	15.400	6.033	13.002	<MDL	1.134	0.778	0.464	0.069
Week 5	13.725	4.299	0.000	<MDL	7.625	5.015	4.066	<MDL	18.300	8.597	24.398	<MDL	16.775	12.896	16.265	<MDL
Week 6	37.800	20.111	0.000	0.283	11.970	6.536	17.884	0.425	20.160	10.055	15.738	1.417	28.980	18.200	14.307	0.283
Week 7	33.075	22.524	21.837	<MDL	12.600	9.854	11.574	<MDL	25.200	15.485	24.021	<MDL	31.500	21.116	30.572	<MDL
Week 8	30.800	28.577	30.622	0.953	4.400	0.985	3.062	<MDL	30.800	19.708	29.091	0.136	28.600	18.230	16.842	0.098
Week 9	35.525	22.172	29.618	<MDL	13.475	13.550	14.809	<MDL	17.150	16.013	22.214	<MDL	22.050	28.331	22.214	0.085
Week 10	29.150	32.278	67.470	<MDL	26.500	24.208	16.867	<MDL	39.750	45.726	40.964	0.261	29.150	29.588	14.458	<MDL
Week 11	61.425	15.083	18.800	0.628	23.400	15.083	21.486	0.377	38.025	36.199	48.343	<MDL	26.325	36.199	24.172	0.377
Week 12	49.400	21.921	26.355	<MDL	36.400	21.921	26.355	<MDL	28.600	41.101	44.804	0.300	20.800	21.921	36.898	0.300

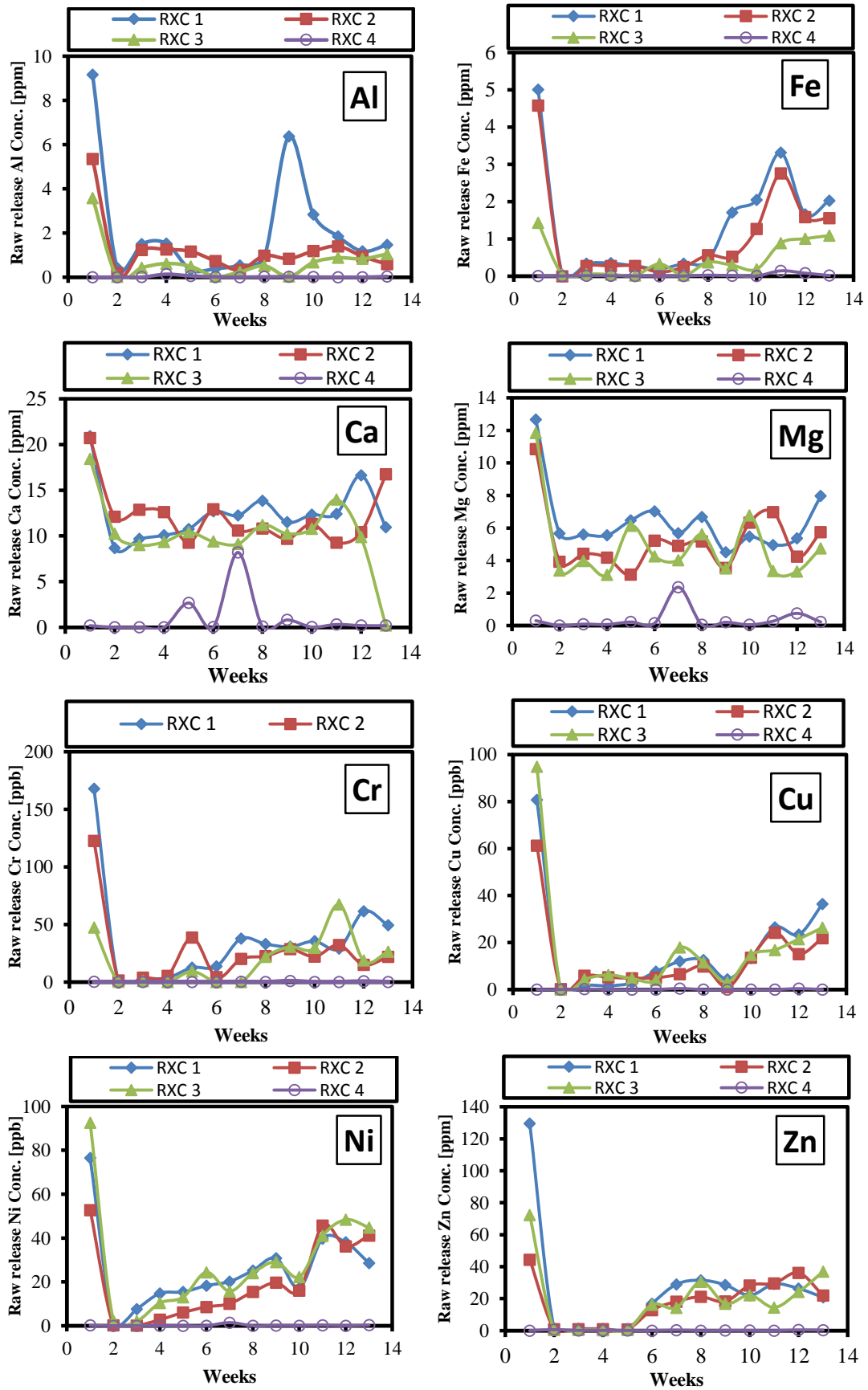


**Figure C-1:** Plots of Raw Release Concentration (non-cumulative) for both Majors and trace Heavy Metals

**Table C-7: Computed Cumulative weighted Concentrations for Major Elements**

	Al (ppm)				Fe (ppm)				Ca (ppm)				Mg (ppm)			
	LAN	DRB	CLV	Control	LAN	DRB	CLV	Control	LAN	DRB	CLV	Control	LAN	DRB	CLV	Control
<b>Week 0</b>	9.165	5.355	3.583	0.002	5.007	4.578	1.434	0.002	20.893	20.715	18.434	0.181	12.667	10.845	11.837	0.305
<b>Week 1</b>	9.584	5.541	3.606	0.005	5.040	4.578	1.480	0.002	29.570	32.823	28.678	0.184	18.325	14.766	15.229	0.306
<b>Week 2</b>	11.081	6.774	4.033	0.011	5.372	4.854	1.541	0.014	39.238	45.686	37.678	0.187	23.916	19.177	19.204	0.396
<b>Week 3</b>	12.610	8.029	4.654	0.145	5.719	5.127	1.586	0.022	49.305	58.286	47.011	0.190	29.465	23.357	22.323	0.464
<b>Week 4</b>	12.947	9.195	5.146	0.204	5.993	5.401	1.604	0.025	60.057	67.540	57.422	2.857	35.933	26.488	28.453	0.687
<b>Week 5</b>	13.333	9.930	5.176	0.219	6.184	5.509	1.932	0.025	72.753	80.444	66.805	2.886	42.960	31.711	32.704	0.830
<b>Week 6</b>	13.868	10.254	5.411	0.222	6.520	5.754	1.957	0.026	84.981	91.007	75.919	11.082	48.634	36.613	36.721	3.193
<b>Week 7</b>	14.801	11.229	5.927	0.240	6.931	6.315	2.326	0.050	98.833	101.818	87.111	11.152	55.301	41.786	42.336	3.244
<b>Week 8</b>	21.174	12.069	5.960	0.262	8.638	6.833	2.617	0.059	110.333	111.488	97.361	11.962	59.815	45.328	45.850	3.448
<b>Week 9</b>	24.009	13.257	6.635	0.270	10.681	8.097	2.802	0.060	122.651	122.795	108.143	11.992	65.280	51.651	52.620	3.498
<b>Week 10</b>	25.862	14.659	7.514	0.273	13.993	10.854	3.692	0.201	135.066	132.048	122.118	12.306	70.233	58.631	55.982	3.773
<b>Week 11</b>	27.038	15.603	8.347	0.273	15.655	12.435	4.696	0.279	151.680	142.455	131.989	12.494	75.594	62.866	59.301	4.526
<b>Week 12</b>	28.501	16.192	9.396	0.309	17.683	13.991	5.782	0.294	162.626	159.183	132.169	12.674	83.558	68.604	64.053	4.751

**Table C-8: Computed Cumulative weighted Concentrations for Trace Elements**

	Cr (ppb)				Cu (ppb)				Ni (ppb)				Zn (ppb)			
	LAN	DRB	CLV	Control												
<b>Week 0</b>	167.875	122.474	47.440	0.181	80.750	61.237	94.880	0.027	76.500	52.790	92.620	0.181	129.625	44.344	72.289	0.000
<b>Week 1</b>	167.875	123.906	47.668	0.219	80.918	61.452	94.880	0.027	78.008	52.991	94.905	0.181	130.932	45.318	72.723	0.612
<b>Week 2</b>	170.925	127.828	48.710	0.279	82.748	67.334	99.255	0.198	85.633	53.122	96.988	0.211	132.152	46.181	73.181	0.732
<b>Week 3</b>	174.613	133.318	48.710	0.421	84.370	72.550	105.505	0.269	100.383	55.867	107.405	0.216	133.317	47.156	73.494	0.874
<b>Week 4</b>	187.213	171.931	57.997	0.476	87.170	77.376	110.148	0.271	115.783	61.900	120.407	0.233	134.451	47.934	73.958	0.943
<b>Week 5</b>	200.938	176.229	57.997	0.476	94.795	82.391	114.214	0.299	134.083	70.497	144.804	0.233	151.226	60.830	90.223	0.943
<b>Week 6</b>	238.738	196.340	57.997	0.760	106.765	88.927	132.098	0.724	154.243	80.553	160.542	1.649	180.206	79.030	104.531	1.227
<b>Week 7</b>	271.813	218.864	79.834	0.788	119.365	98.782	143.672	0.724	179.443	96.038	184.563	1.649	211.706	100.146	135.103	1.227
<b>Week 8</b>	302.613	247.441	110.457	1.741	123.765	99.767	146.734	0.724	210.243	115.746	213.655	1.786	240.306	118.376	151.945	1.325
<b>Week 9</b>	338.138	269.613	140.075	1.746	137.240	113.316	161.544	0.729	227.393	131.759	235.868	1.818	262.356	146.707	174.159	1.409
<b>Week 10</b>	367.288	301.890	207.545	1.778	163.740	137.525	178.411	0.729	267.143	177.486	276.832	2.080	291.506	176.295	188.617	1.409
<b>Week 11</b>	428.713	316.973	226.345	2.405	187.140	152.608	199.897	1.105	305.168	213.685	325.176	2.080	317.831	212.494	212.789	1.786
<b>Week 12</b>	478.113	338.894	252.701	2.405	223.540	174.528	226.253	1.105	333.768	254.786	369.980	2.380	338.631	234.414	249.686	2.086

**Table C-9:** Computation of percentage weekly weathered CaCO<sub>3</sub> in the Lancashire Bowland Shale

1	2	3	4	5	6	7	8	9	10	11	12
Week	VoL Out (mL)	Ca (mg/L)	Ca (mg)	Cum. Ca (mg)	Cum. Ca mg as CaCO <sub>3</sub>	Mg (mg/L)	Mg (mg)	Cum. Mg (mg)	Cum. Mg (mg) as Ca CO <sub>3</sub>	Cum. Ca+Mg as CaCO <sub>3</sub>	*% CaCO <sub>3</sub> Weather each week from 85.52g
0	535	48.32	25.85	25.85	64.63	21.61	11.56	11.56	28.90	93.53	0.10937
1	335	51.80	17.35	43.20	108.01	23.78	7.97	19.53	48.82	156.83	0.18338
2	305	63.40	19.34	62.54	156.35	22.66	6.91	26.44	66.10	222.45	0.26012
3	295	68.25	20.13	82.67	206.69	22.62	6.67	33.11	82.78	289.47	0.33848
4	280	76.80	21.50	104.18	260.45	26.20	7.34	40.45	101.12	361.57	0.42279
5	305	73.25	22.34	126.52	316.30	22.08	6.73	47.18	117.96	434.26	0.50778
6	252	67.05	16.90	143.42	358.54	21.03	5.30	52.48	131.20	489.75	0.57267
7	315	67.95	21.40	164.82	412.05	22.33	7.03	59.52	148.79	560.84	0.65580
8	220	68.32	15.03	179.85	449.63	21.04	4.63	64.14	160.36	609.99	0.71327
9	245	61.55	15.08	194.93	487.33	18.61	4.56	68.70	171.76	659.09	0.77068
10	530	36.52	19.36	214.29	535.72	18.69	9.91	78.61	196.52	732.24	0.85622
11	585	35.45	20.74	235.03	587.56	18.33	10.72	89.33	223.33	810.89	0.94819
12	520	21.60	11.23	246.26	615.64	10.63	5.53	94.86	237.15	852.79	0.99719

Week "0": Initial flush

Column 3: Calcium concentration (mg/L)

Column 4: Mass (in mg) of calcium computed from columns 2 and 3

Column 5: Mass (in mg) of calcium displayed cumulatively

Column 6: Calcium computed as calcium carbonate

Columns 7 through 10 are the same as those described above, but for Magnesium

Column 11: Sum of columns 6 and 10

Column 12: Column 11 divided by the total mass of calcium carbonate equivalent in the column, expressed in percentage

\* % CaCO<sub>3</sub> equivalent used in computing column 12 is derived from the Average NP number (table 4.11 in Chapter 4) and the known mass of sample in a column (table 5.1 in Chapter 5) (i.e. Mass of sample in column (g) × Average NP number (tons/1000 tons CaCO<sub>3</sub> equivalent))

**Table C-10:** Computation of percentage weekly weathered CaCO<sub>3</sub> in the Derbyshire Edale shale

1	2	3	4	5	6	7	8	9	10	11	12
Week	VoL Out (mL)	Ca (mg/L)	Ca (mg)	Cum. Ca (mg)	Cum. Ca mg as CaCO <sub>3</sub>	Mg (mg/L)	Mg (mg)	Cum. Mg (mg)	Cum. Mg (mg) as Ca CO <sub>3</sub>	Cum. Ca+Mg as CaCO <sub>3</sub>	% CaCO <sub>3</sub> Weather each week from 91.47g
0	470	78.10	36.71	36.71	91.77	3.36	1.58	1.58	3.95	95.72	0.104641
1	285	91.22	26.00	62.70	156.76	32.36	9.22	10.80	27.00	183.77	0.200903
2	260	98.36	25.57	88.28	220.70	33.75	8.78	19.58	48.94	269.64	0.294783
3	273	91.50	24.98	113.26	283.14	30.45	8.31	27.89	69.72	352.87	0.385775
4	240	86.50	20.76	134.02	335.04	30.95	7.43	35.32	88.29	423.34	0.462817
5	285	80.35	22.90	156.92	392.29	30.45	8.68	44.00	109.99	502.28	0.549124
6	200	85.90	17.18	174.10	435.24	40.75	8.15	52.15	130.36	565.61	0.618354
7	280	86.75	24.29	198.39	495.97	36.75	10.29	62.44	156.09	652.06	0.712866
8	196	80.36	15.75	214.14	535.35	35.94	7.04	69.48	173.70	709.05	0.775167
9	245	71.80	17.59	231.73	579.32	31.33	7.68	77.16	192.89	772.21	0.844225
10	535	51.40	27.50	259.23	648.07	29.95	16.02	93.18	232.95	881.02	0.963177
11	600	50.33	30.20	289.43	723.57	24.04	14.42	107.60	269.01	992.57	1.085135
12	545	51.02	27.81	317.23	793.08	20.94	11.41	119.02	297.54	1090.62	1.192324

Week "0": Initial flush

Column 3: Calcium concentration (mg/L)

Column 4: Mass (in mg) of calcium computed from columns 2 and 3

Column 5: Mass (in mg) of calcium displayed cumulatively

Column 6: Calcium computed as calcium carbonate

Columns 7 through 10 are the same as those described above, but for Magnesium

Column 11: Sum of columns 6 and 10

Column 12: Column 11 divided by the total mass of calcium carbonate equivalent in the column, expressed in percentage

\* % CaCO<sub>3</sub> equivalent used in computing column 12 is derived from the Average NP number (table 4.14 in Chapter 4) and the known mass of sample in a column (table 5.1 in Chapter 5) (i.e. Mass of sample in column (g) × Average NP number (tons/1000 tons CaCO<sub>3</sub> equivalent))

**Table C-11:** Computation of percentage weekly weathered CaCO<sub>3</sub> in the Whitby Bituminous shale

<b>REACTOR 3- CLEVELAND SHALE</b>											
<b>1</b>	<b>2</b>	<b>3</b>	<b>4</b>	<b>5</b>	<b>6</b>	<b>7</b>	<b>8</b>	<b>9</b>	<b>10</b>	<b>11</b>	<b>12</b>
<b>Week</b>	<b>VoL Out (mL)</b>	<b>Ca (mg/L)</b>	<b>Ca (mg)</b>	<b>Cum. Ca (mg)</b>	<b>Cum. Ca mg as CaCO<sub>3</sub></b>	<b>Mg (mg/L)</b>	<b>Mg (mg)</b>	<b>Cum. Mg (mg)</b>	<b>Cum. Mg (mg) as Ca CO<sub>3</sub></b>	<b>Cum. Ca+Mg as CaCO<sub>3</sub></b>	<b>% CaCO<sub>3</sub> Weather each week from 71.79g</b>
0	511	61.60	31.48	31.48	78.69	52.40	26.78	26.78	66.94	145.64	0.202863
1	455	74.85	34.06	65.53	163.84	49.85	22.68	49.46	123.65	287.48	0.400447
2	415	73.20	30.38	95.91	239.78	49.08	20.37	69.83	174.57	414.35	0.577165
3	415	74.80	31.04	126.95	317.39	44.97	18.66	88.49	221.22	538.61	0.750255
4	370	76.05	28.14	155.09	387.73	43.00	15.91	104.40	261.00	648.73	0.903649
5	405	76.15	30.84	185.93	464.83	40.91	16.57	120.97	302.42	767.25	1.068746
6	285	69.70	19.86	205.80	514.50	25.08	7.15	128.12	320.29	834.78	1.162813
7	435	69.25	30.12	235.92	589.80	35.71	15.53	143.65	359.12	948.93	1.321810
8	305	69.95	21.33	257.26	643.14	28.95	8.83	152.48	381.20	1024.34	1.426854
9	295	62.80	18.53	275.78	689.46	25.72	7.59	160.07	400.17	1089.62	1.517791
10	480	58.00	27.84	303.62	759.06	23.95	11.50	171.56	428.91	1187.96	1.654774
11	535	46.75	25.01	328.63	821.58	25.36	13.57	185.13	462.82	1284.41	1.789120
12	525	43.25	22.71	351.34	878.35	25.03	13.14	198.27	495.68	1374.03	1.913953

Week "0": Initial flush

Column 3: Calcium concentration (mg/L)

Column 4: Mass (in mg) of calcium computed from columns 2 and 3

Column 5: Mass (in mg) of calcium displayed cumulatively

Column 6: Calcium computed as calcium carbonate

Columns 7 through 10 are the same as those described above, but for Magnesium

Column 11: Sum of columns 6 and 10

Column 12: Column 11 divided by the total mass of calcium carbonate equivalent in the column, expressed in percentage

\* % CaCO<sub>3</sub> equivalent used in computing column 12 is derived from the Average NP number (table 4.14 in Chapter 4) and the known mass of sample in a column (table 5.1 in Chapter 5) (i.e. Mass of sample in column (g) × Average NP number (tons/1000 tons CaCO<sub>3</sub> equivalent)

**Table C-12:** Computation of cumulative sulphur weathered from analytical sulphur determination.

Days	<sup>1</sup> Sulphate (LAN) mg/L	<sup>2</sup> Weekly Sulphur Weathered (mg)	<sup>3</sup> % Sulphur Weathered	<sup>4</sup> Cum. % Sulphur	<sup>1</sup> Sulphate (DRB) mg/L	<sup>2</sup> Weekly Sulphur Weathered	<sup>3</sup> % Sulphur Weathered	<sup>4</sup> Cum. % Sulphur	<sup>1</sup> Sulphate (CLV) mg/L	<sup>2</sup> Weekly Sulphur Weathered	<sup>3</sup> % Sulphur Weathered	<sup>4</sup> Cum. % Sulphur
1 (Flush)	274.80	49.01	0.081	0.081	198.20	31.05	0.059	0.059	105.80	18.02	0.034	0.034
7	223.58	24.97	0.041	0.122	213.44	20.28	0.039	0.098	226.04	34.28	0.064	0.098
14	151.76	15.43	0.025	0.147	522.99	45.33	0.087	0.185	292.29	40.43	0.075	0.173
21	164.51	16.18	0.027	0.174	610.66	55.57	0.106	0.291	352.28	48.73	0.091	0.264
28	174.53	16.29	0.027	0.200	508.05	40.64	0.078	0.369	116.71	14.39	0.027	0.291
35	405.97	41.27	0.068	0.268	504.24	47.90	0.092	0.460	115.86	15.64	0.029	0.320
42	411.92	34.60	0.057	0.325	419.65	27.98	0.053	0.514	113.55	10.79	0.020	0.340
49	442.56	46.47	0.076	0.402	403.39	37.65	0.072	0.586	100.81	14.62	0.027	0.367
56	407.10	29.85	0.049	0.451	383.36	25.05	0.048	0.634	96.36	9.80	0.018	0.386
63	492.80	40.25	0.066	0.517	320.96	26.21	0.050	0.684	79.00	7.77	0.014	0.400
70	372.68	65.84	0.108	0.625	324.75	57.91	0.111	0.794	54.65	8.74	0.016	0.417
77	377.99	73.71	0.121	0.746	478.35	95.67	0.183	0.977	54.35	9.69	0.018	0.435
84	367.84	63.76	0.105	0.851	477.28	86.70	0.166	1.143	59.25	10.37	0.019	0.454

<sup>1</sup> Analytical sulphur determination

<sup>2</sup> Weekly mas of sulphur weathered [(Sulphur Conc. ÷3) × weekly leachate collected]

<sup>3</sup> % Sulphur weathered = [Weekly Sulphur weather (g) ÷ Amount of Sulphur in column (g)] × 100

<sup>4</sup> Cumulative percentage sulphur weathered